The Role of Somatostatin 4 Receptors in Analgesia

A thesis submitted to the University of Manchester for the degree of Doctor of Philosophy in the Faculty of Life Sciences

2015

Louise C. J. Gorham

Table of Contents

List of Figures

List of Tables

Abstract

Pain is an unpleasant sensory or emotional experience associated with potential or actual tissue damage; presenting a worldwide debilitating problem. Somatostatin is a regulatory cyclic neuropeptide with inhibitory roles in the central nervous system (CNS) via activation of the five somatostatin receptor subtypes belonging to the family of G protein-coupled receptors (GPCRs). Somatostatin is known to exert analgesic effects, which are in part achieved by activation of the somatostatin 4 (sst_4) receptor subtype. This research aimed to gain a greater understanding of the role of sst_4 receptors in analgesia, with a particular interest in elucidating molecular mechanisms. Using the synthetic sst_4 receptor selective agonist, J-2156, the behavioural analgesic profile was established in four analgesic models: the inflammatory Complete Freund´s Adjuvant (CFA) and monosodium iodacetate (MIA) models; and the neuropathic partial nerve ligation (PNL) and streptozotocin-induced diabetes (STZ) models. Following this mode of action studies were conducted on dissociated dorsal root ganglion (DRG) neurons.

J-2156 has a potent analgesic profile. Maximal analgesic effects were seen at 1 mg/kg in all pain models except the MIA model, which required a dose of 10 mg/kg. Analgesia was long-lasting in inflammatory pain models, where significant improvements were present at 24 hours post compound administration.

J-2156 modulated the activity of a variety of ion channels within DRG neurons. Activation of sst_4 receptors induced a G-protein gated inwardly rectifying potassium channel (GIRK) current and inhibited voltage sensitive calcium channel (Ca_v), transient receptor potential vanilloid channel (TRPV1) and transient receptor potential ankyrin channel (TRPA1) currents. For all ion channels a concentration-dependent effect was observed, with significant effects first being produced at 10 nM and maximal effects reached at 100 nM.

J-2156 caused a significant reduction in paw volume, however this was only seen at doses 10-times that required for analgesia in the CFA model, at 10 mg/kg. This was independent of paw neutrophil and cytokine levels. A significant reduction in inflammatory mediator release from stimulated DRG neurons was observed following incubation with J-2156. The inhibition produced was bell-shaped, where maximal effects were observed at 30 nM.

J-2156 modulated the expression of a number of previously characterised pain, inflammatory and immune genes in both DRG neurons and paw tissue, suggesting that the analgesia is in part due to gene normalisation.

Overall, this work provides a novel insight into the role of sst_4 receptor activation in nociception in chronic pain conditions, indicating contributory molecular mechanisms to the analgesia. From these results it can be concluded that the sst_4 receptor presents an appropriate target for novel broad treatment analgesia.

Declaration

I declare that no portion of the work referred to in the thesis has been submitted in support of an application for another degree or qualification of this or any other university or other institute of learning.

Copyright statement

Acknowledgements

First and foremost I would like to say a massive thank you to my supervisors: Dr Stefan Just, Dr Gillian Edwards and Dr Henri Doods for their continued patience, guidance and support over the past three years, without whom I couldn't have done this.

Secondly I would like to thank the lab leaders within the pain group at BI, who were always available for scientific discussions and suggestions. Particularly Dr Laura Corradini, Dr Janet Nicholson and Gert Kramer. I would also like to thank my advisor Dr Natalie Gardener, for giving me advice and being there when needed.

For conductance of behavioural data I would like to thank Margot Weiland, Anna Menzel, Andreas Kremer and Dr Makoto Shimasaki. For conductance of NGS data I would like to thank Dr Tobias Hildebrant and Sussanne Acker. For help with the pharmacokinetic data I would like to thank Dr Raimund Kuelzer.

Thanks so much to many members of the pain group, including Isabelle Reimann, Nadja Becher, Elisabeth Leibhardt, Rosmarie Ewen, Carsten Hecker, Benjamin Jaehnke, Sylvia Thanner-Hecht and Johannes Freudenreich. You all provided me with great assistance in the lab, teaching me valuable techniques and always being around when I needed help. Also a massive thank you to my friend Dr Graham Goodlad for help with proofreading.

I would like to thank my international BI support. Catherine Sweatman, Dr Niklas Schuelert, Diego Fernandez and Ekaterina Ivanova, as well as Manchester past and present placement students (Stacey, Molly, Gillian, Laura, Luke, Alfie, Kristen and Beth). Thanks to all of you for listening to me complain, giving me advice and putting a smile on my face.

Thank you massively to my amazing friends and family: Sophie Griffin, Kate Brewis, Laura Ruse, Clare Schilizzi, Anthony Hawkins and Matthew Collier for all the fun times, as well as your never ending moral support and confidence in me over the last three years. Also a big thank you to all my friends in Biberach (Anabelle, Nina, Natalie, Paula, Christina, Simon, Valentin, Patrick, Baldu, Elena and Franzi) who welcomed me and made my time here that much more enjoyable!

Last, but definitely not least I would like to thank my Mum, Linda Gorham and Samuel Roch. Both of whom have been rocks to me, providing me with endless love and support.

Abbreviations

AITC	Allyl isothiocynate
AMPA	α-amino-3-hydroxyl-5-methyl-4-isoxazole-propionate receptor
Anxa8	Annexin a8
ASIC	Acid-sensing ion channels
Bdkrb2	Bradykinin receptor b2
Bdnf	Brain derived neurotropic factor
BSA	Bovine serum albumin
cAMP	Cyclic adenosine monophosphate
Ca_v	Voltage sensitive calcium channels
ccl2	Chemokine ligand 2
CCL39	Chinese hamster lung fibroblast cells
CFA	Complete Freund´s Adjuvant
CGRP	Calcitonin gene-related peptide
CHO	Chinese hamster ovary cells
Cmax	Maximal plasma concentration
CNS	Central nervous system
COX	Cyclooxygenase
dH_2O	De-ionized water
DMEM	Dulbecco's Modified Eagle Medium
DMSO	Dimethyl sulfoxide
DPBS	Dulbecco's phosphate buffer saline
DRG	Dorsal root ganglion
FCS	Foetal calf serum
EC_{50}	Half maximal excitatory concentration
Egr1	Early growth response 1
EIA	Enzyme immunoassay
ELISA	Enzyme-linked immunosorbant assay
EP_{1-4}	Prostaglandin receptors
ERAP1	Endoplasmic reticulum aminopeptidase 1
g	grams
GDP	Guanosine diphosphate
GHS-R1a	Growth hormone secretagogue receptor
GIRK	G protein gated inwardly rectifying potassium channel
GPCR	G-protein coupled receptor
GTP	Guanosine triphosphate
Hba1	Hemoglobin alpha 1
HEK	Human embryonic kidney cells
HEPES	Hydroxyethyl piperazineethanesulfonic
HPLC-	High-performance liquid chromatography coupled to tandem mass
HTRF	Homogenous time resolved fluorescent
IBMX	Isobutylmethylxanthine
IC_{50}	Half maximal inhibitory concentration
IL	Interleukin
IL21R	Interleukin 21 receptor
INF	Interferon
i.p	Intraperitoneally

kd	Dissociation constant of the radioligand
kDa	kilo Daltons
Ki	Inhibition constant
LC	Locus coeruleus
LPS	Lipopolysaccharide
MCP1	Monocyte chemoattractant protein 1
mEPSC	Miniature excitatory postsynaptic currents
MgrX2	MAS related gene receptor
MIA	Monosodium iodacetate
ml	Millileters
mM	Millimolar
MPO	Myeloperoxidase
MRGPRD	Mas-related GPCR member D
mRNA	Messenger RNA
m/s	Meters per second
NaOH	Sodium hydroxide
NaCl	Sodium chloride
Na_v	Voltage sensitive sodium channels
NGS	Next generation sequencing
nM	Nanomolar
NMDA	*N*-methyl-*D*-aspartate receptor
NSAIDs	Non-steroidal anti-inflammatory
PAG	Periaqueductal grey matter
PBS	Phosphate buffer saline
PCR	Polymerase chain reactions
pF	Picofarad
PGE_2	Prostaglandin E_2
PKA	Protein kinase A
PKC	Protein kinase C
PNL	Partial nerve ligation model
p.o	Orally administered
PWT	Paw withdrawal threshold
reg3b	Regenerating g islet derived 3 beta
rpkm	Reads per kilobase per million
S1PR3	Sphingosine-1-phosphate receptor 3
s.c	Subcutaneous
S.D.	Standard deviation
S.E.M.	Standard error mean
SNRI	Serotonin-norepinephrine reuptake inhibitors
SP1	Sphingosine-1-phosphate
SRIF	Somatotropin release-inhibiting factor
sst	Somatostatin
sst_{1-5} receptor	Somatostatin receptor subtypes 1-5
STZ	Streptozotocin
TBq	terabecqurel
THBS4	Thrombospondin 4
Tmax	Time of maximal plasma concentration
Tnc	Tenascin-c

TNFα	Tumour necrosis factor α
TRPA	Transient receptor potential ankyrin channels
TRPV1	Transient receptor potential vanilloid 1 ion channel
TTX	Teterodotoxin
µM	Micromolar
WDR	Wide dynamic range neurons

1. Introduction

1.1. Pain

Pain, described in laymen's terms, is an unpleasant sensory or emotional experience associated with potential or actual tissue damage; it therefore provides an important function to alert us to potentially threatening situations. Despite this warning, pain can persist beyond the acute effect, leading to the development of chronic pain. It is estimated that approximately one in five adults within Europe suffer from such conditions, which have constant impacts on their daily lives. Pain can be split into both nociceptive pain, induced by activation of nociceptors by specific stimuli, and neuropathic pain, induced by damage to the somatosensory system. Nociceptive pain is associated with inflammatory diseases such as rheumatoid arthritis and osteoarthritis, whereas neuropathic pain is associated with nerve damage as well as metabolic diseases including diabetes (Schmader, 2002).

1.1.1. Somatosensory system and pain transmission

The sensation of pain arises from the activation of the somatosensory system within the brain. This is part of the sensory system involved in pain processing such as touch, proprioception, temperature and nociception, where each modality has its own receptors, fibres and pathways (Arezzo *et al.*, 1982). Pain can be perceived not only due to the type of fibre being activated, but also due to the pattern of impulses in the nervous system (Persaud *et al.*, 2002). For example a thermal stimulation begins as a warm sensation, however if the stimulation persists this can lead to the development of burning and therefore a painful sensation is perceived.

Nociceptive signalling, i.e. that which is relating to or indicating pain, is comprised of four distinct processes. Transduction involves the transduction of the stimulus energy into electrophysiological activity in primary nociceptive afferents. This electrophysiological signal is conveyed from the periphery to the spinal cord, then to the brainstem and finally in higher brain centres including the thalamus and cortex, by a process known as transmission (Fig. 1.1). At all levels of the central nervous system (CNS) modulation occurs, leading to an increase or decrease of neuronal activity. Pain perception is regulated by cortical regions of the brain, which process the sensory and affective components of pain, combining different aspects implicated in the pain experience.

To allow transmission of nociceptive signals from the periphery to the brain, the entire body is innervated by neurons, specifically primary afferent neurons. The nerve terminals of these are located in peripheral targets where the cell body resides in the dorsal root ganglion (DRG) neurons (McCleskey *et al.*, 1999). Tissue damage occurs as a result of noxious stimulation, of which there are three forms: mechanical, thermal and chemical (Arezzo *et al.*, 1982). Chemical mediators released from the damaged cell, including bradykinin, serotonin, histamine, prostaglandins and protons, are able to recruit peripheral nociceptors. These in turn depolarise the fibre neurons allowing the transmission of nerve impulses to the central dorsal horn of the spinal cord (Latremoliere *et al.*, 2009). Here the nociceptive fibres release excitatory neurotransmitters and peptides enabling the

impulses to be further transmitted across the synaptic cleft. The neurotransmitters known to be involved in nociception include substance P, calcitonin gene-related peptide (CGRP) and glutamate (Tao *et al.*, 2005; de Prado *et al.*, 2009). These are able to activate the spinothalamic (lateral) and the spinoreticular (medial) tract neurons, which further transduce the signals to the lateral and medial thalamus. These subsequently make synaptic contact with the tertiary neurons in the somatosensory cortex and other brain centres to elicit the conscious sensation of pain and the emotional responses involved (McHugh *et al.*, 2000).

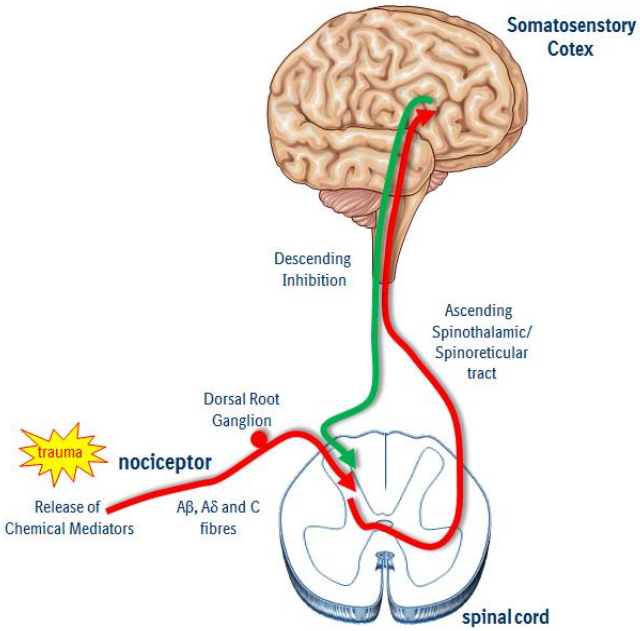

Fig. 1.1. The nociceptive pain pathway. Release of chemical mediators allows for activation of peripheral nociceptors. The noxious stimuli are transduced to electrophysiological signals, which are conveyed from the periphery to the spinal cord, via dorsal root ganglion neurons. These signals are then transmitted to higher brain centres along the ascending spinothalamic and spinoreticular tracts. Modulation of these signals can occur by activation of the descending inhibitory pathway, which controls activity of interneurons in the dorsal horn.

In the periphery, nociceptor stimulation is the first step in pain transmission. Nociceptors are present on nerve endings, responding to nociceptive stimulation via exteroceptive receptors, which detect changes in the environment and proprioceptive receptors, which detect internal changes (Craig, 2003). Nociceptors are polymodal, and are divided into three main types dependent on stimulation: mechanoreceptors, thermoreceptors and chemoreceptors. They are involved in the transduction and transmission processes of nociceptive signals. Technically these are not typical receptors, but rather are unmyelinated, free nerve endings which penetrate the skin, muscle, fascia and viscera tissue. Nociceptors are defined on the basis that they respond proportionally to the intensity of stimulation and have higher thresholds compared to innocuous receptors i.e. activation by a harmless stimulation (Arezzo *et al.*, 1982).

Primary afferent neurons are the first order neurons of nociceptive transmission. These are split into three groups: Aβ, Aδ and C fibres. These are bipolar cells, with axons extending from the main cell body which resides in the DRG neurons to that innervate peripheral and central targets (McCleskey *et al.*, 1999). They are characterised by their conductance velocity. Aβ fibres are large, myelinated fibres with high conductance speeds of 35 - 75 m/s. These are typically involved in non-nociceptive transmission, including mechanical displacement mediating touch, pressure, vibration and

movement. However these fibres are able to modulate nociceptive signalling in both dynamic and tonic ways. Aβ fibres recruit inhibitory interneurons in the substantia gelatinosa of the dorsal horn, thereby allowing innocuous stimuli to reduce nociceptive input (Melzack *et al.*, 1965). This means that blocking input from these large fibres results in an increased response to nociceptive stimuli (Latremoliere *et al.*, 2009). Aδ fibres are relatively large myelinated fibres, with conductance speeds of 5 – 30 m/s. These are responsible for the initial sharp, localisation of pain. There are two types of Aδ fibres: those that are responsible for intense and potentially harmful mechanical stimulation only, known as mechanonociceptors; and those which are responsible for mechanical, thermal and chemical stimulation, known as polymodal nociceptors (Baumgaertner *et al.*, 2012). C fibres are small, unmyelinated fibres with slow conductance speeds of 0.5 – 2 m/s. These are thought to be responsible for secondary pain sensations such as dull and aching pain. These fibres transmit three quarters of all afferent sensory input, and even have some involvement in non-nociceptive signals including itch (Stander *et al.*, 2003).

Primary afferent neurons can be classified into two major neurochemical groups: peptidergic fibres containing neuropeptides, such as CGRP and substance P (Lawson *et al.*, 1997) and non-peptidergic neurons (Snider *et al.*, 1998). Non-peptidergic neurons can be further classified according to their expression of a sensory neuron-specific G-protein coupled receptor (GPCR), the mas-related GPCR member D (MRGPRD), which is expressed on a population of non-peptidergic C fibres (Zylka *et al.*, 2005). Furthermore, expression of the vesicular glutamate transporters (VGluT) differs according to myelination. VGluT1 is present on myelinated afferent neurons while VGluT2 is present on unmyelinated neurons (Oliveira *et al.*, 2003). TRPA1 channel expression is also restricted to a small subpopulation of neurons. Expression is mainly seen on non-, or lightly-myelinated neurons, of which 97% co-express TRPV1 channels (Story *et al.*, 2003).

Second order neurons are located in the spinal cord, specifically on superficial zones of the dorsal horn (lamina I, II) and lamina V (Todd, 2010). These are the neurons which synapse with the primary afferents and further transmit impulses to the higher brain centres. There are two main types: nociceptive-specific neurons and wide dynamic range neurons (WDR). The axonal projections of the second order neurons cross over the midline, resulting in somatosensory information from one side of the body being received in the contralateral side of the brain. As the name suggests nociceptive specific neurons respond only to nociceptive input. These are subdivided depending on which type of primary afferent neurons they are recruited by, Aδ either alone or in combination with C fibres (Marchand, 2008). WDR neurons respond gradually to both innocuous and nociceptive inputs, meaning they are recruited by all types of primary afferents. As the name suggests these are dynamic neurons meaning they undergo change in states of persistent pain. Alterations include differences in their receptive fields, permeability of ion exchange and the discharge frequency (Le Bars *et al.*, 2001).

Secondary neurons are projected to the higher brain centres via two main pathways: the sensory spinothalamic tract and the affective spinorecticular tract. The spinothalamic tract projects neurons from the lamina I and IV – VI of the spinal cord to the lateral nuclei of the ventrobasal thalamus.

These have relatively small receptor fields with rapid conductance (Willis *et al.*, 1979). The spinorecticular tract projects neurons from the deep lamina VII and VIII of the spinal cord to the medial nuclei of the thalamus and brainstem. These have relatively large receptor fields, having specific roles in memory and afferent components of pain (Willis, 1985).

Third order neurons are located in one of the somatosensory nuclei of the thalamus. There are two groups of nuclei: the ventrobasal and the centromedian. The ventrobasal nuclei receive inputs from the spinothalamic tract and transmit these signals to the primary and secondary somatosensory cortices (Talbot *et al.*, 1991). The centromedian nuclei receive input from the spinorecticular tract and transmit these signals to the limbic system. Ultimately, these reach the fourth order neurons, where general and pronociceptive sensations are received and complex sensory information is integrated. In order for pain to be perceived, a complex network of cortical structures needs to be activated. For the sensory discriminative aspect of pain the primary and secondary somatosensory cortexes are activated. For the affective component of pain the anterior cingulate and the insular cortexes are activated (Coghill *et al.*, 1994).

Pain transmission can be modulated along each of these stages. Pain transmission within the dorsal horn is regulated by inhibitory inputs from GABAergic, glycinergic and enkephalinergic interneurons in the spinal cord, these are inhibited by incoming nociceptive fibres. Descending inhibitory pathways from the midbrain and the brainstem regions also modulate nociceptive signalling. This involves input from different brain regions (Pagano *et al.*, 2012). Firstly excitatory neurons within the spinal tract cause activation of noradrenergic neurons located in the locus coeruleus (LC). These then descend to the dorsal horn releasing noradrenaline and activating α2 adrenergic receptors both pre- and post-synaptically, attenuating the pain response (Pertovaara, 2006). Another important region of the brain involved in nociceptive modulation is the periaqueductal grey matter (PAG). Here glutamate excites enkaphalinergic neurons causing the inhibition of GABAergic neurons, which ultimately relieves the inhibition of serotonergic neurons (Vaughan *et al.*, 1997). Serotonin in the dorsal horn activates interneurons, causing the release of enkephalin (Pagano *et al.*, 2012), thus controlling the pain transmission.

A further mechanism contributing to modulation is release of endogenous ligands. An important system involved is the opioid system. Opioids are known to have a central role in nociception by modulating pain sensations. Modulation starts at the periphery and involves several CNS structures (Heinricher *et al.*, 2009). Opioidergic neurotransmission is found throughout the brain and periphery. There are three characterised opioid receptors: mu, delta and kappa, which are activated by the endogenous peptides endorphins, enkephalins and dynorphins respectively (Minami *et al.*, 1995). The receptors modulate nociceptive input via interaction with ion channels and blocking of neurotransmitter release. Endogenous relief occurs via recruitment of opioid-containing immune cells to the site of injury (Stein *et al.*, 1990) or release of peptides from adrenal medulla and sympathetic nerve endings (Bodnar *et al.*, 1980). Indeed this modulation has been reported in humans (Levine *et al.*, 1979) and the opioid receptors are among the most well-established targets for pain relief.

1.1.2. Researching pain

In order to develop novel treatments for chronic pain conditions it is important to have a good understanding of the neurophysiology of pain and the mechanisms involved in the development and maintenance of such conditions. As pain is such a prominent worldwide problem, continual research is being conducted to allow for the development of an effective therapy for optimal management. Despite the fact that pain perception is more complex in humans due to the psychosocial, cultural, developmental and environmental variables, animal models are pivotal for such research. There are two main types of pain: nociceptive and neuropathic, both of which are represented by established and validated animal models. These models do have parallels which mimic persistent pain encountered in the clinic, however cannot simulate all symptoms. Nociceptive models include the Complete Freund´s Adjuvant (CFA) model and the monosodium iodacetate (MIA) model. Neuropathic models include the partial nerve ligation (PNL) model and the diabetic streptozotocin (STZ) model. An additional acute nociceptive model is the carrageenan induced inflammatory pain model. These animal models lead to altered pain processing, which can be measured by analgesic tests, including the Randal and Selitto method for mechanical hyperalgesia and the weight bearing deficit method.

1.1.3. Animal models of nociceptive pain

Nociceptive pain is injury-induced, leading to direct activation of nociceptors and increased sensitivity to noxious stimuli; this often involves inflammatory mediators. Osteoarthritis is an example of a chronic nociceptive pain condition, resulting from both biochemical forces and biochemical changes to the articular cartilage and synovial membrane (Combe *et al.*, 2004). Currently there is no disease-modifying treatment, so medical intervention mainly targets the primary symptoms of pain and disability (Malfait *et al.*, 2013). In patients pain not only worsens with weight bearing and activity, but also with joint stiffness. Mild burns provide an example of acute inflammatory and therefore nociceptive pain, a condition leading to hyperalgesia (Pedersen *et al.*, 1998). Symptoms similar to those in humans can be reflected in validated animal models.

The carrageenan model is more typical of inflammation, which is associated with nociception. It involves an injection of a dose of carrageenan, into the plantar surface on the hind paw. Carrageenan is derived from mucopolysaccharide extract of red alga *Chondrus Crispus*, which initiates activation of inflammatory cascades causing acute oedema. This occurs in two stages, initial swelling at the thirty minute time point (Vinegar *et al.*, 1969) and then again after the three hour time point. Oedema peaks at three to five hours after injection (Winter *et al.*, 1962), making this the most appropriate time for measurements of inflammatory effects. This model is particularly important for research into the development of anti-inflammatory drugs; however it does also results in the development of both thermal (Fecho *et al.*, 2005) and mechanical hyperalgesia (Estebe *et al.*, 2006), meaning it can be used to determine if the anti-inflammatory effects of compounds correlate to the anti-nociceptive effects.

The Complete Freund´s Adjuvant (CFA) model results in the development of injury-induced, persistent inflammatory pain. This model involves injection of the CFA oil into the area of desired local inflammation, for example the hind paw, the knee or the tail (Millan *et al.*, 1988). The oil contains mycobacterium, which stimulates an immune and inflammatory response via the recruitment of neutrophils, macrophages and cytokines (Broderson, 1989). The cutaneous inflammation occurs instantly after injection, while paw oedema peaks at around twenty-four hours. This model results in thermal and mechanical hyperalgesia which lasts for several weeks following the administration of the CFA oil (Lao *et al.*, 2004). A benefit of this model is that the physiological and biochemical effects of the oil seem to be limited to the affected limb (Iadarola *et al.*, 1988), meaning fewer unwanted effects.

The monosodium iodacetate (MIA) model is an established inducer of arthritis (Kalbhen, 1987). This model involves injection of the MIA solution into the knee joint (Combe *et al.*, 2004). MIA is an inhibitor of glycolysis which disrupts chondrocyte metabolism. Since chondrocytes are a requirement for the structural integrity of articular cartilage to remain stable, MIA results in cartilage degeneration in a similar manner to human arthritis (Janusz *et al.*, 2001). Initially there is an inflammatory response, which peaks about three days after injection. This occurs due to the expansion of the synovial membrane by proteinaceous oedema fluid and fibrin and leads to an infiltration of macrophages, neutrophils, plasma cells and lymphocytes (Bove *et al.*, 2003). At this time point weight bearing deficits and mechanical hyperalgesia are present, these last for several weeks following MIA administration (Malfait *et al.*, 2013). The later stages of this model represent the more typical osteoarthritic problems, with exposed subchondral bone and damaged synovium, leading to severe joint pain (Guingamp *et al.*, 1997).

1.1.4. Animal models of neuropathic pain

Neuropathic pain occurs as a result of nerve damage. This is often to peripheral nerves connecting the spinal cord to the rest of the body. Painful neuropathy can arise from various pathological changes such as metabolic disease, viral infection and traumatic injury or can be induced by chemotherapy treatment. This type of pain is a symptom often observed in patients with cancer, AIDS, diabetes and traumatic spinal cord injury (Schmader, 2002; Werhagen *et al.*, 2004). Neuropathic pain can also be caused by endothelial cell damage leading to reduced blood flow to the nerves, resulting in damage and impaired repair mechanisms. Neuropathic conditions are characterised by sensory abnormalities including allodynia, hyperalgesia and spontaneous pain. If these deficits are established in animals, then the physiopathological conditions observed in humans can be modelled.

The partial nerve ligation (PNL) model is based on the principle developed by Seltzer *et al.* (1990), where inflicting injury on a peripheral nerve results in mononeuropathic pain. This model involves the tight ligation of the sciatic nerve in the upper thigh level, just dorsal to the point at which the posterior biceps semitendosus nerve branches (Kim *et al.*, 1997). It results in cold allodynia and mechanical

hyperalgesia, where the effects are seen within one week of surgery and can persist for up to six weeks after nerve ligation (Seltzer *et al.*, 1990). The initial symptoms, occurring within one week of the surgery, can be described as sympathetically-independent pain, i.e. that which is unaffected by the sympathetic nervous system; this then develops into sympathetic-dependent pain, i.e. that which can be relieved by sympathetic block, as time goes on (Kim *et al.*, 1997). This model has been described to produce pain which is similar to that experienced in the human neuropathic conditions (Bennett, 1993).

The streptozotocin (STZ) model is a drug-induced, animal model of peripheral diabetic polyneuropathy. This is a devastating complication of diabetes ultimately leading to sensory loss (Jaggi *et al.*, 2011). Symptoms include abnormal sensations such as paresthesia, allodynia, hyperalgesia and spontaneous pain (Calcutt, 2002). This model involves injection of STZ, a pancreatic β-cell toxin (Courteix *et al.*, 1993), into the intraperitonal cavity. The toxin results in hyperalgesia and a hyper-responsibility of C fibres at two to three weeks after injection (Ahlgren *et al.*, 1993). A problem associated with this model is the development of other metabolic derangements (Jaggi *et al.*, 2011), so it is sometimes described as a model of general disability rather than just a pain model.

1.1.5. Measuring nociception

There are two states of measureable altered pain processing developing in these described animal models of pain: hyperalgesia and allodynia. Hyperalgesia is a heightened pain response to a nociceptive stimulus, resulting in increased pain sensitivity. This is characterised by a decrease in threshold or response latency, combined with an increase in the overall response magnitude. Primary hyperalgesia reflects a greater sensitivity of the peripheral nerve to the stimulus. Secondary hyperalgesia reflects changes in processing of sensory information in the CNS, it refers not directly to the site of injury but an adjacent area. Allodynia is a painful response to a non-nociceptive stimulus. This is therefore not a simple exaggeration of a response, but rather hypersensitivity. Good examples of pain-inducing stimuli for allodynia include tactile or cold sensations, which are not normally perceived as painful. This type of altered pain processing corresponds to hypersensitivity and is reflecting an activation of Aβ or low-threshold Aδ and C fibres (Sandkuhler, 2009).

Hyperalgesia is commonly measured using evoked pain responses, where a nociceptive stimulus is often applied to the hind paw. There are multiple and varied nociceptive stimuli, including heat application, however perhaps the most commonly used is mechanical stimulation (Le Bars *et al.*, 2001). This is measured using a method which was developed by Randall *et al.* (1957), involving a gradually increasing pressure being applied to the punctiform area of the hind paw which is trapped between a plane surface and a blunt point. The device measures the weight pressure applied, where the endpoint of this test is the reflex withdrawal of the paw. Mechanical hyperalgesia is commonly used for carrageenan, CFA, PNL and STZ models of pain, however in the MIA model this is not as effective as it is technically measuring secondary hyperalgesia due to direct localisation of the pain

being in the knee joint (Malfait *et al.*, 2013). Therefore a specific test for the MIA model has been developed.

Osteoarthritis, as seen in the MIA model, leads to altered joint kinematics. The gait is changed meaning the animals develop compensatory movements to minimize joint loading and pain, reflecting the patients' phenotype (Malfait *et al.*, 2013). A method has been developed and is now established, which measures static weight-bearing between the MIA-injected and the contralateral hind limbs using an incapacitance tester. This apparatus is comprised of individual force plates for each hind limb and the amount of body weight distributed between the two hind limbs is measured (Bove *et al.*, 2003). This is a more valid and useful test for pain symptoms seen within the MIA model, furthermore it is similar to a test used in clinics.

Inflammation is often associated with nociception. Both the carrageenan and the CFA models are inducers of localised inflammation, often in the paw, therefore resulting in oedema. A plethysmometer is used to test the effectiveness of anti-inflammatory agents to reduce the paw swelling. It is a piece of apparatus comprised of two tubes and measures the changes in hind paw volume by solution displacement. This is therefore not a nociceptive test, but rather an inflammation test, allowing for anti-inflammatory and anti-nociceptive effects to be correlated.

1.2. Somatostatin and its receptors

Current pain medications are either limited in efficacy to inflammatory pain conditions, or focus on treating pain centrally e.g. anticonvulsants, antidepressants and opioids. Although effective these are often associated with a variety of side effects including sedation, dizziness (Boomershine, 2010; Taylor *et al.*, 2012) and gastrointestinal problems (Grosser *et al.*, 2006; Bruno *et al.*, 2014). These limit their therapeutic use, leaving a significant proportion of patients unsatisfied. Moreover chronic pain is often a mix of pain conditions (i.e. inflammatory, nociceptive and neuropathic pain) and current analgesics have shown limited efficacy in many pain indications, meaning they are only effective in treating one type of pain condition specifically. Therefore it is important for novel, analgesic therapy to target mechanisms that can alleviate a broad pain profile without producing unwanted side effects.

Somatostatin (sst), also known as somatotropin release-inhibiting factor (SRIF) is a cyclic tetradecapeptide (Schulz *et al.*, 2000), first discovered just over 40 years ago in hypothalamic extracts (Krulich *et al.*, 1968). It was quickly characterised as a regulatory peptide, due to its ability to inhibit growth hormone secretion from anterior pituitary cells (Krulich *et al.*, 1968; Brazeau *et al.*, 1973). Somatostatin is produced by multiple cell types including neurons and neuroendocrine, immune and inflammatory cells in response to various factors such as ions, nutrients, neuropeptides, neurotransmitters, hormones, growth factors and cytokines (Patel, 1999). It is a multifunctional neuropeptide that among many roles is able to regulate exocrine secretion, modulate neurotransmitter release and control cell proliferation.

Since the discovery of somatostatin, much progress has been made towards the understanding of its biological roles within different target tissues, and its involvement in the pathology of several diseases. The peptide is widely distributed throughout the body, both in neuronal and non-neuronal tissues (Pinter *et al.*, 2006). It has therefore been ascribed important roles in both the endocrine system and the CNS (Schulz *et al.*, 2000). Somatostatin produces multiple biological effects, and its presence within the circulation allows it to exert a hormonal function, controlling various physiological and pathological conditions. Within the endocrine system somatostatin inhibits secretion of multiple hormones including growth hormone, thyroid-stimulating hormone and adrenocorticotrophic hormone. Such effects are exerted by the action of the peptide on anterior pituitary cells reached via the portal circulation (Brazeau, 1986). Somatostatin also has a role directly within the pancreas, inhibiting glucagon and insulin release (Hauge-Evans *et al.*, 2010), and is able to regulate the release of most gut hormones (Jackson *et al.*, 2011). In addition, somatostatin has a vasoprotective role within the cardiovascular system (Osadchii *et al.*, 1998).

In conjunction with this, somatostatin also has important roles within the central nervous system. It was the first peptide reported to have physiological effects on both the peripheral and central nervous systems (Brazeau, 1986). It is widely distributed within the CNS in a region-specific manner. In general somatostatin exerts inhibitory actions in the nervous system, acting as a neurotransmitter and neuromodulator, thus controlling neuronal firing (Schulz *et al.*, 2000). Somatostatin levels within the CNS affect cognitive function. Depletion of the peptide from the cortical and hippocampal regions of the brain impairs the performance of rats in response to specific behavioural tests, which led to the suggestion that somatostatin plays an important role in Alzheimer's disease (Denoble *et al.*, 1989). In addition, somatostatin levels within the nucleus accumbens influence locomotor activity of rats (Raynor *et al.*, 1993). In the peripheral nervous system, somatostatin inhibits firing of nociceptive dorsal horn and DRG neurons (Schulz *et al.*, 2000); importantly the peptide not only down-regulates nociception but also the neurogenic component of inflammation (Szolcsanyi *et al.*, 1998).

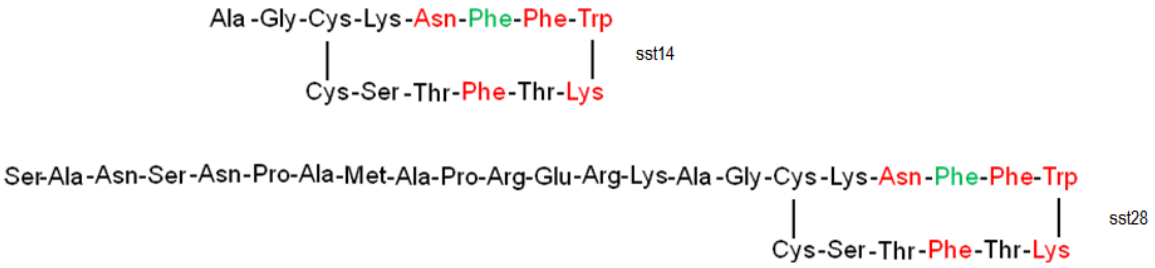

Fig. 1.2. The amino acid sequence of somatostatin. There are two biologically active forms of the cyclic neuropeptitde, somatostatin 14 and the NH_2-terminally extended somatostatin 28 molecule. The amino acids in red indicate those vital for receptor binding; while the green amino acid is important for receptor activation, specifically the sst_4 subtype.

There are two biologically-active forms of somatostatin (Fig. 1.2), each produced from a 116 amino acid precursor protein, pre-pro-somatostatin. Synthesis within cells is initiated by cleavage of the molecule by a signal peptidase. This occurs within the lumen of the endoplasmic reticulum, producing a 92 amino acid molecule pro-somatostatin (Goodman *et al.*, 1983). Further processing and cleaving results in the formation of the two biologically-active products, somatostatin 14 and somatostatin 28. The 14 amino acid cyclic peptide, somatostatin 14, was discovered first (Brazeau *et al.*, 1973). This was followed by the identification of somatostatin 28, a 28 amino acid molecule, which has a NH_2-terminal extension on the originally identified peptide (Pradayrol *et al.*, 1980). Metabolism of the larger peptide can result in the production of somatostatin 14 (Ruggere *et al.*, 1985). These peptide molecules contain specific amino acid residues which are associated with receptor binding $Asn^{5/19}$, $Phe^{7/21}$-$Lys^{9/23}$ and $Phe^{11/25}$ (Moller *et al.*, 2003); or which are specifically associated with receptor activation, for example $Phe^{6/22}$ is the important residue for activation of sst_4 (Lewis *et al.*, 2003) (Fig. 1.2). These two peptide molecules contain the vital amino acids which allow them to bind and activate the receptors, enabling the production of a diverse range of biological activities.

1.2.1. Somatostatin receptors

Somatostatin is of great interest in several research areas since it provides a powerful tool for a greater understanding of multiple pathophysiological conditions ranging from cancers to cognition. However, the role of this peptide and its receptors within nociceptive transmission is of particular interest for this thesis and therefore this area will be discussed further within this report.

Somatostatin has the ability to exert such a broad range of biological effects by associating with the five subtypes of somatostatin receptor, $sst_{1\text{-}5}$, which are widely distributed throughout the body (Pinter *et al.*, 2006). The receptors all belong to the family of G-protein coupled receptors (GPCRs) (Patel *et al.*, 1996). Within the CNS, the region-specific expression levels of the receptor subtypes were initially mapped out using autoradigraphic detection of their mRNA levels. Reubi *et al.* (1985) reported that somatostatin receptors were concentrated in the deep layers of the cerebral cortex and the large areas of the limbic system including the hippocampus, amygdaloid nucleus, medial nabenulla and the septum.

Somatostatin produces a diverse range of biological effects initiated by the binding of the peptide to the different heptahelical membrane-bound receptors (Patel *et al.*, 1996). These are G-protein linked (Sheridan *et al.*, 2000) with the common structure of seven transmembrane helices connected by short intracellular and extracellular loops. The amino N-terminus is extracellular, while the carboxyl C-terminus is intracellular (Pinter *et al.*, 2006) (Fig. 1.3). Specific somatostatin binding was first described by Schonbrunn *et al.* (1978), using the GH_4C_1 cell line derived from the rat pituitary, and confirmed a high-affinity plasma membrane receptor. Since then, five subtypes of human somatostatin receptor have been identified and characterised (Patel *et al.*, 1995). These five receptors range in size from 356 amino acids up to 391 amino acids and there is a 39 – 58% homology in sequence between the different subtypes (Patel, 1999) (Fig. 1.3). The diversity is mainly

seen in the sequence of the N- and C-terminal segments of the receptors. Further subdivision has been described for the subtype 2 somatostatin receptor in which the carboxy-terminal undergoes alternative splicing to give two isoforms sst_{2a} and sst_{2b} (Schulz *et al.*, 2000).

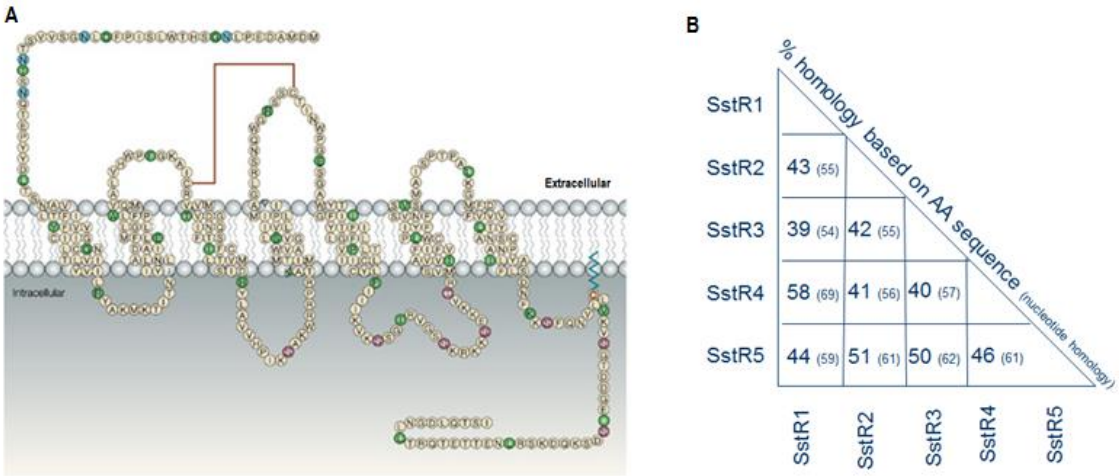

Fig. 1.3. Structure and homology of somatostatin receptors. All somatostatin receptors belong to the family of G-protein coupled receptors, with the common structure of 7 trans-membrane helices, an external N-terminus and an internal C-terminus. Somatostatin binds deep within the membrane, between domains 3 and 7. The sst_2 receptor is shown (A). The individual circles represent the different amino acids, where every tenth is indicated in green. N-linked glycosylation sites are presented by the blue circles and phosphorylation sites are in purple. The disulphide bond between extracellular loops 2 and 3 is presented by the brown line. The membrane anchor site is presented by the brown square on the intracellular C-terminus (Weckbecker *et al.*, 2003). Orthologue data showing homology of the different somatostatin receptor subtypes (B). Similarities in amino acid (AA) sequence between the different subtypes. Subtypes 2, 3 and 5; or subtypes 1 and 4 have most homology, identifying the two distinct groups of SRIF1 and SRIF2 (Pinter *et al.*, 2006).

Based on structural similarities and reactivity for somatostatin analogues, including octreotide, these five receptors have been split into two distinct groups (Patel *et al.*, 1996). The first group, known as SRIF1, consists of receptor subtypes sst_2, sst_3 and sst_5, while the second group, SRIF2, consists of subtypes sst_1 and sst_4 (Pinter *et al.*, 2006) (Fig. 1.3). All receptors possess the ability to be linked to multiple types of G-proteins, thereby interacting with several different effector systems (Sheridan *et al.*, 2000). Similarly the same intracellular pathway may be activated by different receptor subtypes expressed on the same cell (Moller *et al.*, 2003).

Much research has been conducted regarding the binding of somatostatin and its analogues to the receptor. Although it was initially speculated that these receptors have two classes of binding site (Mehler *et al.*, 1980), it is now accepted that somatostatin receptors are modulated by a single class of binding site, as proposed by Sullivan *et al.* (1987). The ligand binding pocket is believed to be located deep within the membrane between transmembrane domains 3 and 7 (Patel *et al.*, 1996). It

is thought that this pocket is lined with hydrophobic and charged amino acid residues, and that the only exofacial structure involved is the second extracellular loop (Sheridan *et al.*, 2000). These suggestions were based on the research of Kaupmann *et al.* (1995) who investigated the molecular nature of selective peptide agonist binding using the somatostatin analogue SMS 201-995 which has high affinity to sst_2 receptors and low affinity to sst_1 receptors. Site–directed mutagenesis illustrated that the important regions for ligand binding lie within the transmembrane domains.

The five somatostatin receptors provide attractive targets of treatments for multiple pathological conditions. Research is therefore on-going to find more receptor specific somatostatin analogues. These would not only allow knowledge about the precise biological effects associated with these receptors to be enhanced, but could also lead to the discovery of new therapies.

1.2.2. Somatostatin and somatostatin receptors in the pain regulatory pathway

Somatostatin and its receptors are widely distributed in both the central and peripheral nervous systems. Many tissues in the body are innervated by peptidergic sensory fibres, which are sub-divided into unmyelinated C fibres and myelinated Aβ and Aδ fibres (Pinter *et al.*, 2006). These transmit pain signals via nerve transmission to the CNS, outlining that the peripheral nervous system, including the DRG neurons are important in nociception. However central expression is also of interest with respect to the response to, and processing of, the nociceptive input.

Nociception involves the transmission of nerve impulses along primary afferent neurons, the cell bodies of which reside in the DRG neurons. These cells contain a diverse group of ligand-gated and voltage-gated ion channels, which are able to transduce noxious stimuli into depolarisations, allowing the nociceptive signals to be conducted along the neuronal axons (McCleskey *et al.*, 1999). Various GPCRs have been reported to be expressed on DRG neurons, including opioid receptors (Shaqura *et al.*, 2004), and $GABA_B$ receptors (Gao *et al.*, 2007). Activation of these receptors can influence the conductance of the DRG neurons, via interactions with the various ion channels. Somatostatin receptors are expressed in the peripheral pain-regulatory pathways, particularly the DRG neurons (Bar *et al.*, 2004).

Direct evidence for a role of somatostatin in pain processing came from the work of Rosenthal *et al.* (1989), providing the initial anatomical basis for somatostatin-induced analgesia. Both light and electron microscopy studies showed the presence of somatostatin immunoreactive structures in lamina II of the lumbar spinal cord in the rat. These structures were present in axons and dendrites, both pre- and post-synaptically. This has also been seen with immunofluorescent imaging techniques indicating the presence of somatostatin and the receptors in small neuronal cell bodies within the spinal ganglion and in fibres in the dorsal horn of the spinal cord (Hokfelt *et al.*, 1976). Interestingly somatostatin is present in different cells to those containing substance P, despite both being associated with nociception. Since these initial findings, the release of somatostatin and distribution of its receptors within the nervous system have been further studied in order to confirm expression in structures that are functionally involved with processing of pain transmission.

The distribution of receptors within lumbar DRG neurons (L1 – L5) has been established using PCR techniques; mRNA for subtypes 1, 2a, 2b and 4 receptors were detected and localisation of these receptor subtypes was confirmed using immunohistochemical techniques. It was seen that 81% of the cell bodies expressed the sst_{2a} receptor, and 79% the sst_{2b} receptor; moreover 45% of cell bodies showed sst_4 receptor-like immunoreactivity (Bar *et al.*, 2004) (Fig. 1.4). A high proportion of other neuronal profiles also showed somatostatin receptor 4 like immunoreactivity, with most intense staining in axons at their connection to the cell body, but also at perinuclear regions and some satellite cells (Bar *et al.*, 2004). It is likely that the receptors are present on a non-peptidergic subpopulation of neurons, as a significant proportion of DRG neurons, of both large- and small- sized cell bodies, expressed receptor subtypes 2a and 2b; which was seen specifically on isolectin B 4 positive neurons (Carlton *et al.*, 2001b). Furthermore, small and medium DRG neurons, which positively express the transient receptor potential vanilloid 1 (TRPV1) channel, have been reported to co-express the somatostatin receptors (Carlton *et al.*, 2004). TRPV1 expressing neurons often also express transient receptor potential ankyrin 1 (TRPA1) channels (Story *et al.*, 2003), suggesting potential co-expression of the somatostatin receptors with this channel family also.

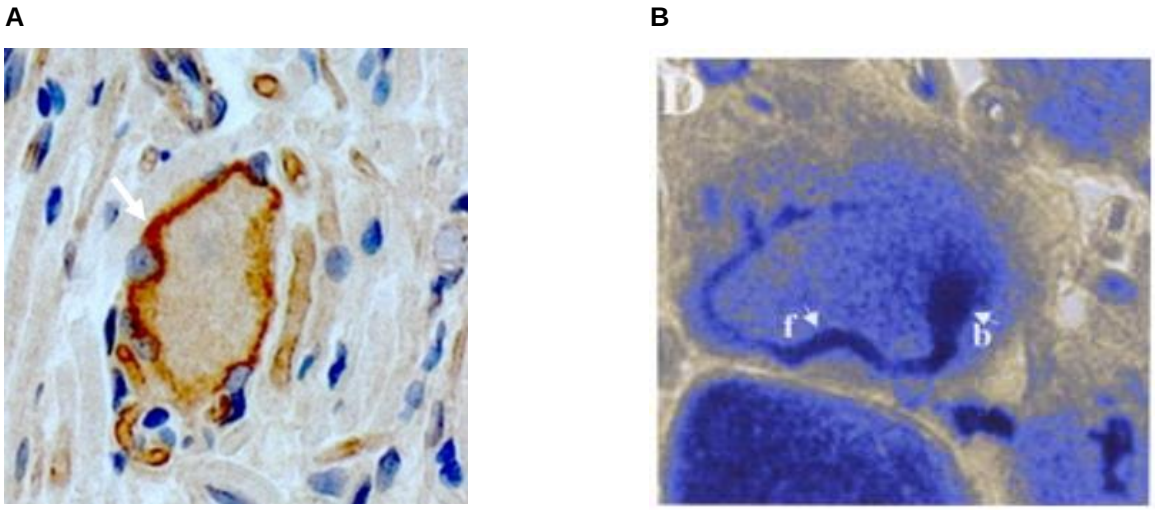

Fig. 1.4. Expression of the sst_4 receptor on DRG neurons. Bar *et al.* (2004) reported that the sst_4 receptor subtype is expressed on 30 – 50% of lumbar DRG neurons and in-house data is consistent with this. The image in (A), obtained in-house (Strierstorfer, unpublished), shows cryosections of DRG neurons at magnification 400x; white arrow shows expression. The published image in (B) Bar *et al.* (2004) show sst_4 receptor immunostaining of neurons at magnification 820x; b shows the origin of the axons, while f shows the course of the labelled axons.

Somatostatin release from rat DRG neurons has been confirmed using lithium-labelled somatostatin. The results showed that this neuropeptide is released from 15% of small DRG neurons, with the highest levels being observed in the lumbar region of the spinal cord (Lawson, 1995). Somatostatin is also produced by fine cutaneous sensory axons, where 35% of small-diameter neurons released the peptide. The release of somatostatin has been recorded from both unmyelinated and myelinated neurons, however a larger proportion was from the C fibres (Carlton *et al.*, 2003). These observations

confirm that there is a peripheral source of somatostatin, indicating that it is a potential candidate for endogenous modulation of nociception.

The emotional response to pain and the processing of nociceptive input is under the control of higher brain centres. Somatostatin and its receptors also have extensive expression profiles within the central nervous system. The hypothalamus appears to be the major site of somatostatin production and activity via activation of receptor subtypes 1-4, which are expressed in this region (Kumar, 2007). Using immunohistochemical and immunocytochemical techniques, subtype-specific receptor antibodies allowed the precise location of the receptors to be established. Somatostatin receptors 1, 2, 3 and 4 are present mainly within the forebrain regions, including the cerebral cortex, structures within the limbic system and the striatum. In contrast the sst_5 receptor is only sparsely distributed in the striatum with, overall, much lower expression levels in comparison to the other receptor subtypes (Stroh *et al.*, 1999).

The distributional patterns of the somatostatin receptors both within the central and peripheral nervous system, and the co-localization with the neuropeptide itself, provides strong evidence to suggest it may have important roles in nociceptive processing.

1.2.3. The effects of somatostatin on nociception

Several recent studies have shown that somatostatin and its receptors have an important role in nociception. There is evidence confirming that endogenously produced somatostatin results in anti-nociception and that central release of somatostatin results in analgesia via the inhibition of spinal nociceptive neurons. Somatostatin was administered via microinjections into the medullary nucleus raphe magnus and the periaqueductal grey matter of anaesthetised cats. *In vivo* electrophysiological studies revealed inhibition of heat-evoked responses, suggesting that centrally produced somatostatin can activate descending sensory neurons involved in pain transmission (Helmchen *et al.*, 1995). Similarly, somatostatin microinjected into the caudate putamen of rats resulted in a significant increase in pain threshold. Mechanical hyperalgaesia was tested using the method described by Randall *et al.* (1957), where increasing pressure was applied to the paw of the animal. Even at the lowest doses a significant analgesic effect was recorded (Tashev *et al.*, 2001), confirming central release induces analgesic effects.

Since there is a direct link between central somatostatin release and receptor activation leading to analgesia based on *in vivo* data, somatostatin has been proposed to be a useful treatment for multiple human pain states, including post-operative relief, cancer pain and inflammatory conditions (Chrubasik *et al.*, 1985). In an early clinical trial, patients having undergone abdominal surgery obtained complete relief from post-operative pain after epidural injections of somatostatin, followed by infusion. In two patients somatostatin even provided adequate analgesia for use intra-operatively (Chrubasik *et al.*, 1985). This has subsequently been confirmed in a more recent clinical trial, suggesting that somatostatin analogues could be beneficial for post-operative analgesia in patients who have adverse effects to opioids (Dahaba *et al.*, 2009). Furthermore, Mollenholt *et al.* (1994)

treated patients with terminal cancer using an intrathecal and epidural administration of somatostatin over an 11 day period and found somatostatin to provide effective pain relief. In osteoarthritic patients, somatostatin injected intra-articularly into the knee over a 4-week period, resulted in significant improvement in joint pain and function. Improvements were seen both at rest and during movement, furthermore the flex angle of the knee was significantly increased (Silveri *et al.*, 1994). Somatostatin is also a useful treatment for pain conditions associated with the inflammatory response. This has been established pre-clinically using *in vivo* models. Using carrageenan, inflammation was induced in rats, and nociceptive effects were determined. Various intraplantary injections of somatostatin were given, resulting in significant decreases in acute pain caused from inflammation (Corsi *et al.*, 1997).

The anti-nociceptive effect of endogenous somatostatin has been compared with that of morphine. Electrophysiological recordings were made from neurons from the lamina I-IV of cats. Stimuli included innocuous mechanical and radiant heat application to glabrous skin of the hind paw. The ability of somatostatin to depress these nociceptive responses by a direct, spinal site of action was quantitively and qualitatively similar to that of morphine (Chrubasik *et al.*, 1984; Sandkuhler *et al.*, 1990). Spinal anti-nociceptive effects were also found in an early study conducted on anaesthetised cats which confirmed the release of somatostatin from dorsal horn neurons in response to nociceptive stimuli and found that somatostatin release was significantly increased by noxious thermal stimulation (Morton *et al.*, 1989).

The therapeutic value of endogenous somatostatin is limited by its broad range of effects mediated by the different receptor subtypes and its short plasma half-life of around three minutes (ten Bokum *et al.*, 1999). This has led to the development of receptor specific and non-specific analogues of the somatostatin peptide. Pharmacological manipulation using such analogues provides further confirmation that this peptide produces analgesic effects.

There are various lines of evidence that suggest that somatostatin is important in nociceptive processing based on observations where the somatostatin receptors are activated by analogues. Such effects include inhibition of nociceptive behaviour (Helyes *et al.*, 2000) and inhibition of dorsal horn neuronal activity (Sandkuhler *et al.*, 1990). Furthermore, in humans various effects using analogues have been reported. Headache or migraine relief, defined as a reduction in severity, was investigated in patients receiving a subcutaneous injection of a somatostatin analogue. The analogue provided significant relief and some patients even became pain free (Kapicioglu *et al.*, 1997). Somatostatin receptor agonists were also effective in patients who were no longer responding to opioids (Paice *et al.*, 1996). This is supported by various *in vivo* studies.

The somatostatin analogue RC-160 induced anti-nociceptive effects. This was measured using the hot plate technique in mice and the tail-flick technique in rats. Significant results lasted up to 12 hours in the rat and 24 hours in the mice (Eschalier *et al.*, 1991). Sandostatin is another stable analogue of somatostatin. Experiments were conducted on rats which had been subcutaneously administered

formalin as a model of long-term nociceptive effects. Intrathecal pre-treatment of sandostatin caused a dose-dependent inhibition of both the first and second phases of the formalin response, confirming that activation of the somatostatin receptors inhibits nociceptive behaviour (Chapman *et al.*, 1992). Capsaicin is a TPRV1 agonist which can be used experimentally to induce nociception. Intra-peritoneal and plantar injection of SCR007, a non-peptide somatostatin analogue, significantly reduced the capsaicin and formalin-induced flinching, lifting and licking nociceptive behaviours in rats (Ji *et al.*, 2006). Moreover, somatostatin antiserum causes increased nociceptive behaviours, which can be blocked with the use of somatostatin analogues (Carlton *et al.*, 2001b).

Antagonists acting at somatostatin receptors enhance the transmission of pain signals. The somatostatin analogue cyclosomatostatin is a well-characterised somatostatin antagonist with affinity for all receptor subtypes. Cyclosomatostatin administration results in increased responses of primary afferents to noxious joint movement in normal knees, confirming that the neuropeptide somatostatin is involved in the sensitivity of primary afferent neurons (Heppelmann *et al.*, 1999). Furthermore, capsaicin-induced nociception was increased in the presence of cyclosomatostatin, whereas the effects were reversed after application of a somatostatin analogue or agonist (Carlton *et al.*, 2003). Nociceptive behavioural studies on formalin-injected animals were significantly increased after intraplantar application of cyclosomatostatin (Carlton *et al.*, 2001b).

Pain transmission pathways involve the activity of dorsal horn neurons, including Aδ fibres and C fibres. Somatostatin and its analogues inhibit these nociceptive transmissions. In various electrophysiological experiments on C-fibres, the somatostatin analogues octreotide and SCR007 were shown to decrease responses to both thermal stimulation and bradykinin-induced excitation. Both effects were reversed by cyclosomatostatin (Carlton *et al.*, 2001a). Moreover, SCR007 was reported to reduce thermal and bradykinin excitation in a dose dependent manner in recordings from glabrous skin-nerve preparations. Again cyclosomatostatin was reported to reverse such effects (Ji *et al.*, 2006).

These data provide good evidence that somatostatin plays an important role in nociception. It not only reduces multiple human pain states, with analgesic effects in different *in vivo* models, but also directly reduces nerve transmission of sensory nociceptive neurons.

1.2.4. Impact of somatostatin 4 receptors on pain transmission

Both the sst_2 and sst_4 receptors are expressed in the pain processing pathway and are thought to be responsible for the analgesic properties associated with somatostatin (Ji *et al.*, 2006). However there are multiple side-effects associated with activation of the sst_2 receptor subtype. For example it is known that somatostatin inhibits the release of growth hormone. Using pharmacological manipulation with both specific agonists (Parmar *et al.*, 1999) and antagonists (Tulipano *et al.*, 2002), the inhibition of growth hormone was shown to be predominantly regulated by the sst_2 and sst_5 receptor subtypes. Stimulation of glucagon secretion also occurs by activation of the sst_2 receptor subtype (Cejvan *et al.*, 2003). The expression profile of the sst_4 receptor means there are fewer unwanted side effects

associated with its activation. Furthermore, pharmacological data (Helyes *et al.*, 2006), as well as knock-out animal studies (Helyes *et al.*, 2009) identify the somatostatin 4 receptor a potential target for novel analgesic drugs.

Although there are multiple agonists which target specific subtypes of the somatostatin receptors, there are few sst_4-selective ligands. Due to both the clinical and research advantages of developing an sst_4 agonist, much work has been and is currently being conducted to develop such compounds. In binding studies, TT-232, a heptapeptide agonist with a cyclopenta ring structure, appeared to have selective affinity for the sst_4 receptor (Pinter *et al.*, 2002). *In vivo* studies found that TT-232, but not octreotide (a sst_2 selective agonist), given intravenously, produced anti-nociceptive effects which were induced by administration of capsaicin (Helyes *et al.*, 2000). This is giving the first indication that the analgesic effects are indeed mediated through the sst_4 receptor. TT-232 has been tested on mice using the phenylquinone-evoked abdominal construction test, and in rats using formalin-induced nociception, both of which were inhibited after the administration of TT-232 (Szolcsanyi *et al.*, 2004). Similarly when hot plate tests were conducted on rats, TT-232 caused an elevation in noxious heat threshold (Szolcsanyi *et al.*, 2004). This sst_4 specific compound is also an effective treatment for mechanical hyperalgesia in both arthritic models (Helyes *et al.*, 2004), and diabetic neuropathy models (Szolcsanyi *et al.*, 2004), again indicating that the sst_4 receptor is indeed involved in nociception.

Another compound that is highly selective for the sst_4 receptor is J-2156. This is a sulfonamido-peptidomimetic compound, which has nanomolar (nM) affinity for the subtype 4 receptor established using binding studies (Engstrom *et al.*, 2005). A minimal selectivity of 400 fold for the sst_4 receptor was seen relative to its binding to the other subtypes. Moreover this compound was shown to have high affinity for the sst_4 receptor over other G-protein coupled receptors (Engstrom *et al.*, 2005). This agonist has been tested in *in vivo* studies; mechanical allodynia is significantly reduced both in arthritic rat models, and in neuropathic models induced by static nerve ligation (Sandor *et al.*, 2006). Multiple anti-inflammatory effects have also been seen in rodents following treatment with J-2156 (Helyes *et al.*, 2006).

The pharmacological data for sst_4 receptor agonists is further supported by animal knock-out studies. Somatostatin receptor subtype 4 gene-deleted mice were tested for various nociceptive and inflammatory responses. These included inflammatory pain in adjuvant-evoked arthritis, carrageen-induced paw oedema, mechanical hyperalgesia and oxazolone-induced hyperalgesia. Mice lacking the sst_4 receptor produced increased inflammatory and nociceptive responses, suggesting impaired defence mechanisms (Helyes *et al.*, 2009), and indicating a vital role for sst_4 in nociceptive responses.

These data support the conclusion that sst_4 receptor is associated with the analgesic effects of somatostatin, meaning this receptor subtype is an attractive target for novel anti-nociceptive compounds. Collectively, anti-nociceptive effects of somatostatin can be attributed to activation of

the sst_4 receptor subtype. The lack of unwanted side-effects means it provides an appropriate target for analgesic therapies.

1.3. G-protein Coupled Receptors (GPCRs) in pain transmission

Receptors are protein macromolecules on or in cells, which act as recognition sites for endogenous ligands. Many drugs used in medicines target these endogenous receptors, either by producing the same response or preventing the action of the endogenous ligand. A specific receptor example is the GPCR, which are present on cell membranes and respond in seconds to stimulation. Signal transduction occurs by the activation of different G-proteins. There are three main types of G-proteins: $G_{\alpha q}$, which is linked to the activation of phospholipase C and $G_{\alpha s}$ and $G_{\alpha i}$, which are linked to the adenylyl cyclase pathway. $G_{\alpha s}$ G-proteins increase cAMP production, while $G_{\alpha i}$ G-proteins inhibit cAMP production. The G-proteins are comprised of three subunits, α, β and γ, which are all involved in modulating effects of receptor activation.

GPCRs have the potential to activate multiple downstream pathways. Binding of an agonist to the GPCR causes a conformational change, resulting in GDP present on the $G\alpha$ subunit being exchanged for GTP. This exchange allows the dissociation of the $G_{\beta\gamma}$ subunit. These subunits can then mediate various physiological actions by interacting with numerous effectors. The effects are terminated by hydrolysis of the GTP, resulting in reuniting of the free $G_{\beta\gamma}$ subunit to the G_α subunit.

Many of the current, well-established pain treatments do, in fact, target GPCRs. Some examples include: opioid receptors (Vanderah, 2010), cannabinoid receptors (Manzanares *et al.*, 2006), serotonin receptors (Marks *et al.*, 2009), metabotropic glutamate receptors (Palazzo *et al.*, 2014), dopamine receptors (Wood, 2008) and adenosine receptors (Zylka, 2011).

A disadvantage of targeting GPCRs is that they are prone to desensitisation. This can be as a result of un-coupling of G-proteins and degradation. All somatostatin receptor subtypes, *except* sst_4, display acute desensitisation (Hukovic *et al.*, 1996), favouring this subtype as an appropriate drug target. Furthermore sst_4, like sst_1, is not readily internalised, whereas the other three subtypes are subject to rapid and marked internalisation (Schreff *et al.*, 2000). For example, exposure to somatostatin 14 resulted in progressive loss of cell-surface sst_2 receptors but not sst_4 receptors (Schreff *et al.*, 2000). This is an important consideration for the development of novel drugs, as the potency needs to remain constant in order for beneficial clinical effects to be produced and lack of analgesic tolerance to develop.

GPCRs have the ability to modulate the activity of a variety of ligand-gated and voltage-sensitive ion channels (McCleskey *et al.*, 1999) (

Fig. 1.5). This enables neurons to adjust their sensitivity in response to activation of a peripheral target (Stone *et al.*, 2009). Examples of ion channels regulated by GPCRs include G protein-gated inwardly-rectifying potassium channel (GIRK), voltage sensitive calcium channels (Ca_v), transient

receptor potential (TRP) channels and voltage sensitive sodium channels (Na_v); all of which would be relevant targets for nociceptive treatment.

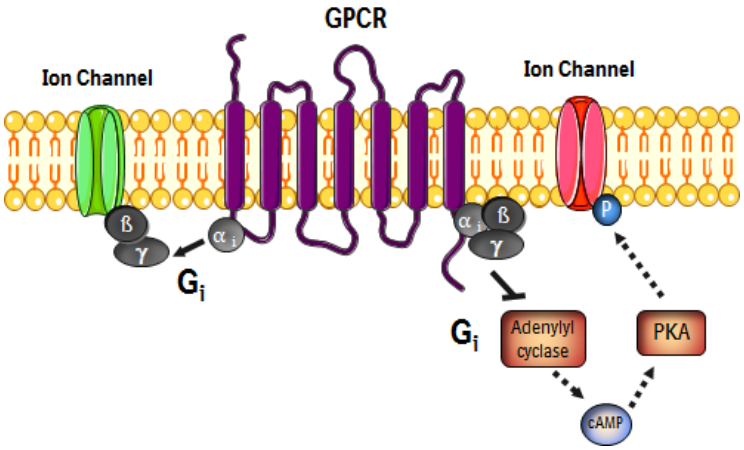

Fig. 1.5. G protein-coupled receptors (GPCRs) modulation of ion channel activity. Binding of an agonist to a GPCRs activates intracellular pathways controlled by the G-protein subunits. Modulation of ion channel activity can be induced by direct binding on the βγ subunit, or by inhibition of the intracellular adenylyl cyclase pathway.

1.3.1. G-protein gated inward rectifying potassium channels

G-protein gated inwardly-rectifying potassium (GIRK) channels belong to the super-family of proteins known as inwardly-rectifying potassium channels (Luscher *et al.*, 2010). To date five GIRK α-subunits have been identified (GIRK1-GIRK5), of which GIRK1-4 have been reported to be expressed in mammalian tissue (Koyrakh *et al.*, 2005).

GIRK channels are composed of four units, each of which consists of two membrane-spanning α helical regions connected by an extracellular membrane-dipping loop, which has the common amino acid sequence GYG and forms the potassium selectivity filter. These units surround a water-filled pore, allowing the movement of potassium ions across the cell membrane. Both the carboxyl and the amino terminus of the protein are intracellular, allowing interaction with molecules present within the cell cytoplasm. The channels are expressed in excitable cells, including the spinal dorsal horn (Walsh, 2011) and DRG neurons, where based on mRNA content GIRK1-4 subunits are present (Gao *et al.*, 2007). These can combine to form either heterotetrameric or homotetrameric proteins (Luscher *et al.*, 2010).

Functionally, the GIRK channels are responsible for maintaining and stabilising the resting membrane potential close to the potassium equilibrium potential (Walsh, 2011). Under basal conditions these channels exhibit low open-state probability (Sadja *et al.*, 2003); their activity is controlled via GPCRs, specifically those comprising of pertussis toxin sensitive $G_{\alpha i}$ G proteins (Luscher *et al.*, 2010). The Gβγ dimers are able to bind directly to the GIRK channels, resulting in activation and opening (Inanobe *et al.*, 1995).

Activation of GIRK channels allows the movement of potassium ions down their electrochemical gradient. This movement of charged ions results in hyperpolarisation of the cell membrane (Luscher

et al., 2010); which inhibits the activation of various voltage dependent Na^+ and Ca^{2+} channels, thus reducing spontaneous action potential formation and inhibiting the release of neurotransmitter (Walsh, 2011). Such effects present the GIRK channel as a good target for excessive cell excitability (Bhave *et al.*, 2010).

Activation of the opioid receptor and the adrenoceptor by compounds such as morphine or clonidine, respectively, results in analgesia which is mediated in part via the GIRK channel activation (Mitrovic *et al.*, 2003). Similarly GIRK1 and GIRK2 knock-out mice exhibit a hyperalgesic behavioural phenotype (Bhave *et al.*, 2010). A specific example of such a knock-out animal is the weaver mutant mouse. This has a mis-sense point mutation in the pore forming region of the GIRK2 subunits (Patil *et al.*, 1995), which reduces coupling to the G-protein and a loss of potassium selectivity. Such mice show significantly reduced analgesia, when treated with morphine, in comparison to wild type mice (Ikeda *et al.*, 2000).

1.3.2. Voltage sensitive calcium channels

Voltage sensitive calcium channels (Ca_v) belong to a family of large multi-protein complexes (Catterall, 2000). To date five subtypes of calcium channels have been identified and are expressed in mammals. These can be subdivided dependent on activation threshold, where L-, N-, P/Q- and R are triggered by strong depolarisations, while T-types are triggered by milder depolarisations (Gribkoff, 2006).

Ca_v channels are formed from a α1-subunit composed of a tetramer of pore-forming domains, each with six α helical transmembrane regions, intracellular carboxyl and amino termini. The selectivity filter is present between transmembrane domains five and six. This α1 subunit is often associated with other auxiliary units including α2, δ, β and γ units. These channels are expressed in all excitable cells, including DRG neurons (Catterall, 2000). Although these are voltage-sensitive, the activity of Ca_v channels can be influenced by GPCR activation. This is either by indirect mechanisms due to $G_{\alpha i}$ inhibition of cAMP production and protein kinase A (PKA) activation, therefore altering phosphorylation and channel trafficking, or directly by the Gβγ dimers binding to the α1 subunit of the channel (Dolphin, 2003).

The main role of these channels involves the transduction of electric activity into biochemical signals (Catterall, 2000). Depolarisation of the cell membrane results in activation of Ca_v channels, causing an influx of calcium ions. As calcium is an important secondary messenger, this allows for the regulation of numerous physiological processes including neuronal excitability and plasticity and the release on neurotransmitters and peptides (Gribkoff, 2006). Furthermore, Ca_v channels affect the excitability of neurons. Inhibition of the channels slows the rate of cell depolarisation, therefore ultimately reducing nerve transmission (Gribkoff, 2006).

Inhibition of Ca_v channels has been implicated in the mechanism underlying the anti-nociception produced by established analgesic compounds. Activation of opioid and cannabinoid 1 (CB1)

receptors, by morphine and CP55,940 respectively, inhibits calcium channel activity. All subtypes of Ca_v channels are inhibited by morphine, however CP55,940 only inhibits N-type (Khasabova *et al.*, 2004). Similarly knock-down of T-type Ca_v channels in DRG neurons resulted in attenuated nociceptive responses after nerve injury (Bourinet *et al.*, 2005). Furthermore, compounds acting directly on the channels, including gabapentine (Wheeler, 2002), can also induce analgesic effects.

1.3.3. Transient receptor potential channels

Transient receptor potential (TRP) channels are a superfamily of ion channels originally identified in *Drosophila melanogaster* where they have a defined role in phototransduction. The trp locus was first identified in 1969 (Cosens *et al.*, 1969). It was later characterised as an ion channel in 1989 (Montell *et al.*, 1989). TRP channels represent a diverse group of cation channels with more than thirty different channels. This group is divided into seven subfamilies, TRPC (canonical), TRPV (vanilloid), TRPM (melastatin), TRPN (no mechanoreceptor potential), TRPP (polycystin), TRPML (mucolipin) and TRPA (ankyrin) (Minke, 2010). Two of the subfamilies involved in pain states are the transient receptor potential vanilloid (TRPV) channels and the transient receptor potential ankyrin (TRPA) channels. In the TRPV subfamily there are six distinct members, which are split into four subtypes, some of which obligate as heteromultimers: TRPV1/2, TRPV3, TRPV4 and TRPV5/6. There is only one member of the TRPA family present in mammals, TRPA1, although four more have been identified in *Drosophila* (Pedersen *et al.*, 2005).

TRP channels are all non-selective cation channels, comprising of four α-subunits, each with the common structure of six α helical transmembrane domains, a pore forming region between transmembrane domains five and six, and intracellular carboxyl and amino termini (Caterina *et al.*, 1997; Cvetkov *et al.*, 2011). Although the channels can be activated by various stimuli they are subject to modulation by GPCRs. Activation of $G_{\alpha i}$ proteins, which ultimately reduces activation of PKA (Mohapatra *et al.*, 2003), prevents channel sensitisation (Law *et al.*, 2000); meaning the threshold required for channel activation remains high, so inhibition occurs.

TRPV1 channels are activated by many different stimuli including mechanical, chemical, thermal and pH changes (Caterina *et al.*, 1997). They were originally named vanilloid receptor 1 channels due to the ability of vanilloid moiety-containing compounds, including capsaicin, to activate them. Capsaicin evokes painful burning via activation of TRPV1 channels, suggesting an important role of this channel in nociception. These channels are predominantly expressed in nociceptive sensory neurons (Caterina *et al.*, 1997), where they have essential roles in the detection and modulation of painful stimuli. Activation of these channels allows the movement of calcium and sodium ions into the cell and potassium ions out of the cell, resulting in an inward depolarising current. This causes cell excitation, triggering action potential propagation and transmission of pain signals (Davis *et al.*, 2000).

Activation of mu-opioid receptors by morphine, a commonly used analgesia, results in inhibition of TRPV1 currents (Endres-Becker *et al.*, 2007). However, direct inhibition using capsazepine a

competitive antagonist of TRPV1 channels (Bevan *et al.*, 1992) is also known to be beneficial. Capsazepine inhibits nocifensive and hyperalgesic responses to capsaicin and other inflammatory agents by directly binding to the channel, therefore offering analgesia via blockage of TRPV1-mediated signals (Rami *et al.*, 2004). Supporting this, TRPV1 knock-out mice showed no response to vanilloid-induced pain, a reduced response to acidification and a greatly reduced response to noxious heat (Caterina *et al.*, 2000).

TRPA1 receptors are so named due to the fourteen ankyrin repeats on the N-terminus region of the receptor (Cvetkov *et al.*, 2011). These channels are activated by a number of pungent chemicals including allyl isothiocynate (AITC) present in mustard oil (Jordt *et al.*, 2004), diallyl thiosulfinate present in garlic and cinnamaldehyde present in cinnamon (Bautista *et al.*, 2006), all of which are known to cause painful sensations. TRPA1 channels have limited expression profiles, but are predominantly expressed in nociceptive sensory neurons (Story *et al.*, 2003), where they modulate pain transmission in a similar manner to TRPV1 channels. The channels are particularly permeable to calcium ions (Kim *et al.*, 2007), and therefore the role of this ion as an important secondary messenger (Gribkoff, 2006) is of importance.

Pharmacological data using selective antagonists confirm that inhibition of TRPA1 channels results in analgesic effects. HC-030031, a selective TRPA1 antagonist, is able to reduce chemically-induced nocifensive behaviour, as well as significantly reverting mechanical hyperalgesia in the CFA inflammatory arthritic pain model (Eid *et al.*, 2008). Another TRPA1 selective antagonist, A-967079, exhibits analgesic efficacy in AITC induced nocifensive behaviour, as well as attenuating cold allodynia in various pain model conditions (Chen *et al.*, 2011). Supporting this, TRPA1 knock-down mice have reduced CFA induced cold hyperalgesia, without loss of acute noxious cold sensation (del Camino *et al.*, 2010).

1.3.4. Voltage sensitive sodium channels

Voltage sensitive sodium channels (Na_v) are a large family of ion channels the function of which is mainly defined by the pore forming α subunit. The α-subunit is composed of four domains each with six α helical transmembrane regions. Within the α-subunit there is a selectivity filter between transmembrane domains five and six, where both the carboxyl and amino termini are intracellular. To date there are nine subtypes of sodium channels which have been identified and are named numerically ($Na_v1.1$ – $Na_v1.9$) (Yu *et al.*, 2003). Na_v channels are split into two distinct pharmacological groups dependent on whether or not they are sensitive to inhibition by teterodotoxin (TTX). The first α subunit from the tetramer has a large extracellular loop which defines TTX sensitivity (Catterall *et al.*, 2005). There are two TTX sensitive channels, $Na_v1.3$ and $Na_v1.7$, and two TTX resistant channels, $Na_v1.8$ and $Na_v1.9$, which are present in DRG neurons (Akopian *et al.*, 1996). The Na_v channels are often associated with β subunits. These are expressed throughout the body, but also specifically in DRGs (Yu *et al.*, 2003). Activity of Na_v channels can be influenced by GPCR activation, despite typically being activated by voltage-stimulations. The $G\beta\gamma$ dimers from GPCRs

are able to directly bind to the channel; or activity can be modulated via indirect mechanisms ultimately altering phosphorylation and channel trafficking (McCleskey *et al.*, 1999).

These channels have a functional role in DRG electrogenesis (Rush *et al.*, 2007). The excitability of nociceptors is initiated by sodium channels generating action potentials and thereby transmitting nerve impulses by repetitive firing. Action potential generation requires both initiation and overshooting, which both occur mainly due to activation and rapid inactivation of specific sodium channels in conjunction with sodium clearance by sodium/potassium ATPase. This change in membrane potential induces depolarisation of neighbouring nerve tissue, again inducing activation of Na_v channels and therefore action potential generation, ultimately resulting in propagation of nerve signals via repetitive firing. Na_v channels therefore contribute to hyper excitability due to the excitation of nociceptors, contributing to both initiation and transmission of pain signals (Swayne *et al.*, 2008).

Indeed several sodium channel blockers have been shown to be beneficial for the treatment of pain due to their ability to reduce excitability of peripheral nerves (Tanelian *et al.*, 1991). This is seen with TTX-sensitive channels, where low doses of TTX reduced both mechanical hyperalgesia and allodynia in neuropathic pain models (Lyu *et al.*, 2000). However it is also true for TTX-resistant channels, where a $Na_v1.8$ selective compound A-803467 reduced mechanical allodynia in all types of pain models tested (Jarvis *et al.*, 2007). Furthermore, DRG-specific $Na_v1.7$ knock-out mice, which have normal expression of $Na_v1.8$, have weakened thermal hyperalgesia but little modulation of mechanical allodynia and hyperalgesia (Nassar *et al.*, 2004). Knock-out models for TTX-resistant channels also show analgesic traits. A $Na_v1.8$ knock-out mouse had pronounced analgesia to mechanical stimuli (Akopian *et al.*, 1996), as well as a $Na_v1.9$ knock-out mouse had decreased hypersensitivity to inflammatory mediators (Priest *et al.*, 2005).

1.3.5. Other ion channels involved in pain transmission

There are other channels which are involved in nociceptive transmission and can be modulated by GPCRs. These include ATP-gated P2X channels and acid-sensing ion channels (ASIC). These channels are both known to be involved in pain transmission and are expressed in nociceptive neurons (Molliver *et al.*, 2005; Wang *et al.*, 2007). These therefore would be appropriate areas of research for specific interests in pain mechanisms and analgesics. However, since these are modulated by $G_{\alpha s}$ coupled GPCRs via the protein kinase C (PKC) pathway (Deval *et al.*, 2004; Wang *et al.*, 2007), and therefore would not be influenced by sst_4 receptor ($G_{\alpha i}$) activation, they are not be considered further in this thesis.

1.3.6. Inflammatory mediators

Increased pain sensitivity (hyperalgesia and allodynia) is one of the most common debilitating symptoms of inflammatory disorders. It involves a variety of interacting humoural inflammatory mediators such as cytokines, chemokines and prostaglandins. These mediate both nervous and neuroendocrine responses, which are intimately associated with the initiation of inflammatory pain,

resulting in sensitisation of neurons i.e. reduced thresholds. Neuronal injury results in the production of these inflammatory mediators by microglia and astrocytes (Scarborough, 1990). Modulation of cytokine levels by GPCRs can therefore influence nociception (Madera-Salcedo *et al.*, 2013).

Cytokines are water soluble, extracellular signalling proteins ranging between 8 and 30 kDa. They provide a means of communication between the immune system and the nervous system, where functionally they mediate the activation of the inflammatory response. There are various types of cytokines including interleukins, tumour necrosis factors and interferons, which can be either pro-inflammatory or anti-inflammatory. Some important examples which have been implicated in nociception and are investigated in this thesis, include interleukin 1 (IL1), interleukin 6 (IL6), tumour necrosis factor α (TNFα) and interferon γ (IFNγ).

There are two forms of IL1: the α subtype (IL1α) and the β subtype (IL1β), which are formed from two independent genes. The cytokines act on two receptor subtypes (IL-RI and IL-RII), the biologically-active receptor is IL-RI. IL-RII acts as a decoy receptor to control excess levels of IL1 by blocking the binding to the active IL-RI receptor (Sims *et al.*, 1994). IL1 is produced by activated macrophages and other inflammatory cells and is released in response to trauma or inflammation. This cytokine is a potent hyperalgesic agent. IL1β, which is three thousand times more potent than IL1α (Ferreira *et al.*, 1988), induces both mechanical and thermal hyperalgesia (Maier *et al.*, 1993) as well as enhancing the response of wide dynamic range (WDR) neurons (Oka *et al.*, 1993). Furthermore, antagonizing the IL-RI, using an antibody against the receptor, results in reduced thermal hyperalgesia and mechanical allodynia in a mouse model of neuropathic pain (Sommer *et al.*, 1999).

IL6 is a secreted glycoprotein and is an example of a prototypic pleiotropic cytokine. It is produced by astrocytes and macrophages, and is up-regulated in disease states with pain symptoms (Arruda *et al.*, 1998). As with other cytokines, IL6 is a potent inducer of hyperalgesic states, particularly thermal hyperalgesia in rats (Oka *et al.*, 1995).

TNFα is a pleiotropic pro-inflammatory cytokine, the mRNA of which is present in normal and lesioned peripheral nerves. It is produced and secreted by monocyte cells for example macrophages. TNFα is an inducer of different states of altered pain processing, including mechanical hyperalgesia in the carrageenan rat model of inflammatory pain (Cunha *et al.*, 1992). This cytokine also increases sensitivity of DRG neurons (Liu *et al.*, 2002). Furthermore, in a neuropathic mouse model when effects of TNFα were inhibited, using specific neutralizing antibodies, both thermal hyperalgesia and mechanical allodynia were reduced (Lindenlaub *et al.*, 2000).

Interferons are glycoproteins released in response to injury from T-cells. There are three main forms of interferons: alpha, beta and gamma. These act on the two receptor subtypes, associating with different signalling pathways. IFNα and IFNβ act on type I receptors. The function of these is not fully understood, although it is thought to be associated with the anti-viral effects associated with

interferons (Taniguchi *et al.*, 2002). The type II receptor is activated by IFNγ and is associated with inflammatory mediation. IFNγ induces pain hypersensitivity (Robertson *et al.*, 1997) as well as increasing spontaneous firing of the dorsal horn (Vikman *et al.*, 2005).

Chemokines are small signalling proteins produced by cells of the immune system that act as chemical messengers attracting activated immune cells to the source of injury. These can be classified into four groups dependent on the position of key cysteine residues, giving C, CC, CXC and CX3C motives (Bajetto *et al.*, 2001). An important example is the monocyte chemoattractant protein 1 (MCP1). This is a highly inducible, CC motif, inflammatory chemokine, known to be a potent chemoattractant of monocytes, activated T cells, natural killer cells and eosinophils. MCP1 acts on CC motif chemokine receptor 2 (CCR2) receptors and contributes to elements of both inflammatory and chronic pain states (White *et al.*, 2007), being a potent inducer of mechanical hyperalgesia in rats (Bogen *et al.*, 2009). Furthermore, inhibition of MCP1 activity by a CCR2/CCR5 receptor antagonist, can reduce both formalin-induced and carrageenan-induced pain reactions (Okamoto *et al.*, 2013).

Prostaglandins are a group of hormone-like fatty acid substances, which contribute to biological functions including inflammation control and vascular permeability. They are formed through the action of the two isoforms of cyclooxygenase (COX) enzymes, COX1 and COX2. COX enzymes catalyse the conversion of arachidonic acid to prostaglandin G_2 (PGG_2) first, then into prostaglandin H_2 (PGH_2), and finally this is converted to active prostaglandins, including PGE_2, an isoform with important roles in inflammation and pain. PGE_2 acts on the four subtypes of membrane receptors (EP_{1-4}), the downstream effects of which include intracellular calcium mobilization (EP_1) and inhibition (EP_3) or activation (EP_{2+4}) of adenylyl cyclase activity, which leads to sensitisation of nociceptors. There are many analgesics which inhibit COX enzymes or block prostaglandin receptors. A COX2 selective inhibitor developed by GlaxoSmithKline has proved to be efficacious against allodynia and hyperaglesia in both nociceptive inflammation and neuropathic pain models (Beswick *et al.*, 2004; Bingham *et al.*, 2005). Furthermore, an EP_4 receptor antagonist developed by Pfizer is effective in various models of inflammatory pain (Nakao *et al.*, 2007).

1.3.7. Mechanism of inflammatory mediator induced pain

Clearly inflammatory mediators are important contributors to altered pain processing. The various underlying molecular mechanisms of this include sensitisation of nociceptors, mimicking neurotransmitters, actions on glutamate transporters and receptors, and influencing the actions of other pain mediators.

The changes cytokines cause in behaviours are paralleled by changes in activity or sensitivity of nerve fibres via actions on ion channels at the molecular level. Often this results in increased excitability of sensory neurons, as seen with MCP1 potentiating excitability of DRG neurons (Sun *et al.*, 2006). The activity of sodium channels, which are important in pain transmission (Swayne *et al.*, 2008), can be increased in the presence of cytokines (Fig. 1.6). Acute application of TNFα to DRG

neurons enhances TTX-resistant sodium currents by activation of the TNF receptor and p38 mitrogen activated protein kinase pathway; this results in direct phosphorylation of $Na_v1.8$ channels leading to increased current density (Jin *et al.*, 2006). Similarly, chronic exposure of IL1β applied to capsaicin-sensitive trigeminal neurons increases the total sodium current without affecting TTX-resistant channels (Liu *et al.*, 2006). Another important channel involved in pain transmission is the TRPV1 channel (Davis *et al.*, 2000), where activity of which can be increased in the presence of cytokines (Fig. 1.6), inducing an inward calcium and sodium current and an outward potassium current. Pretreatment of DRG neurons with TNFα produces an increase in capsaicin sensitive inward current, which seems to be modulated by COX activity (Nicol *et al.*, 1997), therefore, suggesting a potential role for prostaglandins. Furthermore, application of IL1β to nociceptive sensory neurons induces an increase in heat activated inward currents and a shift of activation threshold to lower temperatures (Obreja *et al.*, 2002). In contrast, the activity of potassium channels, which are also implicated in pain transmission (Bhave *et al.*, 2010), can be decreased in the presence of cytokines (Fig. 1.6). An example includes activation of inwardly-rectifying potassium channels in cortical astrocytes by exposure to TNFα, ultimately resulting in a reduction in membrane potential (Köller *et al.*, 1998).

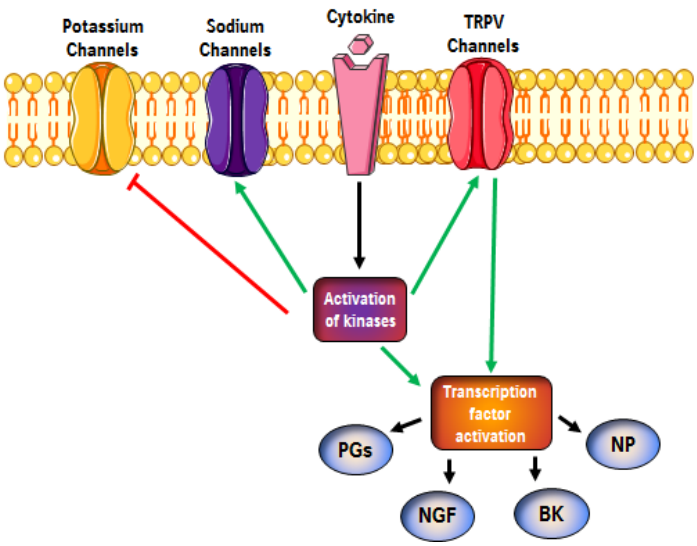

Fig. 1.6. Simplified peripheral mechanism by which cytokines induce pain. Activation of cytokine receptors leads to activation of different intracellular kinases. This in turn inhibits (red) potassium channels and sensitizes (green) sodium and transient receptor potential vanilloid (TRPV) channels. Ultimately there is activation of transcription factors leading to the production or release of proteins including prostaglandins (PGs), nerve growth factor (NGF), bradykinin (BK) and neuropeptides (NP).

The levels of pain mediators, such as neuropeptides, bradykinin and prostaglandins, are influenced by cytokines (Fig. 1.6). Two important neuropeptides involved in pain transmission are substance P and CGRP (Tao *et al.*, 2005). Substance P belongs to the family of tachykinin neuropeptides and acts on neurokinin 1 receptors (NK1R) (Maggi, 1995), which have increased expression following both inflammatory and neuropathic pain conditions (Abbadie *et al.*, 1996). The secretion of substance P is increased by many cytokines including IL1β, IL6, TNFα and MCP1 (Fukuoka *et al.*, 1994; Ding *et al.*, 1995; Malcangio *et al.*, 1996; Jung *et al.*, 2008). Similarly the secretion of CGRP is increased by IL1β and MCP1 (Fukuoka *et al.*, 1994; Qin *et al.*, 2005). This is an inflammatory neuropeptide

acting on the CGRP receptor, which belongs to the family of GPCRs (Conner *et al.*, 2007). Antagonism of this receptor induces anti-nociceptive effects in inflammatory pain models (Hirsch *et al.*, 2013). Bradykinin is a potent algesic peptide which acts on the two receptor subtypes B1 and B2, which have important roles contributing to inflammatory hyperalgesia (Rueff *et al.*, 1993). The activity of these receptors can be influenced by cytokines, IL1β acts on both receptor subtypes (Perkins *et al.*, 1994; Cunha *et al.*, 2007), while TNFα acts on the B2 subtype specifically (Cunha *et al.*, 2007). Various cytokines are also inducers of prostaglandin release, including IL1β (Ferreira *et al.*, 1988) and TNFα (Cunha *et al.*, 1992). Furthermore, cytokines can increase the synthesis and release of naturally occurring anti-nociceptive peptides including opioid peptides (Członkowski *et al.*, 1993) and somatostatin (Scarborough *et al.*, 1989).

Chemokines, which are highly present in the CNS, can act as neuromodulators (Bajetto *et al.*, 2001) and are known to regulate synaptic activity, modulate transmission and evoke second messenger system (White *et al.*, 2007). MCP1 acts as a neuromodulator in the CNS and specifically causes depolarisation of hippocampal membranes as well as increasing excitatory post-synaptic currents, which is proposed to be by potentiation of *N*-methyl-*D*-aspartate receptor (NMDA) and α-amino-3-hydroxyl-5-methyl-4-isoxazole-propionate receptor (AMPA)-induced inward currents (Zhou *et al.*, 2011). In addition, MCP1 negatively modulates GABA-induced currents, facilitating excitatory events (Miller *et al.*, 2008). Glutamate receptors and transporters are involved in pain transmission (Yoshimura *et al.*, 1990) and cytokines, especially TNFα, are thought to alter excitability by effects on these. TNFα down-regulates the expression of the glutamate transporter gene EAAT2/GLT-1 (Sitcheran *et al.*, 2005), but also impairs glutamate re-uptake in the CNS (Korn *et al.*, 2005); together these would increase pain due to the changes in spinal processing (Niederberger *et al.*, 2006).

1.4. The potential mechanism for analgesia

Although the general overall effect of sst_4 receptor activation is somewhat established: inducing analgesia, the precise molecular mechanism behind this is not yet fully elucidated. Comparisons to other receptors, which are known to induce analgesic effects, can be made in order to provide potential mechanisms for the analgesia associated with sst_4 receptor activation.

Early observations that an analogue of somatostatin displaced naloxone from the mu opioid binding site (Gulya *et al.*, 1986) led to speculation that the mode of action of the analogue may involve an agonistic effect at these opioid receptors. However, inhibition of nociceptive dorsal neurons by somatostatin is not antagonized by naloxone (Sandkuhler *et al.*, 1990). Furthermore, MR1452, another antagonist acting at opioid receptors, did not modify the anti-nociceptive effects produced by somatostatin in rat models (Spampinato *et al.*, 1988) again suggesting that somatostatin induces analgesia independently of the opioidergic system. This is further supported by the work of Taddese *et al.* (1995), which showed that somatostatin receptors and opioid receptors are present on different populations of DRGs.

There is a fairly recent concept suggesting that GPCRs might form dimers; this is where different subtypes of receptors can associate together, forming a heterodimer. This can cause alterations to the pharmacology, signalling and internalisation of the different receptors (Prinster *et al.*, 2005). This concept has been reported with δ-opioid and sst_4 receptors (Somvanshi *et al.*, 2014). The heterodimer results in synergistic effects of the agonists on various downstream signalling pathways. These results suggest that a combination therapy, using sst_4 receptor agonists with δ-opioid agonists, might be an appropriate and novel treatment method (Somvanshi *et al.*, 2014). However, the prominent role for sst_4 receptor agonists in reducing pain and the fact that the pathological behavioural effects are not reversed by antagonists, suggests that such heterodimerisation is not vital for the analgesic effects associated with the sst_4 receptor.

1.4.1. Interactions with intracellular secondary messengers

All five subtypes of somatostatin receptor, including the sst_4 subtype, are functionally coupled to adenylyl cyclase activity (Patel *et al.*, 1994), and activation of the receptors results in inhibition of this pathway and therefore reduced cyclic adenosine monophosphate (cAMP) production. The lower levels of cAMP could reduce pain transmission by preventing activation of different protein kinases or altering the function of various ion channels (Fig. 1.4).

Ion channels, including GIRK, Ca_v, TRP and Na_v are important mediators of pain transmission and transduction (Caterina *et al.*, 1997; Story *et al.*, 2003; Gribkoff, 2006; Bhave *et al.*, 2010). The activity of these channels can be influenced by GPCRs or by direct interaction. Modulation of these ion channels has been implicated in the mechanism of numerous analgesic compounds (Mitrovic *et al.*, 2003; Khasabova *et al.*, 2004; Endres-Becker *et al.*, 2007; Eid *et al.*, 2008), and so could also contribute to sst_4 receptor-induced analgesia. More is understood about the role of somatostatin receptors in other physiological and pathological conditions but these could provide hints to the possible mechanisms for their anti-nociceptive effects in pain-processing pathways. Somatostatin's key role in inhibiting insulin release from pancreatic cells is thought to be due to activation of GIRK channels. This was concluded as the ligand was shown to inhibit glucose-induced electrical activity in a pancreatic cell line via induction of an inward potassium current. Utilizing specific blockers and conducting kinetic studies this reduced activity was shown to be by combined activation of ATP sensitive potassium channel and GIRK channel activation (Smith *et al.*, 2001). Similarly, somatostatin causes hyperpolarisation of neuronal endocrine cells via GIRK channel activation (Kailey *et al.*, 2012). Indeed, co-expression of the five somatostatin receptor subtypes with a subunit of the GIRK1 ion channel in xenopus oocytes, has confirmed interaction. Electrophysiological experiments showed currents were induced by both somatostatin 14 and somatostatin 28 application in cells expressing the receptor subtypes 2, 3, 4 and 5, but not 1 (Kreienkamp *et al.*, 1997). This is confirming modulation in recombinant systems, however studies need to be conducted on cultured neuronal tissue in order to make this relevant to the analgesic effects. Voltage sensitive calcium channels are involved in multiple disease conditions. Calcium imaging experiments showed the calcium currents induced by depolarisation in retinal ganglion neurons were significantly reduced after application of an sst_4

receptor selective agonist (Farrell *et al.*, 2010). This means that functional links of the sst_4 receptor to Ca_v channels provide a contributory mechanism to the neuroprotective role of the peptide. Furthermore, in skin nerve preparation of peripheral nociceptors, application of somatostatin significantly reduced TRPV1 capsaicin induced activity and prevents desensitisation (Carlton *et al.*, 2004). Thus, somatostatin's analgesic actions may be partially due modulation of different ion channels, which would need to be established in the pain processing pathway.

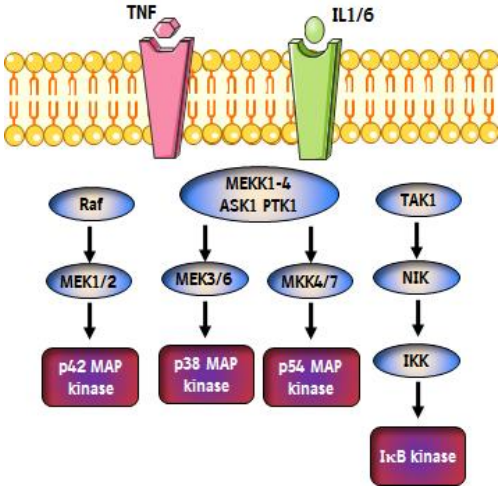

Fig. 1.7. Protein kinase systems known to be activated by IL1 and TNF receptors. The cytokines activated the receptors leading to activation of different intracellular kinases. This could then potentially lead to activation of transcription factors for somatostatin and therefore present a potential mechanism for cytokine induced synthesis. (adapted from (Saklatvala et al., 1996).

1.4.2. Influences in inflammation

Inflammatory mediators are important in controlling chronic pain conditions and can also influence the levels of other pain mediators. The synthesis and secretion of these can be modulated by therapeutic intervention. A reduction in the levels of these mediators is often the mechanism of action of established pain medication. Indeed, various established analgesic compounds target inflammatory pathways. COX inhibitors have potent analgesic effects by reducing levels of PGE_2 (Bingham *et al.*, 2005). Morphine action on opioid receptors is known to prevent lipopolysaccharide (LPS)-induced TNFα secretion from mast cells (Madera-Salcedo *et al.*, 2013) and a fatty acid amide hydrolase (FAAH) inhibitor, VRB597 (which targets the endocannabinoid system) produces anti-nociceptive effects by decreasing levels of IL1β and TNFα release from LPS treated paws (Naidu *et al.*, 2010).

The effects of various cytokines on somatostatin production have also been assessed. Interleukin 1 (IL1) causes increased secretion of somatostatin in primary cultures of foetal rat brain cells. Exposure to this cytokine also results in increased levels of somatostatin mRNA within the brain cultures, confirming it not only increases the secretion but also the synthesis of somatostatin. Such effects were reported even at low concentrations of IL1, showing it is a very potent inducer of synthesis and release (Scarborough *et al.*, 1989). Similar results have been seen after application of tumour necrosis factor (TNFα) and interleukin 6 (IL6) (Scarborough, 1990). Inflammatory pain results in the migration of immune cells to the source of injury. These cells are able to secrete cytokines. The strong link with cytokines to increased somatostatin synthesis and release suggests of a role for somatostatin in analgesia, which might be due to a feedback mechanism associated with sst_4

receptor activation. The mechanism of cytokine induced stimulation of somatostatin synthesis and release is not known. Suggestions have been made indicating a role for the activation of MAP kinases (MAPK) and IκB kinase (Saklatvala *et al.*, 1996) (Fig. 1.7). Another suggestion involves indirect mechanisms, where activation of noradrenergic neurons by the cytokines (Dunn, 1988), results in norepinephrine stimulation of somatostatin release (Peterfreund *et al.*, 1985). Scarborough (1990) showed that the effect is glial dependent, as depletion of this cell type inhibited the induced effects on somatostatin release. Cytokines activate astrocytes, leading to the release of excitatory amino acids including glutamate. Activation of NMDA receptors by glutamate is then able to stimulate somatostatin release (Tapia-Arancibia *et al.*, 1988), indicating an indirect mechanism.

Interaction with various inflammatory mediators could identify potential mechanisms influencing the analgesia of sst_4 receptor activation. There have been suggestions that somatostatin plays a crucial role in inflammation due to expression of receptors on immune cells, including macrophages (ten Bokum *et al.*, 1999; Taniyama *et al.*, 2005). With aspect to the sst_4 receptor, more is understood about the role in lung diseases, where levels of receptor expression are increased in inflammatory conditions in the lung tissue (Varecza *et al.*, 2009). Agonists of the sst_4 receptor have shown to have anti-inflammatory effects. TT-232 reduces both neutrophil infiltration and IL1β secretion in the carrageenan paw of rats (Pintér *et al.*, 2002). While J-2156 reduces substance P and CGRP release in the rat trachea, as well as neutrophil infiltration and IL1β secretion in the rat lung (Helyes *et al.*, 2006). Thus, analgesia caused by sst_4 receptor activation might be in part due to modulation of inflammatory processes.

1.5. Project aims

Pain is a worldwide debilitating problem which affects 20-30% of the population. Although it is one of the most common symptoms for which patients seek medical attention; currently only about 30% of patients reach full pain relief. Continual research is being conducted to identify further approaches to provide effective relief. Somatostatin is a neuropeptide with inhibitory actions on the CNS (Schulz *et al.*, 2000), which produces analgesic effects upon somatostatin 4 receptor activation (Sandor *et al.*, 2006). The global aim of this project was to gain a greater understanding of the role of sst_4 receptors in analgesia and to elucidate the molecular mechanisms underlying this effect, concentrating specifically on peripheral mechanisms. This would therefore lead to the identification of a novel target for the development of analgesic compounds.

2. Materials and Methods

2.1. In vitro: characterising tool compounds

Following identifications of somatostatin receptor agonists from literature, these were characterised using radio ligand binding studies and cAMP functional assays. This allowed for selectivity, affinity and potency to be determined, enabling an appropriate tool compound to be identified.

2.1.1. Compounds

Compound	Stock Solution	Supplier
Corticostatin17	1 mM	BP03465, Bio Trend, Germany.
Example32	10 mM	BI synthesised
J-2156	1 mM	BI synthesised
L803,087	10 mM	Bio Trend, Germany. BN0298
Octreotide	10 mM	Aneosystems, Germany, SP010100B
Somatostatin 14	1 mM	BP0263, Bio Trend, Germany.
Somatostatin 28	1 mM	BP0264, Bio Trend, Germany.
TT-232	10 mM	Bio Trend, Germany, BP0426

Table 2.1. Somatostatin receptor agonists. Selective or non-selective compounds were identified from literature. Binding and functional activation was determined in order to identify an appropriate tool compound. All stock solutions were prepared in DMSO (Merck, Germany) and stored in aliquots. With the exception of octreotide (stored at 4°C), all stock solutions were stored at -20°C and a single aliquot used as required.

2.1.2. Binding studies

Radioligand binding studies were performed in 96-well ELISA plates (NUNC, Denmark) using binding buffer (10 mM/L HEPES; 1 mM/L EDTA; 5 mM/L $MgCl_2x6H_20$) containing 30 μg/mL bacitracin (Sigma, Germany), to ensure the peptide compounds did not interact with the plastic ELISA plates thus the concentration remained stable, and 5 mg/ml protease-free BSA fraction V (Sigma, Germany, A-3059), pH was adjusted to 7.6 using 4 M NaOH. Selectivity of the compounds were determined using membrane preparations from CHO-K1 cells stably-expressing human receptor subtypes sst_{1-5} (Table 2.2). Membrane from CHO-K1 cells (Perkin Elmer, Waltham, MA) expressing the rat sst_4 receptor was also tested at a concentration of 200 μg/well. Each of the compounds (Table 2.1) was tested in duplicates, over a range of concentrations from 10^{-12} M to 10^{-5} M and the endogenous ligand somatostatin 14 (BioTrend, Germany) was run in parallel as a positive control. Binding curves were derived from competitive experiments against 0.05 nM [^{125}I]-Tyr3-somatostatin-(1-14) (ANAWA Trading SA, Switzerland). The final activity of the label was 80.5 TBq/mM. The end volume was 250

μl/well, where initially 25 μl of compound was added to each well, followed by 25 μl of radioligand and then finally 200 μl of cell suspension. Total-binding was defined using only assay buffer and non-specific binding was defined with 1 μM somatostatin 14. The initial incubation was carried out at room temperature (23-24°C) for 3 hours with constant shaking. The reaction was then terminated by rapid filtration through a Packard harvester (Perkin Elmer, Waltham, MA) onto unifilter-96 GF/B filter plates (Perkin Elmer, Waltham, MA) which had been pre-soaked in 0.3% polyethylemeimine (Sigma, Germany). The plates were washed 3 times using ice-cold (4°C) physiological (9 g/L) sodium chloride (NaCl) solution (Merck, USA) at an approximate volume of 300 μL/well. Following addition of 50 μL/well scintillant (Microscint 20, Packard, USA) the plates were further incubated at room temperature (23-24°C) for 1 hour in the dark. Analysis for radioactivity was conducted using the Top Count NXT™ microplate scintilation counter (Packard, USA).

Receptor subtype	Supplier	Concentration/well
Sst_1	Perkin Elmer, Waltham, MA, ES-520-M400UA	40 μg/well
Sst_2	Perkin Elmer, Waltham, MA, ES-521-M400UA	25 μg/well
Sst_3	Perkin Elmer, Waltham, MA, ES-523-M400UA	1.5 μg/well
Sst_4	BioTrend, Germany, A138	0.5 μg/well
Sst_5	Perkin Elmer, Waltham, MA, ES-522-M400UA	25 μg/well

Table 2.2. Somatostatin receptor expressing membranes. The five somatostatin receptor subtypes were expressed in membranes. These were used to determine the affinity of described agonists.

2.1.3. Functional assay: cAMP inhibition

Total cAMP accumulation was measured using the LANCE cAMP detection kit (Perkin Elmer, Waltham, MA), in 384 optical assay plates. The somatostatin analogues (Table 2.1) were tested at concentrations ranging from 10^{-12} M to 10^{-5} M at a volume of 2 μl/well. All dilutions were prepared in stimulation buffer prepared from HBSS 1x solution (Gibco, UK), with an addition of 5 mM HEPES buffer (Gibco, UK), 0.1% BSA (Serva, Germany) and 500 mM Isobutylmethylxanthine (IBMX, Sigma, Germany). IMBX is an inhibitor of cAMP phosphodiaesterases, it was therefore added to prevent the enzymatic breakdown of the produced cAMP. Each concentration of standard or compound was tested in duplicate or triplicate, respectively. The cAMP standard was prepared by diluting 8 μl of the 50 μM standard solution (provided by Perkin Elmer, Waltham) in 92 μl of stimulation buffer, to give a concentration of 1 μM. Serial dilutions were then prepared, using the stimulation buffer, from 1000

nM to 0.01 nM, of cAMP standard. Initially the compounds or standards were pipetted to each well, the plates were then centrifuged to a speed of 1000 cpm, to ensure the solution was at the bottom of the well. Intact H4 cells expressing either human or rat sst_4 receptors (Perkin Elmer, Waltham) were used at 1250 cells/well or 1000 cells/well respectively with a volume of 5 μl/well. The cells were stored in frozen aliquots (1 ml) at – 80°C and defrosted on the day of use. The vial was suspended in 9 ml DPBS solution and the number of cells counted using 0.4% trypan blue stain (Introvegen, life technologies, Germany) and the countless automated cell counter (Introvegen, life technologies, Germany). A pellet was formed by centrifuging the cell suspension at 1200 cpm for 5 minutes, the DPBS was aspirated off and the pellet was re-suspended in the calculated volume of assay stimulation buffer. To this the supplied Alexa Fluor® antibody was added at a dilution of 1:100. The cells were added to the plate next, allowing pre-treatment with the compounds for 10 minutes at room temperature (23-24°C). Again following the addition of the cells the plates were centrifuged to a speed of 1000 cpm. For the standard 5 µl of the supplied Alexa Fluor® antibody was mixed with 495 µl of stimulation buffer and rather than adding cells, 5 µl of the antibody solution was added to the standard wells. After 10 minutes stimulation was then achieved by adding either 10 μM or 30 μM forskolin (Sigma, Germany) for human or rat receptors respectively, again the plates were centrifuged to 1000 cpm. The final volume was 10 μl/well. Plates were incubated for 1 hour at room temperature (23-24°C) with constant shaking. Finally, detection buffer (Perkin Elmer, Waltham) was added (10 μl/well) and the plates were centrifuged to 1000 cpm. This was followed by a further incubation period of 1 hour at room temperature (23-24°C) in the dark. Plates were read using EnVision Xcite 2104 multilabel reader (Perkin Elmer, Waltham, MA) at 665 nm.

2.1.4. Statistics

Graphs were produced in Prism 6.0 for Windows (GraphPad Software, San Diego, USA). Data are expressed as mean±S.E.M, unless exact values are given. For binding studies initially the non-specific binding was subtracted from the total count and then the results were converted to a % of specific binding using Excel 2010 for Windows (Microsoft, Redmond, USA). Ki values were calculated, using Prism 6.0 for Windows, in order to determine the inhibition constant of the drug. For cAMP assays a standard curve was created and the sample concentration was determined by reference to this standard curve using Prism 6.0 for Windows. The results were converted to a % inhibition of the forskolin stimulation using Excel 2010 for Windows. IC_{50} values were calculated, using Prism 6.0 for Windows, in order to determine the concentration of compound which produced 50% of the maximal inhibition.

2.2. In vivo experiments

2.2.1. Animals

Adult male Crl:WI (Han) rats (Charles River, Germany) weighing 300 – 350 g were used in all experiments. These were housed in groups of 5 per cage, in an artificial 12/12 hour light/dark cycle with food and water *ad libitum* in the institutional animal facilities. The room temperature and the humidity were kept constant at 22±2°C and 60±15% respectively. All animal protocols were authorised by the Local Animal Care and Use Committee and carried out according to the local animal care guidelines, AAALAC regulations, and the USDA Animal Welfare Act and followed the guidelines provided by Committee for Research and Ethical Issues of International Association for the Study of Pain (IASP). All experiments were performed under fully-blinded protocols where the primary investigator was unaware of the treatment allocation. A secondary investigator was responsible for randomisation and treatment protocols.

For all models the animals were anaesthetised under 3% isoflurane (Abbvie, Germany) carried in 30/70 O_2/N_2O until the hind paw withdrawal reflex was suppressed. After injection of alogene or surgery (i.e. induction of pain) the rats were returned to their cage and allowed to recover until behavioural studies were performed.

2.2.2. Carrageenan-induced inflammation

Inflammation was induced by a 50 µl intraplantar injection, 1% λ-carrageenan (Sigma-Aldrich, USA) dissolved in 0.9% NaCl physiological saline, into the plantar surface of the left hind paw. A slight pressure was applied to the paw following needle removal to ensure no solution was leaked. Administration was achieved using a 27 G needle (Terumo, Germany). Behavioural studies were performed 3 hours after the injection of carrageenan. *This behavioural data was performed with the help of Margot Weiland.*

2.2.3. Complete Freud´s Adjuvant (CFA)-induced inflammation

Inflammation was induced by a 50 µl intraplantar injection of 25 µg Complete Freud´s Adjuvant (CFA, sigma, USA) into the plantar surface of the left hind paw. For sham experiments 50 µl of buffer was injected. For both alogene and saline injection a 27 G needle (Terumo, Germany) was used. Following this a slight pressure was applied to the paw to ensure the oil remained in the plantar surface. Behavioural studies were conducted 24 hours after CFA injection. *This behavioural data was performed with the help of Margot Weiland.*

2.2.4. Monosodium iodoacetate (MIA)-induced osteoarthritis

Anaesthetised animals were placed in the supine position and the knee was shaved. Osteoathritis was induced by a 50 µl intra-articular injection of 1 mg monosodium iodoacetate (MIA, sigma, USA) through the infrapatellar ligament of the left knee using a 30 G needle (Terumo, Germany). The knee was flexed following injection to allow even distribution of MIA in the synovial space. For sham

experiments 50 µl of buffer was injected. Behavioural studies were performed 3 days after MIA. *This behavioural data was performed with the help of Anna Menzel.*

2.2.5. Streptozotocin (STZ)-induced diabetic neuropathy

Diabetic neuropathy was induced by a single intraperitoneal injection of 65 mg/kg streptozotocin (STZ, Sigma-Aldrich, USA) dissolved in 0.9% NaCl physiological saline. Administration was achieved using a 27 G needle (Terumo, Germany), the syringe was changed after every 4 animals as the STZ is broken down in plastic, so would no longer be active. After injection rats were returned to individual ventilation cages for a minimum of 3 days to prevent any contamination of STZ from excretion matter to other rats within the animal facilities, or to investigators, which could then contaminate other rats. Behavioural studies were conducted 3 weeks after STZ injection. *This behavioural data was performed by Andreas Kremer.*

2.2.6. Partial nerve ligation (PNL) induced neuropathy

Neuropathy was induced using the partial nerve ligation model, described by Seltzer *et al.* (1990). Anaesthetised animals were placed in the supine position and the upper thigh shaved. The left sciatic nerve in the upper thigh region was exposed by blunt dissection through the biceps femoris. The exposed nerve was separated from surrounding connective tissue and the dorsal third was tightly ligated using 6-0 vicryl polyglactin (Ethicon, Germany) sutures. The nerve was gently placed back and the skin incision was closed with 2 sutures using 3-0 vicryl polyglactin (Ethicon, Germany). Behavioural studies were conducted 2 weeks after PNL surgery. *This behavioural data was performed by Makoto Shimasaki.*

2.2.7. Evaluation of mechanical hyperalgesia

Pain thresholds were measured using the method described by Randall *et al.* (1957). Quantificant of the nociceptive pressure threshold was measured using an analgesy-meter (55973v220; Ugo Basile, Italy). The method involves restraining the rat and applying an increasing mechanical force to the middle portion of the dorsum of the rat's hind paw. Nociceptive threshold (in grams, g) was defined as the force which elicits the first sign of pain-associated behaviour in the rat, i.e. paw withdrawal or struggling behaviour. The upper limit of pressure administered was 500 g to prevent tissue damage. The sst_4 receptor agonist J-2156 (in varying doses), or vehicle was administered either at 1 hour or at 24 hours prior to establishment of paw withdrawal threshold. The effect of the positive controls used (described in 2.2.11) was tested at the appropriate time point for the particular models. For each test group n was 8-11 rats. A minimum of 8 rats was used to ensure variability was considered. For positive controls 8 rats were used, the J-2156 treated rats had an n number of 10 and for the vehicle group 11 rats were tested. No exclusion criteria were applied, all rats tested were included in the analysis. This mechanical test for analgesia was used for the carrageenan model, the CFA model, the STZ model and the PNL model.

2.2.8. Weight bearing deficit

Changes in hind paw weight distribution between the left (osteoarthritic) and the right (control) limbs was utilized as an index of joint pain in the osteoarthritic knee. A modified incapacitance tester apparatus (Boehringer Ingelheim, Germany; Fig. 2.1) was used to determine the weight-bearing deficit. The rats were placed in an angled perspex container and positioned so that each hind paw rested on a separate transducer pad. On day 2 after MIA injection, rats were trained and allowed to acclimatise to the testing apparatus. On day 3 after MIA injection measurements were made, the force exerted by each hind paw (g) was averaged over a 10 second period. A baseline measurement was performed initially and then the rats were allocated in groups so that weight bearing measurements were equally distributed in each of the testing groups i.e. the baseline values were the same for each dosing group. The sst_4 receptor agonist J-2156 (in varying doses), positive controls (described in 2.2.11), or vehicle was administered either at 1 hour or at 24 hours prior to the behavioural test being conducted. For each test group there were n = 10 rats.

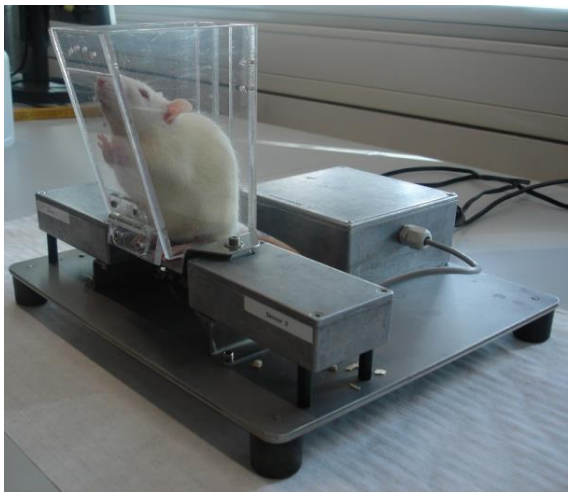

Fig. 2.1. Description of weight-bearing apparatus. Each hind paw on a separate sensor. Rats stand in a forward position, resting front paws on the front side of the perspex chamber. The perspex box has a width of 10.5 cm, a breadth of 6.5 cm and is 13.5 cm in height. The force exerted by each hind paw (g) is averaged over a 10 second period.

2.2.9. Paw Volume in CFA and carrageenan induced swelling

Paw volume was measured by plethysmometry (Ugo Basile, USA) before and 3 hours after carrageenan administration, or 25 hours after CFA administration. The plethysmometer is composed of 2 perspex tubes connected and filled with a conductive solution and an electrode for each chamber. On the hind paw of the rat a mark was made across the ankles, care was taken to ensure this mark is at roughly the same position for each rat. The rat was restrained and the paw was immersed, up to the mark, into the measuring tube causing the displacement of solution, altering the volume in the second tube. This results in a change in conductance between the 2 electrodes, generating an output signal indicating the volume displacement measured (ml). Oedema is expressed as the difference from the baseline paw volume. The sst_4 receptor agonist J-2156 (in varying concentrations), positive controls (described in 2.2.11) or vehicle were administered 1 hour prior to carrageenan or CFA injection. Further injections of J-2156 and celecoxib were given at 8 and 24 hours post CFA injection. There were 10-20 animals per group.

2.2.10. Determination of J-2156 concentrations in the plasma

To determine systemic concentrations of J-2156 in the *in vivo* experiments, blood samples were collected from the sublingual vein and the retinorbital cavity at 1 hour and 24 hours after i.p. compound administration. Blood was collected into EDTA-coated tubes and plasma was generated by centrifugation for 10 minutes at 6200 rpm at 4°C. Total plasma concentrations of J-2156 were determined using HPLC-MS/MS (high-performance liquid chromatography coupled to tandem mass spectrometry). The lower limit of detection in rat plasma was between 1.0 nM and 2.5 nM. *The HPLC-MS/MS data was performed by Raimund Kuelzer.*

2.2.11. Compound administration

For all experiments the sst_4 receptor agonist, J-2156 was dissolved in physiological saline (0.9% NaCl) and all solutions were made fresh on the day of experiment. J-2156 (0.01, 0.1, 1, 3 and 10 mg/kg) or vehicle were administered intraperitoneally (i.p). For carrageenan and CFA mechanical hyperalgesia experiments indomethacin (30 mg/kg) was used as a positive control. Indomethacin was dissolved in 0.01% Tween 80 and 0.5% natrosol and administered orally (p.o), using an 18 G feeding tube (Instech Solomon, USA). In the paw volume study indomethacin was used as a positive control for carrageenan, however celecoxib (30 mg/kg) was used as a positive control in CFA animals. Celecoxib was dissolved in 0.01% Tween 80 and 0.5% natrosol and administered orally. For MIA experiments subcutaneous (s.c) morphine (6 mg/kg) was used as a positive control; morphine was dissolved in physiological saline (0.9% NaCl). For STZ experiments duloxetine (20 mg/kg), dissolved in physiological saline (0.9% NaCl), was used as a positive control and administered intraperitoneally. The positive control for PNL experiments was lamotrigine (30 mg/kg) which was dissolved in 0.01% Tween 80 and 0.5% natrosol and administered orally. Irrespective of administration route, all drugs were given at a volume of 2 ml/kg. The pH of the compounds was always checked, and if necessary, adjusted to approximately pH 7.0.

2.2.12. Obtaining paw samples

Paw muscle tissue was collected from CFA rats following behavioural testing. Rats were anaesthetised then decapitated with a guillotine. Skin tissue was removed using tweezers to raise the tissue and surgical disposable scalpels (Braun, Germany) to excise it. The muscle tissue was then collected in the same way. The muscle of the paw tissue was weighed and approximately 160 mg tissue was immediately placed on dry ice, or for next generation sequencing (NGS) studies (section 2.3.8) the skin tissue was completely submerged in RNAlater® solution (Ambion, life technologies, Germany) and stored at 4°C until use. The samples used for the cytokine release and neutrophil infiltration assays (section 2.3.7) were homogenesised in MSD diluent 6 buffer (Mesoscale discovery, Rockville, MD) at dilutions of 1:5, using Ultra Turax machine (Qiagen, USA). These were then centrifuged for 15 minutes at 10000 rpm at 4°C. Supernatant fractions were kept frozen at -80°C until use.

2.2.13. Sampling DRG neurons

DRG neurons were also obtained from CFA treated animals, following behavioural testing. Rats were anaesthetised and decapitated with a guillotine. The spinal column was then exposed and divided along the coronal plane from the thoracic region to the bottom of the lumbar region allowing access to the spinal cord and the DRG neurons. The L4-L6 DRG neurons were extracted. For the next generation sequencing (NGS) studies (section 2.3.8) the tissue was instantly completely submerged in RNAlater® solution (Ambion, life technologies, Germany) and stored at 4°C until use. For cytokines release studies (section 2.3.7) the DRGs were immediately placed on dry ice. The samples were homogenesized in MSD diluent 6 buffer (Mesoscale discovery, Rockville, MD) at dilutions of 1:5 using Ultra Turax machine (Qiagen, USA), then centrifuged for 15 minutes at 10000 rpm at 4°C for use in the cytokine assay. Pooling of samples was necessary. Supernatant fractions were kept frozen at -80°C until use.

2.2.14. Statistics

Graphs were produced in Prism 6.0 for Windows (GraphPad Software, San Diego, USA). Data are expressed as mean±S.E.M. for behavioural studies and mean±S.D. for plasma levels. For plasma levels the table shows the concentration of J-2156 in nM, for mechanical hyperalgesia the graphs show the paw withdrawal threshold in g, for the weight-bearing deficit the graphs show the imbalance in g and for the paw volume the graphs show the volume in ml. Statistical analysis was carried out on Prism 6.0 for Windows*.* To test for normal distribution the Kolmogorov-Smirnov test was used. Tests evaluated differences between naïve and alogene treated animals, vehicle and compound dosed animals and naïve and compound dosed animals. When one dose was tested, students T-test measurements allowed for significance to be determined. When more than one dose was tested, One-way ANOVA measurements, followed by Bonferroni post-hoc tests allowed for significance to be determined. A P value of <0.05 was deemed significant.

2.3. Ex vivo experiments

2.3.1. Compounds

Compound	Description	Stock Solution	Supplier
A-967079	TRPA1 antagonist	10 mM	BI synthesised
Agatoxin	P/Q type Ca_v blocker	1 mM	Biotrend, Germany
Capsaicin	TRPV1 agonist	1 mM	Sigma, USA
Capsazepine	TRPV1 antagonist	1 mM	Sigma, USA
Celecoxib	Cyclooxygenase 2 inhibitor	10 mM	ChemPasific,USA
Compound 6	TRPA1 agonist	10 mM	BI synthesised
Ω-Conotoxin	N type Ca_v blocker	100 µM	Alomone labs, Jerusalem
Indomethacin	Non-steroidal anti-inflammatory (NSAID) drug	10 mM	Sigma, USA
Mibefradil	T type Ca_v blocker	10 mM	Sigma, USA
Nitrendepine	L type Ca_v blocker	10 mM	Sigma, USA
Pertussis Toxin	Uncouples G_i proteins from GPCRs	100 µg/ml	Sigma, USA
Tertiapin Q	GIRK specific blocker	1 mM	Sigma, USA
Tetrodotoxin	Na_v channel blocker	1 mM	Biotrend, Germany
Veratridine	Na_v channel opener	10 mM	Sigma, USA

Table 2.3. Compounds used as positive controls. Previously described agonists, antagonists and inhibitors were used. Agonists were used for stimulations. Antagonists and inhibitors were used as positive controls to compare the effects induced by the sst_4 receptor agonist. Mibefradil, pertussis toxin, tertiapin Q and tetrodotoxin were prepared in dH_2O, all other compounds were prepared in DMSO (Merck, Germany). With the exception of tetrodotoxin (stored at 4°C), all stock solutions were stored at -20°C and a single aliquot used as required.

2.3.2. Coating coverslips

Glass coverslips, on which DRG primary sensory neurons are grown, were previously sterilized. Multiple 13 mm diameter coverslips were placed in a clean glass culture dish with a diameter of 100 mm and heated at 180°C for 3 hours in a hit air sterilizer (Heraeus, ThermoFisher Scientific, USA). Working under a laminar flow, single sterilized coverslips were placed in wells of a 24 well culture plate (TPP, techno plastic products, Switzerland). The coverslips were coated with 0.1 mg/mL poly-L-lysine (Sigma, Germany, solved in DMSO), at a volume of 1 ml/well and stored at 4°C for 24 – 48 hours. These were then washed 3 times with 1x phosphate buffer saline (PBS) solution (Sigma,

Germany) at an approximate volume of 1 ml/well; before being coated with 2 µg/ml laminin (Sigma, Germany, solved in DMSO) at a volume of 1 ml/well and stored for a minimum of 24 hours at 4°C. On the day of cell preparation the coverslips were again washed 3 times with 1x PBS (1 ml/well) ready for use.

2.3.3. Tissue culture: DRG neuron preparation

Adult DRG neuron cultures were prepared from 6 to 8 week old naïve Crl:WI(Han) (Charles River, Germany) male rats. From CFA or sham-injected rats, only L4-L6 DRGs from the injected side were removed and cultured. DRG neurons were cultured from a minimum of 3 rats for each experiment set, where the n number relates to the number or cells tested or ELISAs conducted. Rats were anaesthetised with isoflurane (Florene, Abott, Germany) before being decapitated with a guillotine. The spinal column was extracted from the thoracic region to the bottom of the lumber region and placed in 1x PBS solution. The next steps were conducted under a laminar flow. The spinal column was cleaned and moved to DMEM solution before being divided along the sagittal plane. DRGs were removed and placed into ice-cold DMEM (c.c.pro., Germany) containing 1% penicillin-streptomycin (Sigma, Germany). These were chemically digested in 4 mg/mL collagenase type IV (Gibco, UK) and 2 mg/mL papain (Sigma, Germany) in DMEM for 90 minutes in a water bath heated to 37°C. This reaction was terminated by aspiration, and addition of DMEM (c.c.pro., Germany) containing 1% penicillin-streptomycin (Sigma, Germany) and 10% FCS (Gibco, UK). The cells were mechanically dispersed using fire-polished pasture pipettes, of gradually decreasing tip diameter, to form a homogenized cell suspension. For electrophysiology and calcium imaging experiments, cells were plated onto coated tissue culture cover slips (Thermo scientific, Germany). For the calcium imaging experiments, 50 µl of the cell suspension was plated onto the centre of the coverslip. These were then left for 2 hours at 37°C, 10% carbon dioxide, before being topped up with 1 ml of culture medium. For neurons which were stimulated and used in the inflammatory mediator ELISAs (section 2.3.7) the cells were re-suspended in 5 ml of culture medium and plated in one well of a 6-well polystyrene plate (Becton Dickinson, France) so these could later be seeded for stimulation. The cells were incubated at 37°C, in an atmosphere of 10% carbon dioxide and with a humidity of 95%. Recordings were made within 48 hours of plating.

2.3.4. Patch clamp electrophysiology

Transmembrane currents and voltages were recorded at room temperature by whole-cell voltage-clamp or current-clamp protocols, using an EPC 10 amplifier, with TIDA 5.2 software (HEKA electronics, Germany) and a PCI-1600 interface (HEKA electronics, Germany). The average cell size of the neurons was between 20 – 35 µm, cells were chosen which appeared round and single. Data were low-pass filtered at 2.9 KHz and sampled at 20 KHz. Patch pipettes were pulled from thick-walled borosilicate glass capillaries (1.5 mm outer diameter) on a Sutter Instruments P-97 puller (Sutter instruments, USA), and had a resistance of 3-5 MΩ. The cells were bathed in normal Ringer's solution containing: 140 mM/L NaCl; 5 mM/L KCl; 10 mM/L glucose; 10 mM/L HEPES; 1.8 mM/L

$CaCl_2$; 0.8 mM/L $MgCl_2$. The pH was adjusted to 7.4 using 1 M NaOH and the osmolarity remained between 300 and 320 mOsmol/l. The pipette solution varied dependent on which protocol was used. The pipette potential was zeroed before seal formation; care was taken to maintain membrane access resistance as low as possible, between 2 and 7 MΩ. Command voltage protocols and data acquisition were performed by TIDA 5.2 (HEKA Electronics, Germany). For the electrophysiology experiments graphs show both original traces and average cell results.

2.3.4.1. G-protein coupled inward rectifying potassium channels (GIRK)

For measurement of GIRK activation whole-cell voltage-clamp recordings were made. The pipette solution consisted of: 20 mM/L NaCl; 120 mM/L KCl; 10 mM/L glucose; 10 mM/L HEPES; 1 mM/L EGTA; 3 mM/L $MgCl_2$, with the addition of 3 mM/L Na_2ATP and 0.3 mM/L NaGTP on the day of testing. The pH was adjusted to 7.4 using 1 M NaOH and the osmolarity remained between 270 and 300 mOsmol/l. In all protocols the cells were exposed to a high potassium extracellular solution containing 100 mM/L NaCl and 45 mM/L KCl and recordings were made while cells were voltage clamped at -80 mV. The initial protocol involved the baseline recording of the cells being measured for 60 seconds, allowing for stabilisation. Following this, the sst_4 receptor agonist, J-2156, was applied for 380 seconds and the effects recorded. However at the 290 second time point the independent blockers were applied in combination with J-2156 until the end of the protocol. To test for different concentrations of J-2156 or different blockers within one protocol a second was established. Again the baseline recording of the cells was measured for 60 seconds, allowing for stabilisation. Then the lower concentration of J-2156 was applied for 380 seconds and the effects recorded. For a further 380 seconds a higher concentration of J-2156 was applied and the effects recorded. At the 690 second time point the first blocker was applied in combination with J-2156. Then at the 790 second time point the second blocker was applied in combination with J-2156 until the end of the protocol. Different concentrations of J-2156 (10, 30 and 100 nM) were tested as well as 2 blockers, barium chloride (BaCl; 300 µM) and tertiapin Q (500 nM) (Table 2.3). The current recorded at the last time point for control baseline (60 seconds), J-2156 (290, 380, 690 seconds) or blocker (380, 780, 880 seconds) application was calculated and an average of the different cells taken. Control experiments were also run; the first was a standard control, applying only vehicle Ringer solution, to indicate stability of recordings. The second was a compound control applying only the sst_4 receptor agonist J-2156, without blocker application, confirming the effects of the blocker, i.e. that there was no reversal of induced current without blockers being applied. Only cells in which J-2156 induced a potassium current of more than 0.5 nA, which was then inhibited by the blockers by more than 0.5 nA, were analysed. These criteria were applied to ensure changes recorded were due to activation of GIRK channels and not through unstable recordings where the seal of the cell might have been lost or leakage was occurring. For these experiments graphs were created which are presenting current change (nA).

2.3.4.2. Transient receptor potential vanilloid 1 (TRPV1) channels

For measurements of TRPV1 inhibition whole-cell voltage-clamp recordings were made with cells held at -60 mV. The pipette solution consisted of: 145 mM/L KCl; 10 mM/L glucose; 10 mM/L HEPES; 1 mM/L $MgCl_2$, with the addition of 2 mM/L Na_2ATP and 0.2 mM NaGTP on the day of testing. The pH was adjusted to 7.4 using 1 M NaOH and the osmolarity remained between 270 and 300 mOsmol/l. The cells were bathed in calcium free Ringer's solution containing: 140 mM/L NaCl; 5 mM/L KCl; 10 mM/L glucose; 10 mM/L HEPES; 1 mM/L $MgCl_2$. Activation of the TRPV1 channels was achieved by application of 300 nM capsaicin for 5 seconds, and cells were considered responsive if the inward current magnitude was at least 100 pA. A protocol was run in which capsaicin (Table 2.3) was applied at two time points 60 and 360 seconds. After the first stimulation (60 seconds), the vehicle control or the different compounds was applied. Therefore the last capsaicin stimulation (360 seconds) was run in the presence of either vehicle control or compound and the ratio of the two peaks was calculated. The sst_4 receptor agonist, J-2156, was tested at a concentration of 100 nM. The TRPV1 specific antagonist capsazepine (10 µM) (Table 2.3) was used as a positive control. The recordings show current change (pA) and the graphs are represented by the ratio of the 2 capsaicin stimulations.

2.3.4.3. Voltage gated sodium channels (Nav)

For measurements of sodium channel modulation both whole-cell voltage-clamp and current-clamp recordings were made. The pipette solution consisted of: 110 mM/L K-gluconate; 8 mM/L NaCl; 20 mM/L KCl; 10 mM/L HEPES; 1 mM/L $MgCl_2$; 10 mM/L EGTA, with the addition of 4 mmol/L Mg-ATP on the day of testing. The pH was adjusted to 7.4 using 1 M NaOH and the osmolarity remained between 270 and 300 mOsmol/l. There were three different protocols used. The first was run in voltage-clamp mode and allowed the sodium current to be analysed. A holding potential of -70 mV was used. A depolarisation from the holding potential to 0 mV for 10 milliseconds was applied at a frequency of 1 Hz for 30 pulses to enable the control current to be established. Compounds: the sst_4 receptor agonist J-2156, tetrodotoxin (TTX) (300 nM) (Table 2.3) or vehicle control were applied for 3 minutes and then the same protocol allowed the compound current to be established. The current at the last time point was calculated for either the control or the test compounds. An average of the different cells was then calculated. To evaluate the excitability of the neurons 2 protocols were run in current-clamp mode, which allowed for the production of action potentials, therefore allowing firing threshold and levels of activity to be determined. The holding current was adjusted to clamp the cell at approximately -70 mV. A fast step protocol was run where the potential was changed 5 times in increasing steps of 80, 160, 240, 320 and 400 pA, every second and held for 0.5 seconds (Fig. 2.2A). The protocol was repeated 3 times, meaning a total recording time of 24 seconds. In the second current-clamp protocol the holding current was gradually increased from the holding current up to 500 pA over a period of 1 second (Fig. 2.2B). The protocol was repeated 3 times, meaning a total recording time of 6 seconds. Threshold of each of the cells was determined by the voltage at which the first action potential was produced. The levels of activity were determined by counting the total

number of action potentials. Firstly the vehicle control current-clamp protocols were run to determine the basal values. The sodium current protocol was then run, followed by a 3 minute pre-incubation time with either of the compounds or vehicle control. Finally the current-clamp protocols were repeated in the presence of compound or vehicle control. The results were normalized to the initial control reading and the % change calculated.

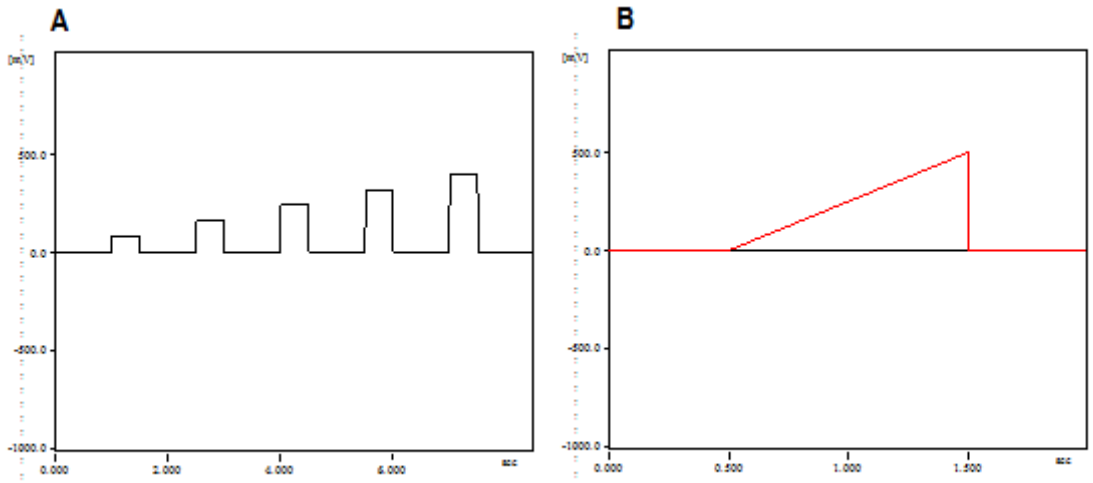

Fig. 2.2. Description of the current clamp protocols. To determine threshold of the cells two protocols were run. The holding current was adjusted to clamp the cell at approximately -70 mV. (A) In the step protocol the potential was quickly changed in increasing steps of 80, 160, 240, 320 and 400 pA, and every second and held for 0.5 seconds. (B) In the ramp protocol the holding current was gradually increased from the holding current up to 500 pA over a period of 1 second. In both protocols (A+B), three repeats were made. The total recording time was therefore 24 or 6 seconds for the step and ramp respectively. Command protocols were performed by TIDA 5.2 (HEKA Electronics, Germany).

2.3.5. Calcium Imaging

The DRG neurons, cultured on coverslips, were pre-loaded with the Ca^{2+} sensitive fluorophore, Fluo-4-AM, 2 µM (Invitrogen, CA) and 1 mM probenecid (Sigma, Germany) for one hour prior to imaging at 37°C, 10% carbon dioxide and with a humidity of 95%. Probenecid is an anion exchange inhibitor, this was used to minimize movement of other positively charged ions across the cell membrane. From this point on care was taken to ensure the cells were always kept in the dark. The cells were then bathed in Ringer buffer (140 mM/L NaCl; 5 mM/L KCl; 10 mM/L glucose; 10 mM/L HEPES; 1.8 mM/L $CaCl_2$; 0.8 mM/L $MgCl_2$; pH was adjusted to 7.4 using 1 M NaOH) until use, to allow the hydrolysis of the AM group of the dye, which leads to the formation of the complex used for measurement. The cells were used within one hour of pre-loading. The coverslips were mounted on a custom made perfusion chamber (10 mm internal diameter) and solutions hand pipetted into the chamber. Excess medium was removed from the chamber by a vacuum pump. Cells were imaged through a Plan Neofluar 20x/0.5 objective, using an Axiovert 200M microscope with inbuilt camera

(Zeiss). Excitation was achieved at 488 nm with an argon laser, and images were collected, at an emission of 510 nm, through a long pass filter, using the computer software Laser Scanning Microscope 510 META version 3,2 SP2 (Zeiss) (Fig. 2.3). The laser power was set to 40% with excitation at 2.1%. The scanning speed was set to 1.97 seconds and the fluorescence signal was optimized by the detector gain and amplifier offset. There were time intervals between image capture, as continuous videoing would cause photolysis of the fluorescent dye.

For the calcium imaging experiments graphs show raw data traces by normalisation of the fluorescent intensity [F/F0]; but also average cell results, representing the ratio of the 2 different stimulations dependent on the protocol. In the case of TRPV1 and TRPA1 data the $\log_{IC50}$ was calculated to determine the concentration of compound, which produces 50% of the maximal inhibition.

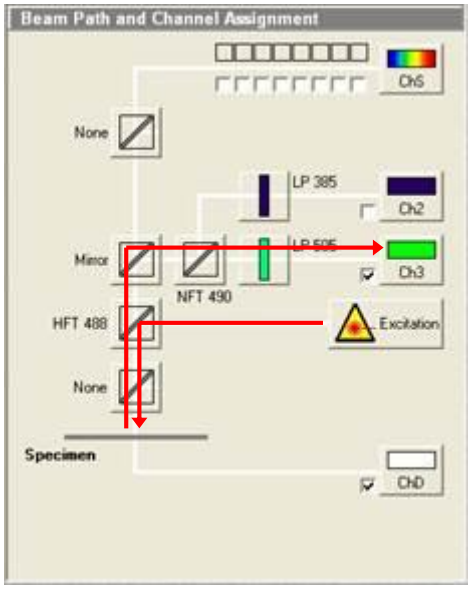

Fig. 2.3. Filter arrangement for LSM 510 meta. The red arrows indicate the path taken by the laser beam. The laser beam passes through the main colour separator (HFT) which only allows wavelengths above 488 nm to pass through. The laser beam is able to excite the fluorescent dye which is bound to the free calcium ions. The emitted light from the dye is passed back through the HFT filter and is reflected by the mirror towards the detector. The second filter (NFT) only allows wavelengths of above 490 nm to pass. A further long pass (LP) filter only allows wavelengths of above 505 nm to pass to the detector.

2.3.5.1. Voltage activated calcium signalling

For measurements of voltage stimulated calcium current inhibition the cells were imaged for 3 seconds per picture. The custom made perfusion chamber (Boehringer Ingelheim) allowed for depolarisation of the cells to be achieved via electrical stimulation. The cover slip was mounted onto the chamber and secured with vaseline. A custom made 'lid' was used, this allowed for solutions to be applied and aspirated away, but also had 2 electrodes which lay flat on the surface of the coverslip. The electrodes were connected to the amplifier (type 215/12; Hugo Sachs Elektronik, Germany) and using voltages between 15-21 V depolarisation was achieved. This was done using a train of 30 pulses (i.e. depolarisations) at a speed of 10 Hz, for 3 seconds. A protocol was run where the voltage stimulation was applied at two time points: 9 and 164 seconds. The compound or vehicle control was applied for 90 seconds prior to the second stimulation. Different concentrations of the sst_4 receptor agonist J-2156 (10, 30 and 100 nM) were tested and the ratio of the peaks at 9

and 164 seconds was calculated. The protocol lasted a total of 180 seconds. Cells were identified as responders to J-2156 if the second peak was less than the mean plus 2 times the S.E.M. of the initial control peak.

To confirm that modulation was via the PKA pathway, experiments were performed in which the cells were pre-treated with pertussis toxin (100 ng/ml) for 16 hours prior to the protocol being run to uncouple G_i proteins from GPCRs (Table 2.3).

For further testing of specific blockers (Table 2.3) to determine which voltage sensitive calcium channels might be influenced, or to establish if the hyperpolarisation caused by GIRK activation influences the inhibition, a triple stimulation protocol was run. Principally the protocol is the same, depolarisation was induced via voltage stimulation, and then 90 seconds prior to the second or third stimulation, compound was applied. With the specific blockers these were applied alone first, then in combination with J-2156 (100 nM) (Fig. 2.4). With the GIRK influence, first the J-2156 (100 nM) effect was established, then in combination with the GIRK specific blocker tertiapin Q (500 nM) (Fig. 2.4).

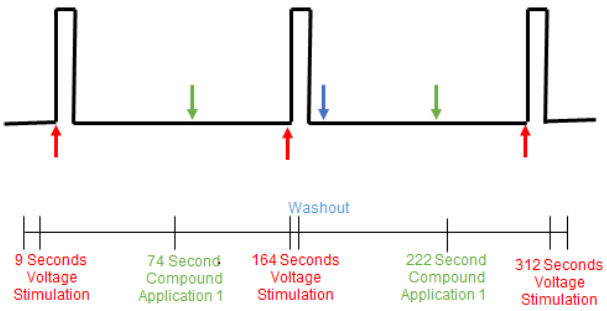

Fig. 2.4. Description of the triple stimulation calcium imaging protocol. The cells were stimulated 3 times with a 3 second voltage at 9, 164 and 312 seconds (red arrows). The specific Ca_v blockers or vehicle control was applied for 90 seconds prior to the second stimulation (green arrow). A second compound application was given at 90 seconds prior to the last stimulation (green arrow). This was either vehicle control, J-2156 in combination with the specific Ca_v blockers or tertiapin Q. A washout of 3 mL Ringer buffer, was applied after the second stimulation (blue arrow). The protocol lasted a total of 330 seconds.

For the triple stimulation protocol the ratio of both the second and the third peaks to the first peak was calculated. Data were normalized to the maximal effect, of all voltage gated calcium channel blockers and graphs represent the relative response.

2.3.5.2. Transient receptor potential vanilloid 1 (TRPV1) channels

Activation of TRPV1 channels was achieved via application of 30 nM capsaicin (Table 2.3) for 30 seconds. The cells were imaged for 15 seconds per image capture. Two protocols were run. The first was a double stimulation protocol where capsaicin was applied at 2 time points: 30 and 430 seconds. After each capsaicin stimulation the cells were washed with 3 ml Ringer buffer. The compound or

vehicle control was applied for 3 minutes prior to the second stimulation, and the effect expressed the ratio of the 2 peaks.

The second protocol involved pre-incubation of the cells for 5 minutes with compound or vehicle control. The cells were then exposed to 30 nM capsaicin for 30 seconds followed by a washout of 3 ml Ringer buffer. Then 3 minutes later depolarisation was induced by 80 mM extracellular potassium solution. The percentage of the potassium response was calculated, i.e. the capsaicin response was normalized to the potassium response. The specific sst_4 agonist J-2156 was tested at different concentrations (0.1 pM – 1 µM) and the TRPV1 specific antagonist capsazepine (10 µM) (Table 2.3) was used as a positive control.

To confirm modulation was via the PKA pathway experiments were repeated in the presence of pertussis toxin (Table 2.3). The cells were pre-treated with pertussis toxin (100 ng/ml) for 16 hours prior to the second protocol being run.

2.3.5.3. Transient receptor potential ankyrin 1 (TRPA1) channels

Activation of TRPA1 channels was achieved by application of 10 µM "compound 6" (Gijsen *et al.*, 2010) (Table 2.3) for 60 seconds. The cells were imaged for 10 seconds per image capture. A double stimulation protocol was run where the cells were firstly pre-incubated with compound or vehicle control for 5 minutes. The cells were then exposed to 10 µM of compound 6 for 60 seconds, followed by a washout of 3 ml Ringer buffer and 80 seconds later depolarisation was induced by 50 mM extracellular potassium solution. The percentage of the potassium response was calculated, i.e. the compound 6 response was determined as a percentage of the potassium response. The TRPA1 antagonist A-967079 (Chen *et al.*, 2011) (Table 2.3) was tested as a positive control, confirming the validity of compound 6 to analyse TRPA1 antagonists. The specific sst_4 agonist J-2156 was tested at different concentrations (0.01 – 1000 nM) and capsazepine (10 µM) tested to confirm TRPA1 selectivity. Pertussis toxin was employed to confirm modulation was via the PKA pathway (Table 2.3). The cells were pre-treated with pertussis toxin (100 ng/ml) for 16 hours prior to the testing.

2.3.6. Myeloperoxidase (MPO) measurement

Myeloperoxidase (MPO) was measured as a biomarker of neutrophil infiltration (Giese *et al.*, 2003). MPO activity in the supernatants of paw samples, prepared as described above (section 2.2.12), was assessed using a peroxidase assay kit (Hycult Biotech, The Netherlands) following the protocol described in the manufacturer's instructions. Firstly 10 ml of the provided 10x dilution buffers A and B were mixed with 40 ml de-ionized water (dH_2O). These solutions were then combined and formed the dilution buffer. The MPO standards were prepared by firstly reconstituting the standard vial in dilution buffer (volume was indicated on vial and is described for each kit set). Serial dilutions were then prepared, using the dilution buffer, from 1:2 through to 1:64 dilution with an end concentration of 3.9 ng/ml. Initially 100 µl of standards or samples were applied to the assay plates in duplicates and incubated for 1 hour at room temperature (23 -24°C). Next, the biotinylated tracer antibody was

added to each well at a volume of 100 µl/well and further incubated for 1 hour at room temperature. The tracer was reconstituted in 1 ml dH_2O. The streptavidin-peroxidase solution was reconstituted in 1 ml dH_2O, then added to each well at a volume of 100 µl/well and the plates were further incubated for 1 hour at room temperature. After each of these steps the whole plate was washed 4 times with the provided assay wash buffer. This involved pipetting approximately 200 µl of wash buffer to each well, then inverting the plate and tapping gently on tissue paper. Finally, 100 µl of the provided tetramethylbenzidine solution was added to each well, followed by 100 µl of stop solution 30 minutes later. The plates were read immediately at 450 nm using an EnVision Xcite 2104 multilable reader (Perkin Elmer, Waltham, MA). A standard curve was created in Prism 6.0 for Windows and the sample concentration extrapolated using Prism 6.0 for Windows. The graph shows the concentration in the sample (pg/ml).

2.3.7. Inflammatory mediator stimulation from DRG neurons

The cells were plated on 96-well plates at 75000 cells/well, using the following method. Cultured DRG neurons were removed from the 6 well plate (section 2.3.3) and suspended in 50 ml DPBS (Sigma, Germany) in a falcon tube. This was centrifuged at 1200 rpm for 5 minutes. The culture medium was aspirated away and the cell pellet was washed by re-suspension in 50 ml DPBS, followed by another centrifuge. This washing step was repeated three times. The cells were counted using 0.4% trypan blue stain (Introvegen, life technologies, Germany) and the countless automated cell counter (Introvegen, life technologies, Germany). After the final wash the DPBS was aspirated off and the cells re-suspended in the appropriately calculated volume of either DMEM (for cytokines and PGE_2) or HEPES buffer (for CGRP).

For determination of cytokine and prostaglandin E_2 (PGE_2) release the cells were exposed 100 ng/ml lipopolysaccharides from Escherichia coli (LPS, Sigma, USA) in the presence of test compound or vehicle control. This was done in DMEM buffer containing 1% penicillin-streptomycin (Sigma, Germany), 1% FCS (Gibco, UK) and 1 µM phosphoramidon (Sigma, USA) for 24 hours at 37°C, 10% carbon dioxide and with a humidity of 95%; the final volume was 200 µl/well. The sst_4 receptor agonist J-2156 was tested over a range of concentrations (1 – 1000 nM); indomethacin (1 µM) (Table 2.3) and celecoxib (1 µM) (Table 2.3) were tested as positive controls.

To measure CGRP release the cells were pre-exposed to the compounds for 30 minutes, the sst_4 receptor agonist J-2156 (1000 nM) was tested, TTX (100 nM) (Table 2.3) and capsazepine (10 µM) (Table 2.3) were used as positive controls. Following this cells were stimulated with either 100 nM capsaicin (Table 2.3), 100 µM veratradine (Table 2.3) or 56 mM potassium solution; all of which were prepared in HEPES buffer (25 mM/L HEPES; 135 mM/L NaCl; 3.5 mM/L KCl; 2.5 mM/L $CaCl_2$; 1 mM/L $MgCl_2$; 3.3 mM/L Glucose; 0.1% BSA; pH adjusted to 7.4 using 1 M NaOH) containing 1 µM phosphoramidon for 30 minutes at 37°C, 10% carbon dioxide and 95% humidity. This was in combination with either the compound or as a vehicle control, where the end volume was 200 µl/well.

For all studies samples were centrifuged for 5 minutes at 1200 rpm. Supernatant fractions were kept frozen at -20°C until use.

2.3.7.1. Measurement of cytokines

Cytokine levels were measured, in preparations of paw samples and DRG neurons, using a custom MSD (Mesoscale discovery, Rockville, MD) analysis kit in conjunction with the MSD system array reader according to the protocol described in the manufacturer's instructions. This was a multi-spot plate and was used to determine the levels of TNFα, IL1β, IL6, MCP1, IFNγ and IL10. Briefly, 25 µl of diluent 6 was added to each well and incubated for 30 minutes with vigorous shaking (600 rpm) at room temperature (23-24°C). This ensured specific binding, meaning diluent 6 coated the base of the well which had no spot of anti-body for the specific cytokine, therefore ensuring no unspecific binding. The same volume of standards or samples was added to duplicated wells and left to incubate overnight at 4°C. The standard solution was prepared by combining 10 µl of each of the individual cytokine stock solutions with 450 µl of diluent 6 and mixing well, where the initial concentration of the standard was 40000 pg/ml of each cytokine. Serial dilutions were then prepared, using diluent 6, firstly with a 1:24 dilution, followed by 1:4 dilutions through to an end concentration of 2.4 pg/ml. The plate was washed 3 times with PBS + 0.05% Tween-20 (Calbiochem, Germany). This was done at a volume of approximately 200 µl/well and the plates were innervated and tapped gently on tissue paper between washes. Following this 25 µl of the detection antibody solution was added to each well and further incubated for 2 hours at room temperature, with vigorous shaking before washing. Finally, 150 µl of the read buffer T was added to each well and the plate analysed on the SECTOR® imager. A standard curve was created in MSD system array reader for Windows and the sample concentration extrapolated. For paw cytokine levels the graphs show the concentration of the cytokines in the sample (pg/ml). With the stimulated DRGs the graphs show the percentage inhibition of the LPS effect, as repeats were run.

2.3.7.2. Prostaglandin E2 (PGE_2) release

PGE_2 levels were measured using a homogeneous time resolved fluorescent (HTRF) detection assay (Cisbio Bioassays, EU), in 384 FIA black plates (Greiner bio-one, Germany), according to the protocol described in the manufacturer's instructions. The PGE_2 standards were prepared by reconstituting the standard vial in reconstitution buffer (volume was indicated on vial and is described for each kit set) to give a concentration of 5000 pg/ml; then serial dilutions were prepared, using the provided assay diluent, from 1:2 through to a final concentration of 2.29 pg/ml. For a negative control the standard was replaced by assay diluent, while PGE2-d2 was replaced by reconstruction buffer. For the positive control only the standard was replaced by assay diluent. Firstly 5 µl of PGE2-d2 was added to each well, then 10 µl of standard or samples run in duplicates and finally 5 µl of anti-PGE2 cryptate. This was incubated overnight at 4°C. The plate was read using an EnVision Xcite 2104 multilable reader (Perkin Elmer, Waltham, MA) at 665 nm. A standard curve was created in Prism 6.0 for Windows, enabling the sample concentrations to be extrapolated. As

repeat experiments were conducted the percentage inhibition of the LPS effect was calculated, and are presented in the graph.

2.3.7.3. Calcitonin gene-related peptide (CGRP) release

CGRP levels were measured using an enzyme immunoassay (EIA) kit (SPI bio, France) according to the protocol described in the manufacturer's instructions. Standards were prepared by reconstitution of the provided CGRP in 1 ml EIA buffer to give a concentration of 500 pg/ml. Serial dilutions were then prepared, using EIA buffer, from 1:2 through to an end concentration of 3.9 pg/ml. Firstly, 100 µl of the standards or samples were added to the wells in duplicates. For the non-specific binding 100 µl of the EIA buffer was used. To allow for immunological reaction, 100 µl of the CGRP tracer was added to each of the wells, except the blank ones. This was then incubated overnight at 4°C. The tracer was prepared by reconstitution of the provided vial with 10 ml EIA buffer. The plate was washed 6 times with assay wash buffer, approximately 300 µl was added to each well, this was then emptied by innervation and excess removed by tapping on tissue paper. The wash buffer was prepared by mixing 1 ml of the provided concentrated wash buffer with 400 ml dH_2O and 200 µl of Tween-20 (Calbiochem, Germany). Finally 200 µl of freshly-prepared Ellman´s reagent was added to each well and the plate was incubated in the dark for 30-60 minutes, with constant shaking (400 rpm) at room temperature (23-24°C). The plate was read on a Flexstation 3 machine (Molecular Devises, Germany) at 414 nm. Using Prism 6.0 for Windows a standard curve was created and the sample concentration extrapolated. The graphs show the ratio of the stimulation to buffer.

2.3.8. Next generation sequencing (NGS)

Total RNA was extracted using the MagMAC-96 Total RNA Isolation kit (Life Technologies, Germany). This was done by following the protocol described in the manufacturer's instructions. Initially a phenol/chloroform extraction was performed and samples were plated on the assay plate. For initial nucleic acid purification 5 µl of the provided bead mix (RNA binding beads) was added to each sample and the plate was shaken for 5 minutes. The beads were magnetically captured using an Ambion 96-well magnetic stand (Life Technologies, Germany) and the supernatant discarded. The wells were then washed using 150 µl of 2 provided wash solutions for 1 minute each while shaking. The provided diluted TURBO DNase was then added at a volume of 50 µl/well and was incubated for 15 minutes with continuous shaking. Next, 100 µl of the provided RNA rebinding solution was added and left for a further 3 minutes while shaking in order to rebind the RNA. The beads were again magnetically captured and the supernatant discarded, these were then washed twice with the provided wash solution 2 at a volume of 150 µl/well. The beads were dried by shaking for 2 minutes and the RNA eluted using 50 µl of the provided elution buffer.

The sequencing library was prepared using 200 ng of total RNA input with the TrueSeq RNA sample prep kit v2 – set B (Illuminae Inc., San Diego, CA). This produced fragments, including adapters, with an average size of 275 bp. Directly before sequencing 8 individual libraries were normalized and pooled together using the adapter indices supplied by the manufacturer. Pooled libraries were then

clustered on the cBot instrument, using the TruSeq SR cluster kit V3 – cBot – HS (Illuminae Inc., San Diego, CA). Sequencing was then performed as S2 bp single reads and 7 base index reads, on an Illuminae HiSeq 2000 instrument using the TruSeq kit HS – V3 (52 cycles) (Illuminae Inc., San Diego, CA). Comparisons were made between the different time points and the different treated groups. Analysis was conducted using Spotfire 6.5 for Windows (TIBCO, USA), with diagrams prepared using Ingenuity® for Windows (Ingenuity, USA). Paw skin and DRGs were analysed. *The NGS data was performed by the lab of Tobias Hildebrant by Sussanne Acker.*

2.3.9. Statistics

Graphs were produced in Prism 6.0 for Windows (GraphPad Software, San Diego, USA). Data are expressed as mean±S.E.M. To test for normal distribution the Kolmogorov-Smirnov test was used, which indicated whether parametric or non-parametric tests should be used. A student's T-test was used when comparing only 2 samples. When more than one concentration was tested, a one-way ANOVA was performed, followed by Bonferroni post-hoc tests. A *P* value of <0.05 was deemed significant.

3. Results

3.1. Characterisation of somatostatin agonists

Within the literature, various somatostatin receptor agonists have been described. In order to identify an appropriate pharmacological tool for future proof of concept and mode-of-action studies, several ligands were characterised in order to establish their selectivity, affinity and potency for the sst_4 receptor.

3.1.1. Selectivity studies

Studies were conducted in order to determine the selectivity and affinity of the various compounds described, to the different somatostatin receptors, identifying those which are selective for the receptor subtype 4. Experiments were performed using cell membranes from CHO-K1 cells which expressed the different receptor subtypes. Competitive radioligand binding assays were conducted using [^{125}I]-Tyr3-somatostatin-(1-14) in order to confirm binding of the ligands to the receptors.

Compound	$Hsst_1$	$Hsst_2$	$Hsst_3$	$Hsst_4$	$Hsst_5$
Somatostatin 14 (N = 6)	-9.27±0.02	-8.67±0.1	-10.16±0.08	-9.55±0.06	-9.18±0.06
Somatostatin 28 (N = 3)	-9.86±0.30	-8.55±0.01	-10.20±0.02	-9.44±0.10	-9.28±0.03
Corticostatin 17 (N = 3)	-8.32±0.10	-7.47±0.01	-8.61±0.02	-8.60±0.06	-8.26±0.05
Example32 (N = 5)	-7.33±0.05	-5.89±0.61	-6.86±0.06	-9.06±0.18	-6.48±0.12
J-2156 (N = 4)	-6.23±0.18	-4.60±0.37	-6.63±0.18	-9.25±0.09	-6.33±0.17
L803,087 (N = 3)	-5.69±0.26	-5.95±0.73	-6.46±0.21	-8.68±0.06	-4.91±0.25
TT-232	-6.58; -5.16	-4.61; -3.11	-4.96; -5.10	-6.85; -6.06	-5.09; -5.34
Octreotide	-6.68; -6.66	-8.38; -8.25	-8.16; -8.20	-3.78; -5.40	-7.74; -7.63

Table 3.1. Selectivity of somatostatin agonists of the human receptor subtypes heterologously expressed in CHO-K1 cell membranes. The affinity and selectivity of various somatostatin agonists for the 5 human somatostatin receptor subtypes were established using radioligand binding assays. The results show the mean±S.E.M.. log Ki of the compounds (N=3-6), unless specific results are indicated (when N= 2). Data were obtained by non-linear regression analysis of the concentration response curves.

Table 3.1 summarizes the affinity, presented as inhibition constant Ki, of the various compounds tested, for the different receptor subtypes. The Cheng Prusoff equation was used to derive the Ki values of the compounds. This was calculated with Prism 6.0 for Windows, using the setting of 'one site – Fit Ki'. Constraints were applied: both the concentration of radioligand in nM (HotNM = 0.05 nM) and the equilibrium dissociation constant (kd) of the radioligand in nM (HotKdNM for sst_1 = 0.85 nM; sst_2 = 1.2 nM; sst_3 = 0.31 nM; sst_4 = 0.45 nM; sst_5 = 2.0 nM). The somatostatin receptor selective endogenous ligands, somatostatin 14 and somatostatin 28, as well as the non-selective endogenous ligand, corticostatin 17, were used as positive controls. These showed nM affinity for all subtypes, therefore indicating no selectivity for a specific receptor subtype, but consistently showed least affinity for the sst_2 receptor. The BI-produced compound 'Example32' had highest affinity for the sst_4 receptor; however this compound was not highly selective, as it also had nM affinity for the receptor subtype 1. Although TT-232 was selective for the sst_4 receptor, the affinity was lower in comparison to the other ligands tested as it only demonstrated μM affinity, additionally comparable affinity was seen for the sst_1 receptor. Octreotide had nM affinity for receptor subtypes 2, 3 and 5, suggesting selectivity to these receptor subtypes; low affinity was seen at the sst_4 receptor. The data identified J-2156 and L803,087 as selective sst_4 receptor agonists with nM affinity for this receptor and over 300 fold selectivity for the sst_4 subtype. Figure 3.1 shows typical selectivity binding curves for somatostatin 14, a non-selective ligand with nM affinity for all receptor subtypes (A) and J-2156, a highly selective compound with low affinity for most receptor subtypes except sst_4 receptors (B).

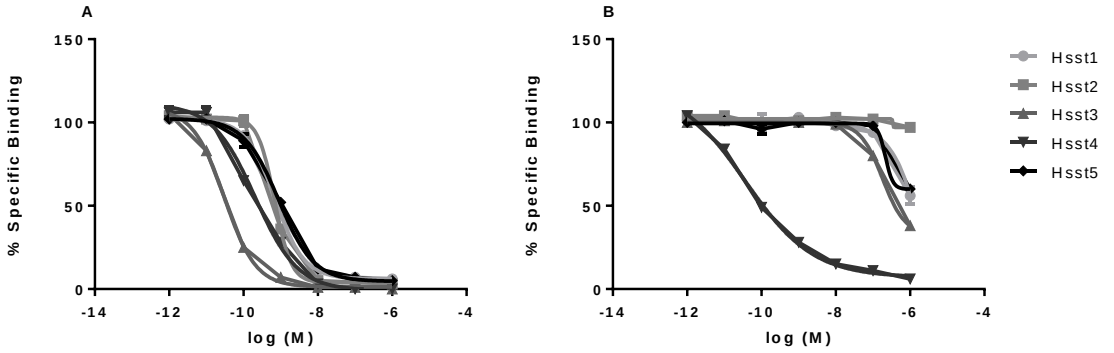

Fig. 3.1. Binding curves for the human somatostatin receptors. Typical binding curves to determine the affinity of somatostatin 14 (A) and J-2156 (B) for the human sst_4 receptor. No selectivity was seen for the endogenous ligand somatostatin 14, while J-2156 was more than 400 fold selective for the sst_4 receptor subtype. Competitive binding assays were run using ^{125}I radiolabelled somatostatin 14 (0.05 nM) in the presence of 0.5 μg protein. The results are presented at % of specific binding.

3.1.2. Affinity for the rat sst$_4$ receptor

The previous data had identified the selectivity and affinity of various agonists for the five human somatostatin receptor subtypes. However, as a basis for future experiments it was important to confirm that these compounds had similar affinity at the rat form of the sst$_4$ receptor subtype. In order to do this, competitive radioligand binding assays were conducted, using cell membranes from CHO-K1 cells which expressed the rat form of the sst$_4$ subtype. The Cheng Prusoff equation was used to derive the Ki values of the compounds, this was calculated as stated above but the kd value for rat sst$_4$ = 0.26 nM.

Compound	Rsst$_4$
Somatostatin 14	-9.42±0.06
Somatostatin 28	-8.83±0.76
Corticostatin 17	-9.04±0.31
Example32	-9.30±0.26
J-2156	-9.05±0.40
L803,087	-8.60±0.53
TT-232	-6.66; -6.87
Octreotide	-6.87; -6.65

Table 3.2. Affinity of somatostatin agonists for the rat sst$_4$ receptor. The affinity of various somatostatin agonists was determined for the rat sst$_4$ receptor subtype using radioligand binding assays. The results show the mean±S.E.M.. log Ki of the compounds (N=3), unless individual results are indicated (N= 2). Data was obtained by non-linear regression analysis of the dose response curves.

Table 3.2 shows the affinity of the various compounds tested on the rat sst$_4$ receptor subtype. The endogenous ligands, somatostatin 14 and somatostatin 28, and corticostatin 17, as well as the peptide mimetics, Example 32, J-2156 and L803087 also showed nM affinity for the rat sst$_4$ receptor. The Ki values were comparable to those for the human receptor, with less than 3 fold difference seen in each case. Again TT-232 and octreotide had low affinity to the sst$_4$ receptor.

3.1.3. Potency of somatostatin agonist: cAMP inhibition

It was also important to confirm that these compounds were able to functionally activate the receptor, i.e. to determine the potency of the compounds. For these experiments intact H4 cells expressing either the human or rat sst_4 receptor were used.

Compound	**$Hsst_4$**	**$Rsst_4$**
Somatostatin 14	-9.7±0.2	-9.8±0.4
Somatostatin 28	-9.1±0.5	-9.7±0.1
Corticostatin 17	-8.5±0.1	-9.0±0.2
Example32	-10.2±0.2	-10.2±0.1
J-2156	-10.3±0.2	-10.1±0.1
L803,087	-10.2±0.2	-9.6±0.1
TT-232	-6.8±0.1	-6.1±0.04
Octreotide	-5.8±0.1	-5.6±0.1

Table 3.3. Potency of somatostatin agonists for the human and rat sst_4 receptor. The efficacy of various somatostatin agonists was determined for both the human (H) and rat (R) sst_4 receptor subtype using cAMP assays. The results show the mean±S.E.M.. log IC_{50} of the compounds. Data was obtained by non-linear regression analysis of the dose response curves. N=3.

Table 3.3 shows the potency of the various compounds tested on the human and rat sst_4 receptor subtypes. These results are presented as IC_{50} values, showing the concentration of ligand producing 50% inhibition of the forskolin-stimulated cAMP production. The IC_{50} values were calculated with Prism 6.0 for Windows using the equation 'log(inhibitor) vs. normalised response'; constraints were applied to the bottom value, which was set to the maximal inhibition produced by somatostatin 14. The endogenous ligands somatostatin 14, somatostatin 28 and corticostatin 17, as well as all the peptide mimetics had nM potency for the human and rat sst_4 receptor. Octreotide was unable to inhibit cAMP production, indicating low potency at either the human or rat sst_4 receptor. Typical cAMP curves for somatostatin 14 and J-2156 are shown in figure 3.2. The potency of the compounds was comparable for the two species; with less than 3-fold difference seen in each case. These results confirm that the sst_4 receptor can functionally couple to the adenylyl cyclase pathway.

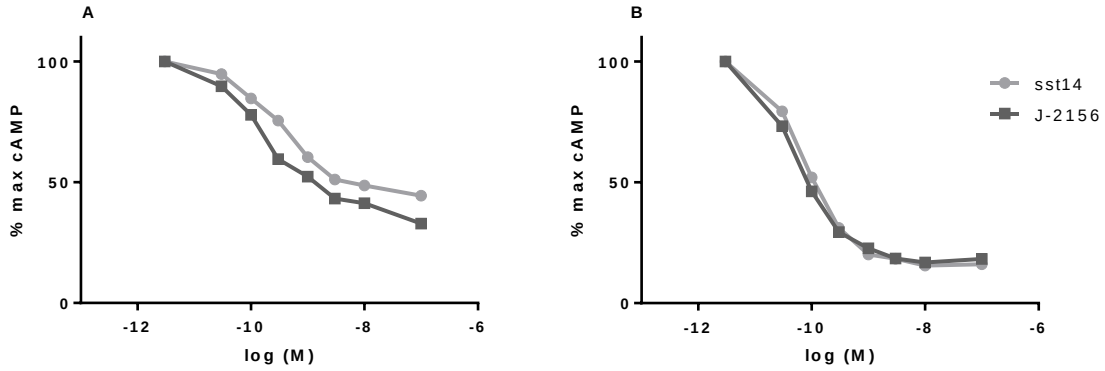

Fig. 3.2. Inhibition of cAMP production by sst_4 receptors. Typical concentration response curves to determine the ability of somatostatin 14 and J-2156 to inhibit cAMP production in H4 cells expressing the rat (A) and the human (B) sst_4 receptor subtypes, stimulated by forskolin (30 µM rat and 10 µM human). The results are presented as % of maximal cAMP concentration.

3.1.4. Identification of tool compounds

These observations showed that, with the exception of octreotide, all the compounds tested had strong affinity as well as potency for both the human and rat sst_4 receptor. Interestingly, while the endogenous ligands had comparable affinity and potency for the receptor, the peptide mimetics had higher potency than affinity. In the case of J-2156 and L803,087 a 11-fold and 34-fold difference was seen respectively for the human receptor (Table 3.1 and Table 3.3); and a 12-fold and 10-fold difference for the rat receptor respectively (Table 3.2 and Table 3.3).

Overall these results identified J-2156 and L803,087 as the most appropriate tool compounds for future experiments, as these not only had nM affinity and potency but were also highly selective for the sst_4 receptor subtype. J-2156 was selected for use in future studies.

3.2. Efficacy of sst_4 receptor agonist, J-2156, on rat pain models

In order to determine whether the sst_4 receptor agonist J-2156 was effective in causing analgesia in both nociceptive and neuropathic pain conditions, established animal models of pain were used. Mechanical hyperalgesia was measured in the Complete Freund´s Adjuvant (CFA), partial nerve ligation (PNL) and streptozotocin (STZ) models, while weight bearing deficits were measured in the monosodium iodacetate (MIA) model. Signs of behavioural side effects were not observed in rats treated with J-2156 in any of the experimental settings. Rats treated with indomethacin were euthanized at the end of the study to prevent lethal gastrointestinal (GI) effects.

3.2.1. Plasma exposure of J-2156

Plasma concentration data of J-2156 from experiments are compiled in Table 3.4. After i.p. administration of 0.1 mg/kg J-2156 to naïve animals the compound showed an early time of maximal plasma concentration (tmax) between 5 and 15 minutes (Fig 3.3). The J-2156 concentrations in plasma samples taken from CFA or MIA pain models treated with higher compound doses and different sampling time points indicate an approximately dose proportional increase of plasma J-2156 concentration following i.p. administration of compound doses ranging from 0.1 mg/kg up to 10 mg/kg (Table 3.4).

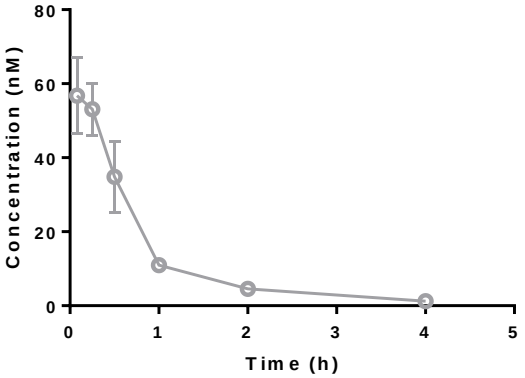

Fig. 3.3. Plasma exposure of J-2156. Naïve rats were administered 0.1 mg/kg (i.p) for assessment of pharmacokinetic properties. Plasma was sampled at regular intervals. After 4 hours the levels of J-2156 in the plasma were below the limit of quantification. A peak in plasma concentration was seen at 5 minutes. The levels decreased exponentially over time. mean±S.D.. N=3.

Dose (mg/kg, i.p.)	**0.1**	**1**	**10**
time [h]	**J-2156 plasma concentration [nM]**		
1	11.0±2.71	-	-
1.5	8.27±6.89[A]	67.3±26.9[A]	-
2	4.54±2.69	-	391±213[B]
4	1.90±1.24	-	162±45[B]
24	Blq	Blq[A]	Blq[B]

Table 3.4. Plasma concentration of J-2156 taken from different in house *in vivo* studies in rats. Blood samples were taken from naïve rats treated with 0.1 mg/kg J-2156, i.p. for basic assessment of pharmacokinetic parameters. Dose proportionality of plasma concentration was confirmed in samples taken from CFA (A) and MIA rats (B). Blq=below limit of quantification (1.0-2.5 nM). – represents the time points at which no plasma was sampled. N=3-8.

3.2.2. Nociceptive pain models

CFA rat model: Intraplantal injection of 25 µg of CFA reduced the pain threshold of rats by 50±3% (P<0.0001 vs. naïve; n=12; Fig 3.4A). Twenty-four hours after CFA injection, doses ranging from 0.01 to 1 mg/kg of J-2156 were administered and behavioural studies performed 1 hour later. J-2156 dose-dependently increased pain threshold. Significant increases in paw withdrawal threshold (PWT) were seen in doses as low as 0.1 mg/kg, with an increase of 39±20% (P<0.05 vs. vehicle; n=10; Fig. 3.4A), producing 73±10% of the sham response. Maximal effects were produced by doses of 1 mg/kg, where J-2156 caused a significant increase in PWT by 77±15% (P<0.01 vs. vehicle; n=10;

Fig. 3.4A). This effect was not significantly different to the control naïve or sham animals, inducing 93±8% of the sham response (NS; n=10; Fig 3.4A). Furthermore, the effect was comparable to that of 30 mg/kg indomethacin (NS; n=10; Fig 3.4A), which was used as a positive control.

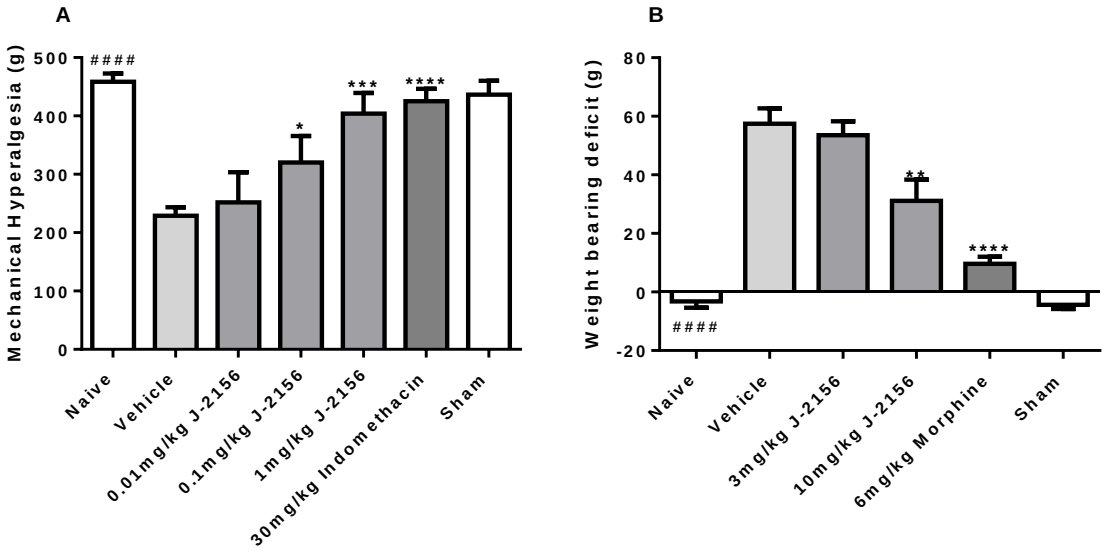

Fig. 3.4. Effect of J-2156 on nociceptive pain models in the rat. (A) Effects of J-2156 on CFA-induced mechanical hypersensitivity in the rat. Twenty-four hours post intraplantarly injection of CFA, vehicle, J-2156 and indomethacin were administered and tests performed 1 hour later. Significant increases in pain threshold were produced by doses as low as 0.1 mg/kg J-2156, and the efficacy of 1 mg/kg was comparable to 30 mg/kg indomethacin. (B) Effects of J-2156 on MIA-induced weight bearing deficit in the rat. At day 3 post intraarticular injection of MIA, vehicle, J-2156 and morphine were administered and at 1 hour after administration significant decreases in weight bearing were produced by 10 mg/kg J-2156 and 6 mg/kg morphine. Data are presented as mean±S.E.M.. N=9-10 rats/group. *P<0.05, **P<0.01, ***P<0.001 and ****P<0.0001 vs. vehicle treated group or $^{####}$P<0.0001 vs. naïve (ANOVA).

MIA rat model: Intraarticular injection of 1 mg MIA induced a weight bearing deficit in rats, with a significant increase compared to the naïve animals (P<0.0001 vs. naïve; n=9; Fig 3.4B). In this model the sst_4 selective agonist, J-2156, was given at 3 days post MIA injection at doses of 3 and 10 mg/kg. Behavioural studies were conducted at 1 hour after compound administration. Experiments showed no efficacy for J-2156 at 0.1 and 1 mg/kg in this model (data not shown). Although 3 mg/kg J-2156 was without effect, 10 mg/kg J-2156 caused a significant reduction in weight bearing deficit of 46±12% (P<0.01 vs. vehicle; n=10-11; Fig. 3.4B), however this was still significantly different from the control naïve and sham rats (P<0.0001 vs. naïve or sham; n=9; Fig 3.4B). In this model 6 mg/kg morphine also showed a significant reversal of weight bearing deficit at 1 hour post compound administration (P<0.0001 vs. vehicle; n=10; Fig. 3.4B).

3.2.3. Neuropathic pain models

STZ rat model: The streptozotocin (STZ) model is a drug-induced model of diabetic neuropathy (Jaggi *et al.*, 2011). Intraperitoneal injection of 65 mg/kg STZ significantly reduced the pain threshold of rats by 46±2% (P<0.0001 vs. naïve; n=8; Fig. 3.5A). Three weeks after the STZ injection, the sst_4 selective agonist, J-2156, was given at doses from 0.01 to 1 mg/kg and behavioural studies were conducted 1 hour after compound administration. J-2156 caused a significant increase in paw withdrawal threshold (PWT) starting from the lowest dose of 0.01 mg/kg with an increase of 38±13% (P<0.05 vs. vehicle; n=8; Fig. 3.5A), producing 74±7% of the naïve response. Maximal effects were reached at 1 mg/kg, where an increase of 51±7% was seen (P<0.001 vs. vehicle; n=8; Fig. 3.5A), which was not significantly different from duloxetine (NS; n=8; Fig. 3.5A). The reversal induced by the highest dose was however significantly different from the naïve result, producing 80±4% of the naïve response (P<0.05 vs. naïve; n=12; Fig. 3.5A).

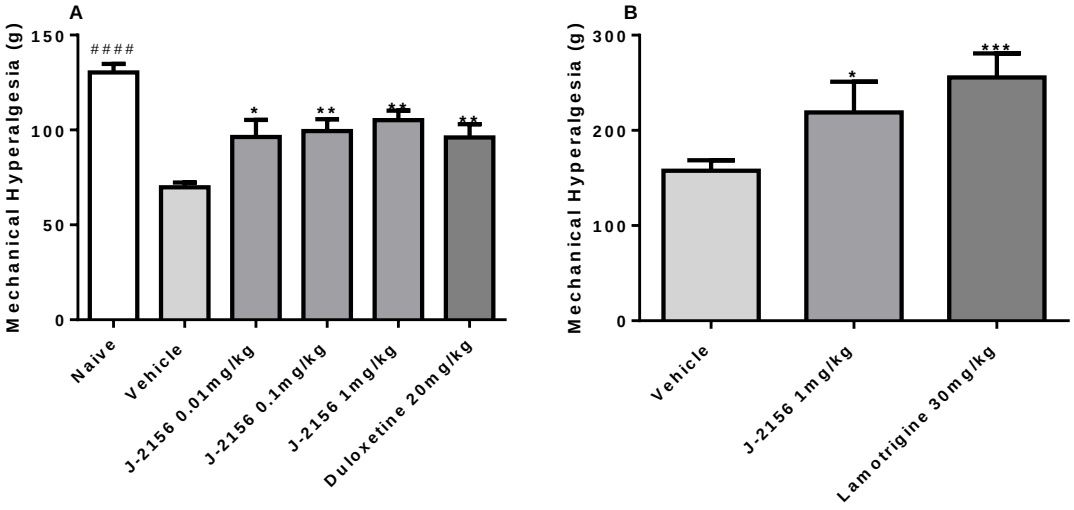

Fig. 3.5. Effect of J-2156 on neuropathic pain models in the rat. (A) Effects of J-2156 on STZ-induced mechanical hypersensitivity in the rat. Three weeks post STZ injection (65 mg/ml, i.p.), J-2156 and duloxetine were administered and mechanical sensitivity was tested 1 hour later. Significant increases in pain threshold were observed at doses as low as 0.01 mg/kg J-2156, which was not significantly different from duloxetine. (B) Effects of J-2156 on PNL-induced mechanical hypersensitivity in the rat. At two weeks after PNL surgery, J-2156 was administered and rats were behaviourally tested 1 hour later. In the same study lamotrigine was administered and rats were tested 2 hours later (as positive control). Data are presented as mean±S.E.M.. N=8-12 rats/group. *P<0.05, **P<0.01 and ***P<0.001 vs. vehicle-treated group or $^{\#\#\#\#}$P<0.0001 vs. naïve (ANOVA).

PNL rat model: Two weeks after nerve injury, PNL rats develop hypersensitivity to noxious stimuli resulting in a significant decrease in PWT (Seltzer *et al.*, 1990). At this time point 1 mg/kg J-2156 was administered and behavioural studies were conducted at 1 hour after compound administration.

J-2156 was only tested at 1 mg/kg as this was shown to be effective in the STZ model and would therefore reduce the number of rats used. This dose caused a 39±20% increase in mechanical threshold (P<0.05 vs. vehicle; n=9; Fig. 3.5B), which was not significantly different from lamotrigine (NS; n=7; Fig. 3.5B). For this model sham rats were not used however previous in-house data has shown a difference in PWT in comparison to the PNL rats, where values of both 324±27 g and 328±7 g have been recorded (results not shown).

3.2.4. Long lasting analgesia in chronic pain models

In order to determine whether the analgesic effects of the sst_4 receptor selective agonist J-2156 were long lasting in the animal models of pain, mechanical hypersensitivity was measured in the CFA and PNL models, while weight bearing deficit was assessed in the MIA model. In a separate study effects were assessed at 1 hour, for confirmation, and then at 24 hours post J-2156 administration, for comparisons, in order to get a time course of the analgesic effect.

CFA rat model: In the CFA model the sst_4 receptor selective agonist, J-2156, was given at a dose of 1 mg/kg, as this was previously established to be a fully efficacious dose (Fig. 3.4A). To confirm these effects, behavioural studies were performed 1 hour after administration at 24 hours after CFA injection. J-2156 caused a significant increase in paw withdrawal threshold by 43±10% (P<0.01 vs. vehicle; n=13; Fig. 3.6A). This effect was not significantly different from the effect of 30 mg/kg indomethacin (NS; n=13; Fig. 3.6A). This confirms the previous data. Prolonged efficacy of J-2156 was assessed by dosing the compound at 24 hours post CFA injection and behavioural tests were assessed 24 hours later, so at 48 hours after CFA injection i.e. a CFA 48 hours model. J-2156 caused a similar effect, increasing the PWT by 54±13% (P<0.01 vs. vehicle; n=13; Fig. 3.6B), which was not different from the acute effect of indomethacin at 1 hour post dosing in the CFA 48 hours model (NS; n=13; Fig. 3.6B). At 48 hours after CFA injection J-2156 caused a significant increase in PWT when tested at 1 hour post dosing (P<0.05 vs. vehicle; n=13-14; results not shown).

MIA rat model: In the MIA model the sst_4 receptor selective agonist, J-2156, was given at 3 days post MIA injection at 10 mg/kg, as this was previously established to be a fully efficacious dose (Fig. 3.4B). Behavioural studies were conducted at 1 and 24 hours after compound administration. At 3 days post MIA injection, J-2156 caused a significant reduction in weight bearing deficit by 37±10% (P<0.05 vs. vehicle; n=10-11; Fig. 3.6C). In this model also 6 mg/kg morphine showed a significant reversal of weight bearing deficit at 1 hour post dosing (P<0.0001 vs. vehicle; n=10; Fig. 3.6C). This confirms the previous data. The analgesic effects of J-2156 were still significant at 24 hours after compound administration (i.e. at day 4 post MIA injection) with a reduction weight bearing deficit of 55±8% (P<0.01 vs. vehicle, n=10-11; Fig. 3.6D). At 4 days after MIA injection J-2156 caused a significant decrease in weight bearing deficit when tested at 1 hour post dosing (P<0.001 vs. vehicle; n=10-11; results not shown). In this model morphine shows a peak at 1 hour and a further decrease over time. By 24 hours the effect of morphine in the MIA model is resolved (Fig. 3.6D). Therefore in this study morphine was used as a positive control, but in another group of rats tested at 1 hour after

administration at the 4 day time point, where analgesic effects were confirmed (P<0.001 vs. vehicle; results not shown).

There were no detectable levels of J-2156 in the plasma at 24 hours post compound administration (Table 3.4), it could therefore be assumed that this long lasting analgesic effect is not directly correlated to the compound exposure at the time of the measurements.

PNL rat model: Experiments were conducted 2 weeks after induction of nerve injury. J-2156 was previously shown to have analgesic effects at 1 hour post compound administration when dosed at 1 mg/kg (Fig. 3.5B). In the same study it was also investigated whether the anti-hypersensitivity effects of J-2156 were still present 24 hours after compound administration. Surprisingly, no increase in paw withdrawal threshold was present at this time point (n=10-14; NS vs. vehicle; Fig. 3.7); lamotrigine was used as positive control and 2 hours after administration induced a significant increase in PWT (P<0.001 vs. vehicle; n=8; Fig. 3.7).

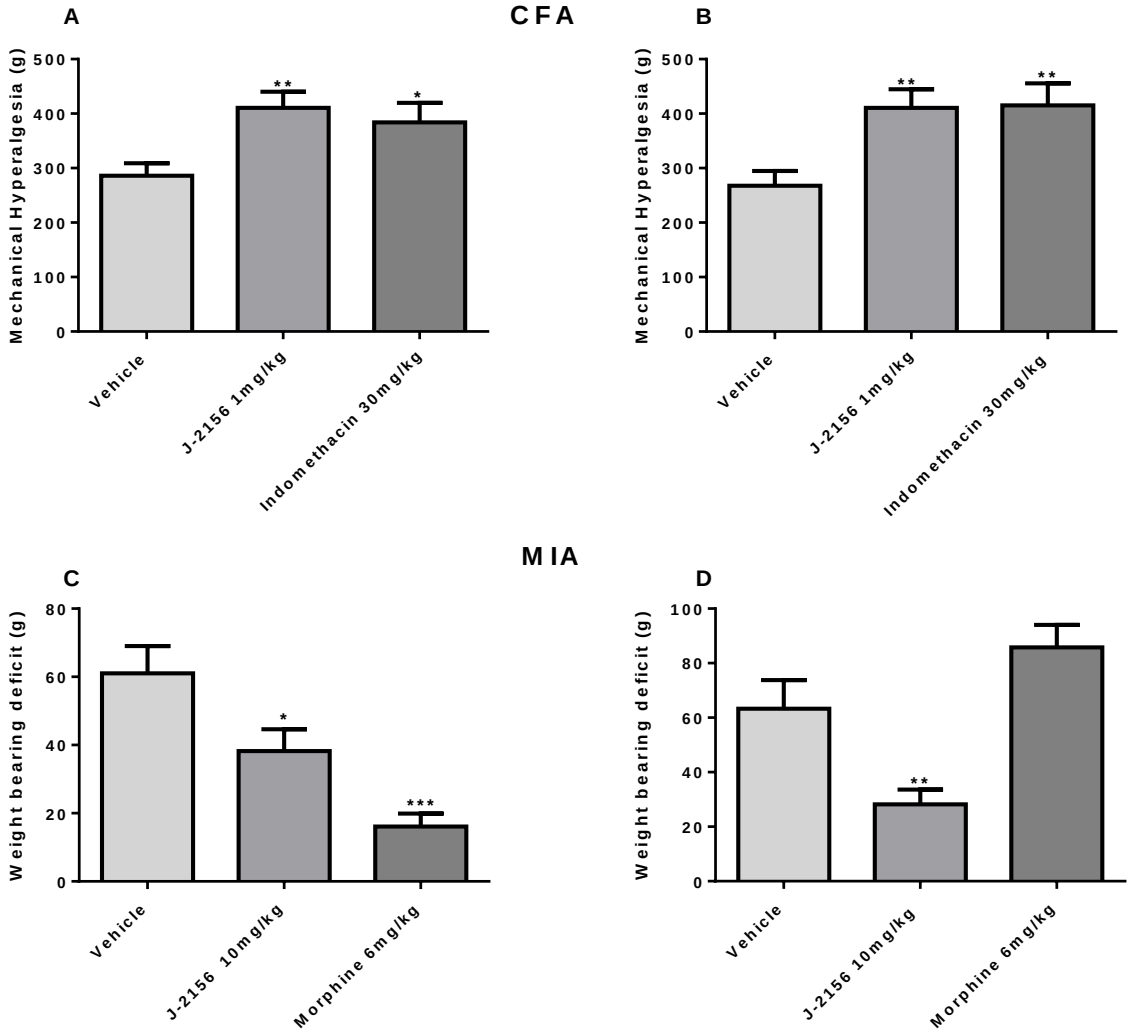

Fig. 3.6. Long lasting effect of J-2156 on nociceptive pain models in the rat. (A, B) Effects of J-2156 on CFA-induced mechanical hypersensitivity in the rat. (A) Twenty-four hours post injection of CFA, J-2156 (1 mg/kg, i.p.) was administered and mechanical sensitivity was tested at 1 hour after administration. (B) Twenty-four hours post intraplantar injection of CFA, J-2156 (1 mg/kg, i.p.), was administered and tested 24 hours later (i.e. 48 hours post CFA injection). In the same studies indomethacin (30 mg/kg, p.o.) was used as a positive control, but at both times tested at 1 hour post compound administration. (C, D) Effects of J-2156 on MIA-induced weight bearing deficit in the rat. (C) At day 3 post intraarticular injection of MIA, J-2156 (10 mg/kg, i.p.) and morphine (6 mg/kg, s.c.) were administered and responses were tested at 1 hour later. (D) Three days post MIA injection, J-2156 (10 mg/kg, i.p.) and morphine (6 mg/kg, s.c.) were administered and tested at 24 hours after administration (i.e. 4 days post MIA injection). Data are presented as mean±S.E.M.. N=9-13 rats/group. *P<0.05 and **P<0.01 vs. vehicle treated group (ANOVA).

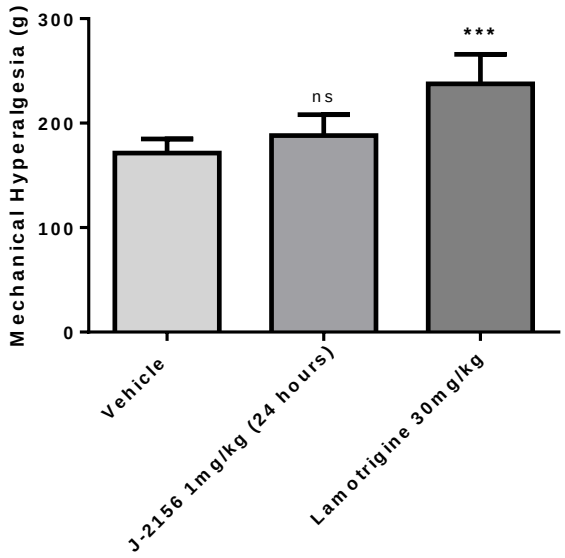

Fig. 3.7. Effect of J-2156 on a neuropathic pain model after 24 hour treatment in the rat. At two weeks after PNL surgery, J-2156 (1 mg/kg, i.p.) was dosed and tested 1 hour (Fig. 3.5B) and 24 hours later. Lamotrigine (30 mg/kg, p.o.) was dosed and tested 2 hours later as positive control. Data are presented as mean±S.E.M.. N=8-12 rats/group. ***P<0.001 vs. vehicle-treated group (ANOVA).

3.3. Functional links to ion channels

Since ion channels are important in pain transmission, functional links of the sst_4 receptor to various ion channels were investigated. Two techniques were used to determine ion movement, electrophysiology and calcium imaging (using fluorescent sensitive dyes). DRG neurons were used as the *ex vivo* pain model.

3.3.1. GIRK channels

In order to determine if the sst_4 receptor is functionally coupled to GIRK channels in DRG neurons, voltage dependent whole-cell currents were recorded from isolated DRG neurons, and the effect of the sst_4 receptor agonist J-2156 was established. The cells had an average capacitance of 50.6±8.1 pF. Control experiments were run (Fig. 3.8A). The first was a standard control, applying only Ringer buffer solution, showing stable readings. The second was a compound control, where only the sst_4 receptor agonist J-2156 was being perfused, without the blocker application, confirming the effects of the blocker. An example recording from one experiment shows the increase in current after J-2156 perfusion, then the blockage after barium chloride ($BaCl_2$) application (Fig. 3.8C).

After 3 minutes of J-2156 perfusion, a significant increase in the magnitude of the inward potassium current was produced by both 30 nM and 100 nM (P<0.001 vs. control). An increase of 103±38% and 134±34% (n=11; Fig. 3.8B) in the current obtained at -80 mV, in 45 mmol/l potassium-containing ringer solution, were recorded respectively. When J-2156 was applied at a lower concentration of 10 nM, there was no significant increase in potassium current (Fig. 3.8B).

The current induced by J-2156 was significantly suppressed not only by the addition of 300 µM $BaCl_2$ by 1.59±0.7 nA (P<0.01 vs. 100 nM J-2156, n=11; Fig. 3.8D), but also by 500 nM tertiapin Q by 1.30±0.7 nA (P<0.05 vs. 100 nM J-2156, n=11; Fig. 3.8D).

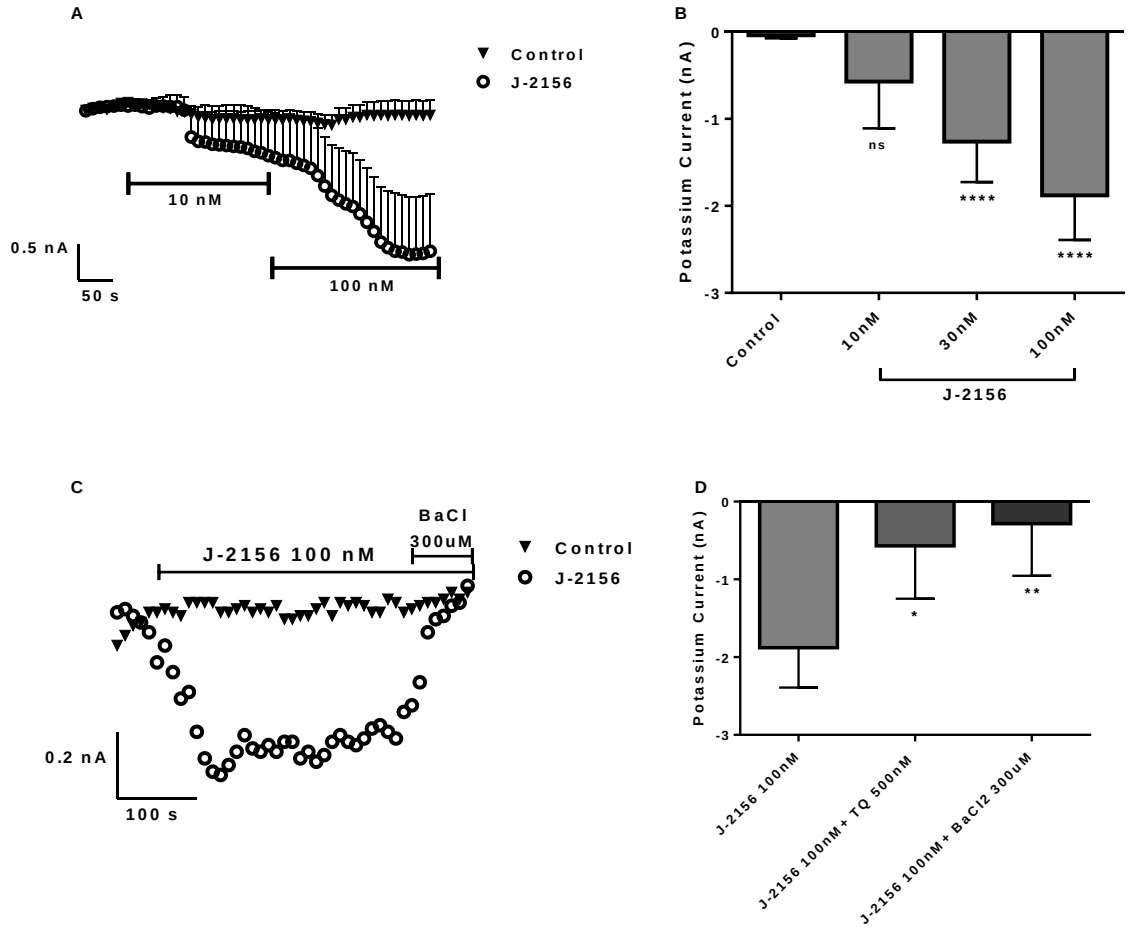

Fig. 3.8. J-2156 increases inward rectifying potassium current of rat DRG neurons. (A) Time-dependent effect of J-2156 (10, 100 nM) induced inwardly rectifying potassium currents obtained at -80 mV in 45 mmol/l potassium containing ringer solution. Application of only Ringer buffer represents control currents. (B) Effects of increasing concentrations of J-2156. The compound induced a potassium current in DRG neurons at 30 nM and 100 nM (ANOVA). (C) Time-dependent effect of J-2156 (100 nM) on inwardly rectifying potassium currents and inhibitory effect of $BaCl_2$ (300 µM). Currents were obtained at -80 mV in 45 mmol/l potassium containing ringer solution. (D) Effects of $BaCl_2$ (300 µM) and tertiapin Q (TQ) (500 nM) on the J-2156 induced potassium current. The current was significantly inhibited by both blockers (ANOVA). These results are presented as potassium current mean±S.E.M.. N=8-11. *P<0.05, **P<0.01, ****P<0.0001 vs. control, or blocker vs. J-2156 100 nM.

3.3.2. Ca_v channels

In order to determine if the sst_4 receptor is able to influence voltage-induced calcium influx in DRG neurons, calcium imaging techniques were used. Application of voltage stimulation (15 – 21 V) for 3 seconds resulted in an increase in intracellular calcium levels, indicating activation of voltage sensitive calcium channels. As shown in figure 3.8A, in control experiments the first and the second stimulations produced similar evoked calcium transients. When J-2156 was applied for 90 seconds the second calcium peak was reduced. J-2156 caused a significant decrease in the voltage induced calcium transient at 10 nM, 30 nM and 100 nM ($P<0.0001$ vs. control) a decrease of 40±11%, 60±9% and 80±4% (n=12-80; Fig. 3.9C) was seen respectively.

To identify the specific Ca_v channels affected by J-2156, specific channel type blockers were applied for 90 seconds before, and again for 90 seconds in combination with J-2156 (100 nM). Ω-Conotoxin (1 µM), agatoxin (200 nM), mibefradil (10 µM) and nitrendipine (10 µM) all caused a significant reduction in the second calcium transient ($P<0.0001$ vs. control; n=13-17; Fig. 3.10). At these concentrations none of the channel inhibitors were as effective as 100 nM J-2156. Significant differences between the sst_4 receptor agonist and the specific blockers can be calculated ($P<0.05$ vs. 100 nM J-2156), suggesting that more than one subtype is influenced by sst_4 receptor activation. When the individual blockers were applied together with J-2156 there was a further reduction in the voltage induced calcium transient amplitude compared to the blocker alone. Ω-Conotoxin, agatoxin, mibefradil and nitrendipine plus 100 nM J-2156 all caused a significant reduction in the calcium transient compared to the blockers alone ($P<0.05$ vs. control; n=13-17; Fig. 3.10). However the combination of Ca_v blockers had a similar effect to the J-2156 agonist alone, where no significant difference was seen in the blockage (results not shown). These results indicate that sst_4 receptors have the ability to interact with multiple subtypes of calcium channels within DRG neurons.

To determine whether the hyperpolarisation caused by GIRK activation (Fig. 3.11) influenced this inhibition of voltage induced calcium influx the GIRK specific blocker tertiapin Q was used. Firstly the sst_4 receptor specific agonist J-2156 was applied alone for 90 seconds and then in combination with 500 nM tertiapin Q for 90 seconds. As previously seen 100 nM J-2156 significantly decreased the voltage induced calcium current by 90±10% ($P<0.0001$ vs. control, n=22; Fig. 3.11). However this inhibition was partially reversed by tertiapin Q, a reversal of 60±16% was seen ($P<0.05$ vs. 100 nM J-2156, n=22; Fig. 3.11). These results indicate that the inhibition of voltage induced calcium influx is in part due to GIRK activation.

In order to determine whether modulation is via the $G_{\alpha i}$, PKA pathway, experiments were performed utilizing pertussis toxin. J-2156 was tested at 100 nM. The cells were pretreated with 100 ng/ml pertussis toxin and the double stimulation protocol was run. The inhibition of voltage induced calcium influx was abolished following pre-treatment with the toxin ($P = 0.23$ vs. control; n=104; Fig. 3.12).

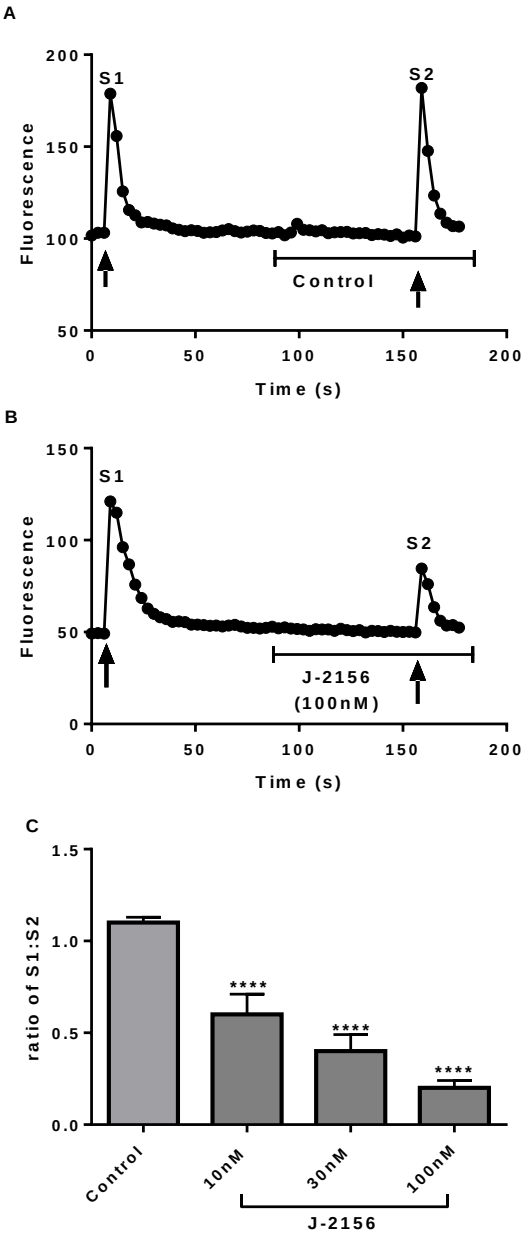

Fig. 3.9. J-2156 inhibits voltage-induced calcium currents of rat DRG neurons. (A,B) Representative examples of responses to 3 second voltage stimulation (15 V, represented by the arrow). The magnitude of increase in calcium influx did not change in the control experiment (A) but inhibition was seen during superfusion with 100 nM J-2156 (B). (C) The sst_4 receptor specific agonist significantly inhibited the calcium current in DRG neurons at 10 nM, 30 nM and 100 nM (ANOVA). These results are presented as ratio of the 2 peaks mean±S.E.M.. N=12-88. ****P<0.0001 vs. control.

Fig. 3.10. Modulation of the inhibitory effects of J-2156 on specific voltage gated calcium channels. Specific blockers were used: 1 µM ω-conotoxin (CTX), 200 nM agatoxin (ATX), 10 µM mibefradil (MIB) and 10 µM nitrendipine (NIT) alone, and then with the addition of 100 nM J-2156 (+). Statistical analysis (ANOVA) of the effects of the blockers showed inhibition of calcium current (P<0.0001 vs. control). Further statistical analysis (ANOVA) revealed further reductions in calcium current following J-2156 application. These results are presented as total blockage relative to the control response mean±S.E.M.. N=13-17. *P<0.05, ***P<0.001 vs. blocker +J-2156.

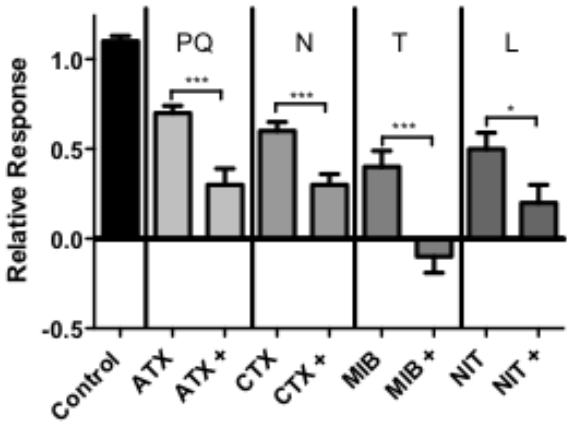

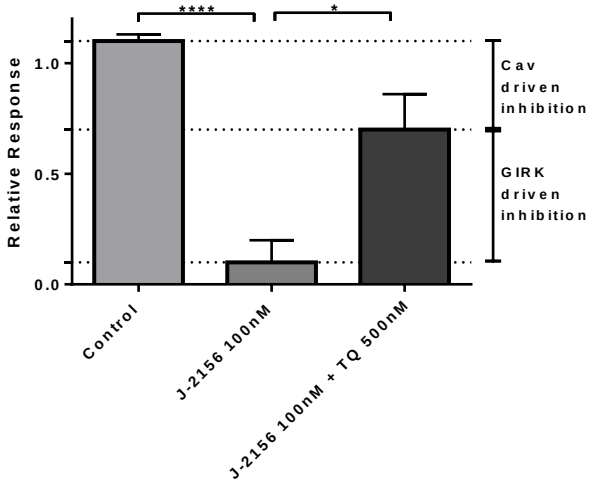

Fig. 3.11. The inhibition of voltage induced calcium current by J-2156 is influenced by GIRK activation. The GIRK specific blocker tertiapin Q (TQ) (500 nM) was used. Statistical analysis (ANOVA) of the effect of this blocker on sst_4 receptor induced calcium influx reduction, revealed significant reversal of this effect. These results are presented as total blockage relative to the control response mean±S.E.M.. N=22. *P<0.05 vs. J-2156 + tratiapin Q, ****P<0.001 vs. control.

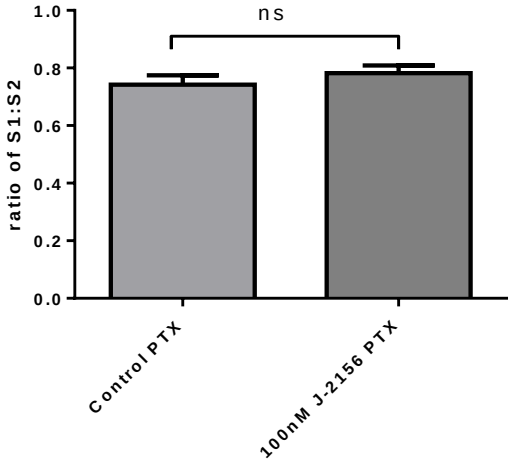

Fig. 3.12. Pertussis toxin inhibits J-2156 modulation of voltage induced calcium currents. Pre-incubation with 100 ng/ml pertussis toxin (PTX) abolished the J-2156 inhibition of voltage induced calcium currents. Under normal conditions 100 nM J-2156 would cause maximal effects. These results are presented as the ratio of the 2 stimulation peaks mean±S.E.M.. N=104.

3.3.3. TRPV1 channels

In order to determine if the sst_4 receptor is functionally coupled to TRPV1 channels in DRG neurons two experimental techniques were used, calcium imaging and patch clamp; the TRPV1 channels were activated using capsaicin, an agonist of TRPV1 channels.

Initially the concentration of capsaicin needed for stimulation of DRG neurons was established. The cells were exposed to capsaicin for 30 seconds. Since there was no significant difference between the calcium influx due to 30 nM and 100 nM capsaicin (data not shown), 30 nM capsaicin was used in all further experiments.

With calcium imaging experiments 2 protocols were run. The first was a double stimulation protocol, where the cells were exposed twice to 30 nM capsaicin for 30 seconds, and the ratio between the two peaks determined. Application of capsaicin resulted in an increase in intracellular calcium levels. In the control experiment the second stimulation produced a slightly reduced evoked calcium transient (Fig. 3.13). When the sst_4 receptor agonist was applied for 3 minutes prior to the second stimulation, the calcium peak was more markedly reduced. J-2156 caused a significant decrease in the capsaicin induced calcium transient at 10 nM ($P<0.01$ vs. control), 100 nM and 1000 nM ($P<0.0001$ vs. control). A decrease of 27±5%, 45±6% and 45±5% was seen respectively (n=23-53 cells; Fig. 3.13A). No effect was produced by 1 nM J-2156 application. The effect of capsazepine, a competitive antagonist for TRPV1 channels (Bevan *et al.*, 1992) was also determined. This caused a significant decrease in capsaicin-evoked calcium transient at 10 µM ($P<0.0001$ vs. control; n=24-53; Fig. 3.13A) of 61±8%. The raw recordings are shown in figure 3.12B+C. Although there was not complete recovery, the slope showing recovery appears to be steeper post compounds application in comparison to the control experiment. So this inhibitory effect is noticeable almost directly after compound application by the heightened rate of recovery seen.

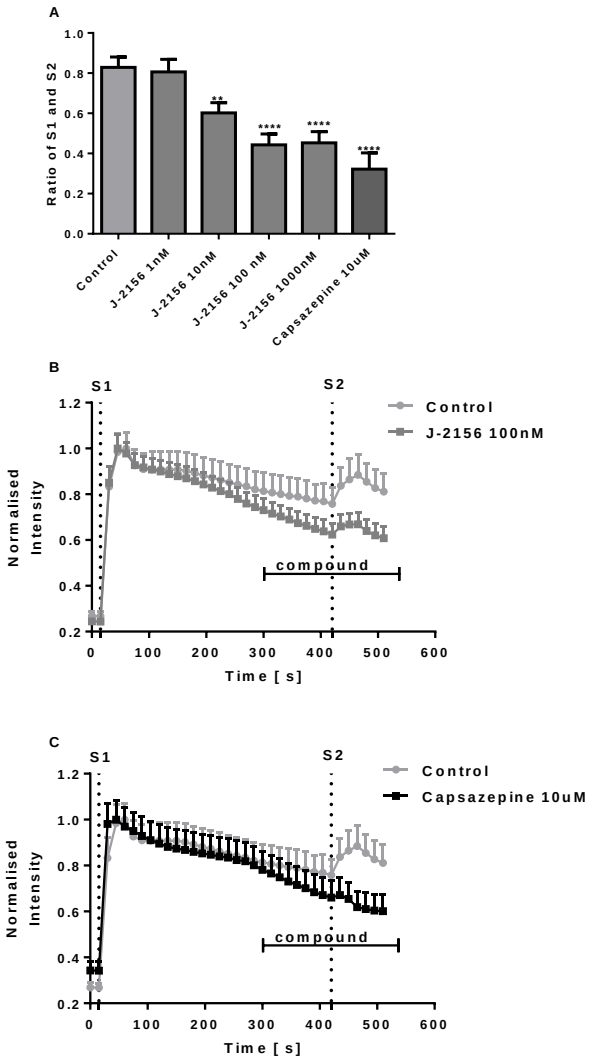

Fig. 3.13. J-2156 inhibits capsaicin-induced calcium currents in rat DRG neurons. (A) Concentration-dependent effects of J-2156. The sst_4 receptor specific agonist significantly inhibited TRPV1 current at 10 nM, 100 nM and 1000 nM (ANOVA). Capsazepine at 10 µM significantly inhibited the TRPV1 current (P<0.0001 vs. control). Averages of the response of 30 nM capsaicin to 100 nM J-2156 (B) and 10 µM capsazepine (C) are shown. These results are presented as the ratio of the two stimulations, S1:S2. mean±S.E.M.. N=24-53. **P<0.01, ****P<0.0001 vs. control.

The second protocol involved pre-incubation of the cells for 5 minutes with J-2156. The cells were then exposed to 30 nM capsaicin for 30 seconds and 3 minutes later depolarisation was induced by 80 mM extracellular potassium solution. The percentage of the potassium response was calculated. Both stimulations resulted in calcium influx in control cells and the potassium response was only slightly greater than the capsaicin response (Fig. 3.14A). Both the sst_4 receptor agonist, J-2156 and the TRPV1 antagonist, capsazepine, reduced the capsaicin-evoked calcium influx, however in their presence, the DRG neurons still responded fully to the potassium. J-2156 caused a significant decrease in the capsaicin-induced calcium transient at 10 nM (P<0.01 vs. control), 100 nM and 1000 nM (P<0.001 vs. control), a decrease of 42±9%, 62±6% and 64±9% was seen respectively (n=17-56 cells; Fig. 3.14B). The Log_{IC50} was -8.27, with 95% confidence intervals of -8.80 to -7.74. This was calculated with Prism 6.0 for Windows using the equation 'log(inhibitor) vs. normalised response', no constraints were applied. At a concentration of 10 µM, capsazepine caused a 92±2% reduction in calcium influx compared to the control (P<0.001 vs. control; n=16-25; Fig. 3.14B).

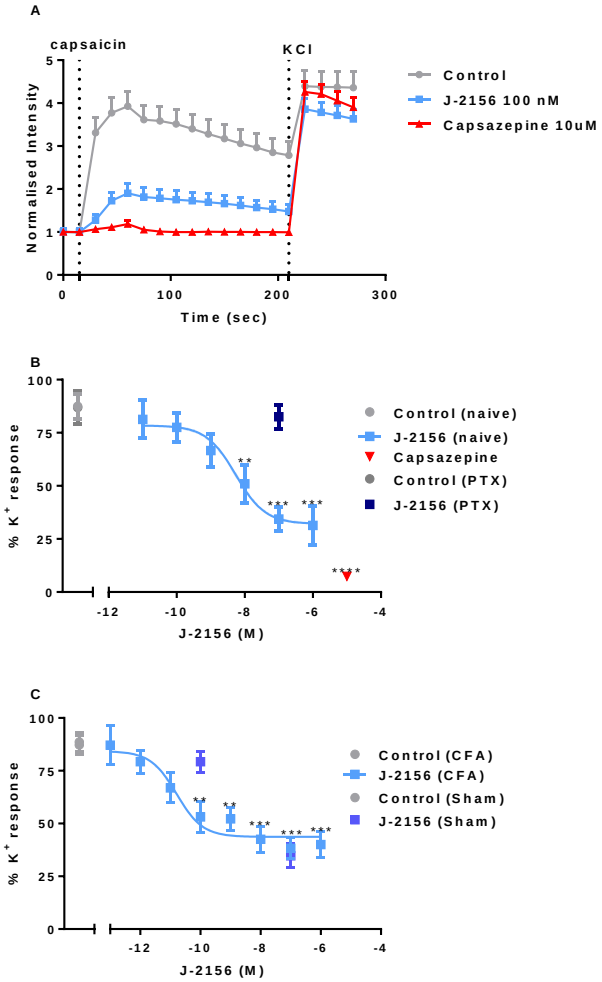

Fig. 3.14. J-2156 inhibition of TRPV1 currents was augmented after CFA treatment. (A) Average response for naïve recordings, showing drug effects. (B) Concentration-dependent effects of J-2156 on naïve DRG neurons. The sst_4 receptor-specific agonist significantly inhibited TRPV1 calcium current at 10 nM, 100 nM and 1000 nM (ANOVA); IC50 = -8.27 M. Capsazepine at 10 µM significantly inhibited the TRPV1 calcium current. Pre-incubation with 100 ng/ml pertussis toxin (PTX) abolished the J-2156 TRPV1 inhibition. (C) Concentration-dependent effects of J-2156 on CFA treated DRG neurons. Significant inhibition of TRPV1 current was seen at concentrations as low as 0.1 nM; maximal effects were reached by 10 nM. IC50 = -10.8 M. Sham treated DRGs responded in the same way as naïve DRGs. These results are presented as the % of potassium response. mean±S.E.M.. N=25-56. **P<0.01, ***P<0.001, ****P<0.0001 vs. control.

To confirm modulation is via the $G_{\alpha i}$, adenylyl cyclase pathway, experiments were performed utilizing pertussis toxin, an agent known to uncouple G_i proteins from GPCRs. J-2156 was tested at 100 nM, as this concentration had maximal efficacy. The cells were pre-treated with 100 ng/ml pertussis toxin and the second protocol run. The inhibition of capsaicin induced calcium influx was abolished following pre-treatment with the toxin (P = 0.32 vs. control; n =56; Fig. 3.14B).

The second protocol was used to establish whether the sst_4 receptor-induced TRPV1 inhibition is augmented after CFA treatment. J-2156 caused a significant decrease in the capsaicin-induced calcium transient at concentrations as low as 0.1 nM (P<0.01 vs. control; n=55; Fig. 3.14C). At this concentration there was a significant difference in the effects J-2156 compared to the naïve DRG neurons (P<0.01 vs. CFA treated neurons; n= 55). Significant effects in the CFA DRG neurons were produced over a range of concentrations from 1 nM (P<0.01 vs. control) to 1000 nM (P<0.001 vs. control; n=50-65; Fig. 3.14C). The Log_{IC50} was -10.8, with 95% confidence intervals of -11.2 to -10.2.

However sham treated animals reacted in the same way as naïve, where no inhibition was seen at 0.1 nM and maximal effects reached at 100 nM of 60±6% (P<0.001 vs. control; n=41; Fig. 3.14C).

Patch clamp experiments were run to test for TRPV1 sodium ion movement. With the electrophysiology experiments a higher concentration of capsaicin was used. It was necessary to use 300 nM capsaicin as when 30 nM was used the number of cells that responded was low. In those cells in which a sodium current was induced by 30 nM capsaicin, the current was 85±16 pA, compared to 384±116 pA with 300 nM (data not shown). This current was considered too small for an appropriate assay window. Thus, a protocol was run where 300 nM capsaicin was applied for 5 seconds at two time points; 60 and 360 seconds. The last application was run in the presence of either vehicle control (Ringer buffer) or the compound. The ratio of the two peaks was calculated. In the control experiment the final stimulation had a slightly reduced effect (Fig. 3.15). When the sst_4 receptor agonist was applied for 5 minutes prior to the final peak the capsaicin response was further reduced in comparison to the control experiment. J-2156 at 100 nM induced a significant decrease in TRPV1 activity of 25±6% (P<0.01 vs. control; n=9-15; Fig. 3.15A). Capsazepine at 10 µM also decreased TRPV1 activity of 67±7% (P<0.0001 vs. control; n=9-15; Fig. 3.15A).

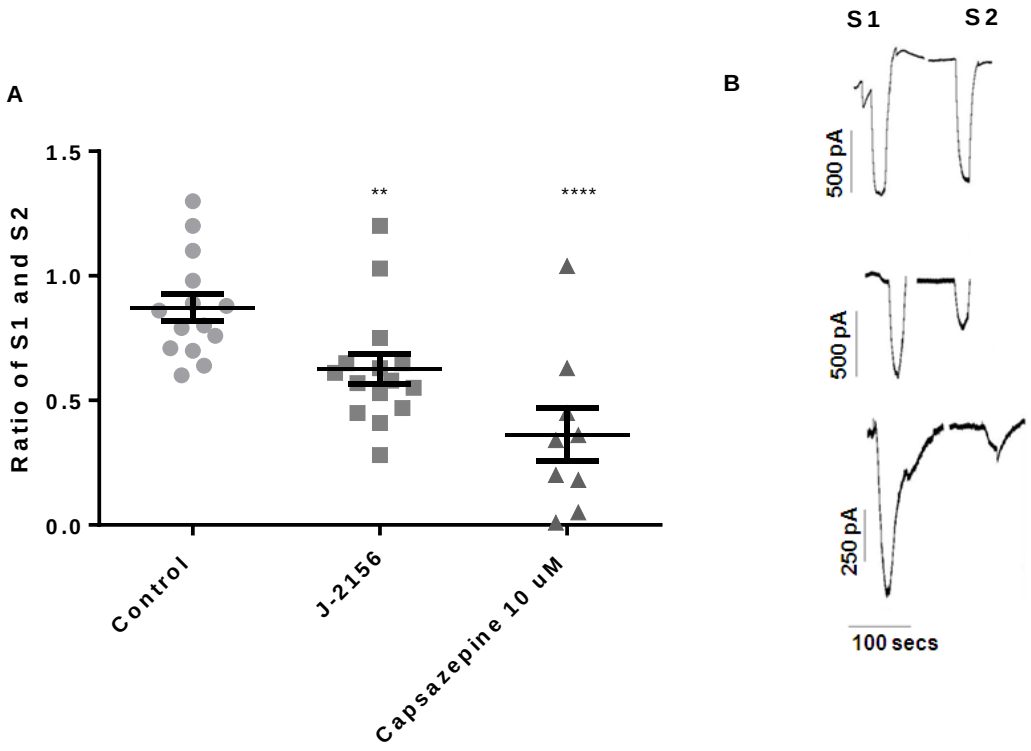

Fig. 3.15. J-2156 inhibits capsaicin induced sodium currents in rat DRG neurons. (A) Effects of the sst_4 receptor specific agonist J-2156 100 nM and Capsazepine 10 µM, both compounds significantly inhibited the capsaicin-stimulated TRPV1 sodium current. (B) Examples of whole-cell current to 300 nM capsaicin stimulations: control (top), J-2156 (middle) and capsazepine (bottom). These results are presented as the ratio of the two stimulations, S1:S2. mean±S.E.M.. N=9-15. **P<0.01, ****P<0.0001 vs. control.

3.3.4. TRPA1 channels

In order to determine if the sst_4 receptor was functionally coupled to TRPA1 channels in DRG neurons calcium imaging experiments were run; the TRPA1 channels were activated using the characterised selective TRPA1 agonist, compound 6 (Gijsen *et al.*, 2010).

Initially the concentration of compound 6 needed for stimulation of the DRG neurons was established. The cells were exposed to compound 6 for 60 seconds and 80 seconds later depolarisation was induced by 50 mM extracellular potassium solution. The response to compound 6 was calculated as percentage of the potassium response. Both 1 µM and 10 µM induced a calcium influx, although 10 µM induced a stronger influx, closer to that of the extracellular potassium, and a greater percentage of the cells responded (data not shown). Therefore 10 µM was used for future experiments.

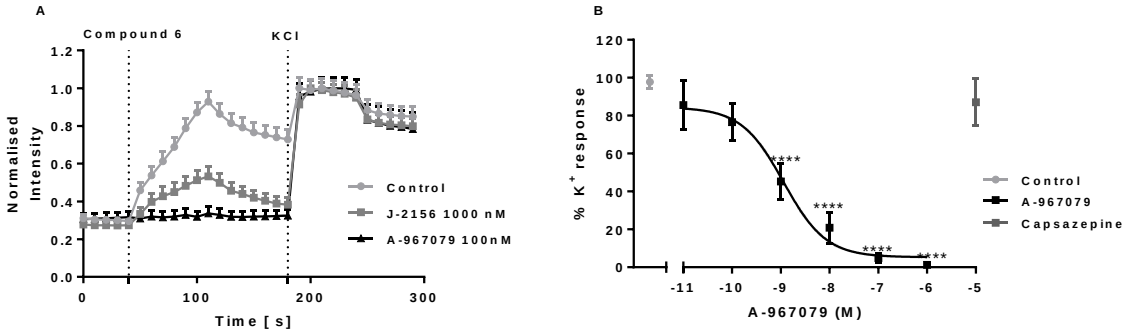

Fig. 3.16. A-967079 inhibits "compound 6" induced calcium currents in rat DRG neurons. (A) Average response for naïve recordings, showing compound response. (B) A-967079 inhibited compound 6 induced calcium currents in rat DRG neurons. Concentration-dependent effects of A-967079 on TRPA1 currents. The TRPA1 specific antagonist, A-967079, completely inhibited TRPA1 current at 100 nM. IC50 = -8.9 M. However the TRPV1 specific antagonist, capsazepine, had no influence of the compound 6 induced calcium influx, at a concentration of 10 µM. These results are presented as the % of potassium response. mean±S.E.M.. N=12-42. ****P<0.0001 vs. control.

To test the effects of the compounds on TRPA1 channel activity the same described protocol was used, however the cells were pre-incubated with the compounds for 5 minutes prior to the exposure to compound 6. Both compound 6 and the high extracellular potassium solution produced calcium influx of a similar magnitude (Fig 3.16A). Both the sst_4 receptor agonist, J-2156 and the TRPA1 antagonist, A-967079 (Chen *et al.*, 2011), reduced TRPA1 calcium influx, but cells still responded fully to the potassium-induced calcium influx. At a concentration of 100 nM, A-967079 was able to fully inhibit the TRPA1 calcium influx (P<0.0001 vs. control, n=12, Fig 3.16B), with a reduction of 95±2%, confirming the validity of compound 6 as a tool to investigate TRPA1 antagonists. The Log_{IC50} of A-967079 was -8.9, with 95% confidence intervals of -9.4 to -8.5. This was calculated with Prism 6.0 for Windows using the equation 'log(inhibitor) vs. normalised response', no constraints were applied. To confirm this inhibition was TRPA1 specific the TRPV1 antagonist, capsazepine (Bevan *et al.*, 1992), was tested. However no inhibition was seen up to concentrations of 10 µM (Fig 3.16B).

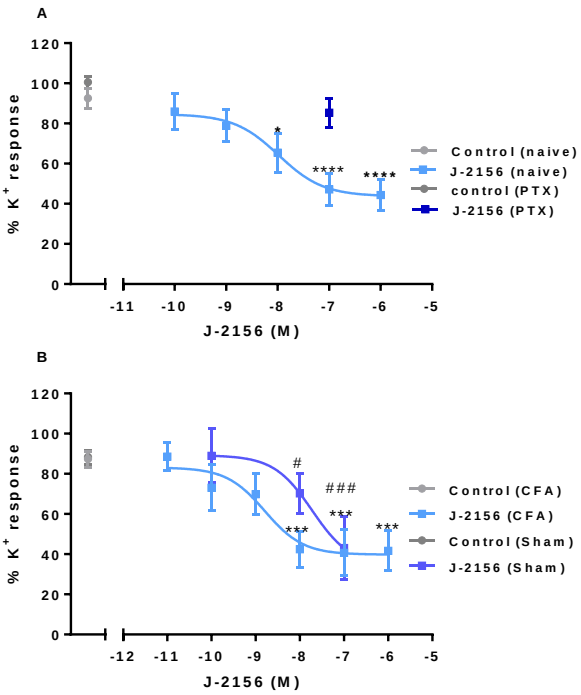

Fig. 3.17. J-2156 inhibits TRPA1 currents in rat DRG neurons. (A) J-2156 inhibited compound 6 induced calcium currents in rat DRG neurons. Concentration-dependent effects of J-2156 on TRPA1 currents; significance is represented by *. The sst_4 receptor specific agonist significantly inhibited TRPA1 current starting from 10 nM (P<0.05 vs. control minimum). IC50 = -8.0 M. Pre-incubation with 100 ng/ml pertussis toxin (PTX) abolished the J-2156 TRPA1 inhibition. (B) J-2156 inhibition of TRPA1 currents in CFA treated DRG neurons. Concentration-dependent effects of J-2156 on DRG neurons; significance is represented by * for CFA neurons and # for sham neurons. The sst_4 receptor specific agonist significantly inhibited TRPA1 currents in CFA neurons starting from 10 nM (P<0.001 vs. control). IC50 = -8.8 M. The sst_4 receptor specific agonist significantly inhibited TRPA1 currents in sham neurons at 10 nM and 100 nM (P<0.05, P<0.001 vs. control respectively). IC50 = -7.7 M. These results are presented as the % of potassium response. mean±S.E.M.. N=25-73.

J-2156 caused a significant decrease in the compound 6-induced calcium transient at 10 nM (P<0.05 vs. control, n=25-73, Fig 3.17A), with a reduction of 29±10%. Maximal effects were reached at 100 nM and 1000 nM J-2156 (P<0.0001 vs. control, n=25-73, Fig 3.17A), where an inhibition of 49±8% and 52±7% was seen respectively. The Log_{IC50} of J-2156 was -8.0, with 95% confidence intervals of -8.5 to -7.5. To confirm modulation was via the $G_{\alpha i}$, PKA pathway, experiments were run utilizing pertussis toxin. The cells were pre-treated with 100 ng/ml pertussis toxin overnight prior to the protocol being run. J-2156 was tested at a concentration of 100 nM as this is where the maximal inhibition is reached. The inhibition of calcium influx via TRPA1 was abolished following pre-treatment of pertussis toxin (P = 0.09 vs. control; n=27; Fig 3.17A).

To establish if the sst_4 receptor induced TRPA1 inhibition was augmented after CFA treatment the protocol was run using inflamed DRG neurons. J-2156 caused a significant reduction in the TRPA1 calcium transient at 10 nM, 100 nM and 1000 nM (P<0.001 vs. control, n=24-30, Fig 3.17B), where an inhibition of 53±9%, 56±12% and 55±10% was seen respectively. The log_{IC50} of J-2156 in inflamed conditions was -8.8, with 95% confidence intervals of -9.8 to -7.8. This inhibitory effect was not

significantly different to the induced inhibition in naïve DRG neurons, at any of the concentrations of J-2156 tested. As a control sham injected animals were used, in this case the cells responded in a similar way to naïve animals. J-2156 caused a significant decrease in the TRPA1 induced calcium transient at 10 nM ($P<0.05$ vs. control, n=13-21, Fig 3.17B), with a reduction of 20±9%. Maximal effects were reached at 100 nM ($P<0.001$ vs. control, n =10-21, Fig 3.17B), where an inhibition of 51±15% was seen. The $\log_{IC50}$ of J-2156 in sham conditions was -7.7, which is comparable to naïve neurons.

3.3.5. Na_v channels

In order to determine if the sst_4 receptor was able to influence the activity of voltage stimulated sodium currents in DRG neurons, whole cell patch clamp experiments were performed, in combination with the sst_4 receptor agonist J-2156. Protocols were run in both current clamp and voltage clamp modes. Although tetrodotoxin (TTX) was tested none of the cells responded to the blocker, indicating that these experiments were mainly investigating functional links to TTX resistant sodium channels.

Two current clamp mode protocols were run to determine the threshold of the cells. The first was a fast step, where the holding potential was changed 5 times in increasing steps of 80, 160, 240, 320 and 400 pA, and every second was held for 0.5 seconds. The second was a medium ramp, where the holding current was gradually increased up to 500 pA over a period of 1 second. These protocols induce action potential generation, which allowed for firing threshold of neurons and levels of activity of the cells to be determined, both of which can be influenced by sodium channel activation. These were run firstly as controls and then as control or compound experiments following 3 minute exposure of the cells to vehicle or drug. For voltage clamp experiments a sodium sweep protocol was run to determine the sodium current at a holding potential of -70 mV. This was established as a control and then the control or compound current was determined 3 minutes later (examples traces are shown in Fig. 3.18).

In control experiments the activation threshold remained stable for both the step (Fig. 3.19B) and the ramp (Fig. 3.19C) protocols. There was no significant difference between the 2 control runs. Similarly, the levels of activity remained stable, where the number of action potentials was also not significantly different (data not shown). Furthermore, the currents were stable throughout the control recordings (Fig. 3.19A).

The compounds were applied for 3 minutes after the initial control values for each protocol had been established. The sst_4 receptor agonist J-2156 was tested at 100 nM. J-2156 caused a significant increase in cell threshold in both the step ($P<0.01$ vs. control, n=15, Fig 3.19B) and in the ramp protocols ($P<0.05$ vs. control, n=9, Fig 3.19C). An increase of 10.51±3.1 mV, or 12.13±5.1 mV was seen respectively. The levels of activity, however, did not significantly change, where the average number of action potentials remained at 21 in the step protocol. A slight effect was seen in the ramp protocol, where a decrease of 4 (21±36%) action potentials was recorded but this was not significant

(data not shown). J-2156 had no effect on the voltage-induced sodium current. There was a slight reduction following J-2156 application of 0.31±0.59 nA, but this was not significant (Fig 3.19A). Example recordings for J-2156 are shown in figure 3.18B. As the effects seen by J-2156 on Na_v were minimal no further concentrations were tested.

Tetrodotoxin (TTX) was tested at 300 nM. After a 3 minute application of TTX no changes were seen. The threshold remained stable for both the step (Fig. 3.19B) and the ramp (Fig. 3.19C) protocols, while the current was consistent (Fig. 3.19A). Furthermore, the levels of activity, known by the number of action potentials also did not change after TTX application (data not shown). These cells reacted in a similar way to control cells, suggesting a resistance to TTX.

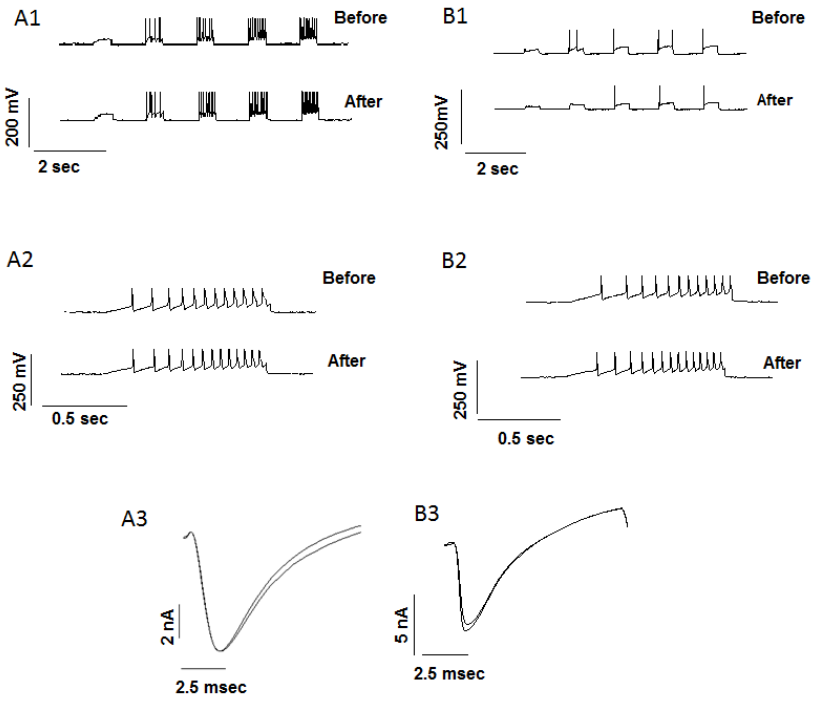

Fig. 3.18. Protocol description of Nav channel patch clamp experiments. Example recordings from control experiments (A) and J-2156 (B). In order to determine threshold and activity levels both step (1) and ramp (2) protocols were run as either control (before) or as a vehicle control or compound (after). Voltage stimulated sodium current was established at a holding potential of -70 mV (3), where control recordings remained stable (A) and a slight, but not significant reduction was seen for J-2156 (B). Small changes were seen with the threshold changes in the presence of J-2156 (B), which might be due to a secondary mechanism independent of Na_v channels, possibly GIRK channel activation.

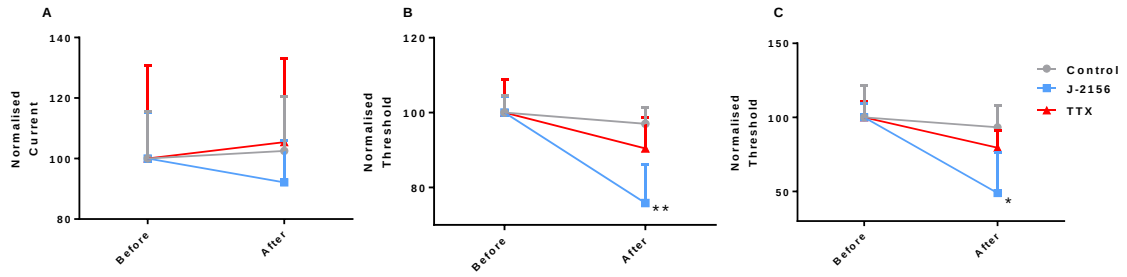

Fig. 3.19. J-2156 influences threshold of DRG neurons. (A) Effects of J-2156 and tetrodotoxin (TTX) on voltage induced sodium current. Stable control recordings were made. J-2156 and TTX had no effect on the sodium current in DRG neurons. These results are presented as the normalised current to that recorded before application of vehicle control or compound. (B+C) Effects of J-2156 and tetrodotoxin (TTX) on cell threshold. J-2156 at 100 nM significantly increased the threshold of DRG neurons in both the step (B) and the ramp (C) protocols (ANOVA). TTX at 300 nM had no effect on threshold. These results are presented as the normalised threshold to that recorded before application of control or compound. mean±S.E.M.. N=5-15. *P<0.05, **P<0.01 vs. control.

3.4. Inflammatory component

Inflammation is an important component of chronic pain. The influence of the sst_4 receptor agonist J-2156 had on inflammation was assessed, by both *in vivo* and *ex vivo* techniques. This was to establish how far these influence the analgesic effects of J-2156.

3.4.1. Effects of J-2156 of paw oedema

In vivo experiments were used to assess anti-oedema properties of J-2156. The CFA model was used alongside the carrageenan inflammation model. Paw oedema was assessed by using plethysmography, a technique that induces a mild distress to animals and therefore can be applied after the assessment of mechanical hypersensitivity without affecting the severity of the model and the quality of the results. No behavioural side effects were observed in rats treated with J-2156 in any of the settings.

Carrageenan rat model: Three hours post carrageenan, oedema occurred in the injected paw**.** This was significantly higher compared to the naïve group ($p<0.0001$ vs. naive; n=10; data not shown). Pre-treatment with 0.1 and 1 mg/kg of J-2156 had no effect on carrageenan-induced paw oedema (NS vs. vehicle; n=10; Fig. 3.20A), whereas, in contrast, analgesic doses of indomethacin significantly reduced paw volume ($P<0.001$ vs. vehicle; n=10; Fig. 3.20A).

In the carrageenan model, effects of J-2156 on pain threshold were also assessed. In this model 0.1 mg/kg had no effect on mechanical hypersensitivity (NS; n=10; Fig. 3.20B); however at 1 mg/kg, J-2156 caused 54±16% increase in paw withdrawal threshold ($P<0.01$ vs. vehicle; n=10; Fig. 3.20B), which was not significantly different from the positive control indomethacin (NS; n=10; Fig. 3.20B).

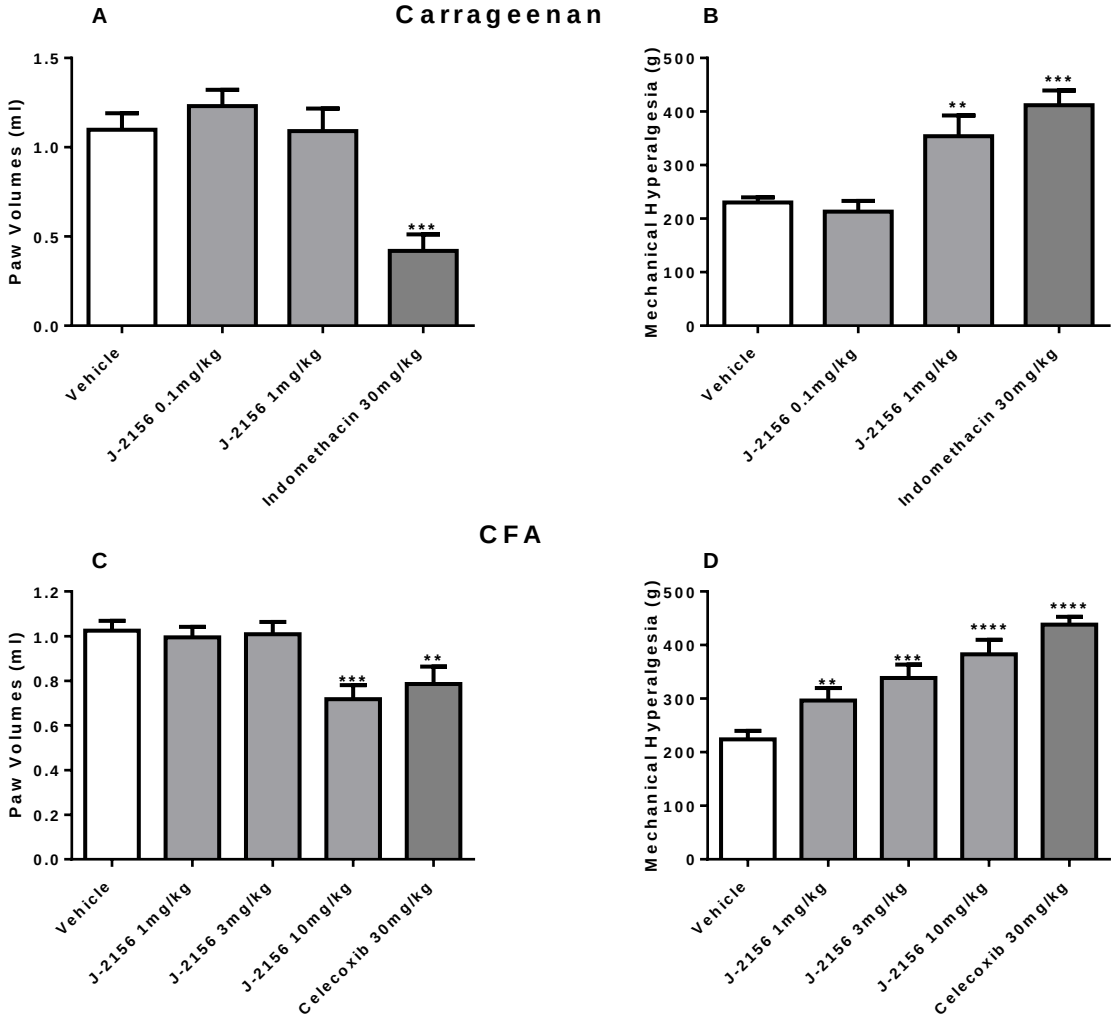

Fig. 3.20. Effect of J-2156 on inflammatory models in the rat. Effects in the carrageenan rat model (A and B). J-2156 (0.1 and 1 mg/kg, i.p.), indomethacin (30 mg/kg, p.o.) and vehicle (2 ml/kg, i.p.) were administered 1 hour prior to the induction of carrageenan paw oedema and effects established 3 hours after carrageenan administration. Indomethacin was used as a positive control. Therefore paw volume was measured at 4 hours post compound administration (A) and mechanical hypersensitivity soon after (B). Although J-2156 increased pain threshold at 1 mg/kg, no effects were seen on paw volume. Effects in the CFA rat model (C and D). J-2156 (1, 3 and 10 mg/kg, i.p.), celecoxib (30 mg/kg, p.o.) and vehicle (2 ml/kg, i.p.) were administered 1 hour prior to the induction of CFA paw oedema, then again at 8 and 24 hours post CFA injection. The animals were tested at 1 hour after the third dosing. Celecoxib was used as a positive control. Paw volume was measured first (C) and paw withdrawal threshold soon after (D). J-2156 at all doses increased pain threshold, however effects on paw volume were only seen in the highest dose of 10 mg/kg. Data are presented as mean±S.E.M.. N=10-20. **P<0.01, ***P<0.001 and ****P<0.0001 vs. vehicle-treated group (ANOVA).

CFA rat model: To confirm and extend further these findings, J-2156 was tested in a subchronic model of inflammatory pain, allowing the compound to be given in multiple doses. Thus, in the CFA model the effects of repeated administration of J-2156 were tested, as well as higher concentrations being used. Intraplantar injection of CFA induced significant paw swelling ($P<0.0001$ vs. naïve; n=20; data not shown). Pre-treatment with 1 and 3 mg/kg J-2156 had no effect on CFA induced paw oedema (NS; n=20; Fig. 3.20C). However a 30±6% reduction in paw volume was observed in rats which had been treated with 10 mg/kg ($P<0.001$ vs. vehicle; n=20; Fig. 3.20C). This effect was not significantly different from that caused by celecoxib (NS; Fig. 3.20C).

Within the same study paw withdrawal was assessed, where J-2156 caused dose-dependent increases in pain threshold (minimum $P<0.05$ vs. vehicle; n=20; Fig. 3.20D). Equally, repeated doses of celecoxib reversed mechanical hypersensitivity in CFA model.

3.4.2. Effects of J-2156 on neutrophil infiltration and cytokine release in rat paws

To characterise further the effects of J-2156 on CFA induced inflammation, inflamed paw tissue was sampled from the previously described *in vivo* study (section 3.4.1.). Neutrophil infiltration and cytokine levels were assessed.

Neutrophil infiltration: Neutrophil infiltration was assessed by measuring myeloperoxidase (MPO) levels in paw samples. Intraplantal injection of CFA induced a significant increase in neutrophil infiltration compared to the naïve animals ($P<0.0001$ vs. naïve; n=10; Fig. 3.21) of 99±5%. Pre-treatment with J-2156 had no effect on CFA induced neutrophil infiltration. At the highest dose of 10 mg/kg there was, however, a slight reduction of 15±6% but this was not significant (NS; n=10; Fig. 3.21). Pre-treatment with celecoxib did significantly reduce CFA induced neutrophil infiltration ($P<0.05$ vs. vehicle; n=10; Fig. 3.21), however there was only a slight reduction of 16±7%.

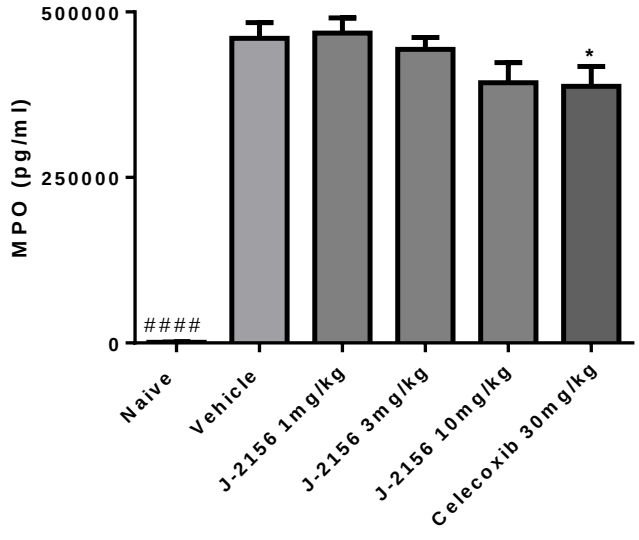

Fig. 3.21. Effect of J-2156 on paw neutrophil infiltration from CFA rats. Effects of J-2156 on neutrophil infiltration. Paw samples were taken from CFA treated animals which had been administered J-2156 (1, 3 and 10 mg/kg, i.p.) at 1 hour prior to CFA induced oedema, then again at 8 and 24 hours post CFA injection. Neutrophil infiltration was assessed using a Hycutt ELISA. Although CFA significantly induced neutrophil infiltration, J-2156 had no effect at any dose. Data are presented as concentration of myeloperoxidase (MPO) in the paw and are expressed as mean±S.E.M.. N=10. *P<0.05 vs. control.

Cytokine levels: The levels of 4 different cytokines in the paw samples were assessed, IL1β (Fig. 3.22A), IFNγ (Fig. 3.22B), IL6 (Fig. 3.22C) and TNFα (Fig. 3.22D). Intraplantal injection of CFA induced a significant increase in the levels of all cytokines compared to the naïve animals (minimum $P<0.05$ vs. naïve; n=5; Fig. 3.22), resulting in an increase of at least 98%. Pre-treatment of J-2156 had no effect on CFA induced cytokine levels. Similarly pre-treatment with celecoxib did not affect CFA induced cytokine release.

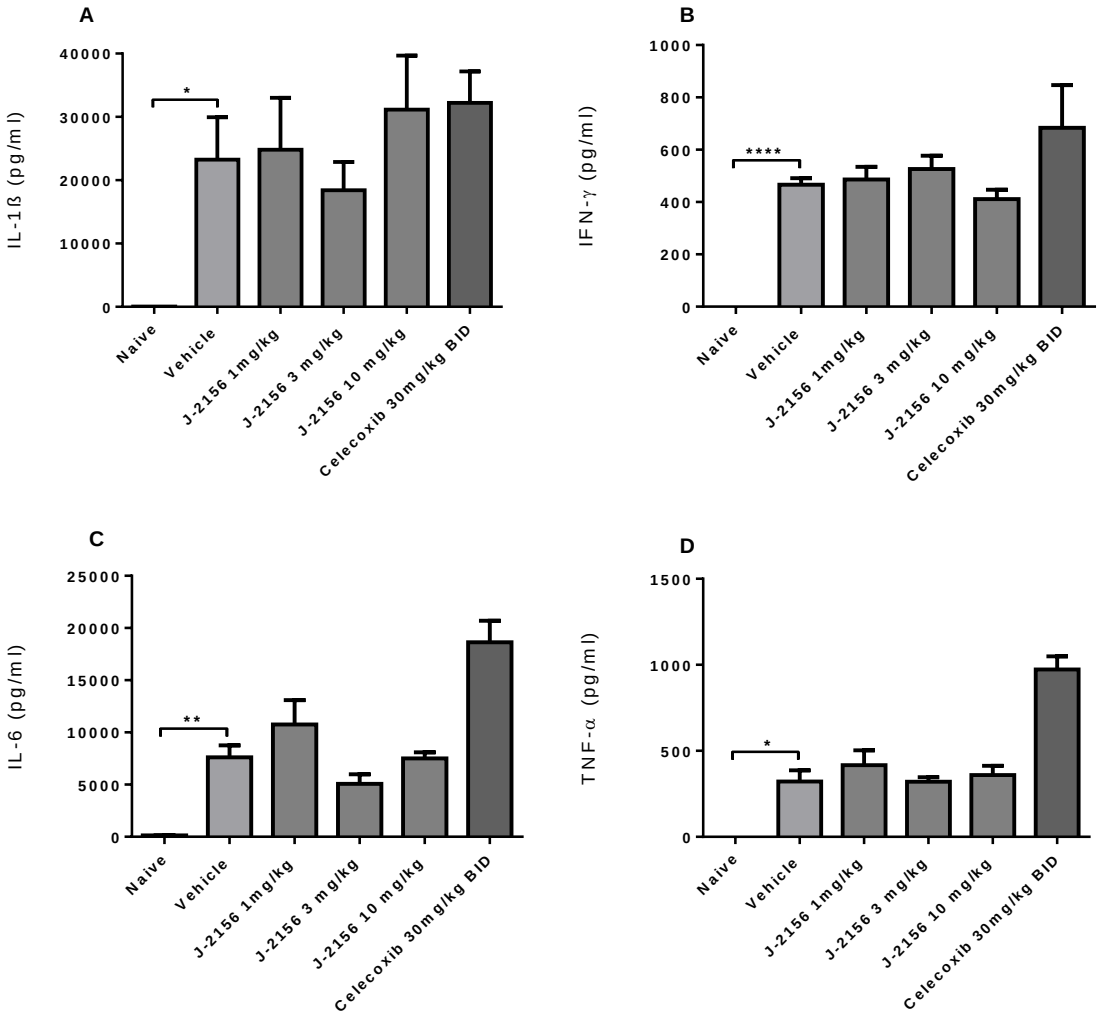

Fig. 3.22. Effect of J-2156 on paw cytokine levels in CFA rats. Effects of J-2156 on paw cytokine levels. Paw samples were taken from CFA treated animals which had been administered J-2156 (1, 3 and 10 mg/kg, i.p.) at 1 hour prior to CFA induced oedema, then again at 8 and 24 hours post CFA injection (BID). Cytokine levels were assessed using a MSD ELISA. Although CFA significantly increased all four tested cytokines: IL1β (A), IFNγ (B), IL6 (C) and TNFα (D), J-2156 had no effect. Data are presented as concentration of the respective cytokine in the paw and are expressed as mean±S.E.M.. N=5. *P<0.05, **P<0.01, ****P<0.0001 vs. naïve.

These data support the *in vivo* behavioural data, where no anti-inflammatory effects were seen in paw tissue at analgesic doses of J-2156. Given that no effects were induced, contralateral paws were not tested.

3.4.3. Effects of 24 hour J-2156 treatment on inflammatory mediators in rat paws

In order to gain further understanding as to what caused the long lasting analgesia in the inflammatory pain models, levels of various inflammatory mediators were investigated. DRG neurons from the inflamed side and inflamed paw tissues were sampled from the CFA rats following the behavioural studies previously described (section 3.2.4). In the DRG neurons, however, the levels of inflammatory mediators were below the detection limits of the assays used, so no results are presented.

The levels of various inflammatory mediators in the inflamed paw were assessed, including IFNγ, IL1β, IL6, TNFα, IL10, MCP1 and PGE_2. As expected, and previously shown (Fig. 3.22), intraplantal injection of CFA induced a significant increase of all the mediators tested at 24 hours post CFA injection ($P<0.05$ vs. naïve minimum; n=3-9; Fig. 3.23). However at 48 hours post CFA injection, significant increases were no longer apparent. Although in most cases the inflammatory mediator levels were higher in CFA injected paws compared to naïve paws, significant effects were only seen for PGE_2 which produced a sustained increase of 64±7% ($P<0.01$ vs. naïve; n=7; Fig. 3.23G).

J-2156 treatment had no effect on CFA induced inflammatory mediator release (Fig. 3.23). As mentioned, the levels of inflammatory mediators did decrease along the time course of the experiment. Lower levels were detected in paws at 48 hours post CFA injection compared to both vehicle and compound treated paws at 24 hours post CFA injection (minimum $P<0.05$ vs. CFA vehicle 24 hours; Fig. 3.23). This contrasted with the behavioural data, where pain threshold still remained low at 48 hours post CFA injection (Fig. 3.6B). Given that J-2156 did not reduced the levels of inflammatory mediators in the inflamed paws, the contralateral paws were not tested.

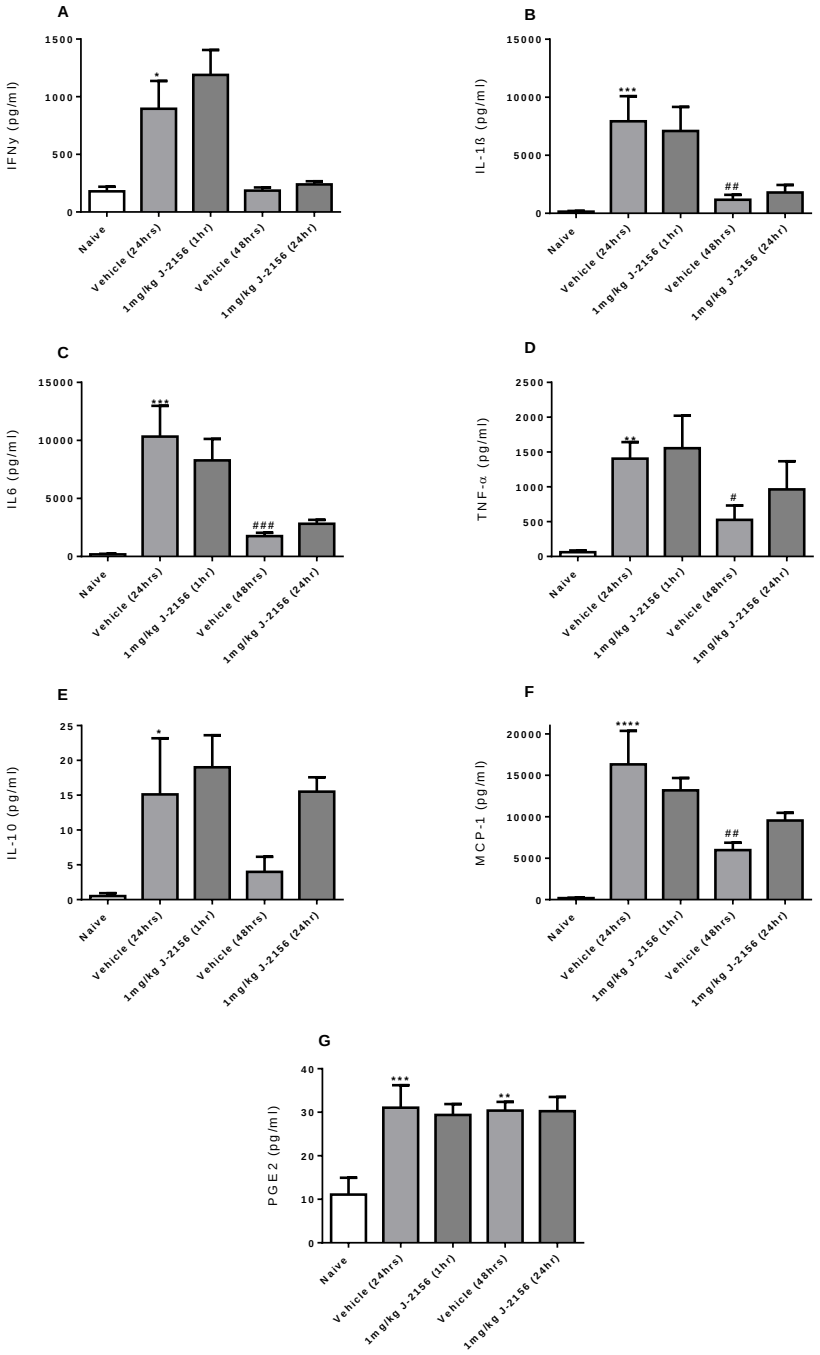

Fig. 3.23. Effects of long lasting treatment of J-2156 on paw inflammatory mediator levels in CFA rats. Effects of J-2156 on paw inflammatory mediator levels. Paw samples were taken from CFA animals which has been administered J-2156 (1 mg/kg, i.p.) for 1 hour (1hr) or 24 hours (24hr) prior to tissue sampling. After 24 hours CFA injection (vehicle (24hrs)) there were significant increases in the levels of all mediators tested: IFNγ (A), IL1β (B), IL6 (C), TNFα (D), IL10 (E), MCP1 (F) and PGE_2 (G), however this effect was not significant 48 hours post CFA injection (vehicle (48hrs)). J-2156 had no effect on any of the inflammatory mediators tested. Data are presented as concentration of the respective cytokine in the paw and are expressed as mean±S.E.M.. N=3-9. *P<0.05, **P<0.01, ***P<0.001, ****P<0.0001 vs. naïve. #P<0.05, ##P<0.01, ###P<0.001 vs. vehicle 24 hrs.

3.4.4. Effects of J-2156 on LPS stimulated inflammatory mediator release

In order to determine if activation of sst_4 receptors in the peripheral nervous system might affect the levels of different inflammatory mediators, various ELISAs were run. DRG neurons were stimulated with LPS to induce the release of cytokines, PGE_2; and capsaicin, veratridine and KCl to induce the release of CGRP and the influence J-2156 had on this was established.

3.4.4.1. Cytokine and chemokine release

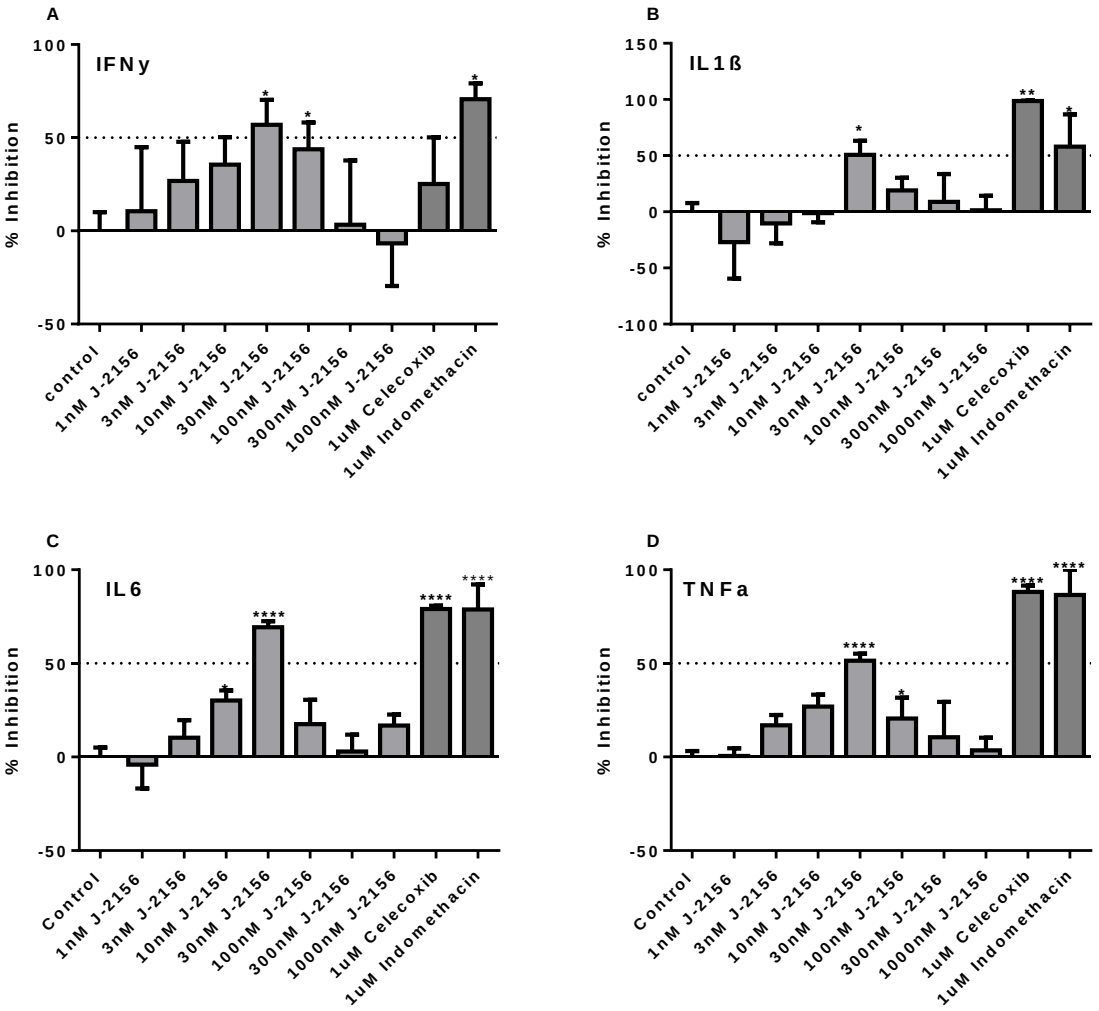

Fig. 3.24. Effect of J-2156 on lipopolysaccharide (LPS) stimulated cytokine release in DRG neurons. Concentration-dependent effects of J-2156 on LPS stimulated cytokine release. DRG neurons were exposed to 100 ng/ml LPS for 24 hours (control). The sst_4 receptor agonist did inhibit the LPS stimulated release of cytokines at 30 nM ($P<0.05$ minimum) in a similar manner to 1 µM celecoxib and indomethacin. Data are presented as the % inhibition of the LPS stimulation. mean±S.E.M.. N=3-6. *P<0.05, **P<0.01, ****P<0.0001 vs. LPS control.

The levels of 4 different cytokines: IFNγ (Fig. 3.24A), IL1β (Fig. 3.24B), IL6 (Fig. 3.24C) and TNFα (Fig. 3.24D) and the chemokine MCP1 (Fig. 3.25) were assessed. The release was stimulated by exposure to 100 ng/ml lipopolysaccharide (LPS) for 24 hours. This consistently caused a significant increase in the levels of all cytokines and the chemokine. An average increase of 71±8%, 58±13%, 71±7% and 78±6% was seen for each cytokine respectively and 70±8% for MCP1 (P<0.0001 vs. buffer; n=3-6; results not shown).

J-2156 caused a significant reduction in the LPS stimulated cytokine and chemokine release. This was however not in a typical concentration dependent manner, rather showing a bell shaped effect. For all cytokines the most efficacious concentration was 30 nM. For IFNγ significant inhibition was reached at 30 nM J-2156 (P<0.05 vs. LPS control; n=4; Fig. 3.24A) and this was still significant at 100 nM (P<0.05 vs. LPS control; n=6; Fig. 3.24A). J-2156 significant inhibited LPS stimulated IL1β release, but only at 30 nM (P<0.05 vs. LPS control; n=4; Fig. 3.24B). In the case of IL6 significant inhibition was first seen at 10 nM J-2156 (P<0.05 vs. LPS control; n=4; Fig. 3.24C), however maximal inhibition was reached at 30 nM (P<0.0001 vs. LPS control; n=4; Fig. 3.24C). TNFα release was significantly inhibited at 30 nM J-2156 (P<0.0001; n=4; Fig. 3.24D) and this was still significant at 100 nM (P<0.05; n=6; Fig. 3.24D). For MCP1 significant inhibition was first induced at 10 nM J-2156, where exposure to 100 nM had similar effects (P<0.01 vs. LPS control; n=4-6; Fig. 3.25). Maximal inhibition was reached at 30 nM J-2156 (P<0.0001 vs. LPS control; n=4; Fig. 3.25).

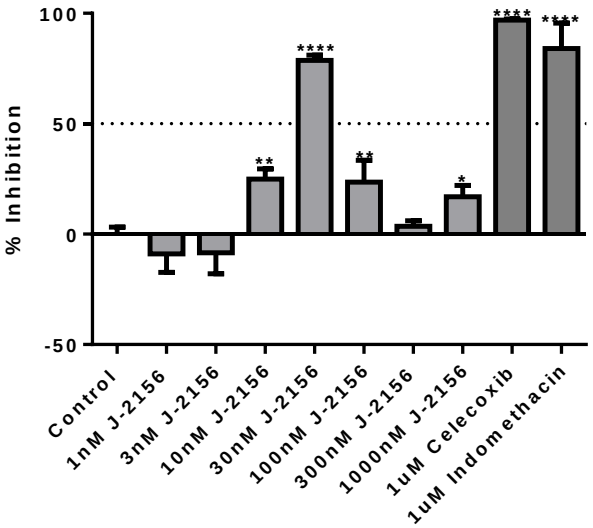

Fig. 3.25. Effect of J-2156 on lipopolysaccharide (LPS) stimulated chemokine release in DRG neurons. Concentration-dependent effects of J-2156 on LPS stimulated chemokine release. DRG neurons were exposed to 100 ng/ml LPS for 24 hours (control). The sst_4 receptor agonist inhibited LPS stimulated release at 30 nM in a similar way to 1 μM celecoxib and indomethacin. Data are presented as % inhibition of the LPS-stimulated release of MCP1. mean±S.E.M.. N=3-6. *P<0.05, **P<0.01, ****P<0.0001 vs. LPS control.

Two positive controls were tested, celecoxib and indomethacin. Interestingly these reacted in a similar way to J-2156, where although significant inhibition was seen this was in a bell shaped response. Maximal inhibition of LPS stimulated inflammatory mediator release, for both celecoxib and indomethacin, was reached at 1 μM, where inhibition was not significantly different to that of 30 nM J-2156. Celecoxib at 1 μM significantly inhibited LPS release of IL1β, IL6 TNFα and MCP1 (P<0.01 vs. LPS control minimum; n=3; Fig. 3.24 and Fig. 3.25). This effect was not as strong at 10

µM celecoxib with reductions of 93±4%, -17±41%, 30±21% and -13±21% were seen for IL1β, IL6 TNFα and MCP1 respectively (results not shown). Indomethacin at 1 µM significantly inhibited LPS release of IFNγ, IL1β, IL6 TNFα and MCP1 ($P<0.05$ vs. LPS control minimum; n=3; Fig. 3.24 and Fig. 3.25), again this effect was not as strong at 10 µM indomethacin with reductions of 57±14%, 58±13%, 49±16%, 29±25% and 35±17% were seen for IFNγ, IL1β, IL6 TNFα and MCP1 respectively (results not shown).

3.4.4.2. Prostaglandin E_2 (PGE_2) release

PGE_2 release in DRG neurons was stimulated by exposure to 100 ng/ml LPS for 24 hours. This consistently caused an increase in the levels of PGE_2 in DRG neurons, with an average increase of 82±2% ($P<0.0001$; n=3-6; results not shown).

J-2156 caused a significant reduction in the LPS stimulated release of PGE_2 however as with the cytokine results this was in a bell shaped response. Significant effects were first seen at 10 nM J-2156 ($P<0.01$ vs. LPS control; n=4; Fig. 3.26). Maximal inhibition was reached at 30 nM J-2156 ($P<0.0001$; n=4; Fig. 3.26) and inhibition was still significant at 100 and 1000 nM ($P<0.05$; n=6; Fig. 3.26). Indomethacin was used as a positive control where maximal inhibition was reached at 10 µM ($P<0.0001$; n=3; Fig. 3.26). This was not significantly different from 30 nM J-2156 (NS; n=3-6; Fig. 3.26).

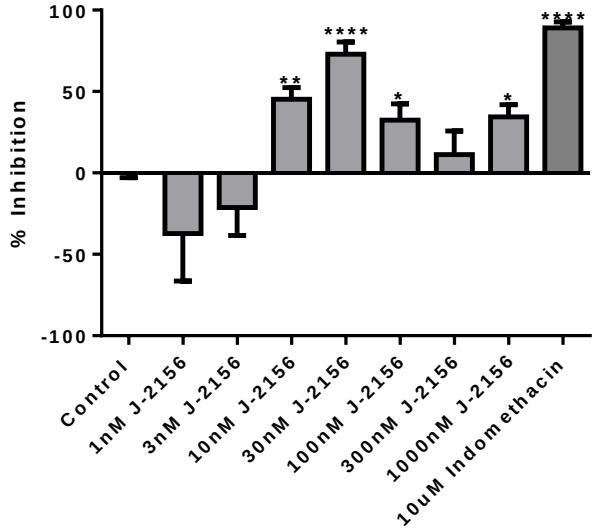

Fig. 3.26. Effect of J-2156 on lipopolysaccharide (LPS) stimulated prostaglandin E_2 (PGE_2) release in DRG neurons. Concentration-dependent effects of J-2156 on LPS stimulated PGE_2 release. DRG neurons were exposed to 100 ng/ml LPS for 24 hours. The sst_4 receptor agonists did inhibit LPS stimulation of PGE_2 at 30 nM in a similar manner to indomethacin. Data are presented as the % inhibition of the LPS stimulation. mean±S.E.M.. N=3-6. *P<0.05, **P<0.01, ****P<0.0001 vs. LPS control.

3.4.5. Calcitonin gene-related peptide (CGRP) release

CGRP release was stimulated in 3 different ways, all of which required 30 minutes exposure of the DRG neurons to the stimulating agent. Capsaicin at 100 nM significantly increased CGRP release by 65±31% (P<0.0001 vs. buffer; n=4; Fig. 3.27A). Veratridine at 100 µM significantly increased CGRP release by 53±11% (P<0.001 vs. buffer; n=10; Fig. 3.27B). High extracellular potassium exposure (56 mM KCl) significantly increased CGRP release by 54±8% (P<0.001 vs. buffer; n=10; Fig. 3.27C).

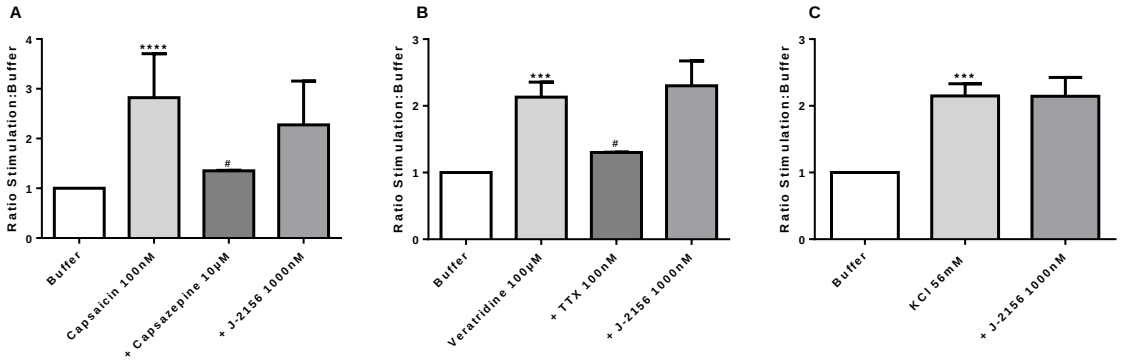

Fig. 3.27. Effect of J-2156 on calcitonin gene-related peptide (CGRP) release in DRG neurons. Effects of J-2156 on stimulated CGRP release. DRG neurons were exposed to either 100 nM capsaicin (A), 100 µM veratridine (B) or 56 mM potassium chloride (KCl) (C) for 30 minutes, all of which significantly increased CGRP release. Significance is represented by ***P<0.001, ****P<0.0001 vs. buffer. J-2156 had no influence on stimulated CGRP release. Capsazepine and tetrodotoxin (TTX) both significantly inhibited either capsaicin or veratridine induced CGRP release respectively. Significance is represented by #P<0.05. Data are presented as the ratio of the stimulation to the buffer. mean±S.E.M.. N=3-10.

J-2156 had no effect on CGRP released from any of the 3 stimulations (Fig. 3.26). Positive controls were tested for 2 of the stimulations. Capsazepine at 10 µM inhibited the capsaicin induced CGRP release by 81±1% (P<0.05 vs. capsaicin; n=3; Fig. 3.27). Tetrodotoxin (TTX) at 100 nM inhibited the veratridine induced CGRP release by 73±1% (P<0.05 vs. veratridine; n=3; Fig. 3.27). The difference in effect of the positive controls, capsazepine and TTX which inhibit CGRP release, compared to J-2156 which has no effect, could be due to expression profile of the sst_4 receptor. The positive controls directly target the channels (TRPV1 and Na_v), which are expressed on both non-peptidergic and peptidergic neurons, thus affecting CGRP release. However it is likely that the somatostatin receptors are only present on non-peptidergic neurons (Carlton *et al.*, 2001b) and therefore activation of the sst_4 receptor has no influence on CGRP release.

3.5. Effects of J-2156 on gene expression

To investigate whether J-2156 treatment might influence gene expression, and therefore result in an analgesic phenotype, next generation sequencing (NGS) studies were performed. This allowed large amounts of genetic information to be extracted from whole biological systems, showing changes in RNA levels. DRG neurons (L4-L6) from the inflamed side and inflamed paw skin tissues were sampled from the CFA rats following the 24 hour behavioural studies previously described (section 3.2.4). Samples were taken from 3 rats from each group: naïve, vehicle treated or compound treated. Various comparisons were made to determine which genes were influenced by the disease development changes, by comparing naïve to vehicle treated CFA tissue samples. Therefore, changes induced by the time course following intraplantal injection of CFA was established. Genes that were either up or down-regulated were identified as CFA-dependent. The effect J-2156 had on those subsets of genes was established, by comparing the vehicle treated CFA neurons to the J-2156 treated CFA neurons. As significance is not so common in such studies (Dawes *et al.*, 2014), restriction criteria were defined for further analysis. This included a factor change of >1.2 compared to naïve or CFA vehicle animals, and a cut off limit of >5 reads per kilobase per million (rpkm) for the CFA sample. The defined restriction criteria were based on advice from Dr Tobias Hildebrant.

3.5.1. DRG neurons

In the DRG neurons, 240 CFA dependent deregulated genes, which would be the likely contributors to the nociception were identified. Approximately a third of these genes (63) were counter-regulated, i.e. the decrease or increase in expression induced by CFA was inhibited by the sst_4 receptor selective agonist, J-2156 (Fig. 3.28).

Fig. 3.28. Venn diagram showing the total number of genes that correlated with 1 hour (A) or 24 hours (B) J-2156 treatment in DRG neurons. Multiple genes were up- or down-regulated by intraplantal injection of CFA and then normalised by treatment with the sst_4 receptor selective agonist J-2156. There were 6 genes which correlated for both time points.

The expression of 6 genes correlated for both 1 hour and 24 hours post administration of J-2156. Those were: fam150b, ccl2, KRT28, Cidea, RT1-A1 and Epha 10, and are listed in table 3.5, where specific genes associated with inflammatory pain and hypersensitivity have been identified.

Ensembl Name	Symbol	Adapted RGD description (http://rgd.mcw.edu/)
ENSRNOG00000005154	fam150B	Family with sequence similarity 150, member B: Found in extracellular region (inferred)
ENSRNOG00000007159	CCL2	Chemokine (C-C motif) ligand 2: Exhibits CCR2 chemokine receptor binding ; it is involved in cellular calcium ion homeostasis and cellular response to ATP ; and participates in granulocyte-macrophage colony-stimulating factor signalling pathway
ENSRNOG00000011846	KRT28	Keratin 28: Exhibits structural molecule activity (inferred)
ENSRNOG00000018505	Cidea	Cell death inducing DFFA-like effector a: Exhibits protein homodimerisation activity (ortholog); it is involved in cell death (ortholog) and lipid metabolic process (ortholog)
ENSRNOG00000038999	RT1-A1	RT1 class Ia: Exhibits beta-2-microglobulin binding; peptide binding; protein heterodimerisation activity; it is involved in positive regulation of T cell mediated cytotoxicity; and is associated with hypersensitivity
ENSRNOG00000045703	Epha10	

Table 3.5. Treatment with J-2156 influences gene expression in DRG neurons. There were 6 genes identified which had altered expression due to treatment with the sst_4 receptor selective agonist J-2156, for both 1 hour and 24 hours. These had already been identified as CFA dependent. Of these ccl2 is known to be important in inflammatory pain. Description information was acquired using the RGD website (http://rgd.mcw.edu/).

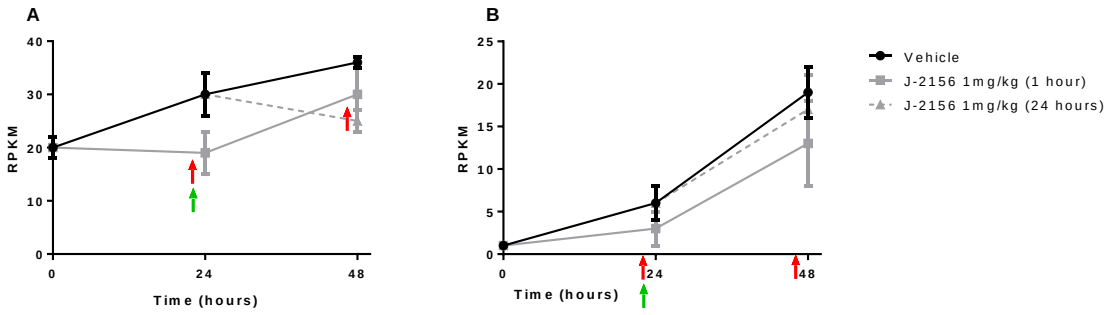

Fig. 3.29. Time profile of chemokine ligand 2 (ccl2) and Regeneration g islet derived 3 beta (reg3b) expression. Intraplantal injection of CFA induced increased expression of ccl2 (A) and reg3b (B) in DRG neurons over time. Treatment with the sst_4 receptor selective agonist, J-2156, reduced this CFA induced increase, where the effect for ccl2 lasted up to 24 post administration. The red arrows indicate administration of J-2156, which was then tested at 1 hour post administration. The green arrows indicate administation of J-2156, which was then tested at 24 hours post administration. Data are presented as reads per kilobase per million (rpkm) and are expressed as mean±S.D.. N=3.

Chemokine ligand 2 (ccl2) and regenerating g islet derived 3 beta (reg3b) are examples where expression is substantially increased over disease development, so expression was higher at both 24 and 48 hours post intraplantral injection of CFA (Fig. 3.29). For ccl2, activation of sst_4 receptors counteracted this expression and the reduced levels persisted up to 24 hours post J-2156 administration (Fig. 3.29A). A similar profile was also seen for reg3b, where reduced levels were seen at 1 hour post compound administration, however these were not apparent at the 24 hour time point (Fig 3.29B).

Table 3.6 and table 3.7 outline all genes which J-2156 induced counter regulation of the CFA effect, at either 1 hour or 24 hours post administration, respectively. These revealed a wide array of genes being regulated, ranging from those involved in DNA binding and protein synthesis, to regulation of hormone activity, or calcium ion binding. Specific genes which have been previously associated with nociception were identified, including reg3b, TRPA1, THBS4 and Hba. Furthermore, genes involved in inflammation were identified including S1PR3, Tnc, Bdnf and Bdkrb2.

Ensembl Name	Symbol	Adapted RGD description (http://rgd.mcw.edu/)
ENSRNOG00000001580	Hoxd9	Homeo box D9: Exhibits DNA binding (ortholog); sequence-specific DNA binding transcription factor activity (ortholog)
ENSRNOG00000002832	slc16a2	Solute carrier family 16, member 2: Exhibits thyroid hormone transmembrane transporter activity; it is involved in hormone transport; thyroid hormone transport
ENSRNOG00000005770	sostdc1	Sclerostin domain containing 1: Involved in hair follicle morphogenesis (ortholog); mammary gland bud morphogenesis (ortholog); negative regulation of BMP signalling pathway (ortholog)
ENSRNOG00000006151	reg3b	Regenerating g islet derived 3 beta: Exhibits carbohydrate binding (inferred); it is involved in defence response to Gram-negative bacterium (ortholog); defence response to Gram-positive bacterium (ortholog)
ENSRNOG00000007354	TRPA1	Transient receptor potential channel, subfamily A, member 1: Exhibits calcium channel activity (ortholog); it is involved in calcium ion transmembrane transport (ortholog); and the detection of chemical stimulus involved in sensory perception of pain (ortholog)
ENSRNOG00000010031	VTN	Vitronectin: Exhibits extracellular matrix binding (ortholog); integrin binding (ortholog)
ENSRNOG00000012471	THBS4	Thrombospondin 4: Exhibits collagen binding; it is involved in behavioural response to pain
ENSRNOG00000013948	ZC3HAV1	Zinc finger CCCH type, antiviral 1 : Exhibits poly(A) RNA binding (ortholog)
ENSRNOG00000014524	S1PR3	Sphingosine-1- phosphate receptor 3: Exhibits integrin binding (ortholog); it is involved in adenylate cyclase-inhibiting G-protein coupled receptor signalling pathway (ortholog); cytokine production (ortholog); inflammatory response (ortholog)
ENSRNOG00000014838	Glipr2	GLI pathogenesis related 2: Exhibits protein homodimerisation activity (ortholog)
ENSRNOG00000016220	RPL12	Ribosomal protein L12: Exhibits poly(A) RNA binding (ortholog)
ENSRNOG00000016408	Kirrel	Kin of IRRE like (Drosophila): Exhibits myosin binding (ortholog)
ENSRNOG00000020270	Anxa8	Annexin A8: Exhibits calcium ion binding (ortholog); calcium-dependent phospholipid binding (ortholog); it is involved in negative regulation of phospholipase A2 activity (ortholog)
ENSRNOG00000020923	Tuft1	Tuftelin 1: Found in cytoplasm (ortholog) ; it is involved in neurotrophin nerve growth factor mediated neuronal differentiation
ENSRNOG00000022609	Mrps10	Mitochondrial ribosomal protein S10: Found in mitochondrion (ortholog) ; it is involved in protein synthesis within the mitochondrion
ENSRNOG00000027513	Rtel1	Regulator of telomere elongation: Exhibits ATP binding (ortholog); ATP-dependent DNA helicase activity (ortholog)
ENSRNOG00000042307	Rybp	RING1 and YY1 binding protein: Exhibits DNA binding (ortholog)
ENSRNOG00000045788		
ENSRNOG00000049585	Tnc	Tenascin C: Exhibits syndecan binding (ortholog); it is involved in cellular response to prostaglandin D stimulus;

ENSRNOG00000045638		
ENSRNOG00000050414	RGD1305704	Interacts with chloroprene
ENSRNOG00000047466	Bdnf	Brain derived neurotrophic factor: Exhibits neurotrophin TRKB receptor binding; it is involved in cellular response to nerve growth factor stimulus; cellular response to norepinephrine stimulus; cellular response to tumour necrosis factor
ENSRNOG00000047019	Bbip1	BBSome interacting protein 1-like: Involved in cilium assembly (ortholog); receptor localization to nonmotile primary cilium (ortholog)
ENSRNOG00000047300	Bdkrb2	Bradykinin receptor B2: Encodes a protein that exhibits bradykinin receptor activity; it is involved in acute inflammatory response to antigenic stimulus
ENSRNOG00000049882	Adcyap1	Adenylate cyclase activating polypeptide 1: Exhibits neuropeptide hormone activity; pituitary adenylate cyclase activating polypeptide activity; it is involved in ATP metabolic process; cAMP-mediated signalling

Table 3.6. A variety of genes were influenced by 1 hour treatment of J-2156 in the DRG neurons. There were 25 genes identified that had altered expression due to treatment with the sst_4 receptor selective agonist, J-2156 for 1 hour. Both pain and inflammation related genes were identified, among other areas. Description information was acquired using the RGD website (http://rgd.mcw.edu/).

Ensembl Name	Symbol	Adapted RGD description (http://rgd.mcw.edu/)
ENSRNOG00000000376	Tmem167b	Transmembrane protein 167B-like: Found in integral component of membrane (inferred)
ENSRNOG00000001416	Vgf	VGF nerve growth factor inducible: Exhibits neuropeptide hormone activity (ortholog); it is involved in regulation of neuronal synaptic plasticity
ENSRNOG00000004659	Creld2	Cysteine-rich with EGF-like domains 2: Exhibits calcium ion binding (inferred)
ENSRNOG00000004837	Limd1	LIM domains containing 1: Exhibits transcription corepressor activity (ortholog)
ENSRNOG00000005457	Lamp5	Lysosomal-associated membrane protein family, member 5: Found in cytoplasmic vesicle membrane (ortholog); dendrite membrane (ortholog); early endosome membrane (ortholog)
ENSRNOG00000005574	Adamts8	ADAM metallopeptidase with thrombospondin motif, 8: Exhibits metalloendopeptidase activity (inferred); zinc ion binding (inferred)
ENSRNOG00000006569	Itgb8	Integrin beta 8: Exhibits receptor binding; extracellular matrix protein binding (ortholog); it is involved it cartilage development (ortholog)
ENSRNOG00000008001	Rab3b	RAB3B member RAS oncogene family: Exhibits GDP binding (ortholog); GTPase activity (ortholog); it is involved in antigen processing and presentation (ortholog)
ENSRNOG00000010841	Col8a2	Collagen type VIII, alpha 2: Involved in camera-type eye morphogenesis (ortholog); epithelial cell proliferation (ortholog)
ENSRNOG00000011348	Snx14	Sorting nexin 14: Exhibits phosphatidylinositol binding (inferred); it is involved in termination of G-protein coupled receptor signaling pathway (inferred)
ENSRNOG00000011994	Perp	PERP, TP53 apoptosis effector: Involved in activation of cysteine-type endopeptidase activity (ortholog); amelogenesis (ortholog); desmosome organization (ortholog)
ENSRNOG00000012881	Fgl2	Fibrinogen like 2: Exhibits peptidase activity (inferred)
ENSRNOG00000014090	Retsat	Retinol saturase: Exhibits all-trans-retinol 13,14-reductase activity (ortholog); oxidoreductase activity (ortholog)
ENSRNOG00000017047	Inip	INTS3 and NABP interacting protein: Involved in cellular response to DNA damage stimulus (ortholog); DNA repair (ortholog); response to ionizing radiation (ortholog)
ENSRNOG00000019422	Egr1	Early growth response 1: Exhibits double-stranded DNA binding; it is involved in cellular response to cAMP; cellular response to drugs
ENSRNOG00000021185	Bola1	BolA family member 1: Found in mitochondrion (ortholog)
ENSRNOG00000022227		
ENSRNOG00000022273	Rfk	Riboflavin kinase: Exhibits riboflavin kinase activity (inferred); it is involved in apoptotic process (ortholog); positive regulation of NAD(P)H oxidase activity (ortholog); reactive oxygen species metabolic process (ortholog)
ENSRNOG00000026646	Ndufs5	NADH dehydrogenase Fe-S protein 5: Involved in mitochondrial respiratory chain complex I assembly (ortholog)

ENSRNOG00000029389		
ENSRNOG00000029886	Hba1	Hemoglobin, alpha 1: Exhibits beta-amyloid binding; it is involved in regulation of sensory perception of pain
ENSRNOG00000030449	Gsta4	Glutathione S- transferase alpha 4: Exhibits drug binding
ENSRNOG00000031896	Stt3a	Subunit of the oligosaccharyltansderase complex: Exhibits glycotransferase activity (ortholog)
ENSRNOG00000033646	Gpr123	G protein coupled receptor 123: Exhibits G-protein coupled receptor activity (inferred); it is involved in G-protein coupled receptor signalling pathway (inferred)
ENSRNOG00000033654	LOC501038	
ENSRNOG00000037341		
ENSRNOG00000049424	Hbb	Haemoglobin beta: Exhibits hemoglobin alpha binding; hemoglobin beta binding; oxygen binding
ENSRNOG00000047321	Hba2	Haemoglobin, alpha 2: Exhibits haptoglobin binding (ortholog); peroxidase activity (ortholog)
ENSRNOG00000049208		
ENSRNOG00000049918	Lrg1	Leucine-rich alpha-2 glycoprotein 1: Exhibits transforming growth factor beta receptor binding (ortholog)
ENSRNOG00000050046		
ENSRNOG00000048286		

Table 3.7. A variety of genes were influenced by 24 hour treatment of J-2156 in the DRG neurons. There were 32 genes identified that had altered expression due to treatment with the sst_4 receptor selective agonist, J-2156 for 24 hours. Genes identified did include those relating to pain perception. Description information was acquired using the RGD website (http://rgd.mcw.edu/).

3.5.2. Paw tissue

In the paw tissue 2055 genes were deregulated (either up or down) by CFA. These would be the likely contributors to nociception. Approximately half of these (885) were counter regulated by the sst_4 receptor selective agonist J-2156 (Fig. 3.30). The expression of 33 genes correlated for both 1 hour and 24 hours post J-2156 treatment; these are listed in table 3.8.

As with the DRG neurons a wide array of genes were regulated (Table 3.8). These included those involved in calcium ion activity, GTP binding and GPCR signaling pathways, and cell growth such as tubulin and fibronectin binding. This shows a large variety of expression, where multiple genes were influenced by CFA. Specific genes which have been previously associated with the immune response and are macrophage or leukocyte molecular markers were identified, including Mx1, cd163, cd38 and fmod.

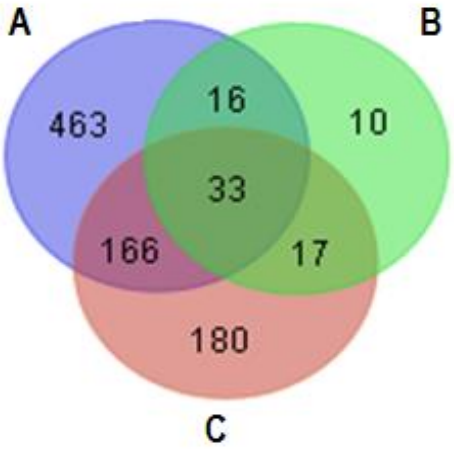

Fig. 3.30. Venn diagram showing the total number of genes that were regulated by CFA and counter regulated by J-2156 treatment in the paw tissue. Multiple genes were up- or down-regulated by intraplantal injection of CFA and then normalised by treatment with the sst_4 receptor selective agonist J-2156, at either 1 hour (A+B) or 24 hours (C) post administration. There were 33 genes which correlated for both time points.

In the paw tissue a large number of genes were either up- or down-regulated by CFA, allowing whole systems or networks to be analysed. Intraplantal injection of CFA induced changes to immunological pathways (Fig. 3.31A). J-2156 seemed to impact those genes regulated by CFA (Fig. 3.31B+C), suggesting possible links to macrophages, monocytes and dendritic cells. Specific gene types were identified which are macrophage or leukocyte molecular markers including cd74, cd7 and cd37. Furthermore, genes involved in inflammation were identified including IL21R. Other systems were investigated where deregulation was seen by CFA, however the sst_4 receptor agonist had little impact on these.

Ensembl Name	Symbol	Adapted RGD description (http://rgd.mcw.edu/)
ENSRNOG00000001959	Mx1	Myxovirus resistace1: Exhibits GTP binding (inferred); it is involved in response to innate immune response (ortholog)
ENSRNOG00000031927	Klk6	Kallikrein related-peptidase 6: Exhibits peptidase activity; it is involved in regulation of neuron projection development; neuron death (ortholog); positive regulation of G-protein coupled receptor protein signalling pathway (ortholog)
ENSRNOG00000027888	Cmss1	Cms1 ribosomal small subunit homolog (yeast): Exhibits poly(A) RNA binding (ortholog)
ENSRNOG00000009311	Fstl3	Follistatin-like 3: Exhibits activin binding (ortholog); fibronectin binding (ortholog)
ENSRNOG00000043325	RGD1562234	Similar to S100 calcium-binding protein, ventral prostate: Exhibits calcium ion binding (inferred)
ENSRNOG00000031851	Ndufa4l2	NADH dehydrogenase (ubiquinone) 1 alpha subcomplex, 4-like 2
ENSRNOG00000049208		
ENSRNOG00000020770	Arl4d	ADP-ribosylation factor-like 4D: Exhibits GTP binding (inferred); it is involved in small GTPase mediated signal transduction (inferred)
ENSRNOG00000031955	Calml3	Calmodulin-like 3: Exhibits calcium ion binding (inferred); it participates in calcium/calcium-mediated signalling pathway
ENSRNOG00000018268	Hhip	Hedgehog-interacting protein: Exhibits hedgehog family protein binding (ortholog); zinc ion binding (ortholog)
ENSRNOG00000011955	RPLP1	Ribosomal protein, large, P1: Exhibits structural constituent of ribosome (inferred)
ENSRNOG00000014204	Pacsin3	Protein kinase C and casein kinase substrate in neurons 3: Exhibits calcium channel inhibitor activity (ortholog); it is involved in negative regulation of calcium ion transport (ortholog)
ENSRNOG00000010253	Cd163	CD163 molecule: Exhibits scavenger receptor activity (inferred)
ENSRNOG00000003069	Cd38	CD38 molecule: Exhibits NAD+ nucleosidase activity; hydrolase activity; it participates in calcium/calcium-mediated signalling pathway
ENSRNOG00000019428	Higd1a	HIG1 hypoxia inducible domain family, member 1A: Involved in cellular response to glucose starvation (ortholog); cellular response to hypoxia (ortholog); negative regulation of apoptotic process (ortholog)
ENSRNOG00000038480	Ppp1r36	Protein phosphatase 1, regulatory subunit 36: Exhibits phosphatase binding (ortholog)
ENSRNOG00000033261	Fam107a	Family with sequence similarity 107, member A: Involved in regulation of cell growth (ortholog)
ENSRNOG00000013380	Rhov	Ras homolog family member V: Exhibits GTP binding (inferred); and is involved in signal transduction
ENSRNOG00000014828	Avpi1	Arginine vasopressin-induced 1: Involved in activation of MAPK activity (ortholog)

ENSRNOG00000005944	Slurp1	Secreted Ly6/Plaur domain containing 1: Involved in locomotory behaviour (ortholog); neuromuscular process controlling posture (ortholog)
ENSRNOG00000031033	MT-ND2	Mitochondrially encoded NADH dehydrogenase 2: Exhibits ionotropic glutamate receptor binding; protein kinase binding; it is invovled in reactive oxygen species metabolic process (ortholog)
ENSRNOG00000016890	Tppp3	Tubulin polymerization-promoting protein family member 3: Exhibits tubulin binding (ortholog); it is involved in microtubule bundle formation (ortholog)
ENSRNOG00000002434	Tmem100	Transmembrane protein 100: Involved in angiogenesis (ortholog); arterial endothelial cell differentiation (ortholog); BMP signaling pathway (ortholog)
ENSRNOG00000037087		
ENSRNOG00000016164	Fcrl2	Fc receptor-like 2: Exhibits SH3/SH2 adaptor activity (ortholog)
ENSRNOG00000003183	Fmod	Fibromodulin: Involved in odontogenesis; wound healing
ENSRNOG00000001295	S100b	S100 calcium binding protein B: Exhibits calcium ion binding; protein homodimerization activity; it participates in calcium/calcium-mediated signalling pathway
ENSRNOG00000023061		
ENSRNOG00000030478		
ENSRNOG00000000875	Fhl1	Four and a half LIM domains 1: Exhibits ion channel binding (ortholog); it is involved in negative regulation of cell growth (ortholog)
ENSRNOG00000006519	Tmem107	Transmembrane protein 107: Involved in cilium assembly (ortholog); embryonic digit morphogenesis (ortholog); neural tube patterning (ortholog)
ENSRNOG00000015411	Apobec1	Apolipoprotein B mRNA editing enzyme, catalytic polypeptide 1: Exhibits cytidine deaminase activity; AU-rich element binding (ortholog)

Table 3.8. Treatment with J-2156 influences gene expression in paw tissue. There were 33 genes identified that had altered expression due to treatment with the sst_4 receptor selective agonist J-2156, at both 1 hour and 24 hours. These had already been identified as CFA dependent. Genes associated with the immune response were identified. Description information was acquired using the RGD website (http://rgd.mcw.edu/).

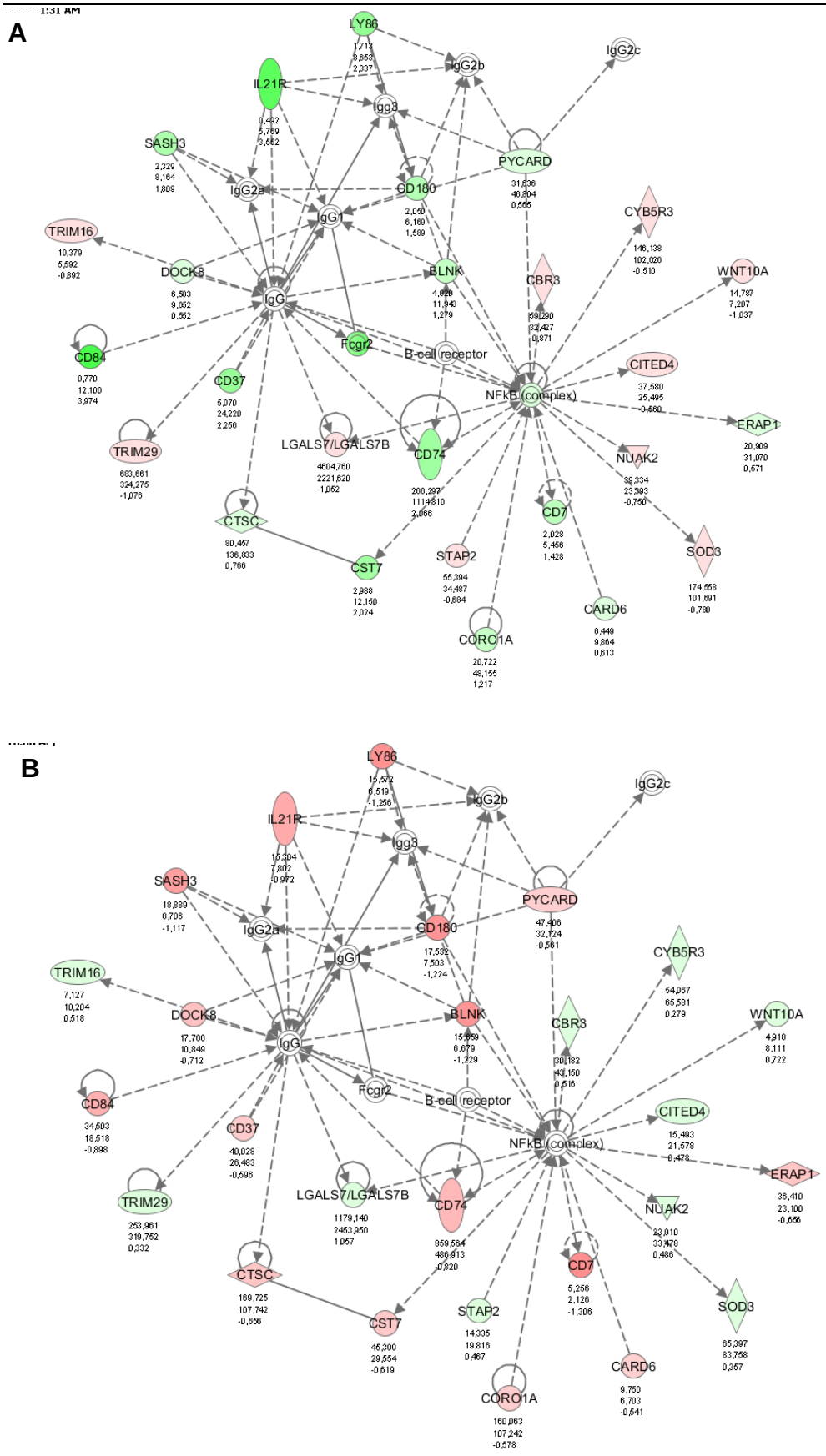
A
LY86
IgG2b
IgG2c
IL21R
Igg3
SASH3
PYCARD
IgG2a
CD180
IgG1
CYB5R3
TRIM16
DOCK8
BLNK
CBR3
WNT10A
IgG
Fcgr2
B-cell receptor
CD84
CD37
CITED4
NFkB (complex)
ERAP1
TRIM29
LGALS7/LGALS7B
CD74
NUAK2
CD7
CTSC
SOD3
STAP2
CST7
CARD6
CORO1A
B
LY86
IgG2b
IgG2c
IL21R
Igg3
SASH3
PYCARD
IgG2a
CD180
IgG1
CYB5R3
TRIM16
DOCK8
BLNK
CBR3
WNT10A
IgG
Fcgr2
B-cell receptor
CD84
CD37
CITED4
NFkB (complex)
ERAP1
TRIM29
LGALS7/LGALS7B
CD74
NUAK2
CD7
CTSC
SOD3
STAP2
CST7
CARD6
CORO1A

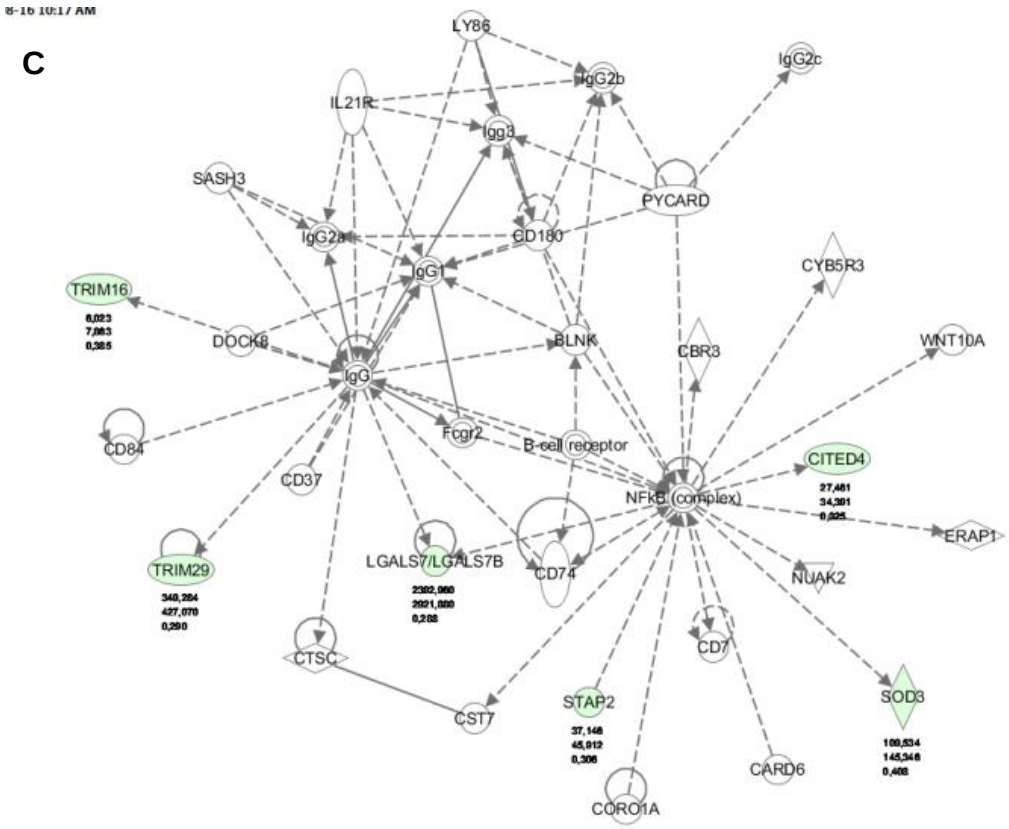

Fig. 3.31. Network analysis revelaed influences on immunological pathways in the paw tissue. Intraplantal injection of CFA influenced genes involved in the humoral immune response (A). At 1 hour (B) or 24 hours (C) post administration of the sst_4 receptor selective agonist, J-2156, counter regulation was seen. This system involved macrophages, leukocytes and inflammatory mediators. Red represents genes that have decreased expression levels, while green represents genes which have increased expression levels.

4. Discussion

Somatostatin is a regulatory neuropeptide, first discovered just over 40 years ago (Krulich *et al.*, 1968). The peptide is widely distributed throughout the body, producing pathological effects via activation of the five receptor subtypes (Patel *et al.*, 1996). Somatostatin has a wide biological profile, having vital roles in both the nervous system and the endocrine system. The peptide has been implicated in analgesia, where activation of somatostatin receptors induces anti-nociceptive effects, a process thought to be in part driven by the sst_4 subtype (Helyes *et al.*, 2000). This was based on the use of an sst_4 receptor agonist TT-232. Subsequently, this compound was reported to have anti-inflammatory and anti-nociceptive effects *in vivo*, using the carrageenan and partial nerve ligation (PNL) pain models, while being devoid of any endocrine effects (Pintér *et al.*, 2002). Supporting this, Szolcsanyi *et al.* (2004) confirmed the anti-nociceptive effects of TT-232 in the acute formalin-induced pain model and the chronic streptozotocin (STZ)-induced diabetic neuropathy model. These studies proposed a primarily peripheral site of action for sst_4 receptor agonists. Indeed, the receptor subtype is expressed on peripheral neurons, including dorsal root ganglion (DRG) neurons (Bar *et al.*, 2004). Later, a novel sulfonamide-peptidomimetic compound J-2156 was developed and found to possess greater affinity and selectivity for the human sst_4 receptor, compared to TT-232 (Engstrom *et al.*, 2005). This compound induces analgesia in the formalin-induced pain model, the adjuvants-evoked inflammatory pain model and the sciatic nerve ligation model of neuropathic pain (Sandor *et al.*, 2006). Moreover, in sst_4 receptor gene deleted mice nociceptive thresholds are decreased (Helyes *et al.*, 2009). Overall, these data indicate that the sst_4 receptor is a potential target for analgesic compounds.

This thesis builds on the knowledge that somatostatin has analgesic properties, which are thought to be mainly driven by activation of the sst_4 receptor subtype. The overall aim of the present study was to gain a greater understanding of the role of sst_4 receptors in analgesia and to elucidate the molecular mechanisms underlying this effect. In order to do this, a tool compound was first identified and characterised. The tool compound, J-2156 was then used for proof of concept studies, as well as mode of action experiments, where functional links to ion channels and inflammatory mediators were investigated. In addition, the influence of sst_4 receptor activation on gene expression was examined. The intention of this work was to investigate whether the sst_4 receptor qualifies as an attractive target to identify novel analgesic compounds that could be developed by the pharmaceutical industry.

4.1. J-2156 is a potent and selective somatostatin 4 receptor agonist

In the present study the selectivity, affinity and potency of various somatostatin agonists, which have been previously listed in published data, was established. J-2156 was identified as an appropriate tool compound for future studies due to its nM affinity and potency, with more than 400-fold selectivity for the sst_4 receptor subtype.

The selectivity of compounds and the affinity for the five somatostatin receptor subtypes were determined using radioligand binding assays. The two known biologically active forms of the endogenous ligand, somatostatin 14 (Brazeau *et al.*, 1973) and somatostatin 28 (Pradayrol *et al.*, 1980) were used as positive controls. Given that these are the endogenous ligands, it was expected that these would have nM affinity for all receptor subtypes. In this report both somatostatin 14 and somatostatin 28 showed nM affinity for all receptor subtypes, confirming the findings of Patel *et al.* (1994). This group conducted radioligand binding assays, using radiolabelled somatostatin 28, [^{125}I]-LTT-SRIF-28, on transfected Chinese hamster ovary (CHO-K1) cells expressing the human somatostatin receptor subtypes. Both endogenous ligands bound with nM affinity to all receptors, subtypes 1-4 preferentially bound somatostatin 14, while subtype 5 preferentially bound somatostatin 28 (Patel *et al.*, 1994).

A different endogenous ligand was also tested, corticostatin 17. This is a neuropeptide which exhibits a structural and functional resemblance to somatostatin, despite being produced from a different gene (Capuano *et al.*, 2011). Corticostatin is also reported to have a wide biological profile. It is not only associated with analgesia, evoking increased thresholds to thermal noxious stimulation in rats (Mendez-Diaz *et al.*, 2004), but also exhibits other neuronal functions including sleep modulation and locomotor activity (Spier *et al.*, 2000). The existence of a specific corticostatin receptor has yet to be identified, although it has been reported to have affinity for the somatostatin receptors (Siehler *et al.*, 1998). This was established using CCL39 cells (Chinese hamster lung fibroblast cells), stably expressing one the five human somatostatin receptor subtypes. Affinity was determined using radiolabelled coritcostatin, [^{125}I]-Tyr10-CST, and high affinity binding was seen for all five somatostatin receptors (Siehler *et al.*, 1998). It has also been suggested that the biological effects of corticostatin might be due to activation of the mas-related-gene receptor (MgrX2) (Robas *et al.*, 2003), or the growth hormone secretagogue receptor (GHS-R1a) (Broglio *et al.*, 2007). Nevertheless, in the present study, corticostatin had nM affinity for the somatostatin receptors, confirming the findings of Siehler *et al.* (1998). Given that activation of the somatostatin receptors is known to induce analgesia (Helyes *et al.*, 2000), one could speculate that it is activation of these receptors which is essential, and therefore responsible for, the analgesic properties of the ligand.

Various peptide mimetics were also characterised. Octreotide was used as a negative control for the sst_4 receptor subtype, as it is known to exhibit affinity for receptor subtypes 2, 3 and 5, with low affinity for subtypes 1 and 4 (Patel, 1999). Two promising compounds were initially identified, J-2156 and L803,087. However the compound chosen for this research was J-2156, as it had slightly higher affinity and potency compared to L803,087 and has been previously reported to induce analgesic effects in pain models (Sandor *et al.*, 2006). J-2156 is a highly selective ligand for the sst_4 receptor subtype and had nM affinity for both the human and rat forms of the receptor. The data produced in this research support the previously published findings of Engstrom *et al.* (2005), who showed that J-2156 has nM affinity for the sst_4 receptor by conducting radioligand binding assays using radiolabeled somatostatin 28 and CHO cells heterologously expressing the human somatostatin

receptor subtypes. In addition, this group reported that J-2156 had no affinity for various other GPCRs tested including bradykinin and opioid receptors (Engstrom *et al.*, 2005). Principally similar experiments were reproduced here, however in the present study radiolabelled somatostatin 14 was used and affinity was determined using CHO cell membrane preparation samples each expressing a separate somatostatin receptor subtype. Despite this, similar affinities were determined for the somatostatin receptors and in this study it was shown for the first time that J-2156 also had nM affinity also for the rat sst_4 receptor subtype.

To measure the potency of compounds a functional assay was conducted to confirm receptor activation. The agonist-induced inhibition of the intracellular adenylyl cyclase pathway was determined by measurements of forskolin-stimulated cAMP production. The endogenous ligands, somatostatin 14, somatostatin 28 and corticostatin 17, as well as the peptide mimetics, were tested on both the human and rat form of the sst_4 receptor. Comparable potencies of the different ligands for both the human and rat receptors were seen. Previous findings, using CHO cells expressing the human sst_4 receptor, showed that somatostatin 14, somatostatin 28 and J-2156 can inhibit forskolin-induced cAMP release (Patel *et al.*, 1994; Engstrom *et al.*, 2005). As cAMP production was also inhibited by J-2156 in the present study, it can be concluded that the sst_4 receptor is functionally coupled to adenylyl cyclase intracellular pathway (Patel *et al.*, 1994). In addition, it was shown in this study for the first time that J-2156 also inhibits forskolin-induced cAMP release by activation of the rat sst_4 receptor subtype. Lowering intracellular cAMP can prevent activation of different protein kinases or alter the function of various ion channels involved in pain transmission. Interestingly some of the peptide mimetics were more potent than the endogenous ligands. Furthermore, the peptide mimetics had higher potency compared to affinity. This was particularly true of J-2156, where a 10-fold difference was calculated.

One possible explanation for this is the receptor reserve phenomenon, which states that often the number of receptors expressed on the cell surface exceeds that which is needed for the full functional effect. Thus the concentration of compound producing 50% of receptor occupancy is often higher than the concentration of compound needed to produce 50% of the maximal response.

Another possible explanation for the inconsistencies seen between the endogenous ligands and the peptide mimetics, particularly J-2156, could be differential binding domains or mechanisms. A homology model of the sst_4 receptor subtype has shown that agonists have two distinctive binding modes (Liu *et al.*, 2012). It could, therefore, be speculated that binding of the endogenous ligands and the peptide mimetics may differ sufficiently to alter the agonistic efficacies. Furthermore, if J-2156 binds differently compared to the endogenous ligands, a conformational change of the receptor could occur. This might stabilise distinct receptor configurations that differ in their ability to interact with the G-protein, meaning that if J-2156 binds there is potentially better coupling to the G-protein.

4.2. J-2156 has a potent analgesic profile

As J-2156 was found to have nM affinity and potency for the sst_4 receptor, its ability to induce anti-nociceptive effects *in vivo* was investigated. Animal models are pivotal for the research and development of analgesic compounds. Chronic pain can be split into nociceptive or neuropathic conditions; therefore the effects of sst_4 receptor activation were investigated in models of both types of pain states. Nociceptive pain is induced by direct activation of nociceptors by specific stimuli and includes conditions associated with inflammation such as rheumatoid arthritis and osteoarthritis. Whereas neuropathic pain is induced by damage to the somatosensory system and includes conditions associated with nerve injury such as diabetic neuropathy. For assessment in nociceptive pain conditions the Complete Freund´s Adjuvant (CFA) and the monosodium iodacetate (MIA) models were used. The CFA model is an injury-induced, persistent inflammatory pain model (Millan *et al.*, 1988) and the MIA model is an established inducer of osteoarthritis (Kalbhen, 1987). Efficacy in neuropathic pain conditions was assessed using the partial nerve ligation (PNL) and the streptozotocin (STZ) induced diabetes models. The PNL model results in mononeuropathic pain produced by injury to a peripheral nerve (Seltzer *et al.*, 1990) and the STZ model a drug-induced model of peripheral diabetic polyneuropathy (Jaggi *et al.*, 2011). All models result in measureable pain processing, including mechanical hyperalgesia and weight bearing deficits.

The sst_4 selective agonist, J-2156, reduced both types of chronic pain states. J-2156 reduced mechanical hyperalgesia in the CFA, PNL and STZ models, as well as ameliorating weight bearing deficits in the MIA model. This confirms that the sst_4 receptor is an appropriate target for novel analgesics and that J-2156 is a suitable treatment for all types of pain conditions. Maximal analgesic effects were seen at 1 mg/kg in all pain models except for the MIA model, which required a dose of 10 mg/kg. Since the analgesic effects of sst_4 receptor agonists most likely act via similar mechanisms, it would be expected that efficacy in MIA would be achieved at the same doses as in other chronic pain models.

There are possible explanations behind the discrepancy in potency between the models. In the MIA model weight-bearing deficit was assessed. Osteoarthritis leads to altered joint kinematics i.e. the animals develop compensatory movements to minimize joint loading and pain (Malfait *et al.*, 2013), therefore measurement of weight-bearing deficit is more of a functional paradigm compared to the Randall Selitto method. This method involves a gradually increasing pressure being applied to the punctiform area of the hind paw which is trapped between a plane surface and a blunt point, where endpoint of this test is the reflex withdrawal of the paw (Randall *et al.*, 1957). Whereas, the weight-bearing deficit method not only requires training sessions to acclimatise the rodents to a novel environment, but also measures changes in posture i.e. no painful stimulus is applied, which suggests a CNS integrated adaption to the non-painful situation. This is of course different from paw withdrawal threshold, which is a spinal reflex with little CNS integrated contribution (Bove *et al.*, 2003). Such discrepancy in the effective dose has been seen with other compounds when comparing weight bearing deficit to mechanical hyperalgesia. Indomethacin and celecoxib are non-steroidal

anti-inflammatory (NSAIDs) compounds used to treat painful conditions associated with inflammation, including osteo- and rheumatoid arthritis. They have slightly different modes of action however as indomethacin is a non-selective COX inhibitor, while celecoxib is a COX2 selective inhibitor (Knights *et al.*, 2010). Boehringer-Ingelheim in-house data has shown that indomethacin also requires a 10 times higher dose in the MIA model compared to that required in the CFA model. Furthermore, celecoxib, which produces analgesia in the CFA model, required prophylactic twice a day treatment for three consecutive days in order to exert efficacy in the MIA model, indicating higher concentrations of compound are required. Both of these examples demonstrate how discrepancies in effective dosing, between the two models and methods, can occur.

Another possible explanation for the inconsistency in effective dose in MIA compared to the other models, might be pharmacokinetic properties. It is known that the distribution of compound in the synovial cavity represent a challenge for novel analgesics. It has been shown that for a small molecule the maximal concentration in the synovial fluid is significantly lower than in the plasma and is only achieved at 4 to 5 hours after the time of maximal concentration in the plasma, where antibodies can even take up to 24 hours to reach a steady state in the synovial fluids (Seideman *et al.*, 1994). Thus, a higher dose of J-2156 (and NSAIDs) may be necessary to obtain a concentration in the synovial fluid might which is sufficient to produce the desired effect.

Chronic pain is still an unresolved problem, with almost two thirds of patients' needs being unmet. Current treatments, examples of which include pregabalin, opioids and COX inhibitors, are often associated with unwanted side effects, such as sedation, dizziness (Boomershine, 2010; Taylor *et al.*, 2012) or gastrointestinal problems (Grosser *et al.*, 2006; Bruno *et al.*, 2014), which limit their use. The sst_4 receptor agonist, J-2156, has shown efficacy in three pain models (Sandor *et al.*, 2006). The findings in this study confirm and extend on that, showing that J-2156 causes analgesic effects in four pain models, suggesting that the sst_4 receptor would be an appropriate target for novel analgesics.

The results presented here demonstrate that this sst_4 receptor agonist can reverse mechanical hyperalgesia to high threshold stimulation in the CFA model, with relative efficacy comparable to indomethacin. Although this is confirming the results of Sandor *et al.* (2006) there are some methodological differences. Despite the CFA model being utilized, Sandor *et al.* (2006) also injected the oil into the root of the rats tails, rather than just an intraplantal injection in the hind paw, which was used in this study. Furthermore, allodynia was tested using the electronic von Frey method, where a touch stimulator, i.e. a non-painful stimulus, is applied to the hind paw of the rats(Sandor *et al.*, 2006). This is different from the results presented here, as hyperalgesia was measured, a painful stimulus was applied to the hind paw, so directly to site of inflammation. It could be speculated that this would be measuring a more chronic pain symptom, as it is a nociceptive stimulus being applied to directly the site of injury. The minimal effective dose found in this study was 0.1 mg/kg J-2156, which was 10-fold higher than required by Sandor *et al.* (2006). This discrepancy could be explained by the dosing schedule, where J-2156 was administered once in this study, compared to 3 times a

day by Sandor *et al.* (2006). The results presented here also show for the first time that J-2156 is efficacious in more complex pain conditions such as osteoarthritic pain. J-2156 reversed weight bearing deficits in the MIA model, thus broadening the prospect of this target in nociceptive pain conditions.

This research also demonstrated a vast potential for the sst_4 receptor agonist in neuropathic pain indications. J-2156 has previously been shown to reverse mechanical hyperalgesia in the PNL model at one week post-surgery when dosed acutely for 20 minutes Sandor *et al.* (2006). The PNL model was established by Seltzer *et al.* (1990), who used the pin-prick method to determine mechanical hyperalgesia. In those conditions hyperalgesia peaked at 1.5 days, correlating to the initial pain produced after surgery. Following this there was a general decrease in mechanical hyperalgesia until day ten, at which point increases were again seen (Seltzer *et al.*, 1990). To ensure a significant decrease in threshold was present, and neuropathy had fully developed, mechanical hyperalgesia was tested at two weeks post-surgery in this study. J-2156 reversed mechanical hyperalgesia in the PNL model, with relative efficacy comparable to lamotrigine. This is anti-convulsant drug, used in the treatment of epilepsy and bipolar disease, however it is also appropriate as an analgesic for neuropathy as it inhibits both voltage-sensitive sodium and voltage-sensitive calcium channels. Efficacy of J-2156 was therefore established in a more chronic nerve injury model, where mechanical hyperalgesia was measured at two weeks after nerve ligation, rather than one week (Sandor *et al.*, 2006). In addition efficacy in the drug-induce diabetic neuropathic STZ model was established. Another sst_4 receptor agonist, TT-232, has shown efficacy the STZ model, inducing significant improvements in mechanical allodynia (Szolcsanyi *et al.*, 2004). The model was tested at a later time point of neuropathy development, at five weeks post induction of nociception (Szolcsanyi *et al.*, 2004) compared to three weeks for the STZ model used in this study. Although TT-232 is described as a selective sst_4 agonist (Szolcsanyi *et al.*, 2004), in the present study the compound had similar affinity for the sst_1 receptor subtype and potency was over a 1000-fold less than J-2156. This sst_4 receptor agonist J-2156 was shown to be efficacious in the STZ model, causing a significant increase in paw withdrawal threshold, at a similar relative efficacy to duloxetine. This drug belongs to the family of serotonin-norepinephrine reuptake inhibitors (SNRI). It is an appropriate compound for treatment of painful conditions including osteoarthritis, but it particularly useful in treating patients with diabetic neuropathy (Bril *et al.*, 2011).

4.3. J-2156 modulates the activity of a variety of ion channels

Since J-2156 was found to be a potent analgesic in four chronic pain models, the potential mechanism of action via functional links to ion channels was investigated. Ion channels are important in pain, with a key role in the transduction and transmission of noxious stimuli from the periphery. Primary sensitive nociceptive afferent fibres have their cells bodies in the DRG neurons. These cells were therefore cultured and used as an *ex vivo* model of pain transmission. Whole cell patch clamp and calcium imaging experiments allowed potassium, calcium and sodium ion movement to be investigated. Activation of the sst_4 receptor with J-2156, resulted in activation of G protein gated

inwardly rectifying potassium (GIRK) channels and inhibition of ion influx through voltage sensitive calcium channels (Ca_v), transient receptor potential vanilloid 1 ion (TRPV1) channels and transient receptor potential ankyrin (TRPA1) channels. Although no effect was seen on voltage sensitive sodium (Na_v) currents, an increase in firing threshold of action potentials in DRG neurons was seen after application of compound. These channels all have important roles in the pain processing pathway (Caterina *et al.*, 1997; Story *et al.*, 2003; Gribkoff, 2006; Bhave *et al.*, 2010), and have all been targeted previously for other analgesic compounds (Mitrovic *et al.*, 2003; Khasabova *et al.*, 2004; Endres-Becker *et al.*, 2007; Eid *et al.*, 2008). The results thus suggest the analgesic effects of J-2156 might be driven by reduced pain transmission from the periphery via modulation of ion channel activity.

Using both polymerase chain reactions (PCR) and immunohistochemistry experiments, Bar *et al.* (2004) found that sst_4 receptors are present on 30 – 60% of DRG neurons. In the present study approximately a third of the cells tested responded to J-2156. The capacitance of the cells recorded in the electrophysiology experiments give some hints of a contribution of medium sized neurons, which could be of Aδ fibre origin. This might help to explain how sst_4 receptor agonists contribute to the analgesia of both inflammatory pain and mechanical hyperalgesia.

Although GIRK channels are functionally responsible for maintaining the resting membrane potential of cells (Walsh, 2011), activation allows for the movement of potassium ions down their electrochemical gradient, resulting in hyperpolarisation of the cell membrane (Luscher *et al.*, 2010). These channels are expressed on DRG neurons (Gao *et al.*, 2007), where activation would reduce pain transmission. It was therefore investigated whether this channel type was activated by J-2156. In a previous report, functional links of the somatostatin receptors to GIRK channels has been seen (Kreienkamp *et al.*, 1997). However, in the earlier publication, the somatostatin receptors were co-expressed with GIRK channels in Xenopus oocytes cells, whole cell patch clamp experiments were run and the endogenous ligands were used to activate the receptors (Kreienkamp *et al.*, 1997). In the present study, although similar electrophysiological protocols were conducted, a sst_4 selective agonist, J-2156, was used to activate receptors in cultured DRG neurons, relating this effect more to the potential analgesic properties. The results showed that the sst_4 receptor specific agonist evoked a concentration-dependent increase in potassium current. Tertiapin Q significantly reduced this induced current, confirming that it is resulting from GIRK channel activation.

Activation of Ca_v channels induces the transduction of electric activity into biochemical signals via an influx of calcium ions (Catterall, 2000). This not only induces cell depolarisation but also allows for continued pain transmission by stimulating the release of neurotransmitters and peptides (Gribkoff, 2006). Given that inhibition of these channels slows the rate of nerve transmission (Gribkoff, 2006), functional links to the sst_4 receptor were investigated. Functional links of the sst_4 receptor to voltage sensitive calcium channels are known. Farrell *et al.* (2010) reported that the sst_4 selective agonist L-803,087 inhibited calcium influx in rat retinal ganglion neurons. The results of the present study showed that the sst_4 receptor specific agonist J-2156 evoked a concentration-dependent decrease

in voltage sensitive calcium current in DRG neurons. In both the publication (Farrell *et al.*, 2010) and within this study, the calcium imaging technique was employed, where similar protocols were conducted but different methods were used to induce the depolarisation of the neurons. In this report a custom built chamber (Boehringer-Ingelheim) allowed for voltage stimulations by an amplifier to be used to induce depolarisation, however Farrell *et al.* (2010) used high extracellular potassium solution (50 mM). The functional link of sst_4 receptors to Ca_v channels in retinal ganglion neurons has recently been confirmed using whole cell patch clamp techniques (Farrell *et al.*, 2014). Relating this mechanism to nociception, functional links of sst_4 receptors to Ca_v channels was confirmed in DRG neurons in the present study.

To establish which specific Ca_v channels were being influenced selective blockers were also applied in combination with J-2156. The sst_4 receptor agonist enhanced the inhibitory effect of each of the blockers. This suggests that the sst_4 receptor is able to modulate multiple types of Ca_v channels, a similar mechanism to that seen for morphine (Khasabova *et al.*, 2004). Morphine significantly inhibited the potassium induced calcium influx in DRG neurons. Co-treatment with selective blockers allowed for the specific Ca_v channels being inhibited to be established. Those results showed that mu-opioid receptors couple with all subtypes of calcium channels (Khasabova *et al.*, 2004). Although J-2156 had a similar profile with an additive inhibition with co-treatment, it does seem that the T-type Ca_v channels are least effected by the sst_4 receptor agonist. When the individual blockers for P/Q-, N- and L-type Ca_v channels were applied in combination with J-2156 there was always some remaining calcium current. This could be due to T-type Ca_v channels, as when J-2156 was applied in combination with the specific T-type blocker, mibefradil, no current remains. Analgesia does not require blockage of all Ca_v channel subtypes. Indeed, another analgesic the cannabinoid 1 receptor agonist CP55,940, does only inhibit one type, the N-type Ca_v channel (Khasabova *et al.*, 2004).

The required concentration of J-2156 to significantly activate GIRK was higher than required to inhibit the other channels investigated, where an effect was seen, or to inhibit cAMP production in the cell lines. This might be due to the specific intracellular pathway being measured, i.e. the specific subunit of the G-protein inducing modulation. GIRK activation is due to the dissociation of the G protein and binding of the $G_{\beta\gamma}$ dimer directly (Inanobe *et al.*, 1995), whereas cAMP inhibition is controlled by the $G_{\alpha i}$ protein (Patel *et al.*, 1994). Indeed, utilizing pertussis toxin, an agent known to inhibit the $G_{\alpha i}$ intracellular pathway (Engstrom *et al.*, 2005), it was shown that inhibition of Ca_v, TRPV1 and TRPA1 channels, by sst_4 receptor activation, was due to protein kinase A (PKA) inhibition. This adenylyl cyclase linked intracellular pathway might be more sensitive to sst_4 receptor activation, requiring lower concentrations compared to dissociation of the $G_{\beta\gamma}$ dimer.

These data suggest that activation of GIRK channels may be important in contributing to the analgesic effects of J-2156. Activation results in hyperpolarisation of the cell membrane (Luscher *et al.*, 2010) and thus inhibits voltage sensitive ion channels and reduces spontaneous action potential formation (Walsh, 2011). In order to establish how far activation of this channel influenced the sst_4 receptor effect on the voltage-stimulated calcium transient, the specific GIRK blocker tertiapin Q was

utilized. In this case a partial reversal of the sst_4 receptor-mediated calcium inhibition was seen. This could indicate an indirect mechanism for the inhibition of voltage stimulated calcium influx by GIRK channel activation. Furthermore, although no effect on voltage stimulated sodium current following J-2156 application was seen, significant increases in firing threshold of DRG neurons were recorded, presumably due to GIRK-induced hyperpolarisation of the cell membrane.

Voltage induced influx of calcium ions results in calcium induced calcium release. Calcium activates ryanodine receptors on the sarcoplasmic reticulum membrane causing an efflux of ions into the cytosol (Shmigol *et al.*, 1995). Thus the reduced voltage stimulated calcium influx might be in part due to decreased release from intracellular calcium stores. Even if the sst_4 induced reduction in intracellular calcium levels is due to reduced release from intracellular calcium stores, the important role this ion plays as a secondary messenger would still be reduced.

TRPV1 and TRPA1 channels are predominantly expressed in nociceptive DRG neurons (Caterina *et al.*, 1997; Story *et al.*, 2003). Activation of these non-selective cation channels in response to noxious stimulation allows the entry of both calcium and sodium ions into the cell and potassium ions out of the cell (Davis *et al.*, 2000; Kim *et al.*, 2007), resulting in depolarising current and ultimately transmission of pain signals. The possibility that these channels could be inhibited by sst_4 receptor activation was therefore investigated. J-2156 produced a concentration-dependent decrease in both TRPV1 and TRPA1 cation currents in DRG neurons. In order to confirm the specific channels being targeted, the effects of the antagonist capsazepine (TRPV1) and A-967079 (TRPA1) were tested. Both the antagonists significantly inhibited the capsaicin (TRPV1 agonist) or compound 6 (TRPA1 agonist) (Gijsen *et al.*, 2010) induced current respectively.

TRPV1 calcium current inhibition was established using calcium imaging experiments and two protocols were run. One was a double stimulation protocol, where the DRG neurons were exposed to capsaicin twice, the second of which was in the presence of the compound, then the ratio of the two stimulations was calculated. As the cells did not fully recover from the first capsaicin stimulation a second protocol was run, this was a pre-exposure protocol. The DRG neurons were pre-incubated with compound for five minutes, then a capsaicin stimulation directly determined the TRPV1 inhibition. To confirm validity of the cell this was then followed by an internal control of potassium induced depolarisation; the percentage of the potassium response was calculated. Both capsazepine and J-2156 were more potent in the pre-exposure protocol. The explanation for capsazepine is likely to be that as the cells have no previous exposure to capsaicin it was not competing for binding to TRPV1 channels. However, J-2156 does not directly bind to TRPV1 channels, since no binding was seen at concentrations of up to 10 µM (unpublished Boehringer-Ingelheim data). Here the explanation could be a reduced calcium-induced calcium release effect (Shmigol *et al.*, 1995), which could be impacting the double stimulation protocol. The remaining calcium present in the cell from the first stimulation contributes to the second stimulation, thus reducing the effects of the compounds; whereas in the second protocol the compound effect on TRPV1 current is shown directly by the first peak.

Electrophysiological experiments were performed to determine inhibition of capsaicin-induced TRPV1 sodium current. In this case in order to get a relevant response it was necessary to use a 100-fold higher concentration of capsaicin than that used to induce calcium influx. The reason for this difference is not clear. In the calcium imaging experiments the response is probably enhanced by release of ions from intracellular stores (Shmigol *et al.*, 1995). However, the effect of capsaicin may be different for the two ions due to the pore size of the channels (Banke *et al.*, 2010). It is assumed that many TRP channels, upon activation are subject to pore dilation, i.e. that the pore size is changed (Nilius *et al.*, 2011). Pore dilation results in increased selectivity of calcium ions and an increased calcium current through the channels (Nilius *et al.*, 2011), again indicating how a lower capsaicin concentration causes an amplification of signalling by the fluro4AM in the calcium imaging experiments.

Somatostatin, released from activated peripheral terminals of capsaicin sensitive primary neurons, inhibits acute inflammation and nociception in the CFA model (Szolcsanyi *et al.*, 1998). This effect was shown to be via sst_4 receptor activation, as resiniferatoxin (a TRPV1 agonist) induced allodynia in rats were dose dependently decreased by the sst_4 selective agonist TT-232 (Szolcsányi *et al.*, 2004). Szolcsányi *et al.* (2004) results confirmed the findings of Pintér *et al.* (2002), who also found that TT-232 significantly reduced both nociceptive and inflammatory responses evoked by 2.5% capsaicin (applied topically to the ear of mice). Those studies indicate that sst_4 receptor agonists affect TRPV1 mediated behavioural effects, whereas the results presented here, confirm direct modulation in an *ex vivo* model. Somatostatin receptor activation has also been shown to play an important role in inhibiting capsaicin-induced nociceptive signaling in the spinal cord, although this effect is shown to be by the sst_2 receptor subtype (Bencivinni *et al.*, 2011). Activation of the sst_2 receptor, using octreotide, not only inhibited capsaicin-induced glutamate release from mouse dorsal horn neurons, but also significantly reduced the capsaicin-induced increase in miniature excitatory postsynaptic currents (mEPSC). These results suggest an important role for this somatostatin receptor subtype in central excitatory nociceptive transmission relating to TRPV1 (Bencivinni *et al.*, 2011). Indeed, it has been suggested that anti-nociceptive and anti-hyperalgesic effects of sst_4 receptor agonists are modulated by inhibition of TRPV1-expressing nociceptors (see review: (Szolcsányi *et al.*, 2011)).

The observed inhibition of TRPV1 channel activity by sst_4 receptor activation, with J-2156, was augmented after CFA treatment. The results showed that the potency of J-2156 was higher during inflammatory pain compared to naïve animals, although the overall efficacy is similar. This is likely to be due to changes in expression and sensitisation of the TRP channels under inflammatory conditions. TRPV1 channels are sensitised and up-regulated during tissue damage (Tominaga *et al.*, 1998) and this is evident in DRG neurons prepared from CFA-injected rats (Ji *et al.*, 2002). This channel is sensitized by inflammatory agents (Cortright *et al.*, 2004) and is responsible for thermal hyperalgesia in carrageenan-induced inflammation (Davis *et al.*, 2000). This indicates the increased potency seen is due to up-regulation and sensitisation of TRPV1; however published data (Sandor

et al., 2006), as well as data presented in this report, show that the sst_4 receptor agonist J-2156 is a particularly potent analgesic for inflammatory pain in the CFA model. It could of course therefore be speculated that this increase in potency of TRPV1 channel inhibition in inflammation is due to increased expression of the sst_4 receptor. This has been seen in both mouse and rat pulmonary tissue, where there is a marked increase in sst_4 receptor expression occurring in inflamed lung tissue (Varecza *et al.*, 2009). Although such increases in expression were established using real-time quantitative PCR, Western blots and immunohistochemistry experiments, there is speculation that the increases seen might be due to increased influx of sst_4 receptor positive macrophages (Varecza *et al.*, 2009). However, in DRG neurons from rats with adjuvants induced inflammation, a model similar to the one used in the experiments presented in this report, no changes in expression were observed under inflammatory conditions at 3 days post alogene injection (Bar *et al.*, 2004). This supports the speculation that this increased expression in lung tissue is due to increased influx of sst_4 receptor positive macrophages and therefore doesn't help explain the sst_4 augmentation of TRPV1.

Inhibition of TRPA1 channel effects by the sst_4 receptor agonist J-2156 has been seen behaviourally. This compound has been reported to inhibit both 1% mustard oil induced ear odeama in mice and 1% mustard oil induced Evans blue leakage in the paw skin of rats (Helyes *et al.*, 2006). The results presented in this study confirm inhibition but show direct modulation in an *ex vivo* model. Somatostatin 4 receptor-induced inhibition of TRPA1 channels was not as efficacious as TRPV1 channels. Calcium ions play a crucial role in controlling the gating behaviour of TRPA1 channels, where elevated intracellular calcium levels induce activation of the channel (Doerner *et al.*, 2007). Thus when analysing inhibition of these channels a double stimulation protocol would be redundant due to the initial calcium influx, plus the calcium-induced calcium release effect (Shmigol *et al.*, 1995), contributing to the second stimulation. TRPA1 channel activity can be modulated by TRPV1 activation (Bautista *et al.*, 2006) due to the influx of calcium ions affecting the gating behaviour. As it was shown that sst_4 receptor activation inhibits TRPV1 calcium currents, the TRPA1 inhibition may, therefore, be a secondary effect of this. However, the TRPV1 competitive antagonist capsazepine had no influence on the TRPA1 activation by compound 6 (TRPA1 agonist, (Gijsen *et al.*, 2010)).

In the present study a higher concentration of the TRPA1 agonist, compound 6, was required to elicit a relevant response of the rat TRPA1 channels in DRG neurons, compared to that seen in human embryonic kidney cells (HEK293) transfected to express the human TRPA1 receptor (Gijsen *et al.*, 2010), despite the same calcium sensitive dye being used. Although, TRPA1 channels are expressed on DRG neurons, this is limited to around 30% of cells (Obata *et al.*, 2005). It is therefore likely that the cell lines (Gijsen *et al.*, 2010) have higher expression, even with perhaps a reserve of receptors, compared to that in the DRG neurons, thus activation can be achieved at a lower concentration. Furthermore, the human TRPA1 receptor might have slight conformational differences, meaning binding and activation of the rat subtype could require higher concentrations of compound 6.

Although high concentrations were needed, specific TRPA1 inhibition by compound was shown as capsazepine had no effect on the compound 6 induced calcium influx.

In addition to their permeability to calcium ions, TRPA1 channels are also permeable to sodium ions and as these are of relevance to pain, this could be of importance. However, TRPA1 channels are most permeable to calcium ions (Kim *et al.*, 2007) and are subject to pore dilation, resulting in a cation selectivity of 30% for calcium ions over sodium ions (Karashima *et al.*, 2010). As sodium ion movement is less sensitive to TRPA1 channel activation it is likely that to elicit a relevant response a high concentration of compound 6 would be required.

Voltage sensitive sodium channels present a valid target for analgesic intervention. These channels are expressed on DRG neurons (Akopian *et al.*, 1996), where the influx of sodium ions means they are responsible for electrogenesis in cells (Rush *et al.*, 2007) and contribute to the transmission of pain signals (Swayne *et al.*, 2008). Since Na_v channels are associated with such properties, functional links to the sst_4 receptor were investigated. The present study showed that activation of the sst_4 receptor had little effect on voltage induced sodium current. Only one concentration of J-2156 (100 nM) was tested, however significant effects on the other ion channels investigated were produced by 100 nM J-2156 (sections 3.3.1-4). In the whole cell current clamp experiments a significant increase in both step and ramp firing thresholds of neurons was observed; but given the influence sst_4 receptor activation has on other ion channels, this is likely to be an indirect GIRK driven secondary effect. This said it has been seen in house that very small changes in voltage induced sodium current can affect cell threshold (unpublished in-house data).

As none of the DRG neurons responded to 300 nM TTX, it could be speculated that predominantly TTX-resistant $Na_{v1.8}$ and $Na_{v1.9}$ channel expressing cells were recorded in the experiments presented here. It could therefore be suggested that the sst_4 receptor agonist has no influence on TTX-resistant current, but could be speculated that activation might influence TTX-sensitive sodium channels. Indeed, $Na_{v1.7}$ channels are known to be activated at lower voltages by slow, small changes in membrane potential (Blair *et al.*, 2002). The results showed that J-2156 does influence the firing threshold of the DRG neurons in the ramp protocol, i.e. when slower, smaller changes in membrane potential are applied. Perhaps those cells that had increased firing threshold in the ramp protocol are expressing TTX-sensitive sodium channels, which are sensitive to sst_4 receptor activation. In order to confirm this, combination experiments would need to be conducted, using both TTX and J-2156, to determine whether an additive effect would occur. However, the sst_4 receptor agonist also increased the threshold of the step protocol, i.e when quicker changes in membrane potential were applied, plus the agonist had no direct influence on the voltage-induced sodium current. Therefore, one would assume that the threshold change is more likely to be driven by GIRK activation, with no direct effect on Na_v channels.

4.4. J-2156 has indirect effects on inflammation

Given that J-2156 was shown to be a potent analgesic in the inflammatory pain models (section 4.2) and the sst_4 receptor modulation of TRPV1 channel activity was augmented under inflammatory condition (section 4.3), the potential mechanisms of analgesia via control of inflammatory effects was investigated. Inflammation is an important component of pathological pain. It involves the recruitment of inflammatory and immune cells, including neutrophils and macrophages, to the site of injury. These release a variety of inflammatory mediators, including cytokines, chemokines and prostaglandins, allowing for communication between the immune system and the nervous system. These mediators have key roles in both induction and maintenance of nociceptive signals. They sensitize nociceptors (Sun *et al.*, 2006), modulate levels of pain mediators (Malcangio *et al.*, 1996), act as neuromodulators (Bajetto *et al.*, 2001) and influence glutamate transporter activity and expression (Sitcheran *et al.*, 2005). The effects of sst_4 receptor activation on these inflammatory effects were therefore investigated using both *in vivo* and *ex vivo* techniques.

The results obtained in the present study demonstrate that sst_4 receptor activation using J-2156 can reduce paw volume. However, this was only seen at doses 10-times that required for anti-nociceptive effects; and independent of neutrophil infiltration and cytokine release. DRG neurons were cultured as an *ex vivo* pain model, where J-2156 was shown to have some influence on stimulated inflammatory mediator release.

For behavioural studies a second established inflammatory model was used. The carrageenan model is one showing acute inflammation (Winter *et al.*, 1962) and is particularly important in accessing anti-inflammatory effects of drugs *in vivo.* Paw volume was assessed in both the carrageenan and the CFA rat models of inflammation using a plethysmometer. As this is a non-invasive technique anti-nociceptive effects, measured using the Randall and Selito method (Randall *et al.*, 1957), could also be established within the same experiments. J-2156 reduced mechanical hyperalgesia in the carrageenan and CFA rat models of inflammatory pain, where significant analgesic effects were seen at a dose of 1 mg/kg. The sst_4 receptor agonist has been reported to have anti-inflammatory actions in rats and mice, examples of which include inhibition of CGRP release, reduction in mustard oil-induced neurogenic inflammation, reduced Evans blue leakage and reduction in carrageenan-induced paw volume (Helyes *et al.*, 2006). It was therefore investigated how far the pain relief produced by J-2156 treatment was due to anti-inflammatory actions.

Although Helyes *et al.* (2006) demonstrated anti-inflammatory properties in animal models of neurogenic and non-neurogenic inflammation this could not be reproduced completely in the present study. Only at doses 10 times higher than those generating analgesia was paw swelling reduced in the CFA rats treated with J-2156. No effect was seen in the carrageenan model for paw volume when J-2156 was dosed acutely up to 1 mg/kg. It cannot be excluded that methodological differences may be contributing to this discrepancy of the data presented in this study and the published study. For example, in the present study a 43% increase in paw swelling was observed compared to 30%

increase seen by Helyes *et al.*, (2006). Indeed, as Helyes *et al.* (2006) used 3% λ-carrageenan, compared to 1%, at a higher volume of 100 µl, compared to 50 µl used in this study, a larger increase in paw volume would be expected. However, the rats were anaesthetised using sodium pentobarbital (Helyes *et al.*, 2006), which according to Bhattacharya *et al.* (1987) can induce anti-inflammatory effects, indicating possibly why a lower oedema was recorded. It could be that the carrageenan-induced increase in paw volume observed in the present study might be too potent to inhibit. Moreover, J-2156 was administered at 15 minutes prior to carrageenan injection (Helyes *et al.*, 2006), whereas 1 hour was used in the study presented here, meaning plasma concentrations of the compound could be higher at the earlier time point. However, lower doses of J-2156 were administered in the Helyes *et al.* (2006) study compared to those used in the present study, so this is unlikely to be of great influence.

Helyes *et al.* (2006) did not observe effects on CFA induced paw oedema when tested within a few days post algogene injection. A significant effect was instead seen at later time points, on the fifth experimental day, where the effect was then comparable to the finding presented here, with a reduction of 30% in paw volume (Helyes *et al.*, 2006). The delay in effect seen in the publication could be due to the discrepancy in dosing, where much higher doses of J-2156 were administered in this study. It could be that by day five of the Helyes *et al.* (2006) study, where the compound was administered three times daily, that the compound exposure is stable and more comparable to that in this study at the earlier time point. At 10 mg/kg the J-2156 induced anti-inflammatory efficacy in the CFA model was comparable to that of the clinically-active NSAID, celecoxib. Thus, sst_4 receptor agonists can reasonably modulate inflammation with a relative efficacy comparable to COX enzymes. This said, given analgesic effects of J-2156 are produced in lower doses than required to reduce inflammation, the anti-inflammatory effect is unlikely to be the main influence on the anti-nociceptive effect.

The paw muscle tissue was sampled from the CFA *in vivo* study to determine how far neutrophil infiltration or cytokine release might be influencing paw volume. Since the presence of neutrophils and cytokines are both known to be important in the inflammatory process leading to nociception (Scarborough, 1990), the effect of J-2156, on the influx of this cell type and the release of these mediators was therefore investigated. J-2156 had a minor influence (15% reduction) on neutrophil infiltration at the highest dose of 10 mg/kg. Given the variability of the assay and the magnitude of the response this is unlikely to be having any impact on paw volume. Moreover, this slight reduction did not correlate to cytokine release, which was found to be unchanged in the present study. This also indicates that peripheral tissue anti-inflammatory effects are not driving the analgesia of J-2156.

Activation of the sst_4 receptor has previously been associated with reduction of granulocyte accumulation determined by myeloperoxidase (MPO) activity. Studies conducted on mice using a LPS-stimulated lung inflammatory model found significant reductions in both neutrophil infiltration and levels of IL1β in the lung tissue (Helyes *et al.*, 2006; Elekes *et al.*, 2008). Contradicting this, however, was the lack of effect of the sst_4 receptor agonist on MPO activity in zymosan- or IL1β-

induced neutrophil accumulation in the back skin tissue of mice (Helyes *et al.*, 2006). Given that granulocytes themselves do not express the sst_4 receptor (Lichtenauer-Kaligis *et al.*, 2000), one could speculate that the observed reductions in neutrophils in the lung tissue might be a secondary effect. Indeed, Helyes *et al.* (2006) suggest that a reduction in the release of neuropeptides, such as substance P, from nerve endings could be influencing inflammatory processes by acting at receptors located on the granulocytes. J-2156 has been shown to inhibit electrically stimulated substance P release (Helyes *et al.*, 2006). Elekes *et al.* (2008) also suggested that the inhibitory effects of J-2156 on granulocyte accumulation was due to reduced chemotactic and neurogenic inflammatory mediators. In contrast, in the skin there is only a localised accumulation of neutrophils, so less influence of neurogenic inflammatory components. This model, therefore, is more comparable to the CFA paw tissue used in the present study, in which there are only localised neutrophils at the site of alogene injection, so influences on neuropeptides are less likely, restricting the potential anti-inflammatory effects.

Another possible explanation as to why only moderate effects on paw tissue inflammatory components are produced by J-2156 might be due to expression of the sst_4 receptor in the paw. It is known that the sst_4 receptor is the predominantly-expressed somatostatin receptor in the rat lung tissue, where only a weak signal for the sst_1 receptor is also seen (Schloos *et al.*, 1997), so the effects of J-2156 on inflammatory cells and mediators would be present. However, to my knowledge, there are no published data showing sst_4 receptor expression in paw tissue, where no in-house studies have been conducted.

As the sst_4 receptors are known to be expressed on DRG neurons (Bar *et al.*, 2004), an *ex vivo* LPS-stimulated inflammatory model was analysed. LPS induced the release of several cytokies including IFNγ, IL1β, IL6 and TNFα, the chemokine MCP1 and the prostaglandin PGE_2, all of which are known to have important roles in pain conditions (Scarborough, 1990; Abbadie *et al.*, 2009). J-2156 concentration-dependently inhibited the release of inflammatory mediators from DRG neurons although the concentration response curve, like that for celecoxib and indomethacin, was bell-shaped. The bell-shaped relationship for J-2156 was not observed in any of the other experiments presented in this study and the explanation for this is unknown. It can however be concluded that the sst_4 receptor is at least as effective in inhibiting inflammatory mediator release in the DRG neurons as the positive controls.

From the data produced in this study, it seems possible that sst_4 receptor-dependent reduction in inflammatory mediator release is specific to neuronal tissue. An inhibition of LPS-stimulated release in DRG neurons was seen, despite no inhibition of CFA-stimulated release in paws. These models are of course different, where CFA leads to localised inflammation in the site of injection (Millan *et al.*, 1988). The reduction observed in the DRG neurons might be due to reduced neurogenic neuroinflammation this leads to increased release of neuropeptides such as substance P and glutamate. Nearby cells of the immune system, including macrophages, mast cells and T cells, which express receptors for these neurogenic inflammatory components are then activated leading to the

release of inflammatory mediators (Xanthos *et al.*, 2014). LPS-stimulation does in fact cause an increase in neuronal activity (Gao *et al.*, 2014) and induces glutamate release (Barger *et al.*, 2007). Thus, the J-2156 inhibition of inflammatory mediator levels, seen in the DRG neurons, is likely to be a secondary effect on reduced neuronal activity, by interacting with ion channels (section 4.3), rather than direct inhibition of mediators.

When stimulated DRG neurons were analysed for CGRP release, no effect of the sst_4 receptor agonist J-2156 was observed. This data contradict previously published findings which indicate that somatostatin receptor activation can reduced CGRP release in lung tissue and trigeminal and brainstem neurons (Helyes *et al.*, 2006; Capuano *et al.*, 2011). Corticostatin is a potent inhibitor of chemically stimulated CGRP release from trigeminal and brain stem neurons (Capuano *et al.*, 2011). Corticostatin has nM affinity for all somatostatin receptor subtypes (Siehler *et al.*, 1998), where the main somatostatin receptors expressed in these neurons are subtypes sst_2 and sst_3 (Capuano *et al.*, 2011). One could therefore speculate that this coricostatin-induced reduction in CGRP release is not driven by activation of sst_4 receptors. Furthermore, Capuano *et al.* (2011) have used different neuronal cultures compared to the DRG neurons used in this study, where they even saw differences in the somatostatin induced inhibition from brain stem cultures compared to trigeminal cultures. Somatostatin significantly inhibited capsaicin-induced CGRP release in trigeminal neurons, but not brainstem neurons (Capuano *et al.*, 2011).

J-2156 specifically has been reported to concentration dependently inhibit the release of CGRP from the peripheral terminals of nerve endings of isolated trachea with a maximal inhibition of around 40% of the electrically induced release at 1000 nM (Helyes *et al.*, 2006). Their methodologies therefore differ from the one employed in the present study with respect to both tissue sampled and stimulation method. Within the sets of experiments reported here some DRG neuronal cultures showed partial inhibition of CGRP release via sst_4 receptor activation. With high extracellular potassium stimulation, for example, some J-2156 dependent inhibition (approximately 30% reduction) was seen in half the experiments. However, collectively the data indicate that J-2156 had no influence of CGRP release from DRG neurons. The poor inhibition in the DRGs compared to the lung might be due to the expression of sst_4 receptors, since in lung tissue it is known to be highly expressed (Schloos *et al.*, 1997).

Inhibition of calcium influx does not always translate to reduced CGRP release. Two examples include xenon (Calcott *et al.*, 2011) and the cannabinoid 1 receptor agonist CP55,940 (Khasabova *et al.*, 2004). Xenon can reduce capsaicin-stimulated TRPV1 calcium currents and is effective in producing analgesia (White *et al.*, 2011). However, when tested in cultured DRG neurons, xenon was ineffective in inhibiting capsaicin stimulated CGRP release (Calcott *et al.*, 2011). CP55,940 is known to inhibit N-type Ca_V channels in DRG neurons (Khasabova *et al.*, 2004) however, when CGRP release was stimulated by potassium-induced depolarisation, the compound showed no inhibition (Khasabova *et al.*, 2004). This group suggest that the L- and P/Q-type currents still remaining are sufficient to overcome the N-type inhibition of CGRP release (Khasabova *et al.*, 2004).

The data presented in the current report show that J-2156 has least effect on T-type Ca_v channels and perhaps the remaining current is sufficient to contribute to CGRP release.

To investigate CGRP release further, electrical stimulation rather than chemical stimulation could be used to make the J-2156 response more comparable to the published data. It might also be important to test "inflamed" DRG neurons. Gabapentin and pregabalin attenuate the capsaicin-evoked release of neuropeptides, including substance P and CGRP, from inflamed rat spinal cord slices, but have no effect on the non-inflamed slices (Fehrenbacher *et al.*, 2003). This suggests that these compounds act on cellular mechanisms that are not active under naïve conditions but only in pathological conditions (Fehrenbacher *et al.*, 2003). This again might help explain why no effects are seen in naïve DRG neurons. In addition the release of other neurogenic inflammatory mediators with important roles in pain such as substance P and glutamate, could be investigated (Snijdelaar *et al.*, 2000; Tao *et al.*, 2005).

4.5. J-2156 normalises expression of nociceptive and immune genes

The results of the present study demonstrate that J-2156 causes significant improvements in nociceptive behavioural tests in inflammatory pain models, which were still apparent at 24 hours post compound administration. Plasma concentrations were established, where analgesic effects were independent of compound exposure at the later time points. It was therefore investigated to what extent J-2156 influences gene expression in DRG neurons and paw skin tissue.

J-2156 has a dose proportional increase in plasma exposure following i.p. administration, this means that as the dose increases the plasma levels increase in a proportional manner. In general nociceptive behavioural *in vivo* studies are conducted at around 1 hour after J-2156 administration, or as close to the time of maximal plasma concentration as possible. The analgesic effects of J-2156 were tested at 1 hour after administration. At this time the plasma levels of the compound, for CFA and MIA models, are within range where maximal effects are seen for modulation of ion channel activity and inflammatory mediator release; thus explaining the analgesia seen. However, the plasma levels of J-2156 decline exponentially over time, where levels are below the detection limit (< 2 nM) at 24 hours post compound administration. Therefore the behavioural effects at this time are independent of plasma exposure.

This is the first study showing notable pain improvements 24 hours after J-2156 administration, a time when levels were no longer detectable in the plasma. Interestingly this long lasting effect was only seen in the inflammatory pain models and not in the neuropathic PNL model, where the inflammatory responses are only partially developed and additionally anti-inflammatory agents are quite ineffective in treating neuropathic pain (Broom *et al.*, 2004; Padi *et al.*, 2004). These results indicate a pharmacodynamic and plasma concentration disconnect for the later time points of J-2156 analgesia. This effect could be driven by longer binding of the compound to the sst_4 receptor, but

given the 24 hour analgesia is not apparent in all models, it can be assumed the compound has normal on-off kinetics.

A long lasting analgesic effect has been shown with a different somatostatin analogue RC-160, which is reported to be most selective for receptor subtypes 5 and 2 (Cai *et al.*, 1986). Behavioural long lasting effects were seen in both the hot plate and tail flick tests, tested in mice or rats respectively. Significant improvements were still present at 24 hours post compound administration (Eschalier *et al.*, 1991); however the group gives no indication of mechanism. This long term analgesia was confirmed by Betoin *et al.* (1994) who observed significant effects in the hot plate and phenylenzoquinene stretch tests in mice and in the paw withdrawal test in rats at both 21 and 24 hours post-administration of the highest doses of RC-160. This group suggests the effect involves a centrally driven opioidergic mechanism as the analgesia was reversed by naloxone. This said, there is contradicting published data showing no reversal of somatostatin receptor induced effects by naloxone (Sandkuhler *et al.*, 1990; Pascual *et al.*, 1991). In electrophysiological recordings made from cat dorsal horn neurons, superfusion of somatostatin was reported to reduce the excitatory responses caused by a mechanical stimuli application to the hindpaw, however this effect was not antagonized by naloxone (Sandkuhler *et al.*, 1990). Indeed, in clinics octreotide provided sufficient pain relief for intractable headaches, where again this effect was not influenced by naloxone (Pascual *et al.*, 1991). Moreover, the J-2156 mediated analgesia is thought to be driven mainly by peripheral rather than central mechanisms, as although J-2156 induced a significant decrease in both peripheral and spinal neuronal excitability, the concentration required to induce effects of spinal neurons was much higher than the effective behavioural dose (Schuelert *et al.*, 2014). It is therefore unlikely that the hypothesized central opioidergic mechanism is causing the long-lasting analgesia of J-2156 shown here.

This 24 hour analgesic presented study could be further developed and characterised by running longer time course experiments, where behavioural studies could be conducted at 48 hours post compound administration, to establish exactly how long the analgesic effect of J-2156 are present. However this was not tested as when comparing to the analgesia of RC-160, effects were no longer present at 48 hours post compound administration (Eschalier *et al.*, 1991; Betoin *et al.*, 1994).

As the 24 hour analgesia was specifically seen in the inflammation dependent pain models and J-2156 has been reported to have anti-inflammatory actions in rats (Helyes *et al.*, 2006), it was investigated how far this pain relief was due to cytokine release in the CFA animals. From the rats in the behavioural study both DRG neurons and paw tissues were sampled and cytokine levels investigated. Unfortunately the levels in the DRG neurons were below the detection limit of the assay. Moreover, as expected from previous data in this study (section 4.4), no influence on CFA induced inflammatory mediator release (IFNγ, IL1β, IL6, IL10 and TNFα, the chemokine MCP1 and the prostaglandin PGE_2) in the paw tissue was seen at either 1 hour or 24 hours post J-2156 administration. As the paw tissue is being investigated in isolation, the reduced neurogenic

neuroinflammation mechanism is not so vital (Xanthos *et al.*, 2014), thus potentially limiting the possible effects.

Given the potent and long lasting analgesia of J-2156 presented in these behavioural studies, the influence of this sst_4 receptor agonist on gene expression was investigated by running NGS studies. Tissues were sampled from the CFA animals. DRG neurons were isolated as the neuronal tissue component, while paw tissues represented the exact site of inflammation. J-2156 counter-regulated the expression of various CFA dependent genes, and in both tissues a wide array of genes were influenced.

In the DRG neurons changes in expression of nine genes were identified which might indicate potential contributors to the analgesia seen with J-2156. Those were ccl2, reg3b, TRPA1, THBS4, Bdnf, Bdkrb2, Hba1, S1PR3 and Tnc. From the genetic description listed in tables 3.5, 3.6 and 3.7 (section 3.5), it is clear that these are involved in the nociceptive and inflammatory processes. All of these genes had increased expression following CFA injection, which at either 1 hour or 24 hours post J-2156 administration, had comparatively reduced expression levels. Of those nine genes some have been previously described as putative biomarkers of nociception, where ccl2 and reg3b are indicated to be of particular importance (LaCroix-Fralish *et al.*, 2011). However THBS4, Bdnf and Bdkrb2 have also all been defined as pain genes (Lotsch *et al.*, 2013).

The role of reg3b within pain conditions is still not understood, however expression is increased in humans with inflammatory disorders which feature pain symptoms, including interstitial cystitis and inflammatory bowel disease (Ogawa *et al.*, 2003; Makino *et al.*, 2010). In this study reg3b expression was shown to be increased in CFA-treated DRG neurons. This confirms previously published data where reg3b expression, determined by immunohistochemistry experiments, has been reported to be increased in DRG neurons following adjuvants-induced inflammation (Averill *et al.*, 2008; He *et al.*, 2010). Expression peaked two days after induction of inflammation (He *et al.*, 2010), a similar profile to that seen in this study, where levels increased from 24 to 48 hours post induction of inflammation. As treatment with J-2156 then inhibited this increased expression of reg3b, this could be a contributing mechanism to the analgesia.

THBS4 and Hba1 are thought to be of more relevance to neuropathic pain conditions. THBS4 is reported to be an important biomarker in neuropathic pain (Wan *et al.*, 2010). Neuropathy was induced in rats using a chronic compression injury model and DNA microarray and real-time PCR experiments showed increased expression of THBS4 in the damaged DRG neurons (Wan *et al.*, 2010). Hba1 is more typically associated with diabetes, representing glycated heamoglobin. In a case-control study, involving 100 diabetic neuropathic patients, Hba1 levels were measured in blood samples. Throughout the 7 year study levels of Hba1 were consistently higher in patients with neuropathy, compared to controls (Coppini *et al.*, 2006). In addition, in another study on diabetic patients, nerve function was assessed based on ability to perceive touch sensations. Hba1 increases correlated to reductions in peripheral nerve function (Paisley *et al.*, 2002). The data presented in this

study was the first to indicate potential roles for THBS4 and Hba1 in the *in vivo* inflammatory pain CFA model, where levels of expression increased under pain conditions and then were lower in those DRG neurons treated with the sst_4 receptor agonist. As these genes are associated with pain conditions, reduced levels induced by J-2156 might add to the anti-nociceptive effects of this compound.

The role of ccl2 is well studied in pain processing (Abbadie *et al.*, 2009; Deshmane *et al.*, 2009), where modulation of the chemokine causes analgesic responses in inflamed conditions (White *et al.*, 2007). In a CFA mouse model, over-expression of ccl2, induced by glial fibrillary acidic protein promoter, induced greater oedemic and hyperalgesic responses. Significant effects were still recorded up to 3 weeks post CFA injection (Menetski *et al.*, 2007). In agreement with the data presented in the present report, increased expression of ccl2 following CFA inflammation has previously been established in DRG neurons using DNA microarrays (Chang *et al.*, 2010). Supporting this, increased expression of ccl2 is apparent in blood, nerve tissue and cerebral spinal fluid of humans with inflammatory conditions that feature pain symptoms, including Guillain-Barre syndrome and experimental autoimmune neuritis (Orlikowski *et al.*, 2003; Press *et al.*, 2003). Given the importance of ccl2 in pain conditions, decreased expression is likely to result in analgesia; therefore the reduced expression levels induced by treatment with the sst_4 receptor agonist could be identifying a contributory mechanism to the anti-nociception.

The role of TRPA1 in nociceptive conditions is also well established (Story *et al.*, 2003). Again with this gene previously published data shows up-regulation of TRPA1 expression following CFA-induced inflammation in DRG neurons, established using in-situ hybridisation histochemistry experiments (Obata *et al.*, 2005). This supports the findings of the present report, where expression was increased in CFA-inflamed DRG neurons compared to naïve DRG neurons and the levels in the DRG neurons prepared from J-2156 treated CFA rats were lower, inhibiting the inflammatory-induced increase. As TRPA1 channels can contribute to pain transmission by movement of positively charged calcium ions (Kim *et al.*, 2007), the lower expression levels in the DRG neurons following treatment with J-2156 might be contributing to the analgesia of this sst_4 receptor agonist.

Brain derived neurotropic factor (Bdnf) is an important contributor to pain conditions (Merighi *et al.*, 2008). Expression in DRG neurons is well accepted (Kashiba *et al.*, 2003). In the present study increased expression was observed in CFA-inflamed DRG neurons, this is confirming published data, where mRNA and protein levels in the dorsal horn have been reported to be increased following peripheral CFA-induced inflammation (Pezet *et al.*, 2002; Duric *et al.*, 2007). Indeed, this increased expression of Bdnf in DRG neurons, established by real time PCRs and Western blots, has been reported to correlate to CFA induced algesia, tested using the von Frey method for mechanical allodynia, a method involving a touch stimulator being applied to the hind paw of the rats (Lin *et al.*, 2011). Moreover, this neurotrophin is thought to specifically contribute to inflammatory pain, rather than neuropathic pain. In a Bdnf knock-out mice model, formalin responses were attenuated in comparison to control mice, however in segmental spinal nerve ligation neuropathic model,

mechanical hyperalgesia was the same in knock-out and control mice (Zhao *et al.*, 2006). In the DRG neurons isolated from the rats treated with the sst_4 receptor agonist, the CFA-induced increase in Bdnf expression was prevented. As this neurotrophin can contribute to nociception, the reduced levels following agonist treatment could be identifying a contributory mechanism to the analgesia of J-2156.

Tnc encodes tenascin-c an extracellular matrix glycoprotein associated with tissue injury and repair; it is specifically expressed in areas of inflammation. The role of this gene is well established in arthritic pain, where intra-articular injection leads to joint inflammation in mice, an affect induced by cytokine release via activation of toll like receptor 4 (TLR4) (Midwood *et al.*, 2009). This receptor is known to have a key role in driving inflammation (O'Neill, 2008). Furthermore, Tnc is associated with prostaglandin D synthase production, which is essential for allodynia symptoms (Eguchi *et al.*, 1999). Given that treatment with the sst_4 receptor agonist, J-2156, prevented the CFA-induced increase in expression of Tnc, regulation of this gene might be identifying a contributing mechanism to the analgesia.

Bradykinin receptors are expressed on sensory neurons. The bradykinin receptor subtype 1 is more extensively described in relation to regulation by inflammation rather than subtype 2 (Bdrk2) (Prado *et al.*, 2002). Bradykinin released from kininogen precursors at the site of tissue injury or inflammation, is able to activate the receptors and contribute to peripheral sensitisation (Rueff *et al.*, 1993). Concentrating specifically on the receptor subtype 2, agonists have the ability to increase dorsal horn neuronal activity, an effect which is inhibited by antagonists. Selective antagonists at the Bdrk2 receptor eliminate the second phase of the formalin test; however have no effect of the first phase. The second phase reflects the level of nociceptive input at the spinal cord, implying the analgesic effect is by reduced central sensitisation. Furthermore, in knock-out Bdrk2 mice, capsaicin-induced allodynia is reduced (Wang *et al.*, 2005). Behavioural studies testing mechanical hyperalgesia, using the Randall-Selitto method, in CFA rats, confirm that B2 antagonists can cause analgesic effects (Khasar *et al.*, 1995). Antagonising the Bdrk2 receptor is obviously beneficial in pain relief, therefore the lower expression levels in those rats treated with J-2156, compared to the CFA vehicle control rats, might also influence the analgesia of this sst_4 receptor agonist.

S1PR3 encodes a receptor which is activated by the biolipid sphingosine-1-phosphate (SP1), a modulator of innate immunity, cell migration and wound healing (Vogler *et al.*, 2003). The biolipid induces nociceptive depolarisation and action potential firing in mouse DRG neurons, as well as resulting in spontaneous pain behaviour *in vivo*, in wild type mice, defined as licking and flinching behaviour. In a S1PR3 knock-out mice model these induced nociceptive effects were significantly reduced. Supporting this, the receptors are expressed on both mice and human DRG neurons, established by in-situ hybridisation immunohistochemistry experiments (Camprubí-Robles *et al.*, 2013). Alterations in expression due to pain conditions has not previously been investigated, however S1PR3 has been defined as an important biomarker in other inflammatory disease, including acute lung injury (Sun *et al.*, 2012), where the data in the present study indicate this could be a biomarker

for inflammatory pain conditions. S1PR3 has roles in nociceptive effects, as J-2156 prevented the CFA-induced up-regulation in the expression levels in the DRG neurons, regulation of this gene could be identifying a potential mechanism to the analgesia associated with this sst_4 receptor agonist.

In the paw tissue there was a magnitude and diversity of genes expressed and influenced following CFA intraplantal injection. Regarding J-2156 the most relevant to the anti-nociceptive properties appear to be the leukocyte and macrophage molecular markers, for example including Mx1, cd163, cd38 and fmod, which all increased following CFA injection and this increased expression was inhibited with the sst_4 receptor agonist treatment.

The CFA oil is known to recruit both inflammatory and immune cells in order to stimulate a response (Broderson, 1989); it is therefore unsurprising that an increase in the markers for such cells is seen in this report. Leukocytes are cells of the immune system that defend against infectious disease and foreign invaders. They are involved in inflammatory nociceptive responses via recruitment to the site of injury. The cells then secrete proalgesic mediators such as cytokines, chemokines and prostaglandins (Rittner *et al.*, 2005), which are all known to induce pain symptoms (Scarborough, 1990; Bingham *et al.*, 2005; Deshmane *et al.*, 2009). Specific leukocyte cell types involved in pain conditions include macrophages.

Macrophages are large phagocytic leukocytes; produced by differentiation of monocytes. These have important roles in disposal of foreign particles. Macrophages have the ability to secrete pain mediators including cytokines (Cavaillon, 1994), prostaglandins (Glatt *et al.*, 1977) and glutamate (Ault *et al.*, 1993). Moreover, the essential role of this cell type in nociception is supported by *in vivo* data, where nociceptive responses, defined as the number of writhes in mice, are induced by both LPS-stimulated macrophages (Thomazzi *et al.*, 1997) and by an increase in resident macrophages, induced by zymosan and acetic acid (Ribeiro *et al.*, 2000). Both of these responses were partially inhibited with the use of cytokine antiserum (Thomazzi *et al.*, 1997; Ribeiro *et al.*, 2000), indicating inflammatory mediators are important but are not the sole contributor to the nociception induced by macrophages. As these cell types are important in pain conditions and CFA-induced increased expression is prevented by treatment with J-2156, these identify potential contributors to the analgesia seen with this sst_4 receptor agonist in the inflammatory pain model specifically.

Another gene identified in the paw skin tissue which is associated with the immune and inflammatory response was IL21R, encoding the interleukin 21 receptor. This genes was up-regulated by CFA and with the sst_4 receptor agonist, J-2156, treatment the up-regulation was prevented. This has previously been described as a biomarker in human diseases that have both inflammatory and painful components, including blood stasis syndrome and early-onset inflammatory bowel disease (Wang *et al.*, 2013; Salzer *et al.*, 2014). Moreover, the IL21R gene has been deemed a risk gene for inflammation in the dark Agouti rat strain, which is particularly susceptible to inflammatory diseases, including rheumatoid arthritis (Backdahl *et al.*, 2014). The IL21R is activated by IL21 and induces pro-inflammatory effects; it is of particular importance in modulating the immune response leading to

chronic inflammation. This receptor subtype causes effects via actions on T cells that are involved in cytokine secretion, activation leads to the secretion of interleukins including IL17 (Weaver *et al.*, 2007). IL17 is important in mediating pro-inflammatory reactions as well as contributing to pain hypersensitivity (Kim *et al.*, 2011). In an IL17 knock-out nerve ligation mouse model, paw withdrawal thresholds to mechanical stimuli were higher compared to the wild-type neuropathic mice (Kim *et al.*, 2011).

These data show that J-2156 prevents the CFA-induced up-regulation of a number of genes involved in inflammation and nociception, however, the molecular pathway behind this has not been investigated so far. The impact on gene expression might be driven by changes in neuronal activity, as it was shown that the sst_4 agonist J-2156 modulated several mechanisms contributing to neuronal excitability. However, it cannot be excluded that this modulation of gene expression might be dependent on recruitment of macrophages or satellite cells, as changed cell numbers would then translate to differentially-expressed genes. Indeed, there are data showing that the sst_4 receptor is expressed on macrophages (ten Bokum *et al.*, 1999; Taniyama *et al.*, 2005), meaning direct effects on these cell types could be induced, and therefore gene levels affected.

The results presented in this report indicate that the previously characterised sst_4 receptor agonist, J-2156, modulates the expression of a variety of genes involved in nociception, thus identifying contributory mechanisms to the analgesia seen with this agonist. Although this is clear, further development of these data is necessary. The next generation sequencing (NGS) data show gene expression in mRNA levels, it is therefore important to establish if this directly translates to protein expression. Immunohistochemistry experiments would support this; however Western Blot analysis would be preferential in order to quantify the data. The conclusions of this study, that the analgesia of J-2156 might be in part due to regulation of genes involved in nociception or inflammation, could also be strengthened using *in vivo* studies with knock-out models of those genes of importance. It would be expected that in such models there would be a reduced analgesic effect of sst_4 receptor agonist treatment. Although some of the genes modulated by J-2156 are known to be relevant in inflammation and nociceptive conditions, the role of others, specifically relating to pain is still unknown. It would therefore be of importance to determine how modulation of those genes influences the analgesia of J-2156, thus potentially identifying novel analgesic targets. Furthermore, the potential intracellular pathways which lead to changes in gene expression could be investigated.

These data not only confirm previous published data, where many genes which have been associated with nociception and the immune and inflammatory response were identified and shown to be CFA-dependently regulated, but also show for the first time that the sst_4 receptor selective agonist J-2156 is able to modulate gene expression. Given the counter regulation of these genes following J-2156 administration, it can be concluded that the analgesic effects of J-2156 are in part due to gene normalisation, resulting in an analgesic phenotype.

4.6. Relevance of this work to other pathological conditions

This research identifies contributing peripheral mechanisms to the analgesic properties of the sst_4 receptor selective agonist J-2156. However, somatostatin and its receptors have been ascribed to have important roles in various pathological conditions including lung disease (Helyes *et al.*, 2006), cognition (Sandoval *et al.*, 2013) and cancers (Evers *et al.*, 1991). Given the importance of this ligand in multiple diseases, the research presented in this report could be applied, and help to contribute towards understanding of those other pathological conditions.

4.6.1. Lung diseases

Lung diseases are induced by airway, lung tissue, or lung circulatory problems. Common examples include asthma and chronic obstructive pulmonary disease. Airway inflammation is an important component of lung disease. The lung is innervated by capsaicin-sensitive primary sensory neurons (Dinh *et al.*, 2004), which contribute to the stretch and pain symptoms of the disease. Pro-inflammatory neurogenic components released from these nerve endings can evoke vasodilation, plasma protein extravasation and leukocyte accumulation in the innervated area. These factors then contribute to the pathological mechanism of several inflammatory disease in the airways (Holzer, 1992), where it is the immune inflammatory changes which are of specific importance (Hogg *et al.*, 2009).

The sst_4 receptor is highly expressed in lung tissue (Schloos *et al.*, 1997) and this subtype specifically is up-regulated in inflamed pulmonary tissues (Varecza *et al.*, 2009). It is already published that the anti-inflammatory effects of sst_4 receptor activation, present it as a suitable target for novel treatments of lung disease (Helyes *et al.*, 2006); however interaction with different ion channels presented in this study could also contribute to beneficial effects. The transient receptor potential channels are of particular relevance. Chronic cough represents a major medical need; it is a common symptom of various lung diseases including asthma (Materazzi *et al.*, 2009). This is a reflex response to protect the airways from allergens and irritants, triggered by activation of peripheral sensory nerve endings in the airway lining (Bessac *et al.*, 2008). Both TRPA1 and TRPV1 channels are known to be expressed in these sensory afferents (Watanabe *et al.*, 2005; Nassenstein *et al.*, 2008). Activation of these channels induces coughing in both rodents and man (Laude *et al.*, 1993; Andrè *et al.*, 2009; Birrell *et al.*, 2009). Given the role of TRP channels in coughing reflexes and the importance they have in inflammatory conditions, these would be appropriate targets for treatment of lung disease (Bessac *et al.*, 2008). Thus, the sst_4 receptor modulation of TRP channels presented in this research (Gorham *et al.*, 2014b) could represent a contributory mechanism to the beneficial effects of sst_4 receptor activation in lung conditions. Furthermore, the NGS studies in this research showed sst_4 receptor induced reduction in S1PR3 expression levels, a known biomarker of inflammatory lung disease (Sun *et al.*, 2012). As increased expression was prevented by sst_4 agonists, this could lead to relief of symptoms.

4.6.2. Alzheimer's disease

Alzheimer's disease is the most common form of dementia associated with cognition problems, including memory, learning and behavioural deficits. The primary pathogenic agent of Alzheimer's disease is amyloid β plaque formation, where reduction of oligomer levels provide a viable means to treat the disease (Saito *et al.*, 2005). Somatostatin levels are consistently decreased in the cortex of Alzheimer's disease patient's brains and cerebrospinal fluid; this is a reproducible marker of the disease (Kumar, 2005). All somatostatin receptor are expressed in cortical neurons, expression has been analysed in frontal cortex sections of control and Alzheimer's disease samples using immunocytochemistry techniques. The sst_1 receptor had similar expression in both control and disease conditions. Immunoreactivity was present in both pyramidal and non-pyramidal neurons, throughout the neuronal structure, the dendrites and processes extending through the neuronal somata in the deep layers of the cortex. Subtypes 2, 4 and 5 had marked reductions in expression in disease states. The sst_2 receptor expression was confined mainly to pyramidal neurons; although levels were decreased in Alzheimer's brains this was not significant, however in dendrites and nerve fibres expression was diminished in disease states. Significant reductions in expression of the sst_4 receptor was observed, immunoreactivity was lost in the majority of Alzheimer's cases, where the receptor was no longer detectable in the dendritic cells of the cortex. Similarly significant reductions in sst_5 receptor were observed, loss was specifically seen in the deep layer of the cortex and in nerve fibres. Contradicting this, the sst_3 receptor had increased expression in disease states. This subtype was shown to be strongly localised to pyramidal neurons, nerve fibres and immune cells in cortex structures. Additionally in Alzheimer's cases expression was also observed in dystrophic neuritis and plaque formations (Kumar, 2005). Taken together these data suggest the ligand and receptors are pathologically involved in Alzheimer's disease (Kumar, 2005). Furthermore, agonizing the somatostatin receptors leads to clearance of amyloid β protein (Saito *et al.*, 2005), where an sst_4 receptor agonist specifically is reported to improve learning and memory (Sandoval *et al.*, 2013).

Neuroinflammation occurs in Alzheimer's disease patients, the mechanisms parallel those seen in the periphery and exaggerates the pathogenesis of the disease (Akiyama *et al.*, 2000). It is therefore suggested that anti-inflammatory treatments can benefit Alzheimer's disease symptoms. The underlying effects identified in this study of J-2156 inhibiting neurogenic neuroinflammation, might contribute to the beneficial effects of sst_4 receptor treatment of dementia. The intracellular calcium levels of neurons from Alzheimer's disease patients are not properly regulated. The amyloid β induces neurotoxic factors which impair cellular calcium homeostasis, rendering the neurons vulnerable to apoptosis and excitotoxicity (Eikelenboom *et al.*, 2006). Thus the reductions in calcium influx following sst_4 receptor activation (Gorham *et al.*, 2014a) would reduce this effect. TRPV1 channels are also thought to contribute to Alzheimer's disease pathology (Yamamoto *et al.*, 2007). These channels are expressed in the cerebrum, hippocampus and hindbrain, suggesting possible roles in neurodegeneration (Tóth *et al.*, 2005). Capsaicin induces cell death in mescencephalic dopamine neurons (Kim *et al.*, 2005) as well as microgilia (Kim *et al.*, 2006). This effect is via calcium signalling and mitochondrial disruption, and is inhibited by capsazepine (Kim *et al.*, 2005). Therefore

the sst_4 receptor modulation of TRPV1 channel activity presented here (Gorham *et al.*, 2014b), indicates a potential mechanisms for the beneficial effects of sst_4 receptor activation in Alzheimer's disease patients, specifically relating to neurodegeneration. Furthermore, the NGS studies in this report show sst_4 receptor activation reduced NDUFS5 expression levels, which is a gene known to participate in Alzheimer's disease via disruption of the mitochondrial respiratory chain complex, so could therefore lead to relief of excitotoxicity.

4.6.3. Cancers

Cancer is a group of diseases, characterised by abnormal growth of cells. This is caused by an imbalance of cell proliferation and cell death, leading to a population of cells that can invade tissues and metastasize to different sites. Somatostatin is produced by various tumours, and receptor expression is seen in different cancer tissue samples including breast (Frati *et al.*, 2014) and bladder (Karavitakis *et al.*, 2014). The endogenous ligand has been shown to have various anti-tumour effects in breast (Setyono-Han *et al.*, 1987), prostate (Murphy *et al.*, 1987), pancreatic (Upp *et al.*, 1988) and lung (Taylor *et al.*, 1991) cancers, although the exact mechanism behind these effects is unknown. Anti-tumour effects have been seen specifically with an sst_4 receptor agonist in malignant pleural mesothelioma (Yamamoto *et al.*, 2014).

Recently, there has been more understood about the role of ion channels in cancers. Specifically TRP channels, which are increasingly recognised as having important roles in the growth, proliferation, migration and invasion of cancer cells, where they are known to be expressed (Chen *et al.*, 2014). These effects are mainly via calcium-dependent mechanisms, such as cytoskeleton remodelling and modulation of intracellular pathways including mitogenactivated protein kinase (MAPK) and extracellular signalling regulated kinases 1 and 1 (ERK1/2) (Nielsen *et al.*, 2014). TRPA1 channel activation specifically is known to inhibit apoptosis and promote cell survival in lung cancers (Schaefer *et al.*, 2013). Furthermore sodium influx promotes invasion of cancers cells (Campbell *et al.*, 2013). Therefore the sst_4 receptor modulation of TRP channels observed in the present study (Gorham *et al.*, 2014b), ultimately leading to reduced calcium and sodium influx, might explain, at least in part, the beneficial effects of sst_4 receptor activation in the treatment of cancers.

Cancers are known to have strong genetic components. From the NGS studies in this research various genes involved in carcinomas were identified and shown to be regulated by the sst_4 receptor agonist J-2156. Two examples include Egr1 and Anxa8, which encode early growth response 1 and annexin a8. Egr1 is defined as a novel target for cancer intervention by gene therapy methods (Baron *et al.*, 2006), it has significant tumour suppressive properties (Liu *et al.*, 1998). Furthermore, expression enhances radio sensitivity of cancer cells (Li *et al.*, 2014). Anxa8 is involved in epidermal differentiation and is up-regulated in squamous carcinomas (Chao *et al.*, 2006). This gene contributes to tumourigenesis via induction of immune responses. It can be used as a diagnosis of cancer (Brichory *et al.*, 2001). In this study sst_4 receptor activation induced increased levels of Egr1

and decreased levels of Anxa8, this could then potentially contribute to the anti-tumour effects of somatostatin.

4.7. Future Perspectives

In this thesis I addressed the role of sst_4 receptors in analgesia, elucidating contributory peripheral molecular mechanisms to the anti-nociceptive effects seen. Although this work is of value to the pharmaceutical industry, some questions still remain unanswered and require further study.

The data presented in this study uses one selective sst_4 receptor agonist, although for truly solid conclusions to be made, it would be necessary to test other selective agonists. Indeed, to confirm the effects seen in these experiments are modulated by sst_4 receptor activation, ideally antagonists would also be tested to determine whether these effects can be reversed. Unfortunately, a sst_4 receptor-selective antagonist has not yet been described in literature. Cyclosomatostatin is described as a non-selective somatostatin receptor antagonist. Intraplantar injection of this compound induced nociceptive behavioural effects in rats, assessed by the number of paw flinches and enhanced the formalin effects; both of which were reversed with co-application with an agonist (Carlton *et al.*, 2001a). Furthermore, cyclosomatostatin can reverse somatostatin agonist induced effects; SCR007 was reported to reduce thermal and bradykinin excitation in a dose dependent manner in recordings from glabrous skin-nerve preparations. An effect which was reversed by cyclosomatostatin (Ji *et al.*, 2006). However, when this compound was tested in the cAMP assay no reversal of J-2156 induced reductions was seen, even though when given alone cyclosomatostatin increased cAMP levels. I therefore chose not to take this forward for future studies. Use of pertussis toxin was perhaps the best inhibitor of sst_4 receptor effects, given this was used in publications to reverse sst_4 receptor induced effects (Engstrom *et al.*, 2005).

In this study, the specific sst_4 receptor agonist was shown to have the ability to modulate the activity of a variety of ion channels involved in pain transmission (Gorham *et al.*, 2014a; Gorham *et al.*, 2014b). To support and develop these data various *in vivo* behavioural studies could be performed. Firstly knock-out models could be used. Such models have been developed for GIRK (Patil *et al.*, 1995), TRPV1 (Caterina *et al.*, 2000) and TRPA1 (del Camino *et al.*, 2010) channels. It could be established whether the analgesic effects of J-2156 are reduced in these models, thus confirming the importance of the contributory mechanism. Furthermore, specific behavioural tests associated with these channels could be conducted. Regarding TRPV1 channels, the effect on capsaicin evoked nociceptive and inflammatory responses could be assessed. For TRPA1 channels effects of J-2156 on cold allodynia could be investigated.

Tissue injury results in the release of inflammatory mediators from recruited immune cells, which are able to activate peripheral nociceptors (Kidd *et al.*, 2001). In the present study, an inhibition effect of the sst_4 receptor selective agonist, J-2156, on cytokine, chemokine and prostaglandin release was observed. These would all contribute to peripheral sensitisation. These data could be developed by

additionally investigating both bradykinin and growth factor release. Bradykinin is released following tissue damage, having important roles in early contribution to the inflammatory cascade. This mediator is known to produce pain, inflammation and hyperalgesia in humans (Meller *et al.*, 1992). Neurotrophic growth factors, such as NGF and Bdnf, produce significant and long lasting contribution to changes in neuronal activity during inflammation (Kidd *et al.*, 2001). Moreover, the bradykinin 2 receptor and Bdnf were identified as important genes contributing to the analgesic effects of J-2156 in the NGS studies presented in this thesis. It would therefore be of relevance to investigate the stimulated release of these mediators and modulation by J-2156.

Sustained activation of primary afferent fibres induces substantial changes to the activation of neurogenic pathways. The released inflammatory mediators and peptide transmitters induce central sensitisation, i.e. an increased response to stimulation due to sensitisation of nociceptive neurons in the dorsal horn of the spinal cord. This is mediated by amplification of the central nervous system via activation of secondary messenger systems, where kinases (Woolf, 1983), and NMDA receptors seem to be of particular importance (Kidd *et al.*, 2001). Effects of sst_4 receptor activation on central sensitisation could be investigated, where peripheral nociceptive mediators investigated in the present study have some influence. However, Schuelert *et al.* (2014) suggest more of a peripheral mechanism for J-2156 induced analgesia, with little influence of central effects. It could therefore be assumed that the analgesia of this specific compound is independent of effects on second order neurons.

It would also be of importance to establish whether the analgesic effect of J-2156 is mainly driven by peripheral or central mechanisms. This could be investigated by comparing the effects of the sst_4 receptor activation on peripheral afferent and spinal neuron activity, determining whether the concentrations required to influence neuronal activity correlate with the effective dose in behavioural studies. J-2156 induces a significant decrease in both peripheral and spinal neuronal excitability, but the concentration required to induce effects of spinal neurons is much higher than the effective dose *in vivo*. This was based on plasma and cerebral spinal fluid exposure of the compound (Schuelert *et al.*, 2014). Therefore, the analgesic effects of J-2156 appear to be mainly driven by the peripheral mechanisms outlined in this thesis.

Another important part of pain transmission is modulation. Descending inhibitory pathways from the midbrain and brainstem regions are able to modulate nociceptive inputs (Pagano *et al.*, 2012). This involves activation of noradrenergic neurons (Pertovaara, 2006) and inhibition of GABAergic neurons (Vaughan *et al.*, 1997). Activation of this system could ultimately lead to control of pain signalling. Such effects could be investigated by measuring stimulated noradrenaline or GABA release and any effect of sst_4 receptor activation on this could be determined. Furthermore, it could be established whether the influences of serotonin and enkaphalin on dorsal horn activity is modulated by J-2156.

GPCRs have the ability to form dimers with receptor subtypes from other receptor families. Recently opioid receptors have been shown to dimerise with somatostatin receptors (Prinster *et al.*, 2005),

including the sst_4 receptor subtype (Somvanshi *et al.*, 2014). Furthermore, it has been seen in-house that the effect of J-2156 on spinal neurons is due to inhibition of morphine sensitive neurons (Schuelert *et al.*, 2014). It could, therefore, be of interest to investigate potential links to the opioidergic system. Immunohistochemistry could be employed to determine co-localization and functional studies could be conducted to see whether the sst_4 receptor-induced effects are either augmented by opioid agonists or reversed by opioid antagonists. Behaviourally, the effects of J-2156 could be determined in opioid receptor knock-out models, to establish whether analgesia is reduced. Finally, effects of sst_4 receptor activation on the release of endogenous opioids could be determined.

4.8. Final summary and conclusions

This research aimed to gain a greater understanding of the role of sst_4 receptors in analgesia with a particular interest in elucidating molecular mechanisms.

J-2156 was identified as an appropriate tool compound for these studies. It has both nanomolar affinity and potency, with more than 400-fold selectivity for the sst_4 receptor subtype. This compound was shown to have a potent analgesic profile, having anti-nociceptive effects in both nociceptive and neuropathic chronic pain models. These *in vivo* anti-nociceptive properties were still significant at 24 hours post compound administration in the inflammatory pain models.

The data show that activation of sst_4 receptors modulates the activity of various ion channels within the pain processing pathway. J-2156 application resulted in an activation of GIRK and inhibition of Ca_V, TRPV1 and TRPA1 channels in the DRG neurons. Modulation of these channels results in hyperpolarisation of cell membranes, leading to increased firing thresholds of neurons and ultimately reduced excitability, thereby inhibiting pain signals. These are therefore identifying contributing molecular mechanisms to the J-2156 induce analgesia. The influence of J-2156 on ion channel activity appears to be the most relevant mechanism contributing to the anti-nociceptive effects of sst_4 receptors. The results indicate that the analgesic properties are independent of peripheral paw tissue inflammation and cytokine concentration. Whereas J-2156 did significantly inhibit inflammatory mediatory release in DRG neurons. However, it is likely that this effect is via indirect mechanisms of reduced neuronal activity and ultimately reduced neurogenic inflammation, as outlined in figure 4.1, again indicating the importance of ion channel modulation.

Finally, J-2156 was shown to modulate the expression of various genes in both DRG neurons and paw skin tissue. Genes, which have been previously described and identified as having important roles in nociception and the immune response, were shown to be counter regulated by sst_4 receptor activation. Thus, the analgesic effects of J-2156 might be in part due to gene normalisation, ultimately resulting in an analgesic phenotype.

Overall, these results indicate that sst_4 receptors are an appropriate and desirable target for novel broad treatment analgesics.

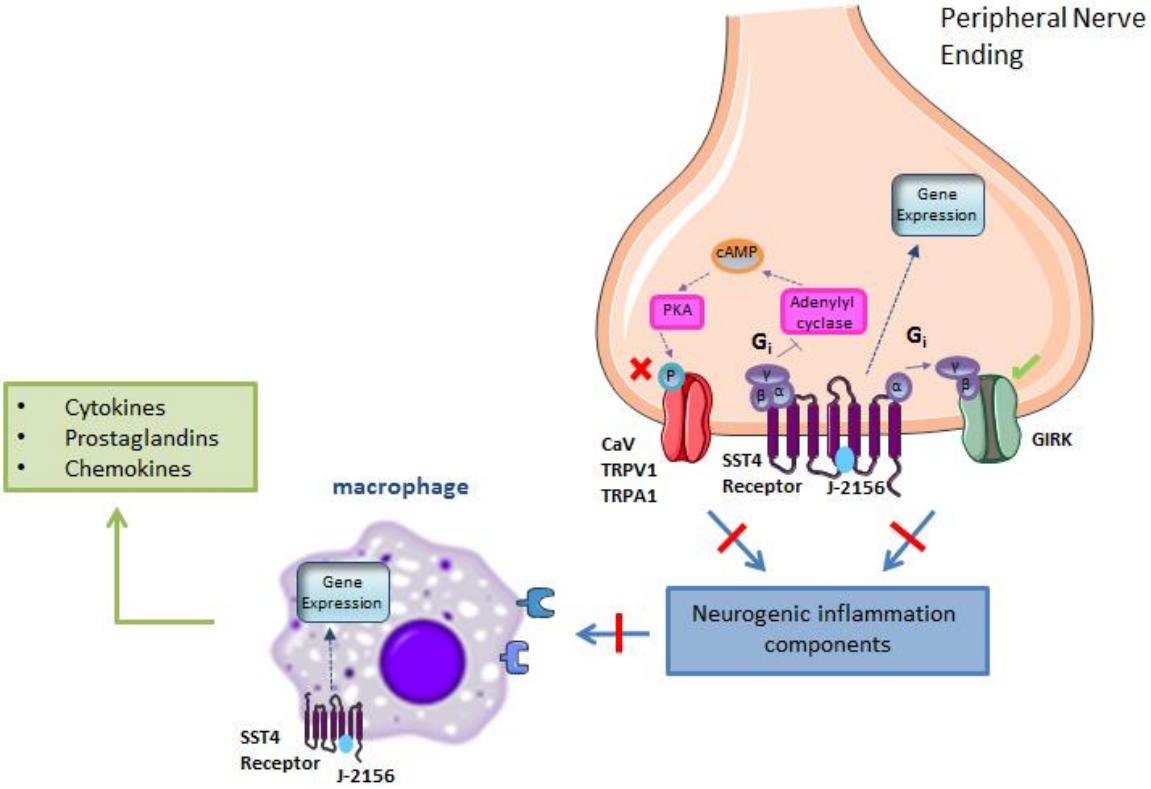

Fig. 4.1. Hypothesized molecular mechanisms contributing to the analgesic effects of J-2156. Activation of sst_4 receptors in peripheral nociceptive fibres results in modulation of various ion channels. The $G_{i\alpha}$ protein inhibits the adenylyl cyclase pathway, reducing cAMP levels and therefore ultimately reduced phosphorylation and sensitization of different ion channels. The $G_{\beta\gamma}$ subunit can also modulate ion channel activity by direct interaction. J-2156 induced a GIRK-dependent current and inhibited Ca_v, TRPV1 and TRPA1 currents, resulting in reduced neuronal excitability, ultimately decreasing the release of neurogenic inflammatory components and pain transmission. A secondary effect would be reduced activation of local inflammatory cells. Inflammatory cells express receptors for neurogenic inflammatory components, once activated these release inflammatory mediators. Therefore the reduced release of neurogenic inflammatory components could lead to reduced inflammatory mediatory release, including cytokines, prostaglandins and chemokines. Furthermore, J-2156 was able to modulate beneficially the expression of various genes which are closely associated with nociception. As macrophages expression sst_4 receptors (ten Bokum *et al.*, 1999; Taniyama *et al.*, 2005), this could be by direct modulation.

5. References

Abbadie C, Bhangoo S, De Koninck Y, Malcangio M, Melik-Parsadaniantz S, White FA (2009). Chemokines and pain mechanisms. *Brain Res Rev* **60**(1)**:** 125-134.

Abbadie C, Brown JL, Mantyh PW, Basbaum AI (1996). Spinal cord substance P receptor immunoreactivity increases in both inflammatory and nerve injury models of persistent pain. *Neuroscience* **70**(1)**:** 201-209.

Ahlgren SC, Levine JD (1993). Mechanical hyperalgesia in streptozotocin-diabetic rats. *Neuroscience* **52**(4)**:** 1049-1055.

Akiyama H, Barger S, Barnum S, Bradt B, Bauer J, Cole GM*, et al.* (2000). Inflammation and Alzheimer's disease. *Neurobiol Aging* **21**(3)**:** 383-421.

Akopian AN, Sivilotti L, Wood JN (1996). A tetrodotoxin-resistant voltage-gated sodium channel expressed by sensory neurons. *Nature* **379**(6562)**:** 257-262.

Andrè E, Gatti R, Trevisani M, Preti D, Baraldi PG, Patacchini R*, et al.* (2009). Transient receptor potential ankyrin receptor 1 is a novel target for pro-tussive agents. *Br J Pharmacol* **158**(6)**:** 1621-1628.

Arezzo JC, Schaumburg HH, Spencer PS (1982). Structure and function of the somatosensory system - a neurotoxicological perspective. *Environmental Health Perspectives* **44**(APR)**:** 23-30.

Arruda JL, Colburn RW, Rickman AJ, Rutkowski MD, DeLeo JA (1998). Increase of interleukin-6 mRNA in the spinal cord following peripheral nerve injury in the rat: potential role of IL-6 in neuropathic pain. *Brain Res Mol Brain Res* **62**(2)**:** 228-235.

Ault B, Hildebrand LM (1993). L-glutamate activates peripheral nociceptors. *Agents Actions* **39 Spec No:** C142-144.

Averill S, Inglis JJ, King VR, Thompson SW, Cafferty WB, Shortland PJ*, et al.* (2008). Reg-2 expression in dorsal root ganglion neurons after adjuvant-induced monoarthritis. *Neuroscience* **155**(4)**:** 1227-1236.

Backdahl L, Ekman D, Jagodic M, Olsson T, Holmdahl R (2014). Identification of candidate risk gene variations by whole-genome sequence analysis of four rat strains commonly used in inflammation research. *BMC Genomics* **15:** 391.

Bajetto A, Bonavia R, Barbero S, Florio T, Schettini G (2001). Chemokines and their receptors in the central nervous system. *Front Neuroendocrinol* **22**(3)**:** 147-184.

Banke TG, Chaplan SR, Wickenden AD (2010). Dynamic changes in the TRPA1 selectivity filter lead to progressive but reversible pore dilation. *Am J Physiol Cell Physiol* **298**(6)**:** C1457-1468.

Bar KJ, Schurigt U, Scholze A, Segond Von Banchet G, Stopfel N, Brauer R*, et al.* (2004). The expression and localization of somatostatin receptors in dorsal root ganglion neurons of normal and monoarthritic rats. *Neuroscience* **127**(1)**:** 197-206.

Barger SW, Goodwin ME, Porter MM, Beggs ML (2007). Glutamate release from activated microglia requires the oxidative burst and lipid peroxidation. *J Neurochem* **101**(5)**:** 1205-1213.

Baron V, Adamson ED, Calogero A, Ragona G, Mercola D (2006). The transcription factor Egr1 is a direct regulator of multiple tumor suppressors including TGFbeta1, PTEN, p53, and fibronectin. *Cancer Gene Ther* **13**(2)**:** 115-124.

Baumgaertner U, Greffrath W, Treede RD (2012). Contact heat and cold, mechanical, electrical and chemical stimuli to elicit small fiber-evoked potentials: Merits and limitations for basic science and clinical use. *Neurophysiologie Clinique-Clinical Neurophysiology* **42**(5)**:** 267-280.

Bautista DM, Jordt SE, Nikai T, Tsuruda PR, Read AJ, Poblete J*, et al.* (2006). TRPA1 mediates the inflammatory actions of environmental irritants and proalgesic agents. *Cell* **124**(6)**:** 1269-1282.

Bencivinni I, Ferrini F, Salio C, Beltramo M, Merighi A (2011). The somatostatin analogue octreotide inhibits capsaicin-mediated activation of nociceptive primary afferent fibres in spinal cord lamina II (substantia gelatinosa). *Eur J Pain* **15**(6)**:** 591-599.

Bennett GJ (1993). An animal model of neuropathic pain: a review. *Muscle Nerve* **16**(10)**:** 1040-1048.

Bessac BF, Jordt SE (2008). Breathtaking TRP channels: TRPA1 and TRPV1 in airway chemosensation and reflex control. *Physiology (Bethesda)* **23:** 360-370.

Beswick P, Bingham S, Bountra C, Brown T, Browning K, Campbell I*, et al.* (2004). Identification of 2,3-diaryl-pyrazolo[1,5-b]pyridazines as potent and selective cyclooxygenase-2 inhibitors. *Bioorg Med Chem Lett* **14**(21)**:** 5445-5448.

Betoin F, Ardid D, Herbet A, Aumaitre O, Kemeny JL, Duchene-Marullaz P*, et al.* (1994). Evidence for a central long-lasting antinociceptive effect of vapreotide, an analog of somatostatin, involving an opioidergic mechanism. *J Pharmacol Exp Ther* **269**(1)**:** 7-14.

Bevan S, Hothi S, Hughes G, James IF, Rang HP, Shah K*, et al.* (1992). Capsazepine: a competitive antagonist of the sensory neurone excitant capsaicin. *Br J Pharmacol* **107**(2)**:** 544-552.

Bhattacharya SK, Das N, Sarkar MK (1987). Inhibition of carrageenin-induced pedal oedema in rats by immobilisation stress. *Res Exp Med (Berl)* **187**(4)**:** 303-313.

Bhave G, Lonergan D, Chauder BA, Denton JS (2010). Small-molecule modulators of inward rectifier K+ channels: recent advances and\ future possibilities. *Future Med Chem* **2**(5)**:** 757-774.

Bingham S, Beswick PJ, Bountra C, Brown T, Campbell IB, Chessell IP*, et al.* (2005). The cyclooxygenase-2 inhibitor GW406381X [2-(4-ethoxyphenyl)-3-[4-(methylsulfonyl)phenyl]-pyrazolo[1,5-b]pyridazine] is effective in animal models of neuropathic pain and central sensitization. *J Pharmacol Exp Ther* **312**(3)**:** 1161-1169.

Birrell MA, Belvisi MG, Grace M, Sadofsky L, Faruqi S, Hele DJ*, et al.* (2009). TRPA1 agonists evoke coughing in guinea pig and human volunteers. *Am J Respir Crit Care Med* **180**(11)**:** 1042-1047.

Blair NT, Bean BP (2002). Roles of tetrodotoxin (TTX)-sensitive Na+ current, TTX-resistant Na+ current, and Ca2+ current in the action potentials of nociceptive sensory neurons. *J Neurosci* **22**(23)**:** 10277-10290.

Bodnar RJ, Kelly DD, Brutus M, Glusman M (1980). Stress-induced analgesia: neural and hormonal determinants. *Neurosci Biobehav Rev* **4**(1)**:** 87-100.

Bogen O, Dina OA, Gear RW, Levine JD (2009). Dependence of monocyte chemoattractant protein 1 induced hyperalgesia on the isolectin B4-binding protein versican. *Neuroscience* **159**(2)**:** 780-786.

Boomershine CS (2010). Pregabalin for the management of fibromyalgia syndrome. *J Pain Res* **3:** 81-88.

Bourinet E, Alloui A, Monteil A, Barrère C, Couette B, Poirot O*, et al.* (2005). Silencing of the Cav3.2 T-type calcium channel gene in sensory neurons demonstrates its major role in nociception. *EMBO J* **24**(2)**:** 315-324.

Bove SE, Calcaterra SL, Brooker RM, Huber CM, Guzman RE, Juneau PL*, et al.* (2003). Weight bearing as a measure of disease progression and efficacy of anti-inflammatory compounds in a model of monosodium iodoacetate-induced osteoarthritis. *Osteoarthritis Cartilage* **11**(11)**:** 821-830.

Brazeau P (1986). Somatostatin - a peptide with unexpected physiological activities. *American Journal of Medicine* **81**(6B)**:** 8-13.

Brazeau P, Vale W, Burgus R, Ling N, Butcher M, Rivier J*, et al.* (1973). Hypothalamic polypeptide that inhibits the secretion of immunoreactive pituitary growth hormone. *Science* **179**(4068)**:** 77-79.

Brichory FM, Misek DE, Yim AM, Krause MC, Giordano TJ, Beer DG*, et al.* (2001). An immune response manifested by the common occurrence of annexins I and II autoantibodies and high circulating levels of IL-6 in lung cancer. *Proc Natl Acad Sci U S A* **98**(17)**:** 9824-9829.

Bril V, England J, Franklin GM, Backonja M, Cohen J, Del Toro D*, et al.* (2011). Evidence-based guideline: Treatment of painful diabetic neuropathy: report of the American Academy of Neurology, the American Association of Neuromuscular and Electrodiagnostic Medicine, and the American Academy of Physical Medicine and Rehabilitation. *Neurology* **76**(20)**:** 1758-1765.

Broderson JR (1989). A retrospective review of lesions associated with the use of Freund's adjuvant. *Lab Anim Sci* **39**(5)**:** 400-405.

Broglio F, Papotti M, Muccioli G, Ghigo E (2007). Brain-gut communication: cortistatin, somatostatin and ghrelin. *Trends in Endocrinology and Metabolism* **18**(6).

Broom DC, Samad TA, Kohno T, Tegeder I, Geisslinger G, Woolf CJ (2004). Cyclooxygenase 2 expression in the spared nerve injury model of neuropathic pain. *Neuroscience* **124**(4)**:** 891-900.

Bruno A, Tacconelli S, Patrignani P (2014). Variability in the response to non-steroidal anti-inflammatory drugs: mechanisms and perspectives. *Basic Clin Pharmacol Toxicol* **114**(1)**:** 56-63.

Cai RZ, Szoke B, Lu R, Fu D, Redding TW, Schally AV (1986). Synthesis and biological activity of highly potent octapeptide analogs of somatostatin. *Proc Natl Acad Sci U S A* **83**(6)**:** 1896-1900.

Calcott G, White JP, Nagy I (2011). Xenon fails to inhibit capsaicin-evoked CGRP release by nociceptors in culture. *Neurosci Lett* **499**(2)**:** 124-126.

Calcutt NA (2002). Potential mechanisms of neuropathic pain in diabetes. *Int Rev Neurobiol* **50:** 205-228.

Campbell TM, Main MJ, Fitzgerald EM (2013). Functional expression of the voltage-gated Na^+-channel Nav1.7 is necessary for EGF-mediated invasion in human non-small cell lung cancer cells. *J Cell Sci* **126**(Pt 21)**:** 4939-4949.

Camprubí-Robles M, Mair N, Andratsch M, Benetti C, Beroukas D, Rukwied R*, et al.* (2013). Sphingosine-1-phosphate-induced nociceptor excitation and ongoing pain behavior in mice and humans is largely mediated by S1P3 receptor. *J Neurosci* **33**(6)**:** 2582-2592.

Capuano A, Curro D, Navarra P, Tringali G (2011). Cortistatin modulates calcitonin gene-related peptide release from neuronal tissues of rat. Comparison with somatostatin. *Peptides* **32**(1).

Carlton SM, Du JH, Davidson E, Zhou ST, Coggeshall RE (2001a). Somatostatin receptors on peripheral primary afferent terminals: inhibition of sensitized nociceptors. *Pain* **90**(3)**:** 233-244.

Carlton SM, Du JH, Zhou ST, Coggeshall RE (2001b). Tonic control of peripheral cutaneous nociceptors by somatostatin receptors. *Journal of Neuroscience* **21**(11)**:** 4042-4049.

Carlton SM, Zhou S, Du J, Hargett GL, Ji G, Coggeshall RE (2004). Somatostatin modulates the transient receptor potential vanilloid 1 (TRPV1) ion channel. In. *Pain*, edn, Vol. 110. Netherlands. p^pp 616-627.

Carlton SM, Zhou S, Kraemer B, Coggeshall RE (2003). A role for peripheral somatostatin receptors in counter-irritation-induced analgesia. *Neuroscience* **120**(2)**:** 499-508.

Caterina MJ, Leffler A, Malmberg AB, Martin WJ, Trafton J, Petersen-Zeitz KR*, et al.* (2000). Impaired nociception and pain sensation in mice lacking the capsaicin receptor. *Science* **288**(5464)**:** 306-313.

Caterina MJ, Schumacher MA, Tominaga M, Rosen TA, Levine JD, Julius D (1997). The capsaicin receptor: a heat-activated ion channel in the pain pathway. *Nature* **389**(6653)**:** 816-824.

Catterall WA (2000). Structure and regulation of voltage-gated Ca2+ channels. *Annual Review of Cell and Developmental Biology* **16:** 521-555.

Catterall WA, Goldin AL, Waxman SG (2005). International Union of Pharmacology. XLVII. Nomenclature and structure-function relationships of voltage-gated sodium channels. *Pharmacol Rev* **57**(4)**:** 397-409.

Cavaillon JM (1994). Cytokines and macrophages. *Biomed Pharmacother* **48**(10)**:** 445-453.

Cejvan K, Coy DH, Efendic S (2003). Intra-islet somatostatin regulates glucagon release via type 2 somatostatin receptors in rats. *Diabetes* **52**(5)**:** 1176-1181.

Chang M, Smith S, Thorpe A, Barratt MJ, Karim F (2010). Evaluation of phenoxybenzamine in the CFA model of pain following gene expression studies and connectivity mapping. *Mol Pain* **6:** 56.

Chao A, Wang TH, Lee YS, Hsueh S, Chao AS, Chang TC*, et al.* (2006). Molecular characterization of adenocarcinoma and squamous carcinoma of the uterine cervix using microarray analysis of gene expression. *Int J Cancer* **119**(1)**:** 91-98.

Chapman V, Dickenson AH (1992). The effects of sandostatin and somatostatin on nociceptive transmission in the dorsal horn of the rat spinal-cord. *Neuropeptides* **23**(3)**:** 147-152.

Chen J, Joshi SK, DiDomenico S, Perner RJ, Mikusa JP, Gauvin DM*, et al.* (2011). Selective blockade of TRPA1 channel attenuates pathological pain without altering noxious cold sensation or body temperature regulation. *Pain* **152**(5)**:** 1165-1172.

Chen J, Luan Y, Yu R, Zhang Z, Zhang J, Wang W (2014). Transient receptor potential (TRP) channels, promising potential diagnostic and therapeutic tools for cancer. *Biosci Trends* **8**(1)**:** 1-10.

Chrubasik J, Meynadier J, Blond S, Scherpereel P, Ackerman E, Weinstock M*, et al.* (1984). Somatostatin, a potent analgesic. *Lancet* **2**(8413)**:** 1208-1209.

Chrubasik J, Meynadier J, Scherpereel P, Wunsch E (1985). The effect of epidural somatostatin on postoperative pain. *Anesthesia and Analgesia* **64**(11)**:** 1085-1088.

Coghill RC, Talbot JD, Evans AC, Meyer E, Gjedde A, Bushnell MC*, et al.* (1994). Distributed processing of pain and vibration by the human brain. *J Neurosci* **14**(7)**:** 4095-4108.

Combe R, Bramwell S, Field MJ (2004). The monosodium iodoacetate model of osteoarthritis: a model of chronic nociceptive pain in rats? *Neurosci Lett* **370**(2-3)**:** 236-240.

Conner AC, Simms J, Barwell J, Wheatley M, Poyner DR (2007). Ligand binding and activation of the CGRP receptor. *Biochem Soc Trans* **35**(Pt 4)**:** 729-732.

Coppini DV, Spruce MC, Thomas P, Masding MG (2006). Established diabetic neuropathy seems irreversible despite improvements in metabolic and vascular risk markers--a retrospective case-control study in a hospital patient cohort. *Diabet Med* **23**(9)**:** 1016-1020.

Corsi MM, Ticozzi C, Netti C, Fulgenzi A, Tiengo M, Gaja G*, et al.* (1997). The effect of somatostatin on experimental inflammation in rats. *Anesth Analg* **85**(5)**:** 1112-1115.

Cortright DN, Szallasi A (2004). Biochemical pharmacology of the vanilloid receptor TRPV1. An update. *Eur J Biochem* **271**(10)**:** 1814-1819.

Cosens DJ, Manning A (1969). Abnormal electroretinogram from a Drosophila mutant. *Nature* **224**(5216)**:** 285-287.

Courteix C, Eschalier A, Lavarenne J (1993). Streptozocin-induced diabetic rats: behavioural evidence for a model of chronic pain. *Pain* **53**(1)**:** 81-88.

Craig AD (2003). Pain mechanisms: labeled lines versus convergence in central processing. *Annu Rev Neurosci* **26:** 1-30.

Cunha FQ, Poole S, Lorenzetti BB, Ferreira SH (1992). The pivotal role of tumour necrosis factor alpha in the development of inflammatory hyperalgesia. *Br J Pharmacol* **107**(3)**:** 660-664.

Cunha TM, Verri WA, Jr., Fukada SY, Guerrero AT, Santodomingo-Garzon T, Poole S*, et al.* (2007). TNF-alpha and IL-1beta mediate inflammatory hypernociception in mice triggered by B1 but not B2 kinin receptor. *Eur J Pharmacol* **573**(1-3)**:** 221-229.

Cvetkov TL, Huynh KW, Cohen MR, Moiseenkova-Bell VY (2011). Molecular architecture and subunit organization of TRPA1 ion channel revealed by electron microscopy. *J Biol Chem* **286**(44)**:** 38168-38176.

Członkowski A, Stein C, Herz A (1993). Peripheral mechanisms of opioid antinociception in inflammation: involvement of cytokines. *Eur J Pharmacol* **242**(3)**:** 229-235.

Dahaba AA, Mueller G, Mattiassich G, Rumpold-Seitlinger G, Bornemann H, Rehak PH*, et al.* (2009). Effect of somatostatin analogue octreotide on pain relief after major abdominal surgery. In. *Eur J Pain*, edn, Vol. 13. England. p^pp 861-864.

Davis JB, Gray J, Gunthorpe MJ, Hatcher JP, Davey PT, Overend P*, et al.* (2000). Vanilloid receptor-1 is essential for inflammatory thermal hyperalgesia. *Nature* **405**(6783)**:** 183-187.

Dawes JM, Antunes-Martins A, Perkins JR, Paterson KJ, Sisignano M, Schmid R*, et al.* (2014). Genome-wide transcriptional profiling of skin and dorsal root ganglia after ultraviolet-B-induced inflammation. *PLoS One* **9**(4)**:** e93338.

de Prado BM, Hammond DL, Russo AF (2009). Genetic Enhancement of Calcitonin Gene-Related Peptide-Induced Central Sensitization to Mechanical Stimuli in Mice. *Journal of Pain* **10**(9)**:** 992-1000.

del Camino D, Murphy S, Heiry M, Barrett LB, Earley TJ, Cook CA*, et al.* (2010). TRPA1 contributes to cold hypersensitivity. *J Neurosci* **30**(45)**:** 15165-15174.

Denoble VJ, Hepler DJ, Barto RA (1989). Cysteamine-induced depletion of somatostatin produces differential cognitive deficits in rats. *Brain Research* **482**(1)**:** 42-48.

Deshmane SL, Kremlev S, Amini S, Sawaya BE (2009). Monocyte chemoattractant protein-1 (MCP-1): an overview. *J Interferon Cytokine Res* **29**(6)**:** 313-326.

Deval E, Salinas M, Baron A, Lingueglia E, Lazdunski M (2004). ASIC2b-dependent regulation of ASIC3, an essential acid-sensing ion channel subunit in sensory neurons via the partner protein PICK-1. *J Biol Chem* **279**(19)**:** 19531-19539.

Ding M, Hart RP, Jonakait GM (1995). Tumor necrosis factor-alpha induces substance P in sympathetic ganglia through sequential induction of interleukin-1 and leukemia inhibitory factor. *J Neurobiol* **28**(4)**:** 445-454.

Dinh QT, Groneberg DA, Peiser C, Mingomataj E, Joachim RA, Witt C*, et al.* (2004). Substance P expression in TRPV1 and trkA-positive dorsal root ganglion neurons innervating the mouse lung. *Respir Physiol Neurobiol* **144**(1)**:** 15-24.

Doerner JF, Gisselmann G, Hatt H, Wetzel CH (2007). Transient receptor potential channel A1 is directly gated by calcium ions. *J Biol Chem* **282**(18)**:** 13180-13189.

Dolphin AC (2003). G protein modulation of voltage-gated calcium channels. *Pharmacological Reviews* **55**(4)**:** 607-627.

Dunn AJ (1988). Systemic interleukin-1 administration stimulates hypothalamic norepinephrine metabolism parallelling the increased plasma corticosterone. *Life Sci* **43**(5)**:** 429-435.

Duric V, McCarson KE (2007). Neurokinin-1 (NK-1) receptor and brain-derived neurotrophic factor (BDNF) gene expression is differentially modulated in the rat spinal dorsal horn and hippocampus during inflammatory pain. *Mol Pain* **3:** 32.

Eguchi N, Minami T, Shirafuji N, Kanaoka Y, Tanaka T, Nagata A*, et al.* (1999). Lack of tactile pain (allodynia) in lipocalin-type prostaglandin D synthase-deficient mice. *Proc Natl Acad Sci U S A* **96**(2)**:** 726-730.

Eid SR, Crown ED, Moore EL, Liang HA, Choong KC, Dima S*, et al.* (2008). HC-030031, a TRPA1 selective antagonist, attenuates inflammatory- and neuropathy-induced mechanical hypersensitivity. *Mol Pain* **4:** 48.

Eikelenboom P, Veerhuis R, Scheper W, Rozemuller AJ, van Gool WA, Hoozemans JJ (2006). The significance of neuroinflammation in understanding Alzheimer's disease. *J Neural Transm* **113**(11)**:** 1685-1695.

Elekes K, Helyes Z, Kereskai L, Sándor K, Pintér E, Pozsgai G*, et al.* (2008). Inhibitory effects of synthetic somatostatin receptor subtype 4 agonists on acute and chronic airway inflammation and hyperreactivity in the mouse. *Eur J Pharmacol* **578**(2-3)**:** 313-322.

Endres-Becker J, Heppenstall PA, Mousa SA, Labuz D, Oksche A, Schäfer M*, et al.* (2007). Mu-opioid receptor activation modulates transient receptor potential vanilloid 1 (TRPV1) currents in sensory neurons in a model of inflammatory pain. *Mol Pharmacol* **71**(1)**:** 12-18.

Engstrom M, Tomperi J, El-Darwish K, Ahman M, Savola JM, Wurster S (2005). Superagonism at the human somatostatin receptor subtype 4. *Journal of Pharmacology and Experimental Therapeutics* **312**(1)**:** 332-338.

Eschalier A, Aumaitre O, Ardid D, Fialip J, Duchenemarullaz P (1991). Long-lasting antinociceptive effect of rc-160, a somatostatin analog, in mice and rats. *European Journal of Pharmacology* **199**(1)**:** 119-121.

Estebe JP, Legay F, Gentili M, Wodey E, Leduc C, Ecoffey C*, et al.* (2006). An evaluation of a polyamine-deficient diet for the treatment of inflammatory pain. *Anesth Analg* **102**(6)**:** 1781-1788.

Evers BM, Parekh D, Townsend CM, Thompson JC (1991). Somatostatin and analogues in the treatment of cancer. A review. *Ann Surg* **213**(3)**:** 190-198.

Farrell SR, Rankin DR, Brecha NC, Barnes S (2014). Somatostatin receptor subtype 4 modulates L-type calcium channels via Gbetagamma and PKC signaling in rat retinal ganglion cells. *Channels (Austin)***:** Epub.

Farrell SR, Raymond ID, Foote M, Brecha NC, Barnes S (2010). Modulation of Voltage-Gated Ion Channels in Rat Retinal Ganglion Cells Mediated by Somatostatin Receptor Subtype 4. *Journal of Neurophysiology* **104**(3)**:** 1347-1354.

Fecho K, Nackley AG, Wu Y, Maixner W (2005). Basal and carrageenan-induced pain behavior in Sprague-Dawley, Lewis and Fischer rats. *Physiol Behav* **85**(2)**:** 177-186.

Fehrenbacher JC, Taylor CP, Vasko MR (2003). Pregabalin and gabapentin reduce release of substance P and CGRP from rat spinal tissues only after inflammation or activation of protein kinase C. *Pain* **105**(1-2)**:** 133-141.

Ferreira SH, Lorenzetti BB, Bristow AF, Poole S (1988). Interleukin-1 beta as a potent hyperalgesic agent antagonized by a tripeptide analogue. *Nature* **334**(6184)**:** 698-700.

Frati A, Rouzier R, Lesieur B, Werkoff G, Antoine M, Rodenas A*, et al.* (2014). Expression of somatostatin type-2 and -4 receptor and correlation with histological type in breast cancer. *Anticancer Res* **34**(8)**:** 3997-4003.

Fukuoka H, Kawatani M, Hisamitsu T, Takeshige C (1994). Cutaneous hyperalgesia induced by peripheral injection of interleukin-1 beta in the rat. *Brain Res* **657**(1-2)**:** 133-140.

Gao F, Liu Z, Ren W, Jiang W (2014). Acute lipopolysaccharide exposure facilitates epileptiform activity via enhanced excitatory synaptic transmission and neuronal excitability in vitro. *Neuropsychiatr Dis Treat* **10:** 1489-1495.

Gao XF, Zhang HL, You ZD, Lu CL, He C (2007). G protein-coupled inwardly rectifying potassium channels in dorsal root ganglion \ neurons. *Acta Pharmacol Sin* **28**(2)**:** 185-190.

Giese MJ, Rayner SA, Fardin B, Sumner HL, Rozengurt N, Mondino BJ*, et al.* (2003). Mitigation of neutrophil infiltration in a rat model of early Staphylococcus aureus endophthalmitis. *Invest Ophthalmol Vis Sci* **44**(7)**:** 3077-3082.

Gijsen HJ, Berthelot D, Zaja M, Brône B, Geuens I, Mercken M (2010). Analogues of morphanthridine and the tear gas dibenz[b,f][1,4]oxazepine (CR) as extremely potent activators of the human transient receptor potential ankyrin 1 (TRPA1) channel. *J Med Chem* **53**(19)**:** 7011-7020.

Glatt M, Kälin H, Wagner K, Brune K (1977). Prostaglandin release from macrophages: an assay system for anti-inflammatory drugs in vitro. *Agents Actions* **7**(3)**:** 321-326.

Goodman RH, Aron DC, Roos BA (1983). Rat pre-prosomatostatin. Structure and processing by microsomal membranes. *J Biol Chem* **258**(9)**:** 5570-5573.

Gorham L, Just S, Doods H (2014a). Somatostatin 4 receptor activation modulates G-protein coupled inward rectifying potassium channels and voltage stimulated calcium signals in dorsal root ganglion neurons. *Eur J Pharmacol* **736:** 101-106.

Gorham L, Just S, Doods H (2014b). Somatostatin 4 receptor activation modulates TPRV1 currents in dorsal root ganglion neurons. *Neurosci Lett* **573:** 35-39.

Gribkoff VK (2006). The role of voltage-gated calcium channels in pain and nociception. *Seminars in Cell & Developmental Biology* **17**(5)**:** 555-564.

Grosser T, Fries S, FitzGerald GA (2006). Biological basis for the cardiovascular consequences of COX-2 inhibition: therapeutic challenges and opportunities. *J Clin Invest* **116**(1)**:** 4-15.

Guingamp C, Gegout-Pottie P, Philippe L, Terlain B, Netter P, Gillet P (1997). Mono-iodoacetate-induced experimental osteoarthritis: a dose-response study of loss of mobility, morphology, and biochemistry. *Arthritis Rheum* **40**(9)**:** 1670-1679.

Gulya K, Pelton JT, Hruby VJ, Yamamura HI (1986). Cyclic somatostatin octapeptide analogs with high-affinity and selectivity toward mu opioid receptors. *Life Sciences* **38**(24)**:** 2221-2229.

Hauge-Evans AC, King AJ, Fairhall K, Persaud SJ, Jones PM (2010). A role for islet somatostatin in mediating sympathetic regulation of glucagon secretion. *Islets* **2**(6)**:** 341-344.

He SQ, Yao JR, Zhang FX, Wang Q, Bao L, Zhang X (2010). Inflammation and nerve injury induce expression of pancreatitis-associated protein-II in primary sensory neurons. *Mol Pain* **6:** 23.

Heinricher MM, Tavares I, Leith JL, Lumb BM (2009). Descending control of nociception: Specificity, recruitment and plasticity. *Brain Res Rev* **60**(1)**:** 214-225.

Helmchen C, Fu QG, Sandkuhler J (1995). Inhibition of spinal nociceptive neurons by microinjections of somatostatin into the nucleus raphe magnus and the midbrain periaqueductal gray of the anesthetized cat. In. *Neurosci Lett*, edn, Vol. 187. Ireland. p^pp 137-141.

Helyes Z, Pinter E, Sandor K, Elekes K, Banvolgyi A, Keszthelyi D*, et al.* (2009). Impaired defense mechanism against inflammation, hyperalgesia, and airway hyperreactivity in somatostatin 4 receptor gene-deleted mice. *Proc Natl Acad Sci U S A* **106**(31)**:** 13088-13093.

Helyes Z, Pintér E, Németh J, Sándor K, Elekes K, Szabó A*, et al.* (2006). Effects of the somatostatin receptor subtype 4 selective agonist J-2156 on sensory neuropeptide release and inflammatory reactions in rodents. *Br J Pharmacol* **149**(4)**:** 405-415.

Helyes Z, Szabo A, Nemeth J, Jakab B, Pinter E, Banvolgyi A*, et al.* (2004). Antiinflammatory and analgesic effects of somatostatin released from capsaicin-sensitive sensory nerve terminals in a Freund's adjuvant-induced chronic arthritis model in the rat. *Arthritis Rheum* **50**(5)**:** 1677-1685.

Helyes Z, Than M, Oroszi G, Pinter E, Nemeth J, Keri G*, et al.* (2000). Anti-nociceptive effect induced by somatostatin released from sensory nerve terminals and by synthetic somatostatin analogues in the rat. *Neuroscience Letters* **278**(3)**:** 185-188.

Heppelmann B, Pawlak M (1999). Peripheral application of cyclo-somatostatin, a somatostatin antagonist, increases the mechanosensitivity of rat knee joint afferents. In. *Neurosci Lett*, edn, Vol. 259. Ireland. p^pp 62-64.

Hirsch S, Corradini L, Just S, Arndt K, Doods H (2013). The CGRP receptor antagonist BIBN4096BS peripherally alleviates inflammatory pain in rats. *Pain* **154**(5)**:** 700-707.

Hogg JC, Timens W (2009). The pathology of chronic obstructive pulmonary disease. *Annu Rev Pathol* **4:** 435-459.

Hokfelt T, Elde R, Johansson O, Luft R, Nilsson G, Arimura A (1976). Immunohistochemical evidence for separate populations of somatostatin-containing and substance P-containing primary afferent neurons in the rat. *Neuroscience* **1**(2)**:** 131-136.

Holzer P (1992). Peptidergic sensory neurons in the control of vascular functions: mechanisms and significance in the cutaneous and splanchnic vascular beds. *Rev Physiol Biochem Pharmacol* **121:** 49-146.

Hukovic N, Panetta R, Kumar U, Patel YC (1996). Agonist-dependent regulation of cloned human somatostatin receptor types 1-5 (hSSTR1-5): subtype selective internalization or upregulation. *Endocrinology* **137**(9)**:** 4046-4049.

Iadarola MJ, Brady LS, Draisci G, Dubner R (1988). Enhancement of dynorphin gene expression in spinal cord following experimental inflammation: stimulus specificity, behavioral parameters and opioid receptor binding. *Pain* **35**(3)**:** 313-326.

Ikeda K, Kobayashi T, Kumanishi T, Niki H, Yano R (2000). Involvement of G-protein-activated inwardly rectifying K+ (GIRK) channels in opioid-induced analgesia. *Neuroscience Research* **38**(1).

Inanobe A, Morishige KI, Takahashi N, Ito H, Yamada M, Takumi T*, et al.* (1995). G beta gamma directly binds to the carboxyl-terminus of the G-protein gated muscarinic K+ channel, GIRK1. *Biochemical and Biophysical Research Communications* **212**(3).

Jackson K, Soutto M, Peng D, Hu T, Marshal D, El-Rifai W (2011). Epigenetic silencing of somatostatin in gastric cancer. *Dig Dis Sci* **56**(1)**:** 125-130.

Jaggi AS, Jain V, Singh N (2011). Animal models of neuropathic pain. *Fundam Clin Pharmacol* **25**(1)**:** 1-28.

Janusz MJ, Hookfin EB, Heitmeyer SA, Woessner JF, Freemont AJ, Hoyland JA*, et al.* (2001). Moderation of iodoacetate-induced experimental osteoarthritis in rats by matrix metalloproteinase inhibitors. *Osteoarthritis Cartilage* **9**(8)**:** 751-760.

Jarvis MF, Honore P, Shieh CC, Chapman M, Joshi S, Zhang XF*, et al.* (2007). A-803467, a potent and selective Nav1.8 sodium channel blocker, attenuates neuropathic and inflammatory pain in the rat. *Proc Natl Acad Sci U S A* **104**(20)**:** 8520-8525.

Ji GC, Zhou ST, Shapiro G, Reubi JC, Jurczyk S, Carlton SM (2006). Analgesic activity of a non-peptide imidazolidinedione somatostatin agonist: in vitro and in vivo studies in rat. *Pain* **124**(1-2)**:** 34-49.

Ji RR, Samad TA, Jin SX, Schmoll R, Woolf CJ (2002). p38 MAPK activation by NGF in primary sensory neurons after inflammation increases TRPV1 levels and maintains heat hyperalgesia. *Neuron* **36**(1)**:** 57-68.

Jin X, Gereau RW (2006). Acute p38-mediated modulation of tetrodotoxin-resistant sodium channels in mouse sensory neurons by tumor necrosis factor-alpha. *J Neurosci* **26**(1)**:** 246-255.

Jordt SE, Bautista DM, Chuang HH, McKemy DD, Zygmunt PM, Högestätt ED*, et al.* (2004). Mustard oils and cannabinoids excite sensory nerve fibres through the TRP channel ANKTM1. *Nature* **427**(6971)**:** 260-265.

Jung H, Toth PT, White FA, Miller RJ (2008). Monocyte chemoattractant protein-1 functions as a neuromodulator in dorsal root ganglia neurons. *J Neurochem* **104**(1)**:** 254-263.

Kailey B, van de Bunt M, Cheley S, Johnson PR, Macdonald PE, Gloyn AL*, et al.* (2012). SSTR2 is the functionally dominant somatostatin receptor in human pancreatic beta- and alpha-cells. In. *Am J Physiol Endocrinol Metab*, edn. p^pp.

Kalbhen DA (1987). Chemical model of osteoarthritis--a pharmacological evaluation. *J Rheumatol* **14 Spec No:** 130-131.

Kapicioglu S, Gokce E, Kapicioglu Z, Ovali E (1997). Treatment of migraine attacks with a long-acting somatostatin analogue (octreotide, SMS 201-995). *Cephalalgia* **17**(1)**:** 27-30.

Karashima Y, Prenen J, Talavera K, Janssens A, Voets T, Nilius B (2010). Agonist-induced changes in Ca(2+) permeation through the nociceptor cation channel TRPA1. *Biophys J* **98**(5)**:** 773-783.

Karavitakis M, Msaouel P, Michalopoulos V, Koutsilieris M (2014). Pattern of somatostatin receptors expression in normal and bladder cancer tissue samples. *Anticancer Res* **34**(6)**:** 2937-2942.

Kashiba H, Uchida Y, Senba E (2003). Distribution and colocalization of NGF and GDNF family ligand receptor mRNAs in dorsal root and nodose ganglion neurons of adult rats. *Brain Res Mol Brain Res* **110**(1)**:** 52-62.

Kaupmann K, Bruns C, Raulf F, Weber HP, Mattes H, Lubbert H (1995). Two amino acids, located in transmembrane domains VI and VII, determine the selectivity of the peptide agonist SMS 201-995 for the SSTR2 somatostatin receptor. *EMBO J* **14**(4)**:** 727-735.

Khasabova IA, Harding-Rose C, Simone DA, Seybold VS (2004). Differential effects of CB1 and opioid agonists on two populations of adult rat dorsal root ganglion neurons. *Journal of Neuroscience* **24**(7)**:** 1744-1753.

Khasar SG, Miao FJ, Levine JD (1995). Inflammation modulates the contribution of receptor-subtypes to bradykinin-induced hyperalgesia in the rat. *Neuroscience* **69**(2)**:** 685-690.

Kidd BL, Urban LA (2001). Mechanisms of inflammatory pain. *Br J Anaesth* **87**(1)**:** 3-11.

Kim CF, Moalem-Taylor G (2011). Interleukin-17 contributes to neuroinflammation and neuropathic pain following peripheral nerve injury in mice. *J Pain* **12**(3)**:** 370-383.

Kim D, Cavanaugh EJ (2007). Requirement of a soluble intracellular factor for activation of transient receptor potential A1 by pungent chemicals: role of inorganic polyphosphates. *J Neurosci* **27**(24)**:** 6500-6509.

Kim KJ, Yoon YW, Chung JM (1997). Comparison of three rodent neuropathic pain models. *Exp Brain Res* **113**(2)**:** 200-206.

Kim SR, Kim SU, Oh U, Jin BK (2006). Transient receptor potential vanilloid subtype 1 mediates microglial cell death in vivo and in vitro via Ca2+-mediated mitochondrial damage and cytochrome c release. *J Immunol* **177**(7)**:** 4322-4329.

Kim SR, Lee DY, Chung ES, Oh UT, Kim SU, Jin BK (2005). Transient receptor potential vanilloid subtype 1 mediates cell death of mesencephalic dopaminergic neurons in vivo and in vitro. *J Neurosci* **25**(3)**:** 662-671.

Knights KM, Mangoni AA, Miners JO (2010). Defining the COX inhibitor selectivity of NSAIDs: implications for understanding toxicity. *Expert Rev Clin Pharmacol* **3**(6)**:** 769-776.

Korn T, Magnus T, Jung S (2005). Autoantigen specific T cells inhibit glutamate uptake in astrocytes by decreasing expression of astrocytic glutamate transporter GLAST: a mechanism mediated by tumor necrosis factor-alpha. *FASEB J* **19**(13)**:** 1878-1880.

Koyrakh L, Lujan R, Colon J, Karschin C, Kurachi Y, Karschin A*, et al.* (2005). Molecular and cellular diversity of neuronal G-protein-gated potassium channels. *Journal of Neuroscience* **25**(49).

Kreienkamp HJ, Honck HH, Richter D (1997). Coupling of rat somatostatin receptor subtypes to a G-protein gated inwardly rectifying potassium channel (GIRK1). *Febs Letters* **419**(1)**:** 92-94.

Krulich L, Dhariwal AP, McCann SM (1968). Stimulatory and inhibitory effects of purified hypothalamic extracts on growth hormone release from rat pituitary in vitro. *Endocrinology* **83**(4)**:** 783-&.

Kumar U (2005). Expression of somatostatin receptor subtypes (SSTR1-5) in Alzheimer's disease brain: an immunohistochemical analysis. *Neuroscience* **134**(2)**:** 525-538.

Kumar U (2007). Colocalization of somatostatin receptor subtypes (SSTR1-5) with somatostatin, NADPH-diaphorase (NADPH-d), and tyrosine hydroxylase in the rat hypothalamus. *J Comp Neurol* **504**(2)**:** 185-205.

Köller H, Allert N, Oel D, Stoll G, Siebler M (1998). TNF alpha induces a protein kinase C-dependent reduction in astroglial K+ conductance. *Neuroreport* **9**(7)**:** 1375-1378.

LaCroix-Fralish ML, Austin JS, Zheng FY, Levitin DJ, Mogil JS (2011). Patterns of pain: meta-analysis of microarray studies of pain. *Pain* **152**(8)**:** 1888-1898.

Lao L, Zhang RX, Zhang G, Wang X, Berman BM, Ren K (2004). A parametric study of electroacupuncture on persistent hyperalgesia and Fos protein expression in rats. *Brain Res* **1020**(1-2)**:** 18-29.

Latremoliere A, Woolf CJ (2009). Central sensitization: a generator of pain hypersensitivity by central neural plasticity. *J Pain* **10**(9)**:** 895-926.

Laude EA, Higgins KS, Morice AH (1993). A comparative study of the effects of citric acid, capsaicin and resiniferatoxin on the cough challenge in guinea-pig and man. *Pulm Pharmacol* **6**(3)**:** 171-175.

Law PY, Wong YH, Loh HH (2000). Molecular mechanisms and regulation of opioid receptor signaling. *Annu Rev Pharmacol Toxicol* **40:** 389-430.

Lawson SN (1995). Neuropeptides in morphologically and functionally identified primary afferent neurons in dorsal root ganglia: substance P, CGRP and somatostatin. *Prog Brain Res* **104:** 161-173.

Lawson SN, Crepps BA, Perl ER (1997). Relationship of substance P to afferent characteristics of dorsal root ganglion neurones in guinea-pig. *Journal of Physiology-London* **505**(1)**:** 177-191.

Le Bars D, Gozariu M, Cadden SW (2001). Animal models of nociception. *Pharmacol Rev* **53**(4)**:** 597-652.

Levine JD, Gordon NC, Fields HL (1979). Naloxone dose dependently produces analgesia and hyperalgesia in postoperative pain. *Nature* **278**(5706)**:** 740-741.

Lewis I, Bauer W, Albert R, Chandramouli N, Pless J, Weckbecker G*, et al.* (2003). A novel somatostatin mimic with broad somatotropin release inhibitory factor receptor binding and superior therapeutic potential. *J Med Chem* **46**(12)**:** 2334-2344.

Li ZL, Liang S, Wang ZC, Li YB, Guo CX, Fang F*, et al.* (2014). Expression of Smac induced by the Egr1 promoter enhances the radiosensitivity of breast cancer cells. *Cancer Gene Ther* **21**(4)**:** 142-149.

Lichtenauer-Kaligis EG, van Hagen PM, Lamberts SW, Hofland LJ (2000). Somatostatin receptor subtypes in human immune cells. *Eur J Endocrinol* **143 Suppl 1:** S21-25.

Lin YT, Ro LS, Wang HL, Chen JC (2011). Up-regulation of dorsal root ganglia BDNF and trkB receptor in inflammatory pain: an in vivo and in vitro study. *J Neuroinflammation* **8:** 126.

Lindenlaub T, Teuteberg P, Hartung T, Sommer C (2000). Effects of neutralizing antibodies to TNF-alpha on pain-related behavior and nerve regeneration in mice with chronic constriction injury. *Brain Res* **866**(1-2)**:** 15-22.

Liu B, Li H, Brull SJ, Zhang JM (2002). Increased sensitivity of sensory neurons to tumor necrosis factor alpha in rats with chronic compression of the lumbar ganglia. *J Neurophysiol* **88**(3)**:** 1393-1399.

Liu C, Rangnekar VM, Adamson E, Mercola D (1998). Suppression of growth and transformation and induction of apoptosis by EGR-1. *Cancer Gene Ther* **5**(1)**:** 3-28.

Liu L, Yang TM, Liedtke W, Simon SA (2006). Chronic IL-1beta signaling potentiates voltage-dependent sodium currents in trigeminal nociceptive neurons. *J Neurophysiol* **95**(3)**:** 1478-1490.

Liu Z, Crider AM, Ansbro D, Hayes C, Kontoyianni M (2012). A Structure-Based Approach to Understanding Somatostatin Receptor-4 Agonism (sst4). *Journal of Chemical Information and Modeling* **52**(1).

Luscher C, Slesinger PA (2010). Emerging roles for G protein-gated inwardly rectifying potassium (GIRK) channels in health and disease. In. *Nat Rev Neurosci*, edn, Vol. 11. England. p^pp 301-315.

Lyu YS, Park SK, Chung K, Chung JM (2000). Low dose of tetrodotoxin reduces neuropathic pain behaviors in an animal model. *Brain Res* **871**(1)**:** 98-103.

Lotsch J, Doehring A, Mogil JS, Arndt T, Geisslinger G, Ultsch A (2013). Functional genomics of pain in analgesic drug development and therapy. *Pharmacol Ther* **139**(1)**:** 60-70.

Madera-Salcedo IK, Cruz SL, Gonzalez-Espinosa C (2013). Morphine prevents lipopolysaccharide-induced TNF secretion in mast cells blocking IκB kinase activation and SNAP-23 phosphorylation: correlation with the formation of a β-arrestin/TRAF6 complex. *J Immunol* **191**(6)**:** 3400-3409.

Maggi CA (1995). The mammalian tachykinin receptors. *Gen Pharmacol* **26**(5)**:** 911-944.

Maier SF, Wiertelak EP, Martin D, Watkins LR (1993). Interleukin-1 mediates the behavioral hyperalgesia produced by lithium chloride and endotoxin. *Brain Res* **623**(2)**:** 321-324.

Makino T, Kawashima H, Konishi H, Nakatani T, Kiyama H (2010). Elevated urinary levels and urothelial expression of hepatocarcinoma-intestine-pancreas/pancreatitis-associated protein in patients with interstitial cystitis. *Urology* **75**(4)**:** 933-937.

Malcangio M, Bowery NG, Flower RJ, Perretti M (1996). Effect of interleukin-1 beta on the release of substance P from rat isolated spinal cord. *Eur J Pharmacol* **299**(1-3)**:** 113-118.

Malfait AM, Little CB, McDougall JJ (2013). A commentary on modelling osteoarthritis pain in small animals. *Osteoarthritis Cartilage* **21**(9)**:** 1316-1326.

Manzanares J, Julian M, Carrascosa A (2006). Role of the cannabinoid system in pain control and therapeutic implications for the management of acute and chronic pain episodes. *Curr Neuropharmacol* **4**(3)**:** 239-257.

Marchand S (2008). The physiology of pain mechanisms: from the periphery to the brain. *Rheum Dis Clin North Am* **34**(2)**:** 285-309.

Marks DM, Shah MJ, Patkar AA, Masand PS, Park GY, Pae CU (2009). Serotonin-norepinephrine reuptake inhibitors for pain control: premise and promise. *Curr Neuropharmacol* **7**(4)**:** 331-336.

Materazzi S, Nassini R, Gatti R, Trevisani M, Geppetti P (2009). Cough sensors. II. Transient receptor potential membrane receptors on cough sensors. *Handb Exp Pharmacol* **187:** 49-61.

McCleskey EW, Gold MS (1999). Ion channels of nociception. *Annu Rev Physiol* **61:** 835-856.

McHugh JM, McHugh WB (2000). Pain: neuroanatomy, chemical mediators, and clinical implications. *AACN clinical issues* **11**(2)**:** 168-178.

Mehler PS, Sussman AL, Maman A, Leitner JW, Sussman KE (1980). Role of insulin secretagogues in the regulation of somatostatin binding by isolated rat islets. *Journal of Clinical Investigation* **66**(6)**:** 1334-1338.

Meller ST, Gebhart GF (1992). A critical review of the afferent pathways and the potential chemical mediators involved in cardiac pain. *Neuroscience* **48**(3)**:** 501-524.

Melzack R, Wall PD (1965). Pain mechanisms: a new theory. *Science* **150**(3699)**:** 971-979.

Mendez-Diaz M, Guevara-Martinez M, Alquicira CR, Guzman Vasquez K, Prospero-Garcia O (2004). Cortistatin, a modulatory peptide of sleep and memory, induces analgesia in rats. In. *Neurosci Lett*, edn, Vol. 354. Ireland. p^pp 242-244.

Menetski J, Mistry S, Lu M, Mudgett JS, Ransohoff RM, Demartino JA*, et al.* (2007). Mice overexpressing chemokine ligand 2 (CCL2) in astrocytes display enhanced nociceptive responses. *Neuroscience* **149**(3)**:** 706-714.

Merighi A, Salio C, Ghirri A, Lossi L, Ferrini F, Betelli C*, et al.* (2008). BDNF as a pain modulator. *Prog Neurobiol* **85**(3)**:** 297-317.

Midwood K, Sacre S, Piccinini AM, Inglis J, Trebaul A, Chan E*, et al.* (2009). Tenascin-C is an endogenous activator of Toll-like receptor 4 that is essential for maintaining inflammation in arthritic joint disease. *Nat Med* **15**(7)**:** 774-780.

Millan MJ, Członkowski A, Morris B, Stein C, Arendt R, Huber A*, et al.* (1988). Inflammation of the hind limb as a model of unilateral, localized pain: influence on multiple opioid systems in the spinal cord of the rat. *Pain* **35**(3)**:** 299-312.

Miller RJ, Banisadr G, Bhattacharyya BJ (2008). CXCR4 signaling in the regulation of stem cell migration and development. *J Neuroimmunol* **198**(1-2)**:** 31-38.

Minami M, Maekawa K, Yabuuchi K, Satoh M (1995). Double in situ hybridization study on coexistence of mu-, delta- and kappa-opioid receptor mRNAs with preprotachykinin A mRNA in the rat dorsal root ganglia. *Brain Res Mol Brain Res* **30**(2)**:** 203-210.

Minke B (2010). The history of the Drosophila TRP channel: the birth of a new channel superfamily. *J Neurogenet* **24**(4)**:** 216-233.

Mitrovic I, Margeta-Mitrovic M, Bader S, Stoffel M, Jan LY, Basbaum AI (2003). Contribution of GIRK2-mediated postsynaptic signaling to opiate and alpha\ 2-adrenergic analgesia and analgesic sex differences. In. *Proc Natl Acad Sci U S A*, edn, Vol. 100. United States. p^pp 271-276.

Mohapatra DP, Nau C (2003). Desensitization of capsaicin-activated currents in the vanilloid receptor TRPV1 is decreased by the cyclic AMP-dependent protein kinase pathway. *J Biol Chem* **278**(50)**:** 50080-50090.

Mollenholt P, Rawal N, Gordh T, Olsson Y (1994). Intrathecal and epidural somatostatin for patients with cancer - analgesic effects and postmortem neuropathologic investigations of spinal-cord and nerve roots. *Anesthesiology* **81**(3)**:** 534-542.

Moller LN, Stidsen CE, Hartmann B, Holst JJ (2003). Somatostatin receptors. *Biochimica Et Biophysica Acta-Biomembranes* **1616**(1)**:** 1-84.

Molliver DC, Immke DC, Fierro L, Paré M, Rice FL, McCleskey EW (2005). ASIC3, an acid-sensing ion channel, is expressed in metaboreceptive sensory neurons. *Mol Pain* **1:** 35.

Montell C, Rubin GM (1989). Molecular characterization of the Drosophila trp locus: a putative integral membrane protein required for phototransduction. *Neuron* **2**(4)**:** 1313-1323.

Morton CR, Hutchison WD, Hendry IA, Duggan AW (1989). Somatostatin - evidence for a role in thermal nociception. *Brain Research* **488**(1-2)**:** 89-96.

Murphy WA, Lance VA, Moreau S, Moreau JP, Coy DH (1987). Inhibition of rat prostate tumor growth by an octapeptide analog of somatostatin. *Life Sci* **40**(26)**:** 2515-2522.

Naidu PS, Kinsey SG, Guo TL, Cravatt BF, Lichtman AH (2010). Regulation of inflammatory pain by inhibition of fatty acid amide hydrolase. *J Pharmacol Exp Ther* **334**(1)**:** 182-190.

Nakao K, Murase A, Ohshiro H, Okumura T, Taniguchi K, Murata Y*, et al.* (2007). CJ-023,423, a novel, potent and selective prostaglandin EP4 receptor antagonist with antihyperalgesic properties. *J Pharmacol Exp Ther* **322**(2)**:** 686-694.

Nassar MA, Stirling LC, Forlani G, Baker MD, Matthews EA, Dickenson AH*, et al.* (2004). Nociceptor-specific gene deletion reveals a major role for Nav1.7 (PN1) in acute and inflammatory pain. *Proc Natl Acad Sci U S A* **101**(34)**:** 12706-12711.

Nassenstein C, Kwong K, Taylor-Clark T, Kollarik M, Macglashan DM, Braun A*, et al.* (2008). Expression and function of the ion channel TRPA1 in vagal afferent nerves innervating mouse lungs. *J Physiol* **586**(6)**:** 1595-1604.

Nicol GD, Lopshire JC, Pafford CM (1997). Tumor necrosis factor enhances the capsaicin sensitivity of rat sensory neurons. *J Neurosci* **17**(3)**:** 975-982.

Niederberger E, Schmidtko A, Coste O, Marian C, Ehnert C, Geisslinger G (2006). The glutamate transporter GLAST is involved in spinal nociceptive processing. *Biochem Biophys Res Commun* **346**(2)**:** 393-399.

Nielsen N, Lindemann O, Schwab A (2014). TRP channels and STIM/ORAI proteins: sensors and effectors of cancer and stroma cell migration. *Br J Pharmacol*.

Nilius B, Prenen J, Owsianik G (2011). Irritating channels: the case of TRPA1. *J Physiol* **589**(Pt 7)**:** 1543-1549.

O'Neill LA (2008). Primer: Toll-like receptor signaling pathways--what do rheumatologists need to know? *Nat Clin Pract Rheumatol* **4**(6)**:** 319-327.

Obata K, Katsura H, Mizushima T, Yamanaka H, Kobayashi K, Dai Y*, et al.* (2005). TRPA1 induced in sensory neurons contributes to cold hyperalgesia after inflammation and nerve injury. *J Clin Invest* **115**(9)**:** 2393-2401.

Obreja O, Rathee PK, Lips KS, Distler C, Kress M (2002). IL-1 beta potentiates heat-activated currents in rat sensory neurons: involvement of IL-1RI, tyrosine kinase, and protein kinase C. *FASEB J* **16**(12)**:** 1497-1503.

Ogawa H, Fukushima K, Naito H, Funayama Y, Unno M, Takahashi K*, et al.* (2003). Increased expression of HIP/PAP and regenerating gene III in human inflammatory bowel disease and a murine bacterial reconstitution model. *Inflamm Bowel Dis* **9**(3)**:** 162-170.

Oka T, Aou S, Hori T (1993). Intracerebroventricular injection of interleukin-1 beta induces hyperalgesia in rats. *Brain Res* **624**(1-2)**:** 61-68.

Oka T, Oka K, Hosoi M, Hori T (1995). Intracerebroventricular injection of interleukin-6 induces thermal hyperalgesia in rats. *Brain Res* **692**(1-2)**:** 123-128.

Okamoto M, Suzuki T, Watanabe N (2013). Modulation of inflammatory pain in response to a CCR2/CCR5 antagonist in rodent model. *J Pharmacol Pharmacother* **4**(3)**:** 208-210.

Oliveira ALR, Hydling F, Olsson E, Shi TJ, Edwards RH, Fujiyama F*, et al.* (2003). Cellular localization of three vesicular glutamate transporter mRNAs and proteins in rat spinal cord and dorsal root ganglia. *Synapse* **50**(2)**:** 117-129.

Orlikowski D, Chazaud B, Plonquet A, Poron F, Sharshar T, Maison P*, et al.* (2003). Monocyte chemoattractant protein 1 and chemokine receptor CCR2 productions in Guillain-Barré syndrome and experimental autoimmune neuritis. *J Neuroimmunol* **134**(1-2)**:** 118-127.

Osadchii OE, Pokrovskii VM (1998). Somatostatin as a regulator of cardiovascular system functions. *Usp Fiziol Nauk* **29**(4)**:** 24-41.

Padi SS, Kulkarni SK (2004). Differential effects of naproxen and rofecoxib on the development of hypersensitivity following nerve injury in rats. *Pharmacol Biochem Behav* **79**(2)**:** 349-358.

Pagano RL, Fonoff ET, Dale CS, Ballester G, Teixeira MJ, Britto LRG (2012). Motor cortex stimulation inhibits thalamic sensory neurons and enhances activity of PAG neurons: Possible pathways for antinociception. *Pain* **153**(12)**:** 2359-2369.

Paice JA, Penn RD, Kroin JS (1996). Intrathecal octreotide for relief of intractable nonmalignant pain: 5-year experience with two cases. *Neurosurgery* **38**(1)**:** 203-207.

Paisley A, Abbott C, van Schie C, Boulton A (2002). A comparison of the Neuropen against standard quantitative sensory-threshold measures for assessing peripheral nerve function. *Diabet Med* **19**(5)**:** 400-405.

Palazzo E, Marabese I, de Novellis V, Rossi F, Maione S (2014). Supraspinal metabotropic glutamate receptors: a target for pain relief and beyond. *Eur J Neurosci* **39**(3)**:** 444-454.

Parmar RM, Chan WW, Dashkevicz M, Hayes EC, Rohrer SP, Smith RG*, et al.* (1999). Nonpeptidyl somatostatin agonists demonstrate that sst2 and sst5 inhibit stimulated growth hormone secretion from rat anterior pituitary cells. *Biochem Biophys Res Commun* **263**(2)**:** 276-280.

Pascual J, Freijanes J, Berciano J, Pesquera C (1991). Analgesic effect of octreotide in headache associated with acromegaly is not mediated by opioid mechanisms. Case report. *Pain* **47**(3)**:** 341-344.

Patel YC (1999). Somatostatin and its receptor family. *Frontiers in Neuroendocrinology* **20**(3)**:** 157-198.

Patel YC, Greenwood M, Panetta R, Hukovic N, Grigorakis S, Robertson LA*, et al.* (1996). Molecular biology of somatostatin receptor subtypes. *Metabolism* **45**(8 Suppl 1)**:** 31-38.

Patel YC, Greenwood MT, Panetta R, Demchyshyn L, Niznik H, Srikant CB (1995). Mini review - the somatostatin receptor family. *Life Sciences* **57**(13)**:** 1249-1265.

Patel YC, Greenwood MT, Warszynska A, Panetta R, Srikant CB (1994). All 5 cloned human somatostatin receptors (hsstr1-5) are functionally coupled to adenylyl-cyclase. *Biochemical and Biophysical Research Communications* **198**(2)**:** 605-612.

Patil N, Cox DR, Bhat D, Faham M, Myers RM, Peterson AS (1995). A potassium channel mutation in weaver mice implicates membrane excitability in granule cell-differentiation. *Nature Genetics* **11**(2).

Pedersen JL, Kehlet H (1998). Hyperalgesia in a human model of acute inflammatory pain: a methodological study. *Pain* **74**(2-3)**:** 139-151.

Pedersen SF, Owsianik G, Nilius B (2005). TRP channels: an overview. *Cell Calcium* **38**(3-4)**:** 233-252.

Perkins MN, Kelly D (1994). Interleukin-1 beta induced-desArg9bradykinin-mediated thermal hyperalgesia in the rat. *Neuropharmacology* **33**(5)**:** 657-660.

Persaud N, Strichartz GR (2002). Micromolar lidocaine selectively blocks propagating ectopic impulses at a distance from their site of origin. *Pain* **99**(1-2)**:** 333-340.

Pertovaara A (2006). Noradrenergic pain modulation. *Progress in Neurobiology* **80**(2)**:** 53-83.

Peterfreund RA, Vale WW (1985). Somatostatin secretion from the hypothalamus. *Adv Exp Med Biol* **188:** 183-200.

Pezet S, Malcangio M, Lever IJ, Perkinton MS, Thompson SW, Williams RJ*, et al.* (2002). Noxious stimulation induces Trk receptor and downstream ERK phosphorylation in spinal dorsal horn. *Mol Cell Neurosci* **21**(4)**:** 684-695.

Pinter E, Helyes Z, Szolcsanyi J (2006). Inhibitory effect of somatostatin on inflammation and nociception. *Pharmacology & Therapeutics* **112**(2)**:** 440-456.

Pinter E, Helyes Z, Németh J, Pórszász R, Pethö G, Thán M*, et al.* (2002). Pharmacological characterisation of the somatostatin analogue TT-232: effects on neurogenic and non-neurogenic inflammation and neuropathic hyperalgesia. *Naunyn Schmiedebergs Arch Pharmacol* **366**(2)**:** 142-150.

Pradayrol L, Jornvall H, Mutt V, Ribet A (1980). N-terminally extended somatostatin - primary structure of somatostatin-28. *Febs Letters* **109**(1)**:** 55-58.

Prado GN, Taylor L, Zhou X, Ricupero D, Mierke DF, Polgar P (2002). Mechanisms regulating the expression, self-maintenance, and signaling-function of the bradykinin B2 and B1 receptors. *J Cell Physiol* **193**(3)**:** 275-286.

Press R, Pashenkov M, Jin JP, Link H (2003). Aberrated levels of cerebrospinal fluid chemokines in Guillain-Barré syndrome and chronic inflammatory demyelinating polyradiculoneuropathy. *J Clin Immunol* **23**(4)**:** 259-267.

Priest BT, Murphy BA, Lindia JA, Diaz C, Abbadie C, Ritter AM*, et al.* (2005). Contribution of the tetrodotoxin-resistant voltage-gated sodium channel NaV1.9 to sensory transmission and nociceptive behavior. *Proc Natl Acad Sci U S A* **102**(26)**:** 9382-9387.

Prinster SC, Hague C, Hall RA (2005). Heterodimerization of g protein-coupled receptors: specificity and functional significance. *Pharmacol Rev* **57**(3)**:** 289-298.

Qin X, Wan Y, Wang X (2005). CCL2 and CXCL1 trigger calcitonin gene-related peptide release by exciting primary nociceptive neurons. *J Neurosci Res* **82**(1)**:** 51-62.

Rami HK, Thompson M, Wyman P, Jerman JC, Egerton J, Brough S*, et al.* (2004). Discovery of small molecule antagonists of TRPV1. *Bioorg Med Chem Lett* **14**(14)**:** 3631-3634.

Randall LO, Selitto JJ (1957). A method for measurement of analgesic activity on inflamed tissue. *Arch Int Pharmacodyn Ther* **111**(4)**:** 409-419.

Raynor K, Lucki I, Reisine T (1993). Somatostatin receptors in the nucleus accumbens selectively mediate the stimulatory effect of somatostatin on locomotor activity in rats. *J Pharmacol Exp Ther* **265**(1)**:** 67-73.

Reubi JC, Maurer R (1985). Autoradiographic mapping of somatostatin receptors in the rat central nervous-system and pituitary. *Neuroscience* **15**(4)**:** 1183-1193.

Ribeiro RA, Vale ML, Thomazzi SM, Paschoalato AB, Poole S, Ferreira SH*, et al.* (2000). Involvement of resident macrophages and mast cells in the writhing nociceptive response induced by zymosan and acetic acid in mice. *Eur J Pharmacol* **387**(1)**:** 111-118.

Rittner HL, Machelska H, Stein C (2005). Leukocytes in the regulation of pain and analgesia. *J Leukoc Biol* **78**(6)**:** 1215-1222.

Robas N, Mead E, Fidock M (2003). MrgX2 is a high potency cortistatin receptor expressed in dorsal root ganglion. *Journal of Biological Chemistry* **278**(45).

Robertson B, Xu XJ, Hao JX, Wiesenfeld-Hallin Z, Mhlanga J, Grant G*, et al.* (1997). Interferon-gamma receptors in nociceptive pathways: role in neuropathic pain-related behaviour. *Neuroreport* **8**(5)**:** 1311-1316.

Rosenthal BM, Ho RH (1989). An electron microscopic study of somatostatin immunoreactive structures in lamina II of the rat spinal cord. In. *Brain Res Bull*, edn, Vol. 22. United States. p^pp 439-451.

Rueff A, Dray A (1993). Sensitization of peripheral afferent fibres in the in vitro neonatal rat spinal cord-tail by bradykinin and prostaglandins. *Neuroscience* **54**(2)**:** 527-535.

Ruggere MD, Patel YC (1985). Hepatic metabolism of somatostatin-14 and somatostatin-28: immunochemical characterization of the metabolic fragments and comparison of cleavage sites. *Endocrinology* **117**(1)**:** 88-96.

Rush AM, Cummins TR, Waxman SG (2007). Multiple sodium channels and their roles in electrogenesis within dorsal root\ ganglion neurons. *J Physiol* **579**(Pt 1)**:** 1-14.

Sadja R, Alagem N, Reuveny E (2003). Gating of GIRK channels: Details of an intricate, membrane-delimited signaling complex. *Neuron* **39**(1).

Saito T, Iwata N, Tsubuki S, Takaki Y, Takano J, Huang SM*, et al.* (2005). Somatostatin regulates brain amyloid beta peptide Abeta42 through modulation of proteolytic degradation. *Nat Med* **11**(4)**:** 434-439.

Saklatvala J, Davis W, Guesdon F (1996). Interleukin 1 (IL1) and tumour necrosis factor (TNF) signal transduction. *Philos Trans R Soc Lond B Biol Sci* **351**(1336)**:** 151-157.

Salzer E, Kansu A, Sic H, Májek P, Ikincioğullari A, Dogu FE*, et al.* (2014). Early-onset inflammatory bowel disease and common variable immunodeficiency-like disease caused by IL-21 deficiency. *J Allergy Clin Immunol* **133**(6)**:** 1651-1659.e1612.

Sandkuhler J, Fu QG, Helmchen C (1990). Spinal somatostatin superfusion in vivo affects activity of cat nociceptive dorsal horn neurons: comparison with spinal morphine. In. *Neuroscience*, edn, Vol. 34. England. p^pp 565-576.

Sandkuhler J (2009). Models and mechanisms of hyperalgesia and allodynia. *Physiol Rev* **89**(2)**:** 707-758.

Sandor K, Elekes K, Szabo A, Pinter E, Engstrom M, Wurster S*, et al.* (2006). Analgesic effects of the somatostatin sst(4) receptor selective agonist J-2156 in acute and chronic pain models. *European Journal of Pharmacology* **539**(1-2)**:** 71-75.

Sandoval KE, Farr SA, Banks WA, Crider AM, Morley JE, Witt KA (2013). Somatostatin receptor subtype-4 agonist NNC 26-9100 mitigates the effect of soluble Abeta(42) oligomers via a metalloproteinase-dependent mechanism. *Brain Res* **1520:** 145-156.

Scarborough DE (1990). Somatostatin regulation by cytokines. *Metabolism-Clinical and Experimental* **39**(9)**:** 108-111.

Scarborough DE, Lee SL, Dinarello CA, Reichlin S (1989). Interleukin-1 beta stimulates somatostatin biosynthesis in primary cultures of fetal rat brain. *Endocrinology* **124**(1)**:** 549-551.

Schaefer EA, Stohr S, Meister M, Aigner A, Gudermann T, Buech TR (2013). Stimulation of the chemosensory TRPA1 cation channel by volatile toxic substances promotes cell survival of small cell lung cancer cells. *Biochem Pharmacol* **85**(3)**:** 426-438.

Schloos J, Raulf F, Hoyer D, Bruns C (1997). Identification and pharmacological characterization of somatostatin receptors in rat lung. *Br J Pharmacol* **121**(5)**:** 963-971.

Schmader KE (2002). Epidemiology and impact on quality of life of postherpetic neuralgia and painful diabetic neuropathy. *Clin J Pain* **18**(6)**:** 350-354.

Schonbrunn A, Tashjian AH (1978). Characterization of functional receptors for somatostatin in rat pituitary cells in culture. *Journal of Biological Chemistry* **253**(18)**:** 6473-6483.

Schreff M, Schulz S, Handel M, Keilhoff G, Braun H, Pereira G*, et al.* (2000). Distribution, targeting, and internalization of the sst(4) somatostatin receptor in rat brain. *Journal of Neuroscience* **20**(10)**:** 3785-3797.

Schuelert N, Just S, Kuelzer R, Corradini L, Gorham LC, Doods H (2014). The somatostatin receptor 4 agonist J-2156 reduces mechanosensitivity of peripheral nerve afferents and spinal neurons in an inflammatory pain model. *Eur J Pharmacol*: Epub.

Schulz S, Handel M, Schreff M, Schmidt H, Hollt V (2000). Localization of five somatostatin receptors in the rat central nervous system using subtype-specific antibodies. *Journal of Physiology-Paris* **94**(3-4)**:** 259-264.

Seideman P, Lohrer F, Graham GG, Duncan MW, Williams KM, Day RO (1994). The stereoselective disposition of the enantiomers of ibuprofen in blood, blister and synovial fluid. *Br J Clin Pharmacol* **38**(3)**:** 221-227.

Seltzer Z, Dubner R, Shir Y (1990). A novel behavioral model of neuropathic pain disorders produced in rats by partial sciatic nerve injury. *Pain* **43**(2)**:** 205-218.

Setyono-Han B, Henkelman MS, Foekens JA, Klijn GM (1987). Direct inhibitory effects of somatostatin (analogues) on the growth of human breast cancer cells. *Cancer Res* **47**(6)**:** 1566-1570.

Shaqura MA, Zollner C, Mousa SA, Stein C, Schafer M (2004). Characterization of mu opioid receptor binding and G protein coupling in rat hypothalamus, spinal cord, and primary afferent neurons during inflammatory pain. *Journal of Pharmacology and Experimental Therapeutics* **308**(2).

Sheridan MA, Kittilson JD, Slagter BJ (2000). Structure-function relationships of the signaling system for the somatostatin peptide hormone family. *American Zoologist* **40**(2)**:** 269-286.

Shmigol A, Verkhratsky A, Isenberg G (1995). Calcium-induced calcium release in rat sensory neurons. *J Physiol* **489 (Pt 3):** 627-636.

Siehler S, Seuwen K, Hoyer D (1998). I-125 Tyr(10)-cortistatin(14) labels all five somatostatin receptors. *Naunyn-Schmiedebergs Archives of Pharmacology* **357**(5).

Silveri F, Morosini P, Brecciaroli D, Cervini C (1994). Intraarticular injection of somatostatin in knee osteoarthritis - clinical-results and igf-1 serum levels. *International Journal of Clinical Pharmacology Research* **14**(2)**:** 79-85.

Sims JE, Giri JG, Dower SK (1994). The two interleukin-1 receptors play different roles in IL-1 actions. *Clin Immunol Immunopathol* **72**(1)**:** 9-14.

Sitcheran R, Gupta P, Fisher PB, Baldwin AS (2005). Positive and negative regulation of EAAT2 by NF-kappaB: a role for N-myc in TNFalpha-controlled repression. *EMBO J* **24**(3)**:** 510-520.

Smith PA, Sellers LA, Humphrey PP (2001). Somatostatin activates two types of inwardly rectifying K+ channels in MIN-6 cells. *J Physiol* **532**(Pt 1)**:** 127-142.

Snider WD, McMahon SB (1998). Tackling pain at the source: New ideas about nociceptors. *Neuron* **20**(4)**:** 629-632.

Snijdelaar DG, Dirksen R, Slappendel R, Crul BJ (2000). Substance P. *Eur J Pain* **4**(2)**:** 121-135.

Sommer C, Petrausch S, Lindenlaub T, Toyka KV (1999). Neutralizing antibodies to interleukin 1-receptor reduce pain associated behavior in mice with experimental neuropathy. *Neurosci Lett* **270**(1)**:** 25-28.

Somvanshi RK, Kumar U (2014). delta-opioid receptor and somatostatin receptor-4 heterodimerization: possible implications in modulation of pain associated signaling. *PLoS One* **9**(1)**:** e85193.

Spampinato S, Romualdi P, Candeletti S, Cavicchini E, Ferri S (1988). Distinguishable effects of intrathecal dynorphins, somatostatin, neurotensin and s-calcitonin on nociception and motor function in the rat. *Pain* **35**(1)**:** 95-104.

Spier AD, de Lecea L (2000). Cortistatin: a member of the somatostatin neuropeptide family with distinct physiological functions. *Brain Research Reviews* **33**(2-3).

Stein C, Gramsch C, Herz A (1990). Intrinsic mechanisms of antinociception in inflammation: local opioid receptors and beta-endorphin. *J Neurosci* **10**(4)**:** 1292-1298.

Stone LS, Molliver DC (2009). In search of analgesia: emerging roles of GPCRs in pain. *Mol Interv* **9**(5)**:** 234-251.

Story GM, Peier AM, Reeve AJ, Eid SR, Mosbacher J, Hricik TR*, et al.* (2003). ANKTM1, a TRP-like channel expressed in nociceptive neurons, is activated by cold temperatures. *Cell* **112**(6)**:** 819-829.

Stroh T, Kreienkamp HJ, Beaudet A (1999). Immunohistochemical distribution of the somatostatin receptor subtype 5 in the adult rat brain: Predominant expression in the basal forebrain. *Journal of Comparative Neurology* **412**(1)**:** 69-82.

Stander S, Steinhoff M, Schmelz M, Weisshaar E, Metze D, Luger T (2003). Neurophysiology of pruritus: cutaneous elicitation of itch. *Arch Dermatol* **139**(11)**:** 1463-1470.

Sullivan SJ, Schonbrunn A (1987). Characterization of somatostatin receptors which mediate inhibition of insulin-secretion in rinm5f insulinoma cells. *Endocrinology* **121**(2)**:** 544-552.

Sun JH, Yang B, Donnelly DF, Ma C, LaMotte RH (2006). MCP-1 enhances excitability of nociceptive neurons in chronically compressed dorsal root ganglia. *J Neurophysiol* **96**(5)**:** 2189-2199.

Sun X, Singleton PA, Letsiou E, Zhao J, Belvitch P, Sammani S*, et al.* (2012). Sphingosine-1-phosphate receptor-3 is a novel biomarker in acute lung injury. *Am J Respir Cell Mol Biol* **47**(5)**:** 628-636.

Swayne LA, Bourinet E (2008). Voltage-gated calcium channels in chronic pain: emerging role of alternative splicing. *Pflugers Arch* **456**(3)**:** 459-466.

Szolcsanyi J, Bolcskei K, Szabo A, Pinter E, Petho G, Elekes K*, et al.* (2004). Analgesic effect of TT-232, a heptapeptide somatostatin analogue, in acute pain models of the rat and the mouse and in streptozotocin-induced diabetic mechanical allodynia. In. *Eur J Pharmacol*, edn, Vol. 498. Netherlands. p^pp 103-109.

Szolcsanyi J, Pinter E, Helyes Z, Oroszi G, Nemeth J (1998). Systemic anti-inflammatory effect induced by counter-irritation through a local release of somatostatin from nociceptors. *British Journal of Pharmacology* **125**(4)**:** 916-922.

Szolcsanyi J, Pintér E, Helyes Z, Petho G (2011). Inhibition of the function of TRPV1-expressing nociceptive sensory neurons by somatostatin 4 receptor agonism: mechanism and therapeutical implications. *Curr Top Med Chem* **11**(17)**:** 2253-2263.

Taddese A, Nah SY, McCleskey EW (1995). Selective opioid inhibition of small nociceptive neurons. *Science* **270**(5240)**:** 1366-1369.

Talbot JD, Marrett S, Evans AC, Meyer E, Bushnell MC, Duncan GH (1991). Multiple representations of pain in human cerebral cortex. *Science* **251**(4999)**:** 1355-1358.

Tanelian DL, Brose WG (1991). Neuropathic pain can be relieved by drugs that are use-dependent sodium channel blockers: lidocaine, carbamazepine, and mexiletine. *Anesthesiology* **74**(5)**:** 949-951.

Taniguchi T, Takaoka A (2002). The interferon-alpha/beta system in antiviral responses: a multimodal machinery of gene regulation by the IRF family of transcription factors. *Curr Opin Immunol* **14**(1)**:** 111-116.

Taniyama Y, Suzuki T, Mikami Y, Moriya T, Satomi S, Sasano H (2005). Systemic distribution of somatostatin receptor subtypes in human: an immunohistochemical study. *Endocr J* **52**(5)**:** 605-611.

Tao Y-X, Gu J, Stephens RL, Jr. (2005). Role of spinal cord glutamate transporter during normal sensory transmission and pathological pain states. *Molecular Pain* **1**.

Tapia-Arancibia L, Astier H (1988). Glutamate stimulates somatostatin release from diencephalic neurons in primary culture. *Endocrinology* **123**(5)**:** 2360-2366.

Tashev R, Belcheva S, Milenov K, Belcheva I (2001). Antinociceptive effect of somatostatin microinjected into caudate putamen. *Peptides* **22**(7)**:** 1079-1083.

Taylor JE, Moreau JP, Baptiste L, Moody TW (1991). Octapeptide analogues of somatostatin inhibit the clonal growth and vasoactive intestinal peptide-stimulated cyclic AMP formation in human small cell lung cancer cells. *Peptides* **12**(4)**:** 839-843.

Taylor R, Raffa RB, Pergolizzi JV (2012). Controlled release formulation of oxycodone in patients with moderate to severe chronic osteoarthritis: a critical review of the literature. *J Pain Res* **5:** 77-87.

ten Bokum AM, Lichtenauer-Kaligis EG, Melief MJ, van Koetsveld PM, Bruns C, van Hagen PM*, et al.* (1999). Somatostatin receptor subtype expression in cells of the rat immune system during adjuvant arthritis. *J Endocrinol* **161**(1)**:** 167-175.

Thomazzi SM, Ribeiro RA, Campos DI, Cunha FQ, Ferreira SH (1997). Tumor necrosis factor, interleukin-1 and interleukin-8 mediate the nociceptive activity of the supernatant of LPS-stimulated macrophages. *Mediators Inflamm* **6**(3)**:** 195-200.

Todd AJ (2010). Neuronal circuitry for pain processing in the dorsal horn. *Nature Reviews Neuroscience* **11**(12)**:** 823-836.

Tominaga M, Caterina MJ, Malmberg AB, Rosen TA, Gilbert H, Skinner K*, et al.* (1998). The cloned capsaicin receptor integrates multiple pain-producing stimuli. *Neuron* **21**(3)**:** 531-543.

Tulipano G, Soldi D, Bagnasco M, Culler MD, Taylor JE, Cocchi D*, et al.* (2002). Characterization of new selective somatostatin receptor subtype-2 (sst2) antagonists, BIM-23627 and BIM-23454. Effects of BIM-23627 on GH release in anesthetized male rats after short-term high-dose dexamethasone treatment. *Endocrinology* **143**(4)**:** 1218-1224.

Tóth A, Boczán J, Kedei N, Lizanecz E, Bagi Z, Papp Z*, et al.* (2005). Expression and distribution of vanilloid receptor 1 (TRPV1) in the adult rat brain. *Brain Res Mol Brain Res* **135**(1-2)**:** 162-168.

Upp JR, Olson D, Poston GJ, Alexander RW, Townsend CM, Thompson JC (1988). Inhibition of growth of two human pancreatic adenocarcinomas in vivo by somatostatin analog SMS 201-995. *Am J Surg* **155**(1)**:** 29-35.

Vanderah TW (2010). Delta and kappa opioid receptors as suitable drug targets for pain. *Clin J Pain* **26 Suppl 10:** S10-15.

Varecza Z, Elekes K, László T, Perkecz A, Pintér E, Sándor Z*, et al.* (2009). Expression of the somatostatin receptor subtype 4 in intact and inflamed pulmonary tissues. *J Histochem Cytochem* **57**(12)**:** 1127-1137.

Vaughan CW, Ingram SL, Connor MA, Christie MJ (1997). How opioids inhibit GABA-mediated neurotransmission. *Nature* **390**(6660)**:** 611-614.

Vikman KS, Siddall PJ, Duggan AW (2005). Increased responsiveness of rat dorsal horn neurons in vivo following prolonged intrathecal exposure to interferon-gamma. *Neuroscience* **135**(3)**:** 969-977.

Vinegar R, Schreiber W, Hugo R (1969). Biphasic development of carrageenin edema in rats. *J Pharmacol Exp Ther* **166**(1)**:** 96-103.

Vogler R, Sauer B, Kim DS, Schäfer-Korting M, Kleuser B (2003). Sphingosine-1-phosphate and its potentially paradoxical effects on critical parameters of cutaneous wound healing. *J Invest Dermatol* **120**(4)**:** 693-700.

Walsh KB (2011). Targeting GIRK Channels for the Development of New Therapeutic Agents. *Frontiers in pharmacology* **2**.

Wan G, Yang K, Lim Q, Zhou L, He BP, Wong HK*, et al.* (2010). Identification and validation of reference genes for expression studies in a rat model of neuropathic pain. *Biochem Biophys Res Commun* **400**(4)**:** 575-580.

Wang C, Gu Y, Li GW, Huang LY (2007). A critical role of the cAMP sensor Epac in switching protein kinase signalling in prostaglandin E2-induced potentiation of P2X3 receptor currents in inflamed rats. *J Physiol* **584**(Pt 1)**:** 191-203.

Wang H, Kohno T, Amaya F, Brenner GJ, Ito N, Allchorne A*, et al.* (2005). Bradykinin produces pain hypersensitivity by potentiating spinal cord glutamatergic synaptic transmission. *J Neurosci* **25**(35)**:** 7986-7992.

Wang J, Yu G (2013). A Systems Biology Approach to Characterize Biomarkers for Blood Stasis Syndrome of Unstable Angina Patients by Integrating MicroRNA and Messenger RNA Expression Profiling. *Evid Based Complement Alternat Med* **2013:** 510208.

Watanabe N, Horie S, Michael GJ, Spina D, Page CP, Priestley JV (2005). Immunohistochemical localization of vanilloid receptor subtype 1 (TRPV1) in the guinea pig respiratory system. *Pulm Pharmacol Ther* **18**(3)**:** 187-197.

Weaver CT, Hatton RD, Mangan PR, Harrington LE (2007). IL-17 family cytokines and the expanding diversity of effector T cell lineages. *Annu Rev Immunol* **25:** 821-852.

Weckbecker G, Lewis I, Albert R, Schmid HA, Hoyer D, Bruns C (2003). Opportunities in somatostatin research: biological, chemical and therapeutic aspects. *Nat Rev Drug Discov* **2**(12)**:** 999-1017.

Werhagen L, Budh CN, Hultling C, Molander C (2004). Neuropathic pain after traumatic spinal cord injury--relations to gender, spinal level, completeness, and age at the time of injury. *Spinal Cord* **42**(12)**:** 665-673.

Wheeler G (2002). Gabapentin. Pfizer. *Current opinion in investigational drugs (London, England : 2000)* **3**(3)**:** 470-477.

White FA, Jung H, Miller RJ (2007). Chemokines and the pathophysiology of neuropathic pain. *Proc Natl Acad Sci U S A* **104**(51)**:** 20151-20158.

White JP, Calcott G, Jenes A, Hossein M, Paule CC, Santha P*, et al.* (2011). Xenon reduces activation of transient receptor potential vanilloid type 1 (TRPV1) in rat dorsal root ganglion cells and in human TRPV1-expressing HEK293 cells. *Life Sci* **88**(3-4)**:** 141-149.

Willis WD (1985). Nociceptive pathways: anatomy and physiology of nociceptive ascending pathways. *Philos Trans R Soc Lond B Biol Sci* **308**(1136)**:** 253-270.

Willis WD, Kenshalo DR, Leonard RB (1979). The cells of origin of the primate spinothalamic tract. *J Comp Neurol* **188**(4)**:** 543-573.

Winter CA, Risley EA, Nuss GW (1962). Carrageenin-induced edema in hind paw of the rat as an assay for antiiflammatory drugs. *Proc Soc Exp Biol Med* **111:** 544-547.

Wood PB (2008). Role of central dopamine in pain and analgesia. *Expert Rev Neurother* **8**(5)**:** 781-797.

Woolf CJ (1983). Evidence for a central component of post-injury pain hypersensitivity. *Nature* **306**(5944)**:** 686-688.

Xanthos DN, Sandkuhler J (2014). Neurogenic neuroinflammation: inflammatory CNS reactions in response to neuronal activity. *Nat Rev Neurosci* **15**(1)**:** 43-53.

Yamamoto J, Ohnuma K, Hatano R, Okamoto T, Komiya E, Yamazaki H*, et al.* (2014). Regulation of somatostatin receptor 4-mediated cytostatic effects by CD26 in malignant pleural mesothelioma. *Br J Cancer* **110**(9)**:** 2232-2245.

Yamamoto S, Wajima T, Hara Y, Nishida M, Mori Y (2007). Transient receptor potential channels in Alzheimer's disease. *Biochim Biophys Acta* **1772**(8)**:** 958-967.

Yoshimura M, Jessell T (1990). Amino acid-mediated epsps at primary afferent synapses with substantia gelatinosa neurons in the rat spinal-cord. *Journal of Physiology-London* **430:** 315-335.

Yu FH, Catterall WA (2003). Overview of the voltage-gated sodium channel family. *Genome Biol* **4**(3)**:** 207.

Zhao J, Seereeram A, Nassar MA, Levato A, Pezet S, Hathaway G*, et al.* (2006). Nociceptor-derived brain-derived neurotrophic factor regulates acute and inflammatory but not neuropathic pain. *Mol Cell Neurosci* **31**(3)**:** 539-548.

Zhou Y, Tang H, Liu J, Dong J, Xiong H (2011). Chemokine CCL2 modulation of neuronal excitability and synaptic transmission in rat hippocampal slices. *J Neurochem* **116**(3)**:** 406-414.

Zylka MJ (2011). Pain-relieving prospects for adenosine receptors and ectonucleotidases. *Trends Mol Med* **17**(4)**:** 188-196.

Zylka MJ, Rice FL, Anderson DJ (2005). Topographically distinct epidermal nociceptive circuits revealed by axonal tracers targeted to Mrgprd. *Neuron* **45**(1)**:** 17-25.

Appendix

A1. Extra results

Cyclosomatostatin has previously described in literature as being an appropriate antagonist for somatostatin receptors. Despite this no experiments were run in this thesis that utilized this compound. Initially the compound was characterized in the same way as the other somatostatin agonists, where radio ligand binding assay were run to determine selectivity and affinity (section 2.1.2) and cAMP assays were run to confirm functional activation and to determine potency (section 2.1.3).

Compound	$Hsst_1$	$Hsst_2$	$Hsst_3$	$Hsst_4$	$Hsst_5$
Cyclosomatostatin	-6.89±0.02	-5.29±0.12	-7.29±0.04	-6.27±0.13	-6.59±0.04

Table A1. Selectivity of cyclosomaostatin a somatostatin antagonist on the human receptor subtypes. The affinity of the described somatostatin antagonist was determined, and the selectivity of these for the 5 human somatostatin receptor subtypes was established using radioligand binding assays. The results show the mean±S.E.M. log Ki of the compounds. Data were obtained by non-linear regression analysis of the dose response curves. N=3.

Cyclosomatostatin had µM affinity for the sst_4 receptor, but was most selective for the sst_3 receptor. For the functional assay 1000 nM somatostatin 14 was used, as this was shown to inhibit cAMP under normal conditions (section 3.1.3; Fig. 3.2) and is 100 fold higher than the calculated IC_{50} (section 3.1.3; Table 3.3). The cells were treated with both 1000 nM somatostatin 14 and increasing concentrations of cyclosomatostatin, where one would expect antagonistic effects by 1000 nM (Fig. A.1). However no reversal of somatostatin induced inhibition was seen at any concentration. Therefore this compound was not used for future experiments.

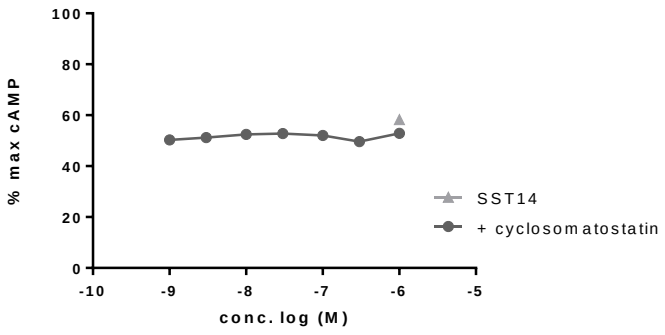

Fig. A.1. Inhibition of cAMP production by sst_4 receptors: Somatostatin alone inhibited cAMP production by activating the rat sst_4 receptor subtype. Cycolosomatostatin had no influence on this induced inhibition. A fluorescent immunoassay developed by Perkin Elmer was conducted using forskolin (30 µM rat and 10 µM human) and intact sst_4 expressing H4 cells. The results are presented as % of maximal cAMP concentration.

A1.1. Extra behavioural data

The characterised sst_4 receptor agonist, J-2156, was tested behaviourally using four validated rat models of pain to confirm that activation of the receptor induces analgesic effects. In the CFA, STZ and PNL models significant improvements in PWT were achieved at 1 mg/kg J-2156 (section 3.2). For the MIA model, weight bearing deficits were measured (section 2.2.8). Significant improvements were only seen under these conditions with higher doses of J-2156 at 10 mg/kg (section 3.2.2; Fig 3.3). Lower doses were tested in the MIA model (Fig. A.2), however no effects were seen. The positive control morphine had significant anti-nociceptive effects.

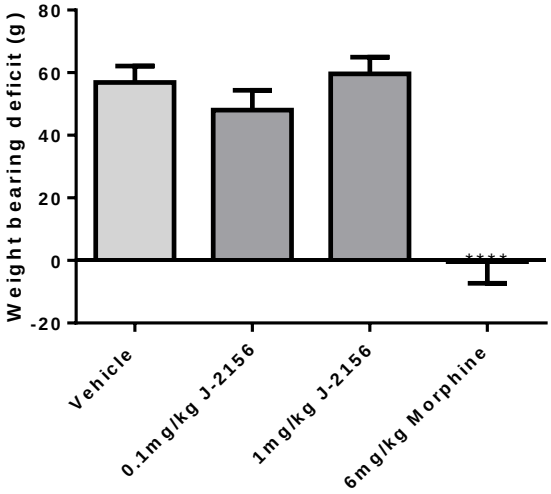

Fig. A.2. Effect of J-2156 on the MIA pain model in the rat: Effects of J-2156 on MIA-induced weight bearing deficit in the rat. At day 3 post intraarticular injection of MIA, J-2156 and morphine was dosed and tested at 1 hour after administration. At lower doses J-2156 had no influence on the MIA induced deficit. Data are presented as mean±S.E.M. N=8 rats/group. ****P<0.0001 vs. vehicle treated group (ANOVA).

The effects of J-2156 were still significant at 24 hours post compound administration in the inflammatory pain models (section 3.2.4). This meant taking behavioural measurements at 48 hours post CFA injection and 4 days post MIA injection. To ensure the acute effect of J-2156 was present at these time points the compound was dosed and behavioural effects were tested 1 hour later. J-2156 caused a significant increase in PWT at 1 hour post dosing at CFA 48 hours ($P<0.05$ vs. vehicle; n=14; Fig. A3A) and significant decreases in weight bearing deficit at MIA 4 days ($P<0.001$ vs. vehicle; n = 11; Fig. A3B). At 4 days post MIA injection morphine also caused a significant decrease in weight bearing deficit, when tested 1 hour post administration ($P<0.001$ vs. vehicle; n=10; Fig. A3B).

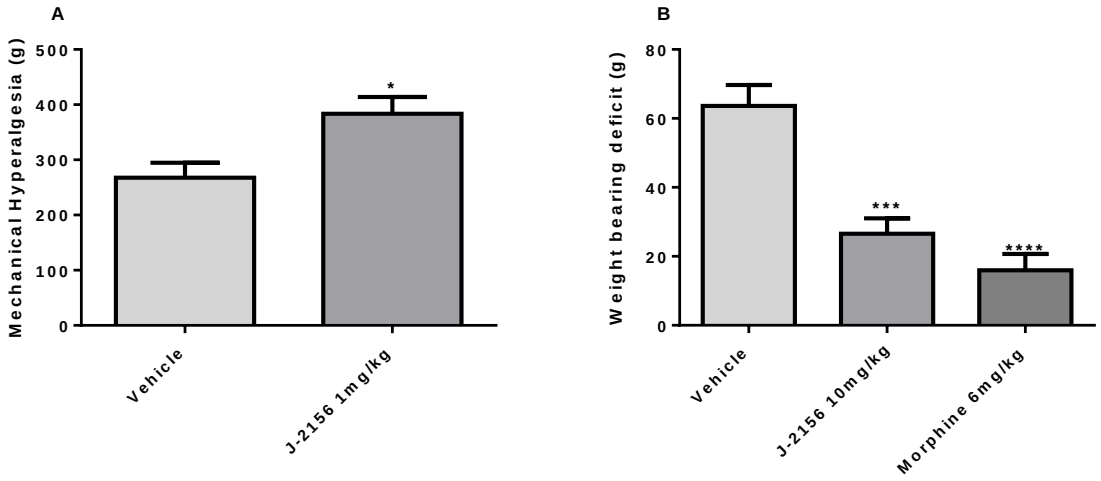

Fig. A.3. Acute effect of J-2156 on later stages nociceptive pain model development. (A) Effects of J-2156 on CFA-induced mechanical hypersensitivity in the rat. Forty-eight hours post injection of CFA, J-2156 (1 mg/kg, i.p.) was administered and mechanical sensitivity was tested at 1 hour after administration. (B) Effects of J-2156 on MIA-induced weight bearing deficit in the rat. At day 4 post intraarticular injection of MIA, J-2156 (10 mg/kg, i.p.) and morphine (6 mg/kg, s.c.) were administered and responses were tested at 1 hour later. Data are presented as mean±S.E.M. N=10-14 rats/group. *P<0.05 and **P<0.01 vs. vehicle treated group (ANOVA).

A1.2. Extra ion channel data

For both TRPV1 and TRPA1 channels selective agonists were used to activate the receptors. It was initially necessary to determine the concentration of these specific agonists.

Capsaicin was used to activate TRPV1 channels. The results are described in section 3.3.3. For calcium imaging experiments 30 nM capsaicin was used to stimulate the cells. At this concentration a large influx of calcium ions was observed by the increase in fluorescence, which was not significantly different to 100 nM (Fig. A.4A). Furthermore, the cells recovered more when 30 nM capsaicin was used (Fig. A.4B).

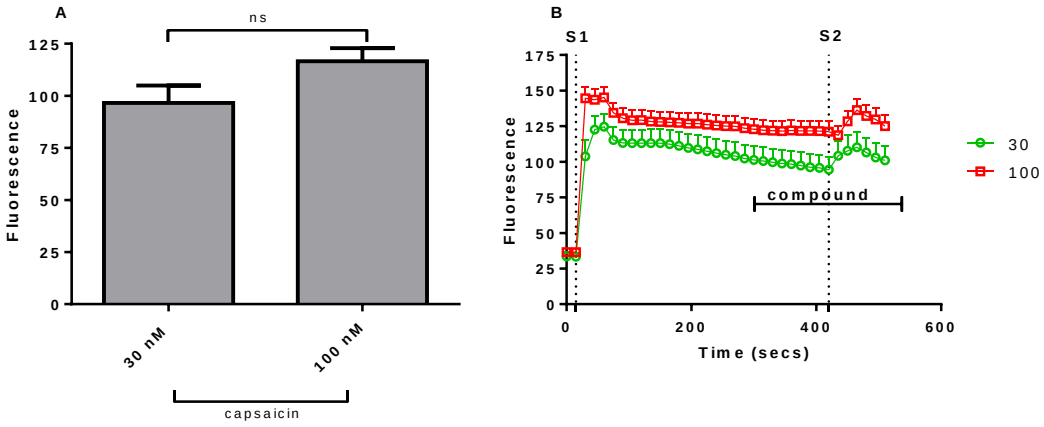

Fig. A.4. Capsaicin induces calcium currents in rat DRG neurons. (A) The effects of capsaicin. The TRPV1 specific agonist induced calcium currents at 30 nM and 100 nM. A similar response was induced. (B) Average raw traces are shown, both concentrations of capsaincin induced calcium current, however the cells recovered more with the 30 nM concentration. Therefore this was used in future experiments. Results are presented as the fluorescence reading. N=24-53.

As TRPV1 channels also allow the movement of sodium ions into the cell, whole cell patch clamp experiments were run. The results are described in section 3.3.3. For these experiments 300 nM capsaicin was required to stimulate the cells. At 30 nM capsaicin the induced current was deemed too small for a viable assay window. Furthermore, at 300 nM the induced current was significantly higher (P<0.001 vs. 30nM; Fig. A.5).

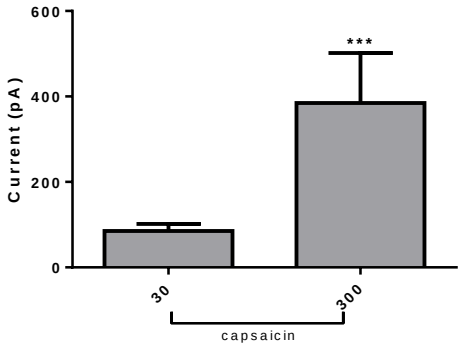

Fig. A.5. Capsaicin induces sodium currents in rat DRG neurons. Concentration-dependent effects of capsaicin. The TRPV1 specific agonist induced calcium currents at 30 nM and 300 nM. The current produced by 30 nM was considered too small for an appropriate assay window. The number of cells responding was too little. Therefore 300 nM was used for future experiments. Results are presented as total current in pA. mean±S.E.M. N=4-15. ***P<0.001.

Compound 6 was used to activate TRPA1 channels. The results are described in section 3.3.4. In the calcium imaging experiments only the higher concentrations of compound 6 elicited an influx of calcium ions (Fig. A.6A). The highest concentration of 10 µM was used for the future experiments as this response was most comparable to that of the 50 mM extracellular potassium response, where the other concentrations tested were significantly lower (Fig. A.6B).

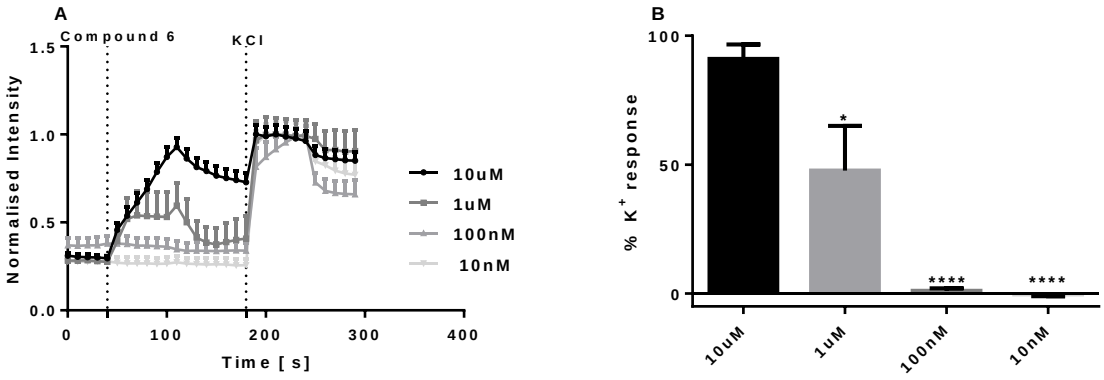

Fig. A.6. Compound 6 induces calcium currents in rat DRG neurons. (A) Protocol description and average response. (B) Concentration-dependent effects of compound 6. The TRPA1 specific agonist induced calcium currents at 10 µM and 1 µM, however that induced by 1 µM was significantly lower. The calcium influx induced by 10 µM was comparable to the high extracellular potassium response, therefore this concentration was used for future experiments. These results are represented as the % of potassium response. mean±S.E.M. N=7. *P<0.05, ****P<0.0001 vs. 10 µM.

Activation of the somatostatin 4 receptor using J-2156 was able to inhibit TRP channel currents, where the effect was augmented under inflammatory conditions. This effect was more pronounced for TRPV1 channels, where the number of cells responding to capsaicin was significantly higher in the CFA DRG neurons compared to the naive DRG neurons (Fig. A7). For TRPA1 channels, the number of cells responding was similar for CFA and naïve DRG neurons, with a difference of only 3% (Fig. A8).

Fig. A.7. Inflamed DRG neurons are more responsive to capsaicin. The TRPV1 specific agonist induced calcium currents in both naïve and inflamed DRG neurons. The Complete Freund Adjuvants (CFA) inflammatory pain model was used. A significantly higher number of cells responded to capsaicin in the inflamed DRG neurons. The results are presented as the % of the total number of cells which responded to the high extracellular potassium exposure. mean±S.E.M. N=10. ***P<0.001 vs. naïve.

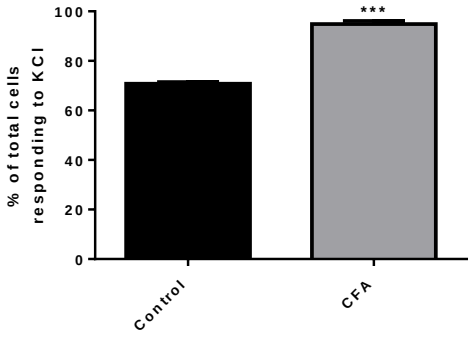

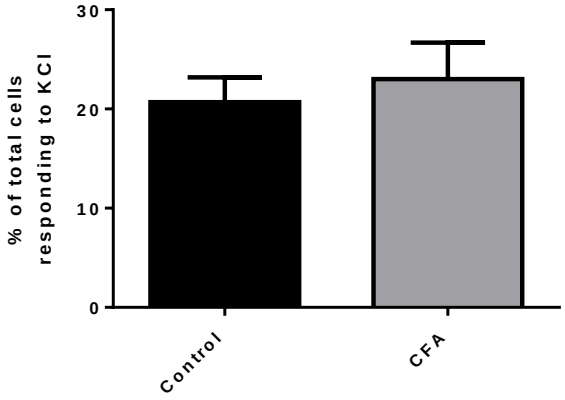

Fig. A.8. Response of DRG neurons to compound 6. The TRPA1 specific agonist induced calcium currents in both naïve and inflamed DRG neurons. The Complete Freund Adjuvants (CFA) inflammatory pain model was used. A slightly higher number of cells responded to compound 6 in the inflamed DRG neurons, although this was not significant. The results are presented as the % of the total number of cells which responded to the high extracellular potassium exposure. mean±S.E.M. N=12.

Functional links to voltage sensitive sodium channels was investigated using whole cell patch clamp experiments. Two protocols were run in current clamp mode to establish the threshold of the cell and the levels of activity (protocols described in section 2.3.4.3). The sst_4 receptor agonist induced a significant increase in threshold of the cells, however there was no influence of the level of activity, which was established by counting the total number of action potentials produced in each protocol. The results are described in section 3.3.5. Stable control recordings were made, no differences in action potential numbers was seen following either 100 nM J-2156 or 300 nM TTX application (Fig. A.9).

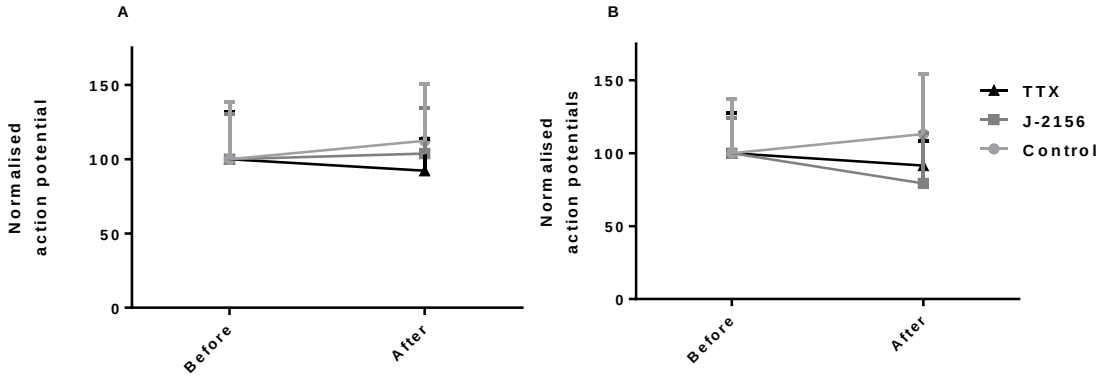

Fig. A.9. Influences on the number of action potentials produced. The effects of J-2156 and tetrodotoxin (TTX) on the number of action potentials produced. J-2156 had no effect in both the step (A) and the ramp (B) protocols at 100 nM. TTX also had no effect at 300 nM. These results are presented as the normalised threshold recorded before and after application of control or compound. mean±S.E.M. N=5-15.

A1.3. Extra inflammatory data

In order to stimulate the release of inflammatory mediators, including cytokines, chemokines and prostaglandins, the DRG neurons were exposed to 100 ng/ml LPS for 24 hours (section 2.3.7). The results are described in section 3.4.4. Treatment with LPS caused a significant increase in the levels of all inflammatory mediators tested (Fig. A.10).

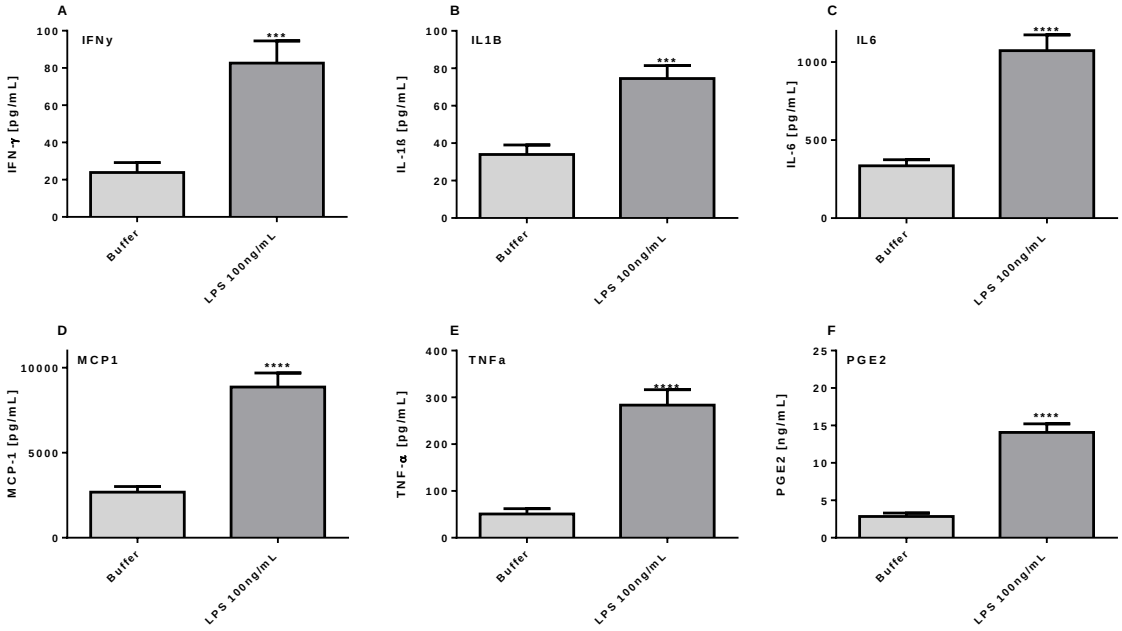

Fig. A.10. Effect of J lipopolysaccharide (LPS) stimulating cytokine and prostaglandin release in DRG neurons. Statistical analysis (paired t-test) of the effects of LPS stimulated to stimulate cytokine and prostaglandin release. DRG neurons were exposed to 100 ng/ml LPS for 24 hours. This significantly increased the levels of all assessed inflammatory mediator levels: IFNγ (A), IL1β (B), IL6 (C), MCP1 (D), TNFα (D) and PGE_2 (F). Data are represented as the concentration of the respective inflammatory mediator. mean±S.E.M.. N=3-6. ***P<0.001, ****P<0.0001 vs. Buffer.

The somatostatin 4 receptor agonist J-2156 significantly inhibited LPS induced inflammatory mediator release. The effects however were bell shaped. Interestingly such responses were also seen with both positive controls tested – celecoxib and indomethacin. The results are described in section 3.4.4.1. The exact graphs are shown in Fig. A.11 and A.12.

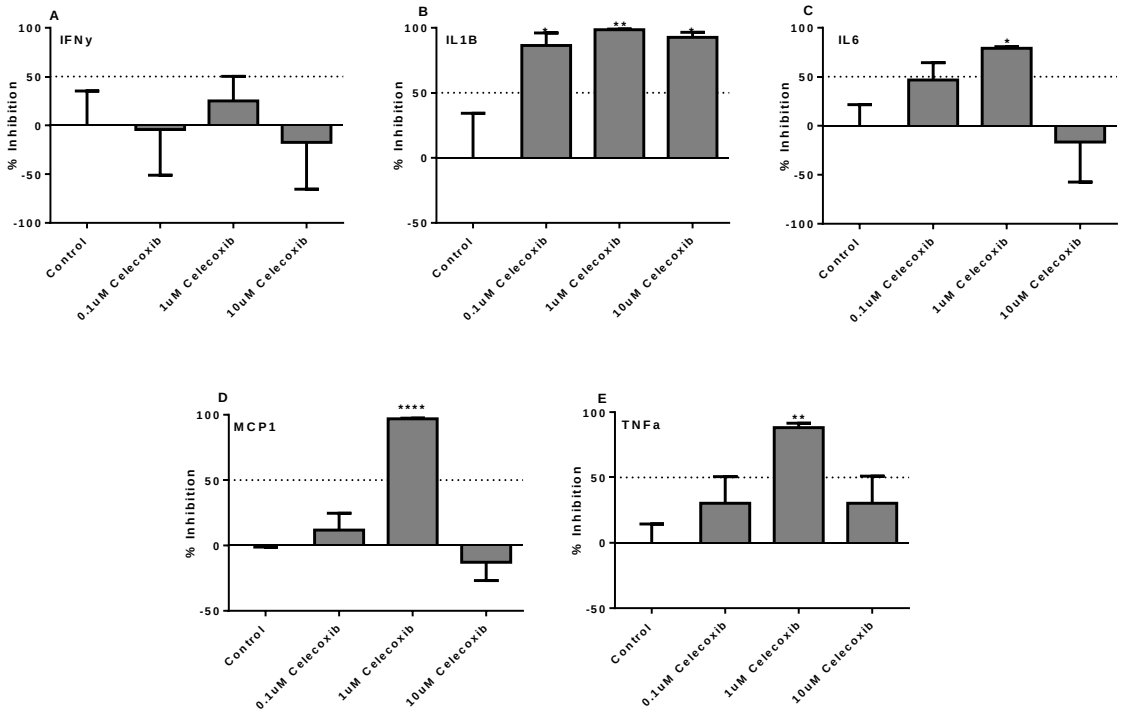

Fig. A.11. Effect of celecoxib on lipopolysaccharide (LPS) stimulated cytokine release in DRG neurons. Statistical analysis (ANOVA) of the effects of celecoxib on LPS stimulated cytokine release. DRG neurons were exposed to 100 ng/ml LPS for 24 hours (control). This significantly increased the levels of all assessed cytokine levels: IFNγ (A), IL1β (B), IL6 (C), MCP1 (D) and TNFα (E). Celecoxib inhibited LPS stimulation at 1 µM ($P<0.05$ minimum). The effects were bell shaped. Data are represented at the % inhibition of the LPS stimulation. mean±S.E.M.. N=3. *$P<0.05$, **$P<0.01$, ****$P<0.0001$ vs LPS control stimulation.

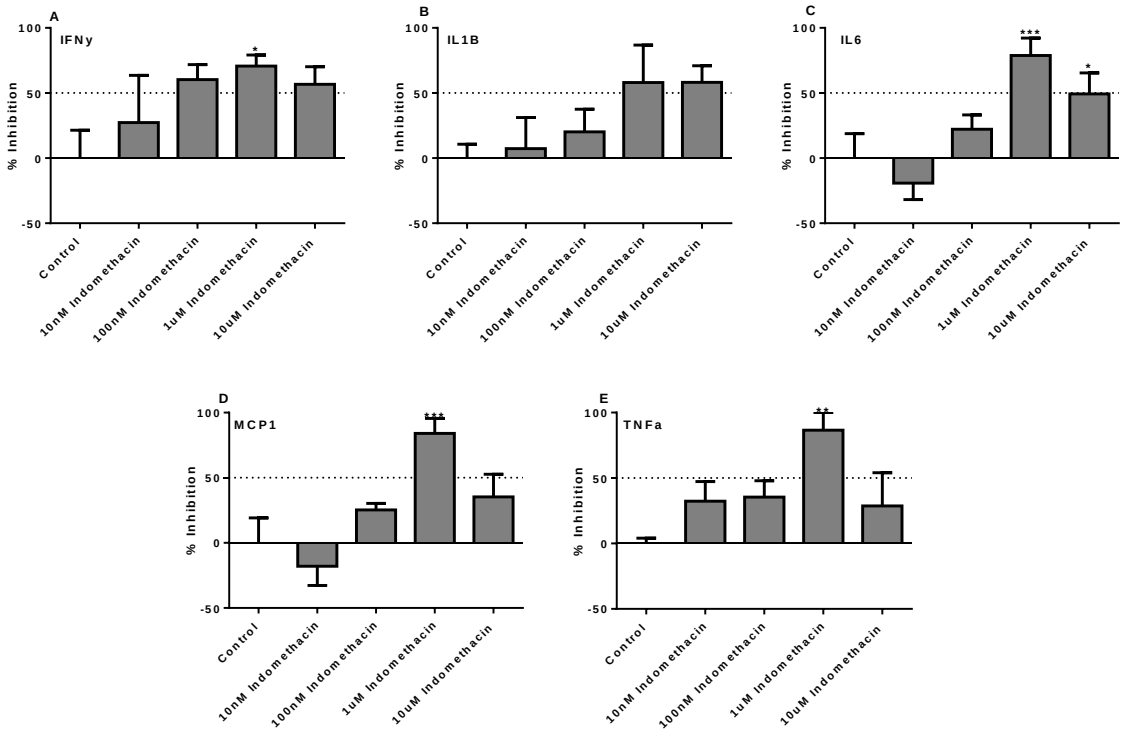

Fig. A.12. Effect of Indomethacin on lipopolysaccharide (LPS) stimulated cytokine release in DRG neurons. Statistical analysis (ANOVA) of the effects of indomethacin on LPS stimulated cytokine release. DRG neurons were exposed to 100 ng/ml LPS for 24 hours (control). This significantly increased the levels of all assessed cytokine levels: IFNγ (A), IL1β (B), IL6 (C), MCP1 (D) and TNFα (E). Indomethacin inhibited LPS stimulation at 1 µM ($P<0.05$ minimum). The effects were bell shaped. Data are represented at the % inhibition of the LPS stimulation. mean±S.E.M.. N=3. *$P<0.05$, **$P<0.01$, ***$P<0.001$ vs LPS control stimulation.

A2. Publications

A2.1. Gorham L, Just S, Doods H (2014). Somatostatin 4 receptor activation modulates G-protein coupled inward rectifying potassium channels and voltage stimulated calcium signals in dorsal root ganglion neurons. *Eur J Pharmacol* **736:** 101-106.

A2.2. Gorham L, Just S, Doods H (2014). Somatostatin 4 receptor activation modulates TPRV1 currents in dorsal root ganglion neurons. *Neurosci Lett* **573:** 35-39.

A2.3. Schuelert N, Just S, Kuelzer R, Corradini L, Gorham L, Doods H (2014). The somatostatin receptor 4 agonist J-2156 reduces mechanosensitivity of peripheral nerve afferents and spinal neurons in the CFA inflammatory pain model. *Eur J Pharmacol*: In press.

European Journal of Pharmacology 736 (2014) 101–106

Contents lists available at ScienceDirect

European Journal of Pharmacology

journal homepage: www.elsevier.com/locate/ejphar

Neuropharmacology and analgesia

Somatostatin 4 receptor activation modulates G-protein coupled inward rectifying potassium channels and voltage stimulated calcium signals in dorsal root ganglion neurons

Louise Gorham, Stefan Just*, Henri Doods

Boehringer Ingelheim Pharma GmbH & Co. KG, Department of CNS Diseases Research Germany, Birkendorfer Strasse 65, 88397 Biberach an der Riss, Germany

ARTICLE INFO

Article history:
Received 30 September 2013
Received in revised form
10 April 2014
Accepted 10 April 2014
Available online 21 April 2014

Keywords:
Sst_4 receptor
Somatostatin agonist J-2145
Dorsal root ganglion
GIRK
Ca_v
GPCR

ABSTRACT

Somatostatin has a wide biological profile resulting from its actions on the five receptor subtypes (sst_{1-5}). Recently somatostatin was shown to exert analgesic effects via activation of the sst_4 receptor. Although the analgesia in pain models is established, the precise molecular mechanism has yet to be fully elucidated. This research aimed to identify possible anti-nociceptive mechanisms, showing functional links of the sst_4 receptor to G-protein coupled inward rectifying potassium (GIRK) channels and reduction of voltage stimulated calcium influx within the pain processing pathway. Whole cell voltage clamp experiments and calcium imaging experiments were conducted on DRG neurons prepared from adult rats. Application of an sst_4 receptor selective agonist, J-2156, on DRG neurons induced a GIRK modulated potassium current, and inhibited voltage sensitive calcium current. Both mechanisms are thought to contribute to the analgesic properties of sst_4 receptor agonists.

1. Introduction

Somatostain (sst), also known as somatostatin releasing-inhibiting factor (SRIF), is a cyclic tetradecapeptide (Schulz et al., 2000), first discovered just over 40 years ago in hypothalamic extracts. It was quickly characterized as a regulatory peptide (Krulich et al., 1968), and has been ascribed important roles both in the endocrine system and in the central nervous system (CNS) (Schulz et al., 2000). Somatostatin has the ability to exert such a broad range of biological effects by associating with the five receptor subtypes, sst_{1-5}, which are widely distributed throughout the body (Pinter et al., 2006). The receptors all belong to the family of G-protein coupled receptors (GPCRs) (Patel et al., 1996).

Several recent studies have shown that somatostatin and its receptors have roles in analgesia, where the specific receptor involved is the sst_4 receptor. This was concluded on the basis of data using a highly selective sst_4 receptor agonist, J-2156 (Engstrom et al., 2005), which significantly reduced mechanical allodynia in arthritic and neuropathic pain models (Sandor et al., 2006) and exhibits multiple anti-inflammatory effects in rodents (Helyes et al., 2006). In addition mice lacking the sst_4 receptor have increased inflammatory and nociceptive responses suggesting impaired defense mechanisms (Helyes et al., 2009). Somatostatin receptors are expressed in peripheral pain regulatory pathways, particularly DRG neurons, where 45% of cells showed sst_4 receptor-like immunoreactivity (Bar et al., 2004).

Although the analgesic effect of sst_4 receptor agonists is established, the precise molecular mechanism behind this has yet to be fully elucidated. Potential mechanisms could be unfolded via links to various ion channels involved in nerve transmission.

Pain transmission involves activation of multiple potassium channels, including GRIK. These belong to the superfamily of G-protein coupled inwardly-rectifying potassium channels which influence a wide spectrum of physiological processes (Luscher and Slesinger, 2010). Functionally the GIRK channels are responsible for maintaining the resting membrane potential close to that of potassium equilibrium (Walsh, 2011). Activation of GIRK channels results in hyperpolarization of the cell membrane (Luscher and Slesinger, 2010), thus reducing spontaneous action potential formation (Walsh, 2011). Such effects present the GIRK channel as a good target for excessive cell excitability, including pain (Bhave et al., 2010).

Voltage gated calcium channels (Ca_v) belong to a family of large multi-protein complexes (Catterall, 2000). These channels are expressed in all excitable cells and are able to transduce electrical activity into biochemical signals (Catterall, 2000). Ca_v can be

Abbreviations: ATP, adenosine triphosphate; CNS, central nervous system; DMEM, Dulbecco's Modified Eagle Medium; DRG, dorsal root ganglion neurons; GIRK, G-protein inward rectifying potassium channels; GPCR, G protein coupled receptor; GTP, guanosine triphosphate; HEPES, hydroxyethyl piperazineethanesulfonic; nM, nanomolar; sst, somatostatin; SRIF, somatotropin release-inhibiting factor; Ca_v, voltage gated calcium channels

* Corresponding author. Tel.: +49 7351 54 5949; fax: +49 7351 54 5128.
E-mail address: stefan.just@boehringer-ingelheim.com (S. Just).

http://dx.doi.org/10.1016/j.ejphar.2014.04.016
0014-2999/

influenced by GPCRs by either direct binding or influence of phosphorylation and channel trafficking (Dolphin, 2003). Inhibition results in reduced cell excitability and release of neurotransmitters and peptides. Such effects present calcium channels, so reduce intracellular calcium ion content, as good targets for treatment of chronic pain (Gribkoff, 2006).

The objective of this study is to investigate the actions of the sst_4 receptor signaling on membrane excitability in rat DRG neurons. In the present report we show that the sst_4 receptor is functionally coupled to GIRK and is able to inhibit voltage stimulated calcium influx in DRG neurons.

2. Methods

2.1. Culture of DRG neurons

Adult DRG neuron cultures were prepared from 6 to 8 week old Crl:WI(Han) (Charles River, Germany) male rats. DRGs were removed and placed into DMEM (c.c.pro., Germany, FM-13-L) containing 1% penicillin–steptomycin (Sigma, Germany, P4333-100). These were digested in 4 mg/mL collagenase (Gibco, UK, 17104-019) and 2 mg/mL papain (Sigma, Germany, P4762) for 75 min in a water bath heated to 37 °C. This reaction was terminated by aspiration, and addition of DMEM (c.c.pro., Germany, FM-13-L) containing 1% penicillin–steptomycin (Sigma, Germany, P4333-100) and 10% FCS (Gibco, UK, 10500-064). Using fire-polished pasture pipettes the cells were mechanically dispersed into a homogenized cell suspension. Cells were plated on to 0.1 mg/mL poly-L-lysine (Sigma, Germany, P-7886) and 2 μg/mL laminin (Sigma, Germany, C2020-IMG) coated 35 mm tissue culture cover slips (Thermo scientific, Germany). The cells were stored at 37 °C, 10% carbon dioxide and with a humidity of 95%. Recordings were made within 48 h of plating. For the calcium imaging experiments, plated cells were left for 2 h at 37 °C, 5% CO_2 before being topped up to 1 mL of culture medium.

2.2. Whole cell patch clamp

Transmembrane currents were recorded by whole-cell voltage-clamp using an EPC 10 amplifier, with the TIDA 5.2 software (HEKA electronics, Germany) and a PCI-1600 interface (HEKA electronics, Germany) at room temperature. The average cell size of the neurons was approx. 35 μm. Data were low-pass filtered at 2.9 KHz and sampled at 20 KHz. Patch pipettes were pulled from thick-walled borosilicate glass capillaries (1.5 mm outer diameter) on a Sutter Instruments P-97 puller (Sutter instruments, USA), and had a resistance of 3–5 MΩ. The pipette solution consisted of: 20 mmol/l NaCl; 120 mmol/l KCl; 10 mmol/l glucose; 10 mmol/l HEPES; 1 mmol/l EGTA; 3 mmol/l $MgCl_2$, with the addition of 3 mmol/l Na_2ATP and 0.3 mmol/l NaGTP on the day of testing. The cells were bathed in normal Ringer's solution containing: 140 mmol/l NaCl; 5 mmol/l KCl; 10 mmol/l glucose; 10 mmol/l HEPES; 1.8 mmol/l $CaCl_2$; 0.8 mmol/l $MgCl_2$. The pH was adjusted to 7.4 using NaOH and the osmolarity remained between 300 and 320 mOsmol/l. Activation of the GIRK channels was achieved with a high potassium extracellular solution containing 100 mmol/l NaCl and 45 mmol/l KCl. The pipette potential was zeroed before seal formation; care was taken to maintain membrane access resistance as low as possible, between 3 and 7 MΩ. Command voltage protocols and data acquisition were performed by TIDA 5.2 (HEKA electronics, Germany). Cells were analyzed when J-2156 induced a potassium current of more than 0.5 nA, which was then reduced by more than 0.5 nA, Statistical analysis was carried out using the prism5 software. Data are expressed as mean ± S.E.M.. To test for normal distribution the Kolmogorov–Smirnov test was used. *t*-Test measurements allowed for significance to be determined.

2.3. Calcium imaging

The DRG neurons were pre-loaded with the Ca^{2+}-sensitive fluorophore, Fluo-4-AM, 2 μM (Invitrogen, CA) and 1 mM probenecid (Sigma, Germany) for one hour prior to imaging. The cells were then washed in Ringer buffer (140 mmol/l NaCl; 5 mmol/l KCl; 10 mmol/l glucose; 10 mmol/l HEPES; 1.8 mmol/l $CaCl_2$; 0.8 mmol/l $MgCl_2$. The pH was adjusted to 7.4 using NaOH) until use. The cells were used within one hour of pre-loading. Cells were imaged through a plan neofluar 20 × /0,5 objective, using an Axiovert 200 M microscope with inbuilt camera (Zeiss). Excitation was achieved at 488 nm with an argon laser, and images were collected, at an emission of 510 nm, through a long pass filter, using the computer software Laser Scanning Microscope 510 META version 3,2 SP2 (Zeiss). The fluorescent signal was optimized by the detector gain and amplifier offset. The cells were mounted on a custom made perfusion chamber. Depolarization of the cells was achieved via electrical stimulation of voltages between15–21 V, using an amplifier (HSE, Germany). The voltage was tested by a train of 40 pulses as 10 Hz, for 3 s. Cells were identified as responders to J-2156 if a greater effect was seen than the mean plus 2 times the S.E.M. of the control result. Statistical analysis was carried out using the prism5 software. Data are expressed as mean ± S.E.M., normalized to the maximal effect, of all voltage gated calcium channel blockers. To test for normal distribution the Kolmogorov–Smirnov test was used. *t*-Test measurements allowed for significance to be determined.

3. Results

In order to determine if the sst_4 receptor is functionally coupled to GIRK channels in DRG neurons, voltage dependent whole-cell currents from isolated DRG neurons were recorded, utilizing the sst_4 receptor selective agonist J-2156 (Engstrom et al., 2005).

Within each protocol 2 different concentrations of compound were applied, followed by potassium channel blockers. Around 30% of the cells tested responded to the sst_4 receptor agonist. These cells had an average capacitance of 50.75 ± 8.11 pF. Control experiments were run (Fig. 1A), the first was a standard control, applying only vehicle control ringer solution, showing stable readings. The second was a compound control, applying only the sst_4 receptor agonist J-2156, without the blocker application, confirming the effects of the blocker. A recording from one experiment shows the increase in current after J-2156 perfusion, then the blockage after barium chloride ($BaCl_2$) perfusion (Fig. 1C).

After 3 min of compound perfusion, a significant increase in the magnitude of the inward potassium current was seen at both 30 nM and 100 nM ($P < 0.001$). An increase of 1.22 ± 0.5 nA and 1.84 ± 0.5 nA ($n = 11$; Fig. 1B) in the current obtained at −80 mV, in 45 mmol/l potassium-containing ringer solution, was recorded respectively. When J-2156 was applied at a lower concentration of 10 nM, there was no significant increase in potassium current (Fig. 1B).

The current induced by J-2156 was significantly suppressed not only by the addition of 300 μM $BaCl_2$ by 1.59 ± 0.7 nA ($P < 0.01$, $n = 11$; Fig. 1D); but also by 500 nM tertiapin Q by 1.30 ± 0.7 nA ($P < 0.05$, $n = 11$; Fig. 1D). These results confirm that the potassium induced current is as a result of GIRK channel activation, indicating that the sst_4 receptor is functionally coupled to GIRK channels within DRG neurons.

In order to determine if the sst_4 receptor is able to influence voltage induced calcium influx in DRG neurons, calcium imaging

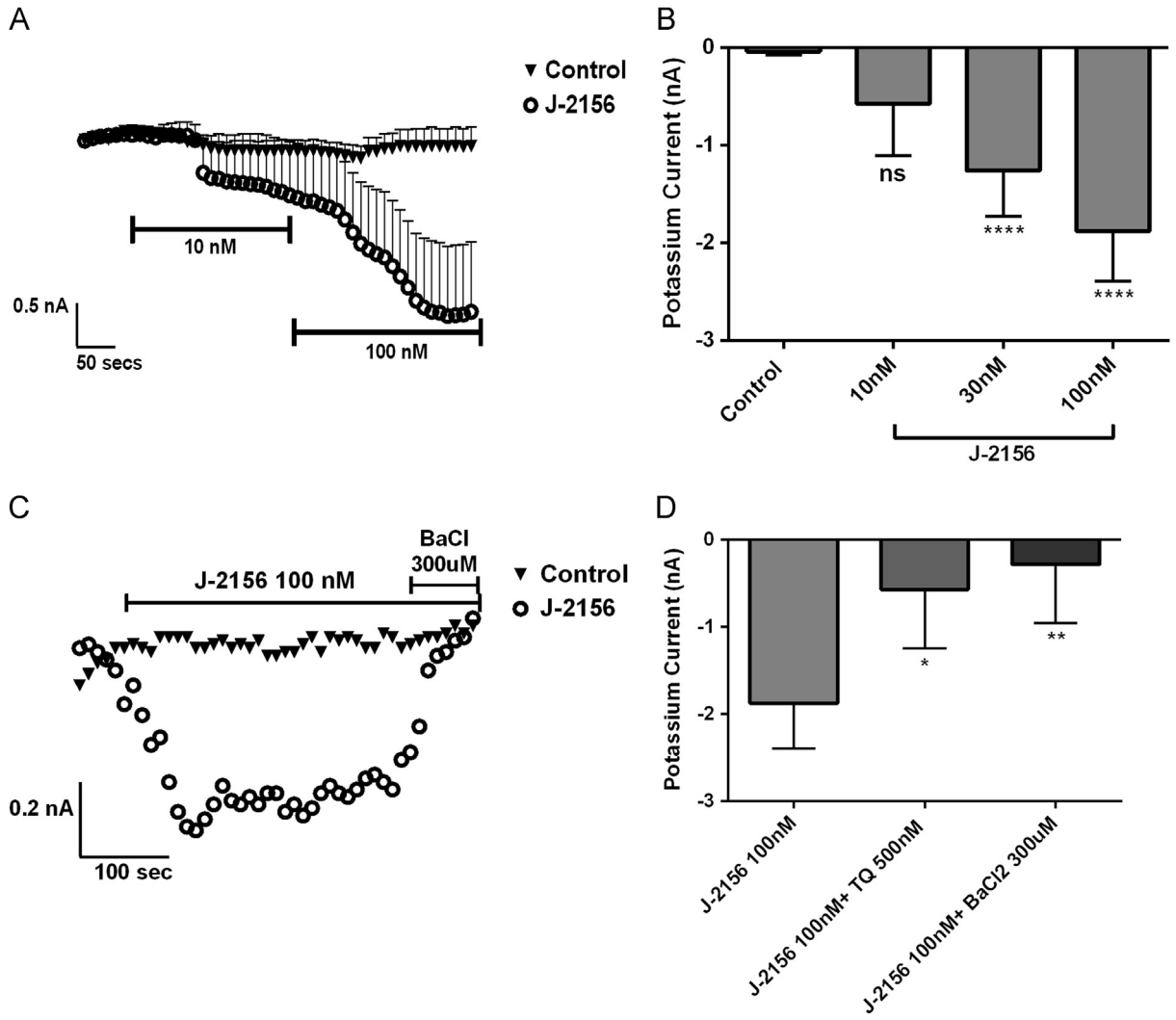

Fig. 1. J-2156 increases inward rectifying potassium current of rat DRG neurons. (A) *I–V* curve of J-2156 (30, 100 nM) effect on inwardly rectifying potassium currents was obtained at −80 mV in 45 mmol/l potassium containing ringer solution, where control currents are shown. (B) Statistical analysis (*t*-test) of the effects of increasing concentrations of J-2156. The sst_4 receptor specific agonist significantly induced a potassium current in DRG neurons at 30 nM and 100 nM ($P<0.001$ *vs* control). These results are represented as potassium current (nA) mean ± S.E.M. $N=8–11$. (C) *I–T* curve of J-2156 (100 nM) effect on inwardly rectifying potassium currents was obtained at −80 mV in 45 mmol/l potassium containing ringer solution, where the effect of $BaCl_2$ (300 μM) is seen. (D) Statistical analysis (*t*-test) of the effects of $BaCl_2$ (300 μM) and tertiapin Q (TQ) (500 nM) on the J-2156 induced current. The current was significantly inhibited by both blockers ($P<0.01$, $P<0.05$ *vs* J-2156 respectively). These results are represented as potassium current (nA) mean ± S.E.M. $N=8–11$.

techniques were used, in combination with the sst_4 receptor selective agonist J-2156 (Engstrom et al., 2005). Around 30% of cells reacted to the sst_4 receptor agonist. Application of voltage stimulation for 3 s resulted in an increase in intracellular calcium levels, indicating activation of voltage sensitive calcium channels. As seen in Fig. 2A a stable control was run, where the second stimulation produced the same evoked calcium transient. When the compound was applied for 90 s the second calcium peak was reduced. J-2156 caused a significant decrease in the voltage induced calcium transient at 10 nM, 30 nM and 100 nM ($P<0.0001$) a decrease of 40 ± 11%, 60 ± 9% and 80 ± 4% ($n=12–80$; Fig. 2C) was seen respectively.

Following this reduction of voltage induced calcium transient, it was investigated if specific Ca_v were being influenced. We applied specific channel type blockers before, for 90 s, and again for 90 s, in combination with J-2156. Conotoxin (1 μM), agatoxin (200 nM), mibefradil (10 μM) and nitrendipine (10 μM) all caused a significant reduction in the second calcium transient of 40 ± 5%, 30 ± 4%, 60 ± 9% and 50 ± 9% respectively ($P<0.0001$, $n=13–17$; Fig. 3). These effects are not as potent as 100 nM J-2156, where significant differences between the sst_4 receptor agonist and the specific blockers can be calculated ($P<0.05$), indicating more than one subtype is influenced by sst_4 receptor activation. When the individual blockers and J-2156 were applied together there was a further reduction in the voltage induced calcium transient amplitude compared to the blocker alone. Conotoxin (1 μM), agatoxin (200 nM), mibefradil (10 μM) and nitrendipine (10 μM) plus 100 nM J-2156 all caused a significantly increased reduction in the second calcium transient compared to the blockers alone, of 70 ± 6%, 70 ± 9%, > 100 ± 9% and 80 ± 10% respectively ($P<0.05$; Fig. 3). However the combination of Ca_v blockers had similar potency to the J-2156 agonist alone, where no significant difference is seen in the blockage (results not shown here). These results indicate that sst_4 receptors have the ability to interact with all subtypes of calcium channel within DRG neurons.

To determine if the hyperpolarization caused by GIRK activation (Fig. 1) influences this inhibition of voltage induced calcium influx we utilized the GIRK specific blocker tertiapin Q. Firstly the sst_4 receptor specific agonist J-2156 was applied for 90 s and then in combination with 500 nM tertiapin Q for 90 s. As previously seen 100 nM J-2156 significantly decreased the voltage induced calcium current by 90 ± 10% ($P<0.0001$, $n=22$; Fig. 4). However this inhibition was partially reversed by tertiapin Q, a reversal of 60 ± 16% ($P<0.05$,

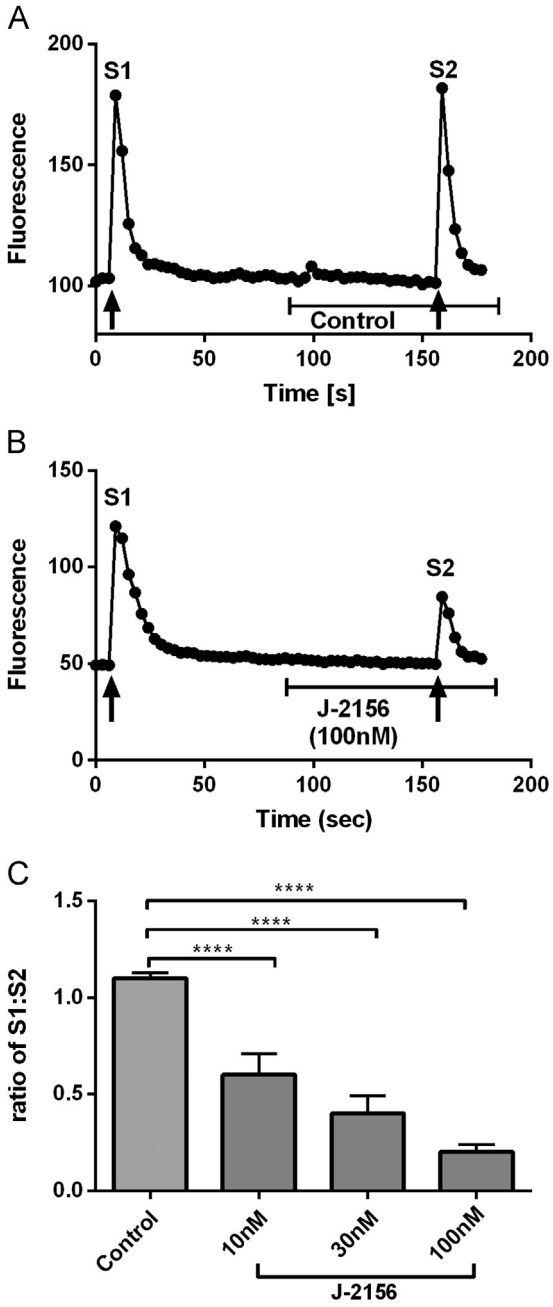

Fig. 2. J-2156 inhibits voltage induced calcium currents of rat DRG neurons. (A,B) Representative examples of responses to 3 s voltage stimulation (represented by the arrow). The magnitude of increase in calcium influx did not change in the control experiment (A); where inhibition is seen during superfusion with 100 nM J-2156 (B). (C) Statistical analysis (*t*-test) of the effects of increasing concentrations of J-2156. The sst_4 receptor specific agonist significantly inhibited the calcium current in DRG neurons at 10 nM, 30 nM and 100 nM ($P<0.0001$ vs control). These results are represented as % of total blockage mean ± S.E.M. $N=12–88$.

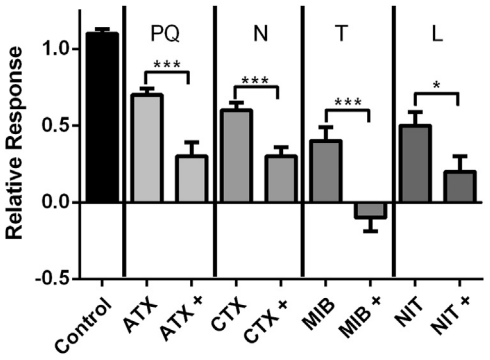

Fig. 3. Modulation of the inhibitory effects of J-2156 on specific voltage gated calcium channels. Specific blockers were used: 1 μM Conotoxin (CTX), 200 nM agatoxin (ATX), 10 μM mibefradil (MIB) and 10 μM nitrendipine (NIT) alone, and then with the addition of 100 nM J-2156 (+). Statistical analysis (*t*-test) of the effects of the blockers showed inhibition of calcium current ($P<0.0001$ vs control). Further statistical analysis (*t*-test) revealed significant reductions in calcium current following J-2156 application ($P<0.05$ vs blocker +J-2156). These results are represented as % of total blockage mean ± S.E.M., relative to the control response. $N=13–17$.

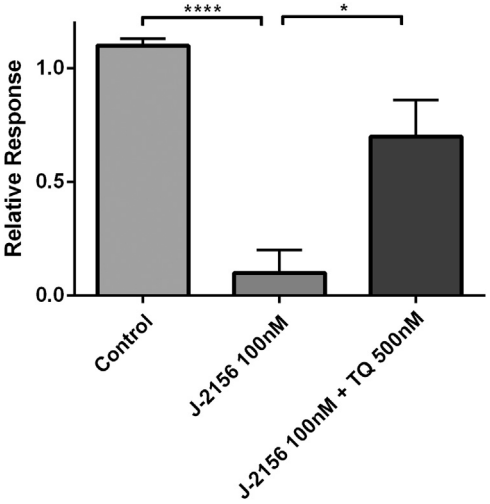

Fig. 4. The inhibition of voltage induced calcium current by J-2156 is influenced by GIRK activation. The GIRK specific blocker tertiapin Q (TQ) (500 nM) was used. Statistical analysis (*t*-test) of the effect of this blocker on sst_4 receptor induced calcium influx reduction revealed significant reversal of this effect ($P<0.05$ vs blocker +J-2156). These results are represented as % of total blockage mean ± S.E.M., relative to the control response. $N=22$.

$n=22$; Fig. 4) was seen. These results indicate that the inhibition of voltage induced calcium influx is in part due to GIRK activation.

4. Discussion

In the present study we were able to show that activation of the sst_4 receptor results in activation of GIRK channels and inhibition of voltage stimulated calcium influx within DRG neurons.

Functional links of other somatostatin receptor subtypes to GIRK channels provide the mechanism behind other physiological and pathological effects of this neuropeptide. Somatostatin´s key role in stimulating glucose release from pancreatic cells via sst_2 receptoractivation is due to activation of GIRK channels (Smith et al., 2001). Similarly somatostatin causes hyperpolarization of neuronal endocrine cells via GIRK activation (Kailey et al., 2012). Our findings are also confirming previous data showing functional links of the sst_4 receptor subtype to GIRK channels where Xenopus oocytes were used (Kreienkamp et al., 1997); however the current results using DRG neurons indicate a partial contribution to analgesic properties of sst_4 receptor agonists.

Whole cell voltage clamp recordings were made, utilizing the sst_4 receptor specific agonist J-2156 (Engstrom et al., 2005) and the GIRK blocker tertiapin Q (Kanjhan et al., 2005), allowing functional links to GIRK channels to be established.

These results showed that the sst_4 receptor specific agonist evokes a concentration dependent increase in potassium current in DRG neurons. In order to obtain evidence that this induced current was as a result of GIRK activation, tertiapin Q was used, which significantly reduced this induced current, representing a

potential mechanism behind the anti-nociceptive effects of sst_4 receptor agonists.

Activation of postsynaptic GIRK channels has been implicated in the mechanism underlying the anti-nociception produced by well-established analgesic compounds. Activation of opioid receptors and adrenergic receptors results in analgesia, mediated in part via GIRK activation (Ikeda et al., 2000). Supporting this GIRK1 and GIRK2 knock-out mice exhibit hyperalgesia behavioral phenotypes (Bhave et al., 2010). The weaver mutant mouse has a missense point mutation in the pore forming region of GIRK2 subunits; this reduced coupling of G-proteins (Patil et al., 1995). These mice show significantly reduced analgesia when treated with morphine, in comparison to wild type mice (Ikeda et al., 2000).

Additionally it was shown that activation of the sst_4 receptor is able to inhibit voltage induced calcium influx within DRG neurons. Calcium imaging experiments were run, utilizing the sst_4 receptor specific agonist J-2156 (Engstrom et al., 2005). The reduced calcium influx could be in part due to several reasons including: inhibition of voltage gated calcium channels, reduced excitability of DRG neurons via opening of potassium channels or reduced release from intracellular stores.

These results show that the sst_4 receptor specific agonist evokes a concentration dependent decrease in voltage induced calcium current in DRG neurons, indicating functional links to voltage gated calcium channels. In order to establish which specific voltage gated calcium channel was influenced selected blockers were also applied, where an additive effect was seen in all cases, representing a potential mechanism behind the anti-nociceptive effects of sst_4 receptor agonists. Our results suggest that the sst_4 receptor is able to modulate all types of voltage gated calcium channels to a similar extent. This would be a similar mechanism to that which has been seen for morphine (Khasabova et al., 2004), which showed that other GPCRs are able to modulate all subtypes of Ca_vs.

Inhibition of the voltage induced calcium influx via sst_4 receptor activation may be in part modulated via GIRK channel activation. In order to establish how activation of this channel influences the sst_4 receptor effect on calcium transient, the specific GIRK blocker tertiapin Q was utilized. In this case a partial reversal of the sst_4 receptor inhibition was seen. This could indicate an indirect mechanism for inhibition of the voltage stimulated calcium influx. Activation of GIRK channels results in hyperpolarization of the neuronal cell membrane (Kailey et al., 2012) this in turn would modulate voltage sensitive ion channels, including voltage gated calcium channels.

Calcium channels play key roles within DRG neurons. Inhibition of these would affect the excitability of the DRG neurons, slowing the rate of cell depolarization and therefore ultimately reducing nerve transmission. Lowering intracellular calcium would also alter its secondary messenger effects including control of neuropeptide release (Gribkoff, 2006); it has been previously reported that the J-2156 sst_4 receptor agonist has been reported to inhibit substance P and CGRP release from trachea cells (Helyes et al., 2006). The ability of this agonist to inhibit the voltage gated calcium channels provides a potential mechanism behind this reduced release of these neuropeptides; providing further explanation as to how sst_4 receptor agonists cause analgesic effects.

Inhibition of voltage gated calcium channels has been implicated in the mechanism underlying the anti-nocipception produced by well-established analgesic compounds. This is not only true for other GPCRs including opioid and CB1 receptor agonists (Khasabova et al., 2004); but other analgesic compounds act directly on voltage gated calcium channels, including gabapentine (Wheeler, 2002). Supporting this, functional links of the sst_4 receptor to voltage gated calcium channels provide a contributory mechanism to other physiological and pathological effects of this neuropeptide. Somatostatin´s neuroprotective role within retinal ganglion neurons was shown to be as a result of inhibition of voltage gated calcium channels via activation of sst_4 receptors (Farrell et al., 2010).

Voltage induced influx of calcium ions would result in calcium induced calcium release. This is where the cytosolic concentration of calcium can be increased via the release of calcium ions from intracellular stores. Calcium is able to activate ryanodine receptors present on the sarcoplasmic reticulum membrane causing an efflux of ions into the cytosol (Shmigol et al., 1995). Therefore this reduced calcium influx could also be in part due to decreased release from intracellular calcium stores, meaning the important roles this ion plays as a secondary messenger would be reduced.

Our results confirm the findings of Bar et al. (2004), which reported that sst_4 receptors are present on 30–60% of DRG neurons. In both the electrophysiology and the calcium imaging experiments around a third of the cells tested responded to application of this sst_4 receptor agent. The capacitance of the cells recorded might give some hints of a contribution of medium sized neurons, which could be of origin Aδ fibers. As in both data sets a similar number of cells responded we can confirm previously published data and conclude that the analgesic actions of this sst_4 receptor agonist are in part due to the peripheral mechanisms. Similarly this might help to explain how sst_4 receptor agonists contribute to the analgesia of both inflammatory pain and mechanical allodynia (Sandor et al., 2006).

In summary, our results indicate that activation of sst_4 receptors in DRG neurons leads to opening of GIRK channels and inhibition of voltage stimulated calcium influx. Both mechanisms are thought to contribute to the analgesic effects of sst_4 receptor agonists.

Acknowledgments

The authors would like to thank Rosemarie Ewen, Carsten Hecker, Benjamin Jaehnke and Gert Kramer for their technical assistance.

References

Bar, K.J., Schurigt, U., Scholze, A., Segond Von Banchet, G., Stopfel, N., Brauer, R., Halbhuber, K.J., Schaible, H.G., 2004. The expression and localization of somatostatin receptors in dorsal root ganglion neurons of normal and mono-arthritic rats. Neuroscience 127, 197–206.

Bhave, G., Lonergan, D., Chauder, B.A., Denton, J.S., 2010. Small-molecule modulators of inward rectifier K+ channels: recent advances and\ future possibilities. Future Med. Chem. 2, 757–774.

Catterall, W.A., 2000. Structure and regulation of voltage-gated Ca^{2+} channels. Annu.Rev. Cell Dev. Biol. 16, 521–555.

Dolphin, A.C., 2003. G protein modulation of voltage-gated calcium channels. Pharmacol. Rev. 55, 607–627.

Engstrom, M., Tomperi, J., El-Darwish, K., Ahman, M., Savola, J.M., Wurster, S., 2005. Superagonism at the human somatostatin receptor subtype 4. J. Pharmacol. Exp. Ther. 312, 332–338.

Farrell, S.R., Raymond, I.D., Foote, M., Brecha, N.C., Barnes, S., 2010. Modulation of voltage-gated ion channels in rat retinal ganglion cells mediated by somatostatin receptor subtype 4. J. Neurophysiol. 104, 1347–1354.

Gribkoff, V.K., 2006. The role of voltage-gated calcium channels in pain and nociception. Semin. Cell Dev. Biol. 17, 555–564.

Helyes, Z., Pinter, E., Nemeth, J., Sandor, K., Elekes, K., Szabo, A., Pozsgai, G., Keszthelyi, D., Kereskai, L., Engstroem, M., Wurster, S., Szolcsany, J., 2006. Effects of the somatostatin receptor subtype 4 selective agonist J-2156 on sensory neuropeptide release and inflammatory reactions in rodents. Br. J. Pharmacol. 149, 405–415.

Helyes, Z., Pinter, E., Sandor, K., Elekes, K., Banvolgyi, A., Keszthelyi, D., Szoke, E., Toth, D.M., Sandor, Z., Kereskai, L., Pozsgai, G., Allen, J.P., Emson, P.C., Markovics, A., Szolcsanyi, J., 2009. Impaired defense mechanism against inflammation, hyperalgesia, and airway hyperreactivity in somatostatin 4 receptor gene-deleted mice. Proc. Natl. Acad. Sci. USA 106, 13088–13093.

Ikeda, K., Kobayashi, T., Kumanishi, T., Niki, H., Yano, R., 2000. Involvement of G-protein-activated inwardly rectifying K+ (GIRK) channels in opioid-induced analgesia. Neurosci. Res., 38.

Kailey, B., van de Bunt, M., Cheley, S., Johnson, P.R., Macdonald, P.E., Gloyn, A.L., Rorsman, P., Braun, M., 2012. SSTR2 is the functionally dominant somatostatin receptor in human pancreatic\ beta- and alpha-cells, Am. J. Physiol. Endocrinol. Metab..

Kanjhan, R., Coulson, E.J., Adams, D.J., Bellingham, M.C., 2005. Tertiapin-Q blocks recombinant and native large conductance K+ channels in a use-dependent manner. J. Pharmacol. Exp. Ther. 314, 1353–1361.

Khasabova, I.A., Harding-Rose, C., Simone, D.A., Seybold, V.S., 2004. Differential effects of CB1 and opioid agonists on two populations of adult rat dorsal root ganglion neurons. J. Neurosci. 24, 1744–1753.

Kreienkamp, H.J., Honck, H.H., Richter, D., 1997. Coupling of rat somatostatin receptor subtypes to a G-protein gated inwardly rectifying potassium channel (GIRK1). Febs Lett. 419, 92–94.

Krulich, L., Dhariwal, A.P., McCann, S.M., 1968. Stimulatory and inhibitory effects of purified hypothalamic extracts on growth hormone release from rat pituitary in vitro. Endocrinology 83, 783–790.

Luscher, C., Slesinger, P.A., 2010. Emerging roles for G protein-gated inwardly rectifying potassium (GIRK) channels in health and disease. Nat. Rev. Neurosci., 301–315.

Patel, Y.C., Greenwood, M., Panetta, R., Hukovic, N., Grigorakis, S., Robertson, L.A., Srikant, C.B., 1996. Molecular biology of somatostatin receptor subtypes. Metabolism 45, 31–38.

Patil, N., Cox, D.R., Bhat, D., Faham, M., Myers, R.M., Peterson, A.S., 1995. A potassium channel mutation in weaver mice implicates membrane excitability in granule cell-differentiation. Nat. Genet., 11.

Pinter, E., Helyes, Z., Szolcsanyi, J., 2006. Inhibitory effect of somatostatin on inflammation and nociception. Pharmacol. Ther. 112, 440–456.

Sandor, K., Elekes, K., Szabo, A., Pinter, E., Engstrom, M., Wurster, S., Szolcsanyi, J., Helyes, Z., 2006. Analgesic effects of the somatostatin sst(4) receptor selective agonist J-2156 in acute and chronic pain models. Eur. J. Pharmacol. 539, 71–75.

Schulz, S., Handel, M., Schreff, M., Schmidt, H., Hollt, V., 2000. Localization of five somatostatin receptors in the rat central nervous system using subtype-specific antibodies. J. Physiol.-Paris 94, 259–264.

Shmigol, A., Verkhratsky, A., Isenberg, G., 1995. Calcium-induced calcium release in rat sensory neurons. J. Physiol. 489 (Pt 3), 627–636.

Smith, P.A., Sellers, L.A., Humphrey, P.P., 2001. Somatostatin activates two types of inwardly rectifying K+ channels in MIN-6 cells. J. Physiol. 532, 127–142.

Walsh, K.B., 2011. Targeting GIRK channels for the development of new therapeutic agents. Front. Pharmacol., 2.

Wheeler, G., 2002. Gabapentin. Pfizer. Curr. Opin. Investig. Drugs 3, 470–477 (London, England: 2000).

Neuroscience Letters 573 (2014) 35–39

Contents lists available at ScienceDirect

Neuroscience Letters

journal homepage: www.elsevier.com/locate/neulet

Somatostatin 4 receptor activation modulates TPRV1 currents in dorsal root ganglion neurons

Louise Gorham*, Stefan Just, Henri Doods

Boehringer Ingelheim Pharma GmbH & Co. KG, Dept. CNS Diseases Research Germany, Birkendorfer Strasse 65, 88397 Biberach an der Riss, Germany

HIGHLIGHTS

- Influence of a SSTR4 agonist, J-2156, on TRPV1 activity in DRG neurons was assessed.
- J-2145 concentrationally inhibited capsaicin induced calcium influx.
- J-2156 concentrationally inhibited capsaicin induced sodium influx.
- J-2145 inhibition of capsaicin induced calcium influx is augmented after CFA treatment.
- This inhibition identifies a contributing mechanism to the analgesic effects of J-2156.

ARTICLE INFO

Article history:
Received 24 March 2014
Received in revised form 16 April 2014
Accepted 28 April 2014
Available online 5 May 2014

Keywords:
sst_4 Receptor
Somatostatin agonist J-2145
DRG
TRPV1
GPCR

ABSTRACT

Somatostatin (sst) is a cyclic neuropeptide known to have inhibitory roles in the central nervous system. It exerts its biological effects via the activation of the 5 sst receptor subtypes, which belong to the family of G-protein coupled receptors (GPCR). This peptide has analgesic properties, specifically via the activation of the sst_4 receptor subtype. Although this is established, the precise molecular mechanisms causing this have not yet been fully elucidated. This research aimed to identify a possible anti-nociceptive mechanism, showing functional links to the transient receptor potential vanilloid type 1 (TRPV1) within the pain processing pathway. Calcium imaging and whole cell voltage clamp experiments were conducted on DRG neurons prepared from adult rats, utilizing capsaicin stimulations and the sst_4 receptor specific agonist J-2156. The complete Freund's adjuvant (CFA) inflammatory pain model was used to examine if effects are augmented in pain conditions. The sst_4 receptor agonist J-2156 was able significantly to inhibit capsaicin induced calcium and sodium influx, where the effect was more potent after CFA treatment. This inhibition identifies a contributory molecular mechanism to the analgesic properties of sst_4 receptor activation.

1. Introduction

The neuropeptide somatostatin (sst) is widely distributed throughout the body, having critical roles within the central nervous system (CNS) [22]. It exerts such a broad range of biological effects by associating with the 5 receptor subtypes, sst_{1-5}, which all belong to the family of G-protein coupled receptors (GPCRs) [17].

This neuropeptide has recently been implicated in analgesia, where activation of sst receptors results in inhibition of nociceptive behaviors [11]. Similarly sst analogs inhibit neuronal activity [20] and decrease responses of joint mechanoreceptors to noxious rotation [24]. Of the five sst receptor subtypes it is the sst_4 receptor that is thought to be responsible for the analgesic properties associated with sst. This was concluded on the basis of pharmacological data [21], as well as knock out animal studies [10].

The sst_4 receptor is expressed in the peripheral pain regulatory pathways, specifically DRG neurons [2]. Nociception involves the transmission of nerve impulses along primary afferent neurons, known as dorsal root ganglion neurons (DRGs). These cells contain a diverse group of ligand-gated and voltage-gated ion channels which are able to transduce noxious stimulation into depolarizations, allowing nociceptive signals to be conducted along neuronal axons [13].

Although it is well established that activation of sst_4 receptors results in analgesia, the precise molecular mechanisms involved have yet to be fully elucidated. A family of channels associated with pain onset is the transient receptor potential channels, for

Abbreviations: ATP, adenosine triphosphate; CFA, complete Freund's adjuvant; CNS, central nervous system; DMEM, Dulbecco's modified Eagle medium; DRG, dorsal root ganglion neurons; GPCR, G protein coupled receptor; HEPES, hydroxyethyl piperazineethanesulfonic; PKA, protein kinase A; sst, somatostatin; TRPV1, transient receptor potential vanilloid 1.

* Corresponding author. Tel.: +49 7351 54 7028; fax: +49 7351 54 5128.
E-mail address: louise_catherine_josephine.gorham@boehringer-ingelheim.com (L. Gorham).

http://dx.doi.org/10.1016/j.neulet.2014.04.042
0304-3940/

example, the transient receptor potential vanilloid type 1 (TRPV1). These channels are predominantly expressed in nociceptive sensory neurons [5], where they have essential roles in the detection and modulation of painful stimuli [7].

TRPV1 channels are known to be activated by many different stimuli including mechanical, chemical, thermal and pH changes [5]. Additionally they can be modulated by GPCRs. Activation of G_i proteins results in the inhibition of adenylate cyclase, leading to inhibition of cyclic adenosine monophosphate (cAMP) formation, causing a reduced activation of protein kinase A (PKA) [14]. The lack of PKA activation ultimately prevents TRPV1 sensitization [12]. This mechanism is reversed by pertussis toxin, where the inhibitory effect on cAMP via sst_4 receptor activation is abolished following pretreatment with the toxin [9].

The objective of this study was to investigate the actions of sst_4 receptor activation on TRPV1 channel signaling. In the present study we show that sst_4 receptor activation modulates TRPV1 channel currents in DRG neurons, which was abolished following pertussis toxin pre-treatment. As the sst_4 receptor agonist J-2156 is particularly potent in the complete Freund's adjuvant (CFA) model of inflammatory pain [21], we investigated if this functional link was augmented in this pain model. We found the effects were more potent post CFA injection.

2. Methods

2.1. Animals and CFA-induced inflammation

Adult male Crl:WI (Han) rats (Charles River, Germany) weighing 300–350 g were used in all experiments. Inflammation was induced by a 50 μl subcutaneous injection of 25 μg Complete Freund's Adjuvant (CFA, Sigma, USA) into the plantar surface of the left hind paw. For sham experiments 50 μl of buffer was injected. All intraplantar injections were performed under brief isoflurane (Abbott GmbH, Germany) anesthesia. All animal protocols were authorized by the Local Animal Care and Use Committee and carried out according to the local animal care guidelines, AAALAC regulations, and the USDA Animal Welfare Act. These followed the guidelines provided by Committee for Research and Ethical Issues of IASP. DRG neurons were sampled 24 h after CFA injection.

2.2. Cell culture: DRG neurons

Adult DRG neuron cultures were prepared from 6 to 8 week old Crl:WI (Han) (Charles River, Germany) male rats. From CFA injected rats only L4-L6 DRGs from the inflamed side were removed and cultured. DRGs were removed and placed into DMEM (C.C. Pro., Germany, FM-13-L). Digestion of cells was achieved using 4 mg/ml collagenase (Gibco, UK, 17104-019) and 2 mg/ml papain (Sigma, Germany, P4762) at 37 °C for 75 min. This reaction was terminated by aspiration, and addition of 10% FCS (Gibco, UK, 10500-064). The cells were dissociated by mechanical agitation and plated onto 0.1 mg/ml poly-L-lysine (Sigma, Germany, P-7886) and 2 μg/ml laminin (Sigma, Germany, C2020-IMG) coated cover slips (Thermo Scientific, Germany). The cells were stored at 37 °C, 10% carbon dioxide and with a humidity of 95%. Recordings were made within 24 h of plating.

2.3. Calcium imaging

The DRG neurons were pre-loaded with the Ca^{2+}-sensitive fluorophore, Fluo-4-AM, 2 μM (Invitrogen, CA) and 1 mM probenecid (Sigma, Germany) for one hour prior to imaging. The cells were then washed in Ringer buffer (140 mM NaCl; 5 mM KCl; 10 mM glucose; 10 mM HEPES; 1.8 mM $CaCl_2$; 0.8 mM $MgCl_2$; pH 7.4 using NaOH) until use. The cells were used within one hour of pre-loading. Cells were imaged through a plane neofluar 20×/0,5 objective, using an Axiovert 200M microscope with inbuilt camera (Zeiss). Excitation was achieved at 488 nm with an argon laser, and images were collected, at an emission of 510 nm, through a long pass filter, using the computer software Laser Scanning Microscope 510 META version 3,2 SP2 (Zeiss). The fluorescent signal was optimized by the detector gain and amplifier offset. The cells were mounted on a custom made perfusion chamber. Activation of TRPV1 channels was achieved via application of 30 nM capsaicin for 30 s.

2.4. Electrophysiology

Transmembrane currents were recorded by whole-cell voltage-clamp at −60 mV holding potential, using an EPC 10 amplifier, with TIDA 5.2 software (HEKA Electronics, Germany) and a PCI-1600 interface (HEKA Electronics, Germany). Data were low-pass filtered at 2.9 kHz and sampled at 20 kHz. Patch pipettes were pulled from borosilicate glass capillaries (1.5 mm outer diameter) on a Sutter Instruments P-97 puller (Sutter Instruments, USA), and had a resistance of 3–5 MΩ. The pipette solution consisted of: 145 mM KCl; 10 mM glucose; 10 mM HEPES; 1 mM $MgCl_2$, with the addition of 2 mM Na_2ATP and 0.2 mM NaGTP on the day of testing. The cells were bathed in calcium free Ringer's solution containing: 140 mM NaCl; 5 mM KCl; 10 mM glucose; 10 mM HEPES; 1 mM $MgCl_2$. The pH was adjusted to 7.4 using NaOH and the osmolarity remained between 300 and 320 mOsmol/l. Activation of the TRPV1 channels was achieved with a 300 nM capsaicin application for 5 s, where cells were considered responsive if the inward current magnitude was at least 100 pA. The pipette potential was zeroed before seal formation; care was taken to maintain membrane access resistance as low as possible, between 3 and 7 MΩ. Command voltage protocols and data acquisition were performed by TIDA 5.2 (HEKA Electronics, Germany).

2.5. Statistics

Statistical analysis was carried out using prism5 software. Data are expressed as mean ± S.E.M. Normal distribution was testing using the Kolmogorov–Smirnov test. One-way ANOVA measurements, followed by Bonferroni post-hoc tests, allowed for significance to be determined. The $\log_{IC50}$ was calculated to determine the concentration of compound which produces 50% of the maximal inhibition. Raw data traces are shown by normalization of the fluorescent intensity [F/F_0].

3. Results

In order to determine if the sst_4 receptor is functionally coupled to TRPV1 channels in DRG neurons we used two experimental techniques; calcium imaging and patch clamp. A previous described sst_4 receptor specific agonist J-2156 [9] was utilized, where the TRPV1 channels were activated using capsaicin.

Initially the concentration of capsaicin needed for stimulation of DRG neurons was established. The cells were exposed to capsaicin for 30 s; both 30 nM and 100 nM were able to induce a calcium influx, where no significant difference is calculated (data not shown). We therefore chose to continue with 30 nM capsaicin for future experiments, as with this concentration less desensitization was observed.

With calcium imaging experiments 2 protocols were run. The first was a double stimulation protocol, where the cells were exposed twice to 30 nM capsaicin for 30 s, and the ratio between the two peaks determined. Application of capsaicin resulted in an increase in intracellular calcium levels. A control experiment was run, where the second stimulation had a slightly reduced

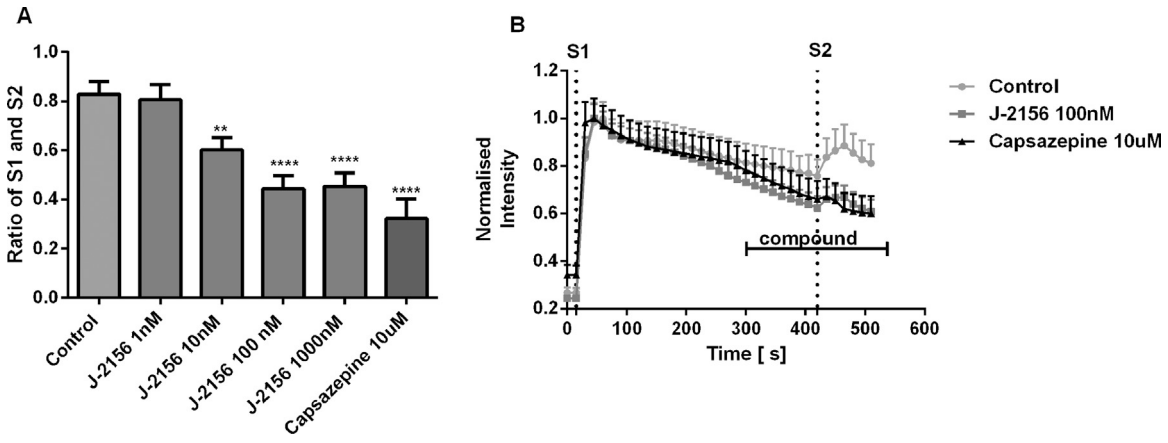

Fig. 1. *J-2156 inhibits capsaicin induced calcium currents in rat DRG neurons.* (A) Statistical analysis (ANOVA) of the effects of J-2156. The sst_4 receptor specific agonist significantly inhibited TRPV1 current at 10 nM, 100 nM and 1000 nM ($P < 0.01$, $P < 0.0001$, $P < 0.0001$ vs. control, respectively). Capsazepine at 10 μM significantly inhibited the TRPV1 current ($P < 0.0001$ vs. control). Averages of the response to 30 nM capsaicin are shown (B). These results are represented as the ratio of the two stimulations, S1:S2. $N = 24–53$.

evoked calcium transient (Fig. 1). When the sst_4 receptor agonist was applied for 3 min prior to the second stimulation, the calcium peak was reduced. J-2156 caused a significant decrease in the capsaicin induced calcium transient at 10 nM ($P < 0.01$ vs. control), 100 nM and 1000 nM ($P < 0.0001$ vs. control). A decrease of 27 ± 5%, 45 ± 6% and 45 ± 5% was seen, respectively ($n = 23–53$ cells; Fig. 1A). No effect was seen at 1 nM J-2156 application. The effect of capsazepine, a competitive antagonist of TRPV1 channels [3] was also determined. This caused a significant decrease in capsaicin evoked calcium transient at 10 μM ($P < 0.0001$ vs. control; $n = 24–53$; Fig. 1A) of 61 ± 8%. The raw recordings are shown in Fig. 1B; although there was not complete recovery, the slope showing recovery is steeper post compounds application in comparison to the control experiment. So this inhibitory effect is noticeable almost directly after compound application by the heightened rate of recovery seen.

The second protocol involved pre-incubation of the cells for 5 min with the compound. The cells were then exposed to 30 nM capsaicin for 30 s and 3 min later depolarization was induced by 80 mM extracellular potassium solution. The percentage of the potassium response was calculated. The control cells resulted in a calcium influx by both stimulations, where there was only a slight increase in the potassium response (Fig. 2A). Both the sst_4 receptor agonist, J-2156 and the TRPV1 antagonist, capsazepine, reduced the capsaicin evoked calcium influx, however, they still fully responded to the potassium. J-2156 caused a significant decrease in the capsaicin induced calcium transient at 10 nM ($P < 0.01$ vs. control), 100 nM and 1000 nM ($P < 0.001$ vs. control), a decrease of 42 ± 9%, 62 ± 6% and 64 ± 9% was seen, respectively ($n = 17–56$ cells; Fig. 2B). The $\log_{IC50}$ is −8.269. At a concentration of 10 μM, capsazepine caused a significantly reduced calcium influx compared to the control ($P < 0.001$ vs. control; $n = 16–25$; Fig. 2B), where reduction of 92 ± 2% was seen.

To confirm modulation is via the PKA pathway, experiments were run utilizing pertussis toxin, an agent known to uncouple G_i proteins from GPCRs. J-2156 was tested at 100 nM, as this concentration had maximal efficacy. The cells were pretreated with 100 ng/ml pertussis toxin and the second protocol run. The inhibition of capsaicin induced calcium influx was abolished following pretreatment with the toxin ($P = 0.3209$ vs. control; $n = 56$; Fig. 2B).

This second protocol was used to establish if the sst_4 receptor induced TRPV1 inhibition is augmented after CFA treatment. J-2156 caused a significant decrease in the capsaicin induced calcium transient at concentrations as low as 0.1 nM ($P < 0.01$ vs. control; $n = 55$; Fig. 2C). Significant effects were seen at 1 nM ($P < 0.01$ vs. control), 10 nM, 100 nM and 1000 nM ($P < 0.001$ vs. control), a decrease of 40 ± 5%, 52 ± 6%, 57 ± 4% and 55 ± 6% was seen, respectively ($n = 50–65$ cells; Fig. 2C). The $\log_{IC50}$ is −10.79. However sham treated animals reacted in the same way as naïve, where no inhibition was seen at 0.1 nM and maximal effect at 100 nM of 60 ± 6% ($P < 0.001$ vs. control; $n = 41$; Fig. 2C).

With the electrophysiology experiments a higher concentration of capsaicin was used. It was necessary to use 300 nM capsaicin as when 30 nM was used the number of cells that responded was low. Those cells which responded had an induced sodium current of 85 ± 16 pA at 30 nM, compared to 384 ± 116 pA with 300 nM (data not shown). This current was considered too small for an appropriate assay window. A protocol was run where 300 nM capsaicin was applied for 5 s at two time points; 60 and 360 s. The last application was run in the presence of either vehicle control or the compound and the ratio of the two peaks was calculated. Application of capsaicin resulted in an induced sodium current. A control experiment was run, where the final stimulation had a slightly reduced effect (Fig. 3). When the SSTR4 agonist was applied for 5 min prior to the final peak the capsaicin response was further reduced. J-2156 at 100 nM induced a significant decrease in TRPV1 activity ($P < 0.01$ vs. control) of 25 ± 6% ($n = 9–15$; Fig. 3A). Capsazepine at 10 μM also induced a significant decrease in TRPV1 activity ($P < 0.0001$ vs. control) of 67 ± 7% ($n = 9–15$; Fig. 3A).

4. Discussion

In the present study we were able to show that activation of the sst_4 receptor results in inhibition of TRPV1 channels within DRG neurons. Two experimental techniques were conducted utilizing the sst_4 receptor agonist J-2156 [9], and the TRPV1 agonist capsaicin [3]. These results showed that the J-2156 evokes a concentration dependent decrease in TRPV1 cation current in DRG neurons.

The sst_4 receptor agonist, J-2156, is a particularly potent analgesia for inflammatory pain [21]. We therefore tested whether the observed inhibition of TRPV1 current by sst_4 receptor activation was augmented after CFA treatment. These results showed that the potency of J-2156 is higher during inflammatory pain compared with naïve animals, although the overall efficacy is similar.

TPRV channels play key roles within nociception. Relating directly to pain transmission, activation of these channels allows the movement of sodium and calcium ions into the cell and potassium ions out of the cell, resulting in an inward depolarizing current. This would lead to cell excitation, triggering action potential propagation and transmission of pain signals [15]. Relating to

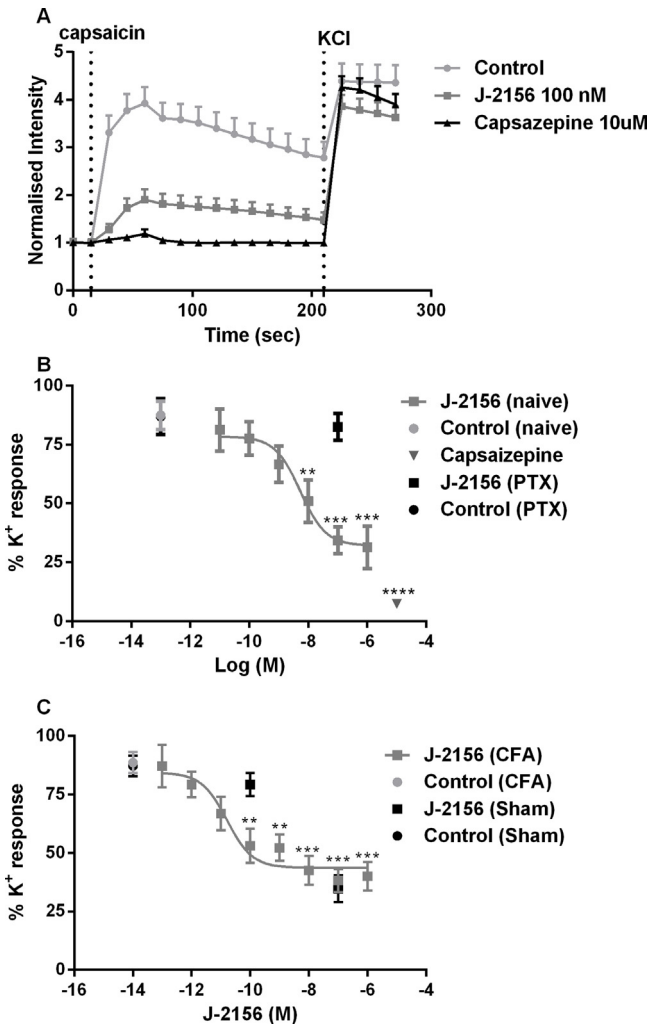

Fig. 2. *J-2156 inhibition of TRPV1 currents is augmented after CFA treatment.* (A) Protocol description and average response for naïve recordings. (B) Statistical analysis (ANOVA) of the effects of J-2156 on naïve DRG neurons. The sst_4 receptor specific agonist significantly inhibited TRPV1 current at 10 nM, 100 nM and 1000 nM ($P < 0.001$, $P < 0.0001$ vs. control, respectively). IC50 = −8.269 M. Capsazepine at 10 μM significantly inhibited the TRPV1 current ($P < 0.0001$ vs. control). Pre-incubation with 100 ng/ml pertussis toxin abolished the J-2156 TRPV1 inhibition. (C) Statistical analysis (ANOVA) of the effects of J-2156 on CFA treated DRG neurons, where significant inhibition of TRPV1 current was seen at concentrations as low as 0.1 nM ($P < 0.05$ vs. control); maximal effects were reached by 10 nM ($P < 0.0001$ vs. control). IC50 = −10.79 M. Sham treated DRGs responded in the same way as naïve DRGs. These results are represented as the % of potassium response. $N = 25–56$.

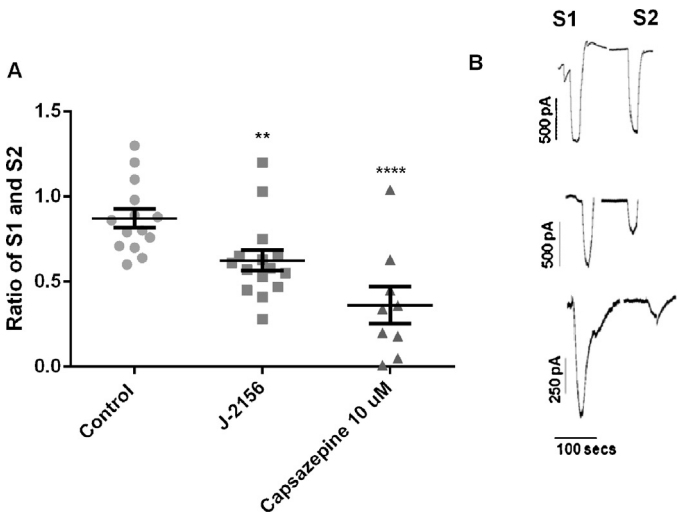

Fig. 3. *J-2156 inhibits capsaicin induced sodium currents in rat DRG neurons.* (A) Statistical analysis (ANOVA) of the effects of the sst_4 receptor specific agonist J-2156 100 nM and Capsazepine 10 μM, both compounds significantly inhibited the TRPV1 current ($P < 0.01$, $P < 0.0001$ vs. control, respectively). (B) Examples of whole-cell current to 300 nM capsaicin stimulations: control (top), J-2156 (middle) and capsazepine (bottom). These results are represented as the ratio of the two stimulations, S1:S2. $N = 9–15$.

expression, TRPV1 channels are predominantly expressed in nociceptive specific neurons [5], these are sensitized and up-regulated during tissue damage, confirming roles within pain [25]. Supporting this Caterina et al. [4] reported that TRPV1 knock-out mice showed no response to vanilloid induced pain, a reduced response to acidification and a greatly reduced response to noxious heat. These data therefore identify that inhibition of TRPV1 channels provides a useful mechanism for analgesia. TRPV1 has also been implicated in inflammatory pain. This channel is sensitized by inflammatory agents [6] and is essential for thermal hyperalgesia in inflammation but not neuropathy [7]. Furthermore expression of this channel is increased in all types of DRG neurons after CFA injection [8], giving an explanation regarding the augmented effect we see in inflamed DRG neurons.

Inhibition of TRPV1 channels has been implicated in the mechanism underlying the anti-nociception produced by well-established compounds. This is not only true for other GPCRs including opioid receptors [8]; but also capsazepine a competitive antagonist of the TRPV1 channel [3]. Capsazepine is able to inhibit nocifensive and hyperalgesic responses to capsaicin and other inflammatory agents by direct binding to the channel, therefore offering analgesia via blockage of TRPV1 mediated signals [19].

Our results confirm the findings of Pintér et al. [18], who conducted in-vivo experiments using the sst_4 receptor specific agonist TT-232. This compound was able significantly to reduce both nociceptive and inflammatory responses evoked by capsaicin, indicating that sst_4 receptor agonists affect TRPV1 activity, where our results confirm direct modulation in an ex-vivo model.

In the calcium imaging experiments two protocols were run, seen in Figs. 1B and 2A, one a double stimulation protocol and the other a pre-exposure protocol. The effects of capsazepine are more pronounced in the pre-exposure protocol (Fig. 2A); in this case the cells have no previous exposure to capsaicin, meaning capsazepine does not have to compete for binding. This enhanced effect of the second protocol is also true for the sst_4 receptor agonist J-2156. This compound does not directly bind to the TRPV1 channel, where no binding is seen at concentrations of up to 10 μM (unpublished data). However another explanation could be the calcium induced calcium release effect [23] impacting the double stimulation protocol. The remaining calcium present in the cell from the first stimulation contributes to the second, thus reducing the effect of the compounds; whereas in the second protocol the compound effect is shown directly by the first peak.

With the electrophysiology experiments it was necessary to use a 100 fold higher concentration of capsaicin to get a relevant response. The two experimental techniques are measuring different ions. In the calcium imaging experiments the response can be enhanced by release of ions from intracellular stores [23]. Similarly, the effect of capsaicin may be different for the two ions due to the pore size of the channels [1]. It is assumed that many TRP channels, upon activation, are subject to pore dilation, meaning the pore size is changed. Pore dilation results in an increased selectivity of calcium ions and an increased calcium current through the channel [16], again indicating how a lower capsaicin concentration causes a larger current in the calcium imaging experiments.

In conclusion, our results indicate that activation of sst_4 receptor in DRG neurons leads to inhibition of transient receptor potential

vanilloid type 1 (TRPV1) channels, where the effect is augmented after CFA treatment. These observations demonstrate a contributory mechanism underlying the analgesic effects of peripherally acting sst_4 receptor agonist J-2156 in inflammatory pain.

Acknowledgments

The authors would like to thank Luke Bryden, Rosmarie Ewen, Carsten Hecker, Benjamin Jaehnke, Gert Kramer and Margot Weiland for their technical assistance.

References

[1] T.G. Banke, S.R. Chaplan, A.D. Wickenden, Dynamic changes in the TRPA1 selectivity filter lead to progressive but reversible pore dilation, Am. J. Physiol.: Cell Physiol. 298 (2010) C1457–C1468.
[2] K.J. Bär, U. Schurigt, A. Scholze, G. Segond Von Banchet, N. Stopfel, R. Bräuer, K.J. Halbhuber, H.G. Schaible, The expression and localization of somatostatin receptors in dorsal root ganglion neurons of normal and monoarthritic rats, Neuroscience 127 (2004) 197–206.
[3] S. Bevan, S. Hothi, G. Hughes, I.F. James, H.P. Rang, K. Shah, C.S. Walpole, J.C. Yeats, Capsazepine: a competitive antagonist of the sensory neurone excitant capsaicin, Br. J. Pharmacol. 107 (1992) 544–552.
[4] M.J. Caterina, A. Leffler, A.B. Malmberg, W.J. Martin, J. Trafton, K.R. Petersen-Zeitz, M. Koltzenburg, A.I. Basbaum, D. Julius, Impaired nociception and pain sensation in mice lacking the capsaicin receptor, Science 288 (2000) 306–313.
[5] M.J. Caterina, M.A. Schumacher, M. Tominaga, T.A. Rosen, J.D. Levine, D. Julius, The capsaicin receptor: a heat-activated ion channel in the pain pathway, Nature 389 (1997) 816–824.
[6] D.N. Cortright, A. Szallasi, Biochemical pharmacology of the vanilloid receptor TRPV1. An update, Eur. J. Biochem. 271 (2004) 1814–1819.
[7] J.B. Davis, J. Gray, M.J. Gunthorpe, J.P. Hatcher, P.T. Davey, P. Overend, M.H. Harries, J. Latcham, C. Clapham, K. Atkinson, S.A. Hughes, K. Rance, E. Grau, A.J. Harper, P.L. Pugh, D.C. Rogers, S. Bingham, A. Randall, S.A. Sheardown, Vanilloid receptor-1 is essential for inflammatory thermal hyperalgesia, Nature 405 (2000) 183–187.
[8] J. Endres-Becker, P.A. Heppenstall, S.A. Mousa, D. Labuz, A. Oksche, M. Schäfer, C. Stein, C. Zöllner, Mu-opioid receptor activation modulates transient receptor potential vanilloid 1 (TRPV1) currents in sensory neurons in a model of inflammatory pain, Mol. Pharmacol. 71 (2007) 12–18.
[9] M. Engstrom, J. Tomperi, K. El-Darwish, M. Ahman, J.M. Savola, S. Wurster, Superagonism at the human somatostatin receptor subtype 4, J. Pharmacol. Exp. Ther. 312 (2005) 332–338.
[10] Z. Helyes, E. Pinter, K. Sandor, K. Elekes, A. Banvolgyi, D. Keszthelyi, E. Szoke, D.M. Toth, Z. Sandor, L. Kereskai, G. Pozsgai, J.P. Allen, P.C. Emson, A. Markovics, J. Szolcsanyi, Impaired defense mechanism against inflammation, hyperalgesia, and airway hyperreactivity in somatostatin 4 receptor gene-deleted mice, Proc. Nat. Acad. Sci. U.S.A. 106 (2009) 13088–13093.
[11] Z. Helyes, M. Than, G. Oroszi, E. Pinter, J. Nemeth, G. Keri, J. Szolcsanyi, Anti-nociceptive effect induced by somatostatin released from sensory nerve terminals and by synthetic somatostatin analogues in the rat, Neurosci. Lett. 278 (2000) 185–188.
[12] P.Y. Law, Y.H. Wong, H.H. Loh, Molecular mechanisms and regulation of opioid receptor signaling, Annu. Rev. Pharmacol. Toxicol. 40 (2000) 389–430.
[13] E.W. McCleskey, M.S. Gold, Ion channels of nociception, Annu. Rev. Physiol. 61 (1999).
[14] D.P. Mohapatra, C. Nau, Desensitization of capsaicin-activated currents in the vanilloid receptor TRPV1 is decreased by the cyclic AMP-dependent protein kinase pathway, J. Biol. Chem. 278 (2003) 50080–50090.
[15] I. Nagy, P. Sántha, G. Jancsó, L. Urbán, The role of the vanilloid (capsaicin) receptor (TRPV1) in physiology and pathology, Eur. J. Pharmacol. 500 (2004) 351–369.
[16] B. Nilius, J. Prenen, G. Owsianik, Irritating channels: the case of TRPA1, J. Physiol. 589 (2011) 1543–1549.
[17] Y.C. Patel, M. Greenwood, R. Panetta, N. Hukovic, S. Grigorakis, L.A. Robertson, C.B. Srikant, Molecular biology of somatostatin receptor subtypes, Metabolism 45 (1996) 31–38.
[18] E. Pintér, Z. Helyes, J. Nemeth, R. Porszasz, G. Petho, M. Than, G. Keri, A. Horvath, B. Jakab, J. Szolcsanyi, Pharmacological characterisation of the somatostatin analogue TT-232: effects on neurogenic and non-neurogenic inflammation and neuropathic hyperalgesia, Naunyn Schmiedebergs Arch. Pharmacol. 366 (2002) 142–150.
[19] H.K. Rami, M. Thompson, P. Wyman, J.C. Jerman, J. Egerton, S. Brough, A.J. Stevens, A.D. Randall, D. Smart, M.J. Gunthorpe, J.B. Davis, Discovery of small molecule antagonists of TRPV1, Bioorg. Med. Chem. Lett. 14 (2004) 3631–3634.
[20] J. Sandkühler, Q.G. Fu, C. Helmchen, Spinal somatostatin superfusion in vivo affects activity of cat nociceptive dorsal horn neurons: comparison with spinal morphine, Neuroscience (England) 34 (1990) 565–576.
[21] K. Sandor, K. Elekes, A. Szabo, E. Pinter, M. Engstrom, S. Wurster, J. Szolcsanyi, Z. Helyes, Analgesic effects of the somatostatin sst(4) receptor selective agonist J-2156 in acute and chronic pain models, Eur. J. Pharmacol. 539 (2006) 71–75.
[22] S. Schulz, M. Handel, M. Schreff, H. Schmidt, V. Hollt, Localization of five somatostatin receptors in the rat central nervous system using subtype-specific antibodies, J. Physiol. (Paris) 94 (2000) 259–264.
[23] A. Shmigol, A. Verkhratsky, G. Isenberg, Calcium-induced calcium release in rat sensory neurons, J. Physiol. 489 (Pt 3) (1995) 627–636.
[24] F. Silveri, P. Morosini, D. Brecciaroli, C. Cervini, Intraarticular injection of somatostatin in knee osteoarthritis—clinical-results and IGF-1 serum levels, Int. J. Clin. Pharmacol. Res. 14 (1994) 79–85.
[25] M. Tominaga, M.J. Caterina, A.B. Malmberg, T.A. Rosen, H. Gilbert, K. Skinner, B.E. Raumann, A.I. Basbaum, D. Julius, The cloned capsaicin receptor integrates multiple pain-producing stimuli, Neuron 21 (1998) 531–543.

European Journal of Pharmacology 746 (2015) 274–281

Contents lists available at ScienceDirect

European Journal of Pharmacology

journal homepage: www.elsevier.com/locate/ejphar

Neuropharmacology and analgesia

The somatostatin receptor 4 agonist J-2156 reduces mechanosensitivity of peripheral nerve afferents and spinal neurons in an inflammatory pain model

Niklas Schuelert [a,*], Stefan Just [a], Raimund Kuelzer [b], Laura Corradini [a], Louise C.J. Gorham [a], Henri Doods [a]

[a] Department of CNS Diseases Research, Boehringer Ingelheim Pharma GmbH & Co KG, 88397 Biberach, Germany
[b] Department of Drug Discovery and Support, Boehringer Ingelheim Pharma GmbH & Co KG, 88397 Biberach, Germany

ARTICLE INFO

Article history:
Received 11 September 2014
Received in revised form
4 November 2014
Accepted 4 November 2014
Available online 12 November 2014

Keywords:
Somatostatin receptor 4
Spinal cord
Primary afferent
In vivo electrophysiology
Inflammatory pain
Rat

ABSTRACT

Somatostatin (SST) is a peptide hormone that regulates the endocrine system and affects neurotransmission via interaction with G protein-coupled SST receptors and inhibition of the release of different hormones. The aim of this study was to investigate whether the analgesic properties of the selective SSTR4 agonist J-2156 are mediated via peripheral and/or spinal receptors.

Effect on mechanical hyperalgesia in the Complete Freund's Adjuvant (CFA) model was measured after intraperitoneal application of J-2156. Electrophysiological neuronal recordings were conducted 24 h after injection of CFA or vehicle into the paw of Wistar rats. Mechanosensitivity of peripheral afferents of the saphenous nerve as well as of spinal wide dynamic range (WDR) and nociceptive-specific (NS) neurons were measured after systemic or spinal application of J-2156.

In CFA animals J-2156 dose dependently reduced hyperalgesia in behavioral studies. The minimal effective dose was 0.1 mg/kg. Mechanosensitivity of peripheral afferents and spinal neurons was significantly reduced by J-2156. NS neurons were dose dependently inhibited by J-2156 while in WDR neurons only the highest concentration of 100 μM had an effect. In sham controls, J-2156 had no effect on neuronal activity.

We demonstrated that J-2156 dose-dependently reduces peripheral and spinal neuronal excitability in the CFA rat model without affecting physiological pain transmission. Given the high concentration of the compound required to inhibit spinal neurons, it is unlikely that the behavioral effect seen in CFA model is mediated centrally. Overall these data demonstrated that the analgesic effect of J-2156 is mediated mainly via peripheral SST4 receptors.

1. Introduction

Somatostatin (SST) is a peptide hormone widely distributed in the central nervous system and peripheral tissues (Gamse et al., 1981). SST is involved in a variety of functions including modulation of hormone and neurotransmitter release as well as cognitive and behavioral processes (ten Bokum et al., 2000). These effects are mediated via five different G-protein-coupled receptor subtypes which can be divided into two main groups on the basis of their sequence similarities and their binding profile towards synthetic SST analogs. One group comprises the SSTR2, SSTR3 and SSTR5 receptors and the other group contains the SSTR1 and SSTR4 receptors (Hoyer et al., 1995; Reisine and Bell, 1995). Exogenously administered SST has been shown to inhibit neurogenic inflammation and nociception in a variety of experimental assessments (Chrubasik et al., 1984; Fioravanti et al., 1995; Karalis et al., 1994; Lembeck et al., 1982). However, low doses of intrathecally applied SST have been shown to elicit scratching and biting behavior which has been interpreted as signs of pain or itch (Kardon et al., 2014; Seybold et al., 1982; Wiesenfeld-Hallin, 1985; Wiesenfeld-Hallin, 1986). In the peripheral sensory nervous system, SST is stored in nociceptive afferents which express the transient receptor potential vanilloid 1 (TRPV1) capsaicin receptor (Carlton et al., 2004; Clapham, 2003; Szolcsanyi et al., 2011). SSTR4 is a $G_{\alpha i}$ coupled GPCR (Patel et al., 1994) which has been shown to modulate G-protein gated inward rectifying potassium channels (GIRK), voltage gated calcium signaling (Gorham et al., 2014a) and transient receptor potential vanilloid (TRPV1) channels (Gorham et al., 2014b) in DRG neurons. SST is also expressed by glutamatergic interneurons in the dorsal horn and release of the peptide could

* Corresponding author. Tel.: +49 73515496041; fax: 49 7351545128.
E-mail address: niklas.schuelert@boehringer-ingelheim.com (N. Schuelert).

http://dx.doi.org/10.1016/j.ejphar.2014.11.003
0014-2999/

act on receptors expressed by the central terminals of primary afferents (Todd, 2010). In response to stimulation, SST is released from these capsaicin-sensitive nociceptors and induces anti-nociceptive and anti-inflammatory actions (Morton et al., 1989; Szolcsanyi et al., 1998a, 1998b). In addition to the peripheral site of action, several studies have also shown an inhibitory action of SST on spinal neurons (Jiang et al., 2003; Kim et al., 2002; Murase et al., 1982; Yasaka et al., 2010). In fact, the action of SST on spinal neurons appears to be mediated by SSTR2, which is selectively expressed by inhibitory interneurons in the superficial dorsal horn (Iwagaki et al., 2013). The therapeutic value of endogenous SST is limited by its broad range of effects mediated by the different receptor subtypes and its short plasma half-life (ten Bokum et al., 2000). However, SST receptor agonists acting on SSTR4 on peripheral and central neurons could be promising for analgesic drug development. This is supported by the potent and broad spectrum of anti-nociceptive effects of selective SSTR4 agonists (Helyes et al., 2000, 2006; Pinter et al., 2002; Sandor et al., 2006). The novel sulfonamido-peptidomimetic compound, J-2156 [(1′S,2S)-4-amino-N-(1′-carbamoyl-2′-phenylethyl)-2-(4″-methyl-1″-naphthalenesulfonamino)] butanamide possesses nanomolar affinity for the human SSTR4 and is over 400-fold more selective for this receptor than for other human SST receptor subtypes (Engstrom et al., 2005). J-2156 has been shown to be an effective analgesic in different pain models in rodents (Helyes et al., 2006;Sandor et al., 2006). Due to the expression of SSTR4 on rat dorsal root ganglia (Bar et al., 2004), a primarily peripheral site of action for SSTR4 agonists has been proposed (Helyes et al., 1996; Pinter et al., 2002; Szolcsanyi et al., 2004). However, the SSTR4 receptor is also expressed in the rat spinal cord (Somvanshi and Kumar, 2014) and therefore a central site of action cannot be excluded.

In the present study we characterized, for the first time, the effect of J-2156 on in vivo electrophysiological responses of peripheral nerve afferents and spinal cord neurons in the rat Complete Freund's Adjuvant (CFA)-induced inflammatory pain model. The aim was to evaluate whether the analgesic effect of the SSTR4 agonist is mediated exclusively peripherally or if a central component might contribute to the analgesia.

2. Materials and methods

2.1. Animals

Male Han-Wistar rats (200–420 g body weight, Charles River Laboratories, Germany) were housed in groups of 5 per cage. The room temperature and the humidity were kept constant at 22 ± 2 °C and 60 ± 15%, respectively. A 12:12 h light–dark cycle was applied with food and water ad libitum in the institutional animal facilities. All experimental procedures were approved by the Ethics Committee and the Regierungspräsidium Tübingen and adhered to the guidelines of the Committee for Research and Ethical Issues of IASP 1983.

2.2. Complete Freund's adjuvant (CFA) pain model

Rats were anesthetized under 5% isoflurane in 50% O_2 and 50% air and were maintained at 2% isoflurane during the injection period. Animals received an intraplantar (i.pl.) injection in the left hind paw with CFA suspension (25 μg in 50 μl, Sigma-Aldrich). Sham animals were injected with 50 μl of physiological saline as vehicle control.

2.3. Mechanical hyperalgesia

The mechanical paw withdrawal threshold in gram (PWT, g) of the ipsilateral inflamed paws was determined by paw pressure test (Randall-Selitto, Ugo Basile Equipment) at 24 h post CFA injection. The SSTR4 agonist J-2156 (0.01; 0.1 and 1 mg/kg) or vehicle (0.5% Natrosol and 0.01% tween 80) were administered i.p. (2 ml/kg). Indomethacin (30 mg/kg, orally, p.o.) was used as a positive control. Mechanical hyperalgesia was assessed 1 h post dosing. Analgesic activity was evaluated by comparing the PWT of the inflamed paw in the vehicle- and J-2156-treated groups. In this assay a maximal force of 500 g (i.e. cut-off) was applied to prevent tissue damage.

2.4. Surgical procedure

Animals were anesthetized in a chamber using 5% isoflurane in 50% O_2 and 50% air and were thereafter maintained at 2% isoflurane during surgery. An acceptable depth of anesthesia was continuously monitored by the absence of the hind paw withdrawal reflex. Animals were placed on a heated plate and core body temperature was maintained at 37 °C. A longitudinal midline incision was made in the neck of the animal and the trachea was exposed and cannulated (tip of a plastic transfer pipette). The cannula was connected to an UNO Micro ventilator (UNO Roestvastaal BV, Zevenaer, NL) with 50% O_2 and 50% air (stroke volume of 2–2.5 ml; breath frequency 70 strokes/min). The left carotid artery was exposed and cannulated with a fine-bore catheter (Intromedic Polyethylene tubing, PE-50) containing heparinized physiological saline (0.9% NaCl + Heparin 100 i.u./ml). The cannula was connected to a pressure transducer and a custom-made blood pressure monitor to allow continuous monitoring. A catheter with heparised physiological saline was placed in the jugular vein for intravenous compound and physiological saline administration.

2.5. Peripheral nerve recordings

A longitudinal skin incision was made along the medial aspect of the hind limb and the skin was fixed to a plastic 'O' ring to create a pouch which was filled with warm paraffin oil to prevent tissue desiccation throughout the experiment. The saphenous nerve was isolated in the inguinal region and cut centrally to prevent any spinally mediated reflexes. The saphenous nerve stump containing afferents from the paw and ankle region was placed on a small plastic stage. Under a dissecting microscope, the perineurium was removed and fine neurofilaments were dissected from the nerve using fine watchmaker forceps. Neurofilaments were then placed over a platinum electrode to record single afferent fiber activity. The receptive field of the recorded afferent was identified by the elicitation of a response to gentle probing with a fine von Frey filament. The afferents included in this study had a receptive field on the plantar hind paw and responded to increased mechanical force in a graded manner with coding of increasing intensity. All recorded afferents had a mechanical threshold below 6 g, therefore the 8 g von Frey filament was used as a supra-threshold stimulus. The von Frey filament was applied for 10 s into the center of the receptive field. Recordings were made before (baseline control) and every 5 min after intravenous administration of vehicle, followed by intravenous administration of J-2156 (1 and 5 mg/kg bolus). The conduction velocity of the nerve fibers (C-fibers < 2 m/s; Aδ-fibers 2–10 m/s) was determined by electrical stimulation of the receptive field with a bipolar silver wire electrode (1–10 V, 0.5 ms pulse width). The conduction velocity was calculated by dividing the distance between the receptive field and the electrode by the latency between the stimulus artifact and the evoked action potential. Percentage

changes in the nerve firing rate before and after administration of the vehicle and J-2156 were calculated. Neuronal activity was recorded using a differential amplifier (DAM80, WPI, USA) and a capturing interface with software (Notochord-hem 3.5, Notochord Systems, Croissy-sur-Seine, France) and then stored on a microcomputer for offline analysis.

2.6. Spinal cord recordings

A laminectomy was performed to expose L4–L6 segmental region of the spinal cord which receives afferent input from the hind paw. The dura mater was cut along the exposed area with fine spring scissors. The surrounding muscle on bone structures created a pool which was continuously filled with warm saline to prevent desiccation. A 1 MΩ Tungsten electrode (WPI, TM33B10) was advanced into the dorsal horn of the spinal cord in 10 μm increments using a hydraulic drive to a depth of 500–1200 μm from dorsal surface of the dorsal horn. The signal was amplified using a differential amplifier (DAM80, WPI, USA) and recorded using a capturing interface with software (Notochord-hem 3.5, Notochord Systems). Neurons with a defined receptive field on the CFA treated hind paw were used for further characterization. Different mechanical stimuli (brush, 8 g, 60 g von Frey) were applied for 10 s to the plantar surface of the hind paw and neuronal activity of dorsal horn neurons was recorded. The stimulation interval was fixed to 5 min. Baseline conditions of at least five stable control responses (less than 10% variability) were achieved for each parameter before vehicle (physiological saline) and compound application. Vehicle (physiological saline) and J-2156 were applied directly onto the spinal cord (cumulative doses were administered every 20 min to the same neuron). A 100 μl pipette was used for topical application onto the spinal cord, creating a pool directly above the recording site. After the administration of the highest dose of J-2156 and a 30 min washout period with physiological saline, the firing rate of spinal neurons returned to baseline levels and morphine (100 μM) was applied topically onto the spinal cord to the same neuron as a positive control. Spinal neurons were classified as wide dynamic range (WDR) neurons when they responded to stimulation with a fine brush and to non-noxious (8 g von Frey) and noxious (60 g von Frey) stimulation. Nociceptive-specific (NS) neurons were classified as neurons that did not respond to brush stimulation or the 8 g von Frey filaments but just responded to high force stimulation (60 g von Frey). At the end of each experiment, lidocaine (1% in physiological saline) was administered topically onto the spinal cord to ensure that compounds reached the recorded neuron. Recordings were not included if lidocaine did not inhibit a mechanical response.

2.7. Determination of compound concentrations in the plasma and cerebrospinal fluid

The exposure of the compound was monitored during the course of the experiments. In electrophysiological experiments, plasma samples were taken from arterial blood 45 min after i.v. administration of J-2156 and 15 min after topical application of the compound on the spinal cord. In behavioral studies plasma (collected from retinorbital cavity) and cerebrospinal fluid (CSF; collected from the foramen magnum) were taken at the end of the experimental procedure (at 1.5–2 h after i.p. administration) in euthanized animals. The total plasma and CSF concentrations of J-2156 were determined by HPLC–MS/MS (high performance liquid chromatography coupled to tandem mass spectrometry).

2.8. Compound administration

For all experiments J-2156 was dissolved in physiological saline (0.9% NaCl) and solutions were made fresh on the day of experiment. For peripheral nerve recordings, different cohorts of animals were administered J-2156 (1 and 5 mg/kg) or vehicle intravenously (i.v.) via a bolus injection (2 ml/kg). For spinal neuron recordings, J-2156 (100 nM, 1 μM, 10 μM, 100 μM), morphine (100 μM, Caesar Loretz) or vehicle were applied topically on the exposed spinal cord surface (volume: 100 μl). Indomethacin was dissolved in 0.01% Tween 80 and 0.5% natrosol. For behavioral studies, J-2156 (0.01, 0.1, 1 mg/kg, i.p.) or Indomethacin (30 mg/kg, p.o.) were administered in a volume of 2 ml/kg.

2.9. Statistics

Basal firing frequencies in CFA-treated and sham animals were analyzed using an unpaired *t*-test. The effect of compounds in the bahavioural assessment was analyzed by a one-way ANOVA with a Bonferroni's multiple comparison test. Compound effects on afferent nerve activity were analyzed using a two-way ANOVA with repeated measures and a Turkey's multiple comparison test. For the spinal recordings, dose dependency was analyzed by one-way ANOVA, for comparison of animal groups and neuron subgroups a 2-way ANOVA was used with individual points being compared using a one-sample *t*-test. All differences were considered statistically significant at a P value less than 0.05. All data passed a normality test (Shapiro–Wilk normality test); therefore a Gaussian distribution can be assumed and parametric statistics were applied. All data were expressed as means ± S.E.M for "*n*" observations, peripheral afferents and spinal neurons.

3. Results

3.1. Effect of J-2156 on CFA-induced mechanical hyperalgesia

Mechanical hyperalgesia was tested on the ipsilateral paw in CFA-injected animals. Twenty-four hours after the injection of CFA, the paw showed edema and erythema formation as well as a significant decrease in the mechanical withdrawal threshold. These are typical signs of inflammation and pain. CFA-induced inflammation significantly reduced the mechanical threshold which is around 400 g in naïve animals. Twenty four hour post-CFA injection, rats received an i.p. dose of vehicle or J-2156 (0.01, 0.1 and 1 mg/kg). One hour post-dosing behavioral test was performed. J-2156 dose dependently reduced hyperalgesia in CFA-injected animals (one-way ANOVA, $P < 0.001$). The effect of the highest dose was comparable to the effect of 30 mg/kg orally administered indomethacin while the minimal effective dose (MED) was achieved at 0.1 mg/kg (Fig. 1A).

3.2. Electrophysiological effect of J-2156 on mechanosensitivity of peripheral afferents

A total of 20 units in CFA-treated animals and 6 units in sham animals were recorded. One fiber was recorded in each animal. The conduction velocity of recorded afferents was between 0.9 and 11 m/s, which confirmed them as either C- or Aδ-fibers. One, presumably Aβ-fibre with a conduction velocity of 24 m/s was recorded. Only units with a receptive field restricted to the plantar surface of the inflamed paw were included in the study. The average firing rate of afferents in response to a 10 s stimulation period with a supra-threshold stimulus 15 g von Frey was not significantly different between groups.

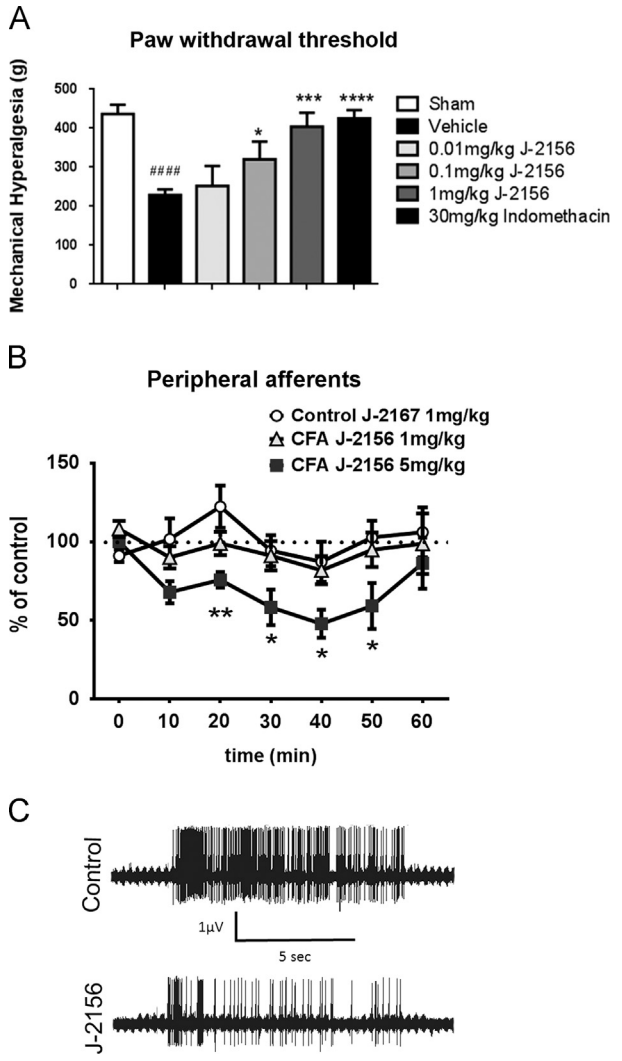

Fig. 1. (A) The SSTR4 agonist J-21256 significantly reduced CFA induced hyperalgesia in a dose-dependent manner ($P<0.05$). The effect of the highest dose (1 mg/kg) is comparable to Indomethacin (30 mg/kg). $N=8$–12 animals per group. (B) J-2156 (5 mg/kg) significantly reduced afferent nerve firing in CFA-treated animals, but has no effect in sham control animals ($n=6$–20 afferents). (C) An original spike train of an afferent fibre from a CFA-treated animal before and after application of 5 mg/kg J-2156.

i.v. administration of physiological saline as a vehicle had no effect on peripheral afferent activity. Administration of J-2156 (1 mg/kg, i.v.) had no significant effect on evoked firing while a dose of 5 mg/kg significantly reduced the firing rate up to 48% of the baseline firing in the CFA-treated animal. 5 mg/kg J-2156 had no effect in sham-treated animals (Fig. 1B). There was a significant difference between the effect of 5 mg J-2156 in CFA and control animals between 20 and 50 min-post drug application. All 3 groups were compared using the 2 way ANOVA with a multiple comparison test. An original recording of an afferent fiber is shown before and after i.v. administration of J-2156 (Fig. 1C).

3.3. Effect of J-2156 on spinal neurons

In CFA-injected animals, a total of 13 WDR neurons and 5 NS neurons were recorded. The average recording depth was 725 ± 42 μm for WDR neurons and 804 ± 39 μm for NS neurons. The average firing rate of spinal NS neurons to the 60 g von Frey filament was higher in CFA-treated animals (650 spikes) compared to controls (541 spikes) but this increase was not significant. In vehicle-treated animals, 2 WDR neurons and 6 NS neurons were recorded. The average recording depth was 780 ± 42 μm for WDR neurons and 740 ± 39 μm for NS neurons. The variability of the absolute number of action potentials to mechanically-evoked stimulation was very high in control and CFA neurons. In CFA animals the 60 g von Frey filament elicited a firing rate between 26.5 and 117.1 Hz from NS neurons and between 37.9 and 110.3 Hz from WDR neurons. In control animals the 60 g von Frey filament elicited a firing rate between 15.9 and 112.8 Hz from NS neurons and between 101.5 and 150.9 Hz from WDR neurons. Due to this high variability firing rate before compound administration was normalized to 100% as the baseline response. In CFA-treated animals, J-2156 significantly reduced the firing rate of spinal neurons to a 60 g von Frey stimulus, but had no effect in sham-treated animal (Fig. 2A). Spinal neurons were grouped according to their response characteristics in WDR- (response to brush, 8 g von Frey, 60 g von Frey) and NS-neurons (response to 60 g von Frey). In WDR neurons, only a subgroup of neurons responded to topical spinal application of the highest dose (100 μM) of J-2156 which resulted in an overall inhibition of firing rate to about 74% of control baseline, comparable to the effect of morphine (Fig. 2B). In NS neurons, concentrations of 1 μM already significantly reduced the firing rate to about 44% of control baseline and the effect was dose-dependent (one-way ANOVA, $P<0.05$). In addition, in all recorded NS neurons, morphine had a stronger inhibitory effect than in WDR neurons. Comparing the changes in firing rate of both neuronal subgroups in CFA animals, the inhibitory effect of J-2156 on NS neurons was significantly higher compared to the effect on WDR neurons ($P<0.05$, two-way ANOVA). In sham control rats (i.e. i.pl. injected with saline), J-2156 had no significant effect at any concentrations tested on WDR or NS neurons. Only, approximately 50% of neurons were inhibited by morphine and therefore did not reach significance (Fig. 2C). The difference regarding the effect of J-2156 on spinal NS neurons in CFA-treated and sham animals was highly significant (2-way ANOVA, $P<0.001$). In most NS neurons in CFA animals, the maximal inhibitory effect was seen 15 min after compound application. For further analysis of data, all recorded neurons were also grouped according to their sensitivity to morphine. Neurons with less than 30% inhibition by morphine were counted as morphine-insensitive and neurons showing morphine inhibition above 30% as morphine-sensitive (Fig. 2D). In morphine sensitive neurons the inhibitory effect of J-2156 was significantly higher compared to the morphine-insensitive neurons (unpaired t-test, $P<0.01$). An original recording of a spinal NS neuron is shown before and after administration of 100 μM J-2156 (Fig. 2E).

3.4. Plasma and CSF concentrations of J-2156

Plasma concentrations of J-2156 were determined in CFA animals after intraperitoneal (i.p.), intravenous, and topical spinal administration. i.v. administration resulted in a total plasma concentration of 205 nM with 1 mg/kg and 1537 nM with 5 mg/kg after 45 min. i.p. administration resulted in a total plasma concentration of 67 nM after 1.5–2 h. After topical spinal administration of J-2156, the systemic plasma levels remained below the detection threshold of 2.5 nM for all concentrations tested. Concentrations in the cerebrospinal fluid (CSF) remained below the detection limit after 1 mg/kg i.p. dosing (Table 1). Since only peripheral effects on primary afferents were measured after i.v. administration, CSF levels were not assessed for this study.

4. Discussion

In this study we demonstrated that the SSTR4 selective agonist is a potent analgesic in the CFA model of acute inflammatory pain.

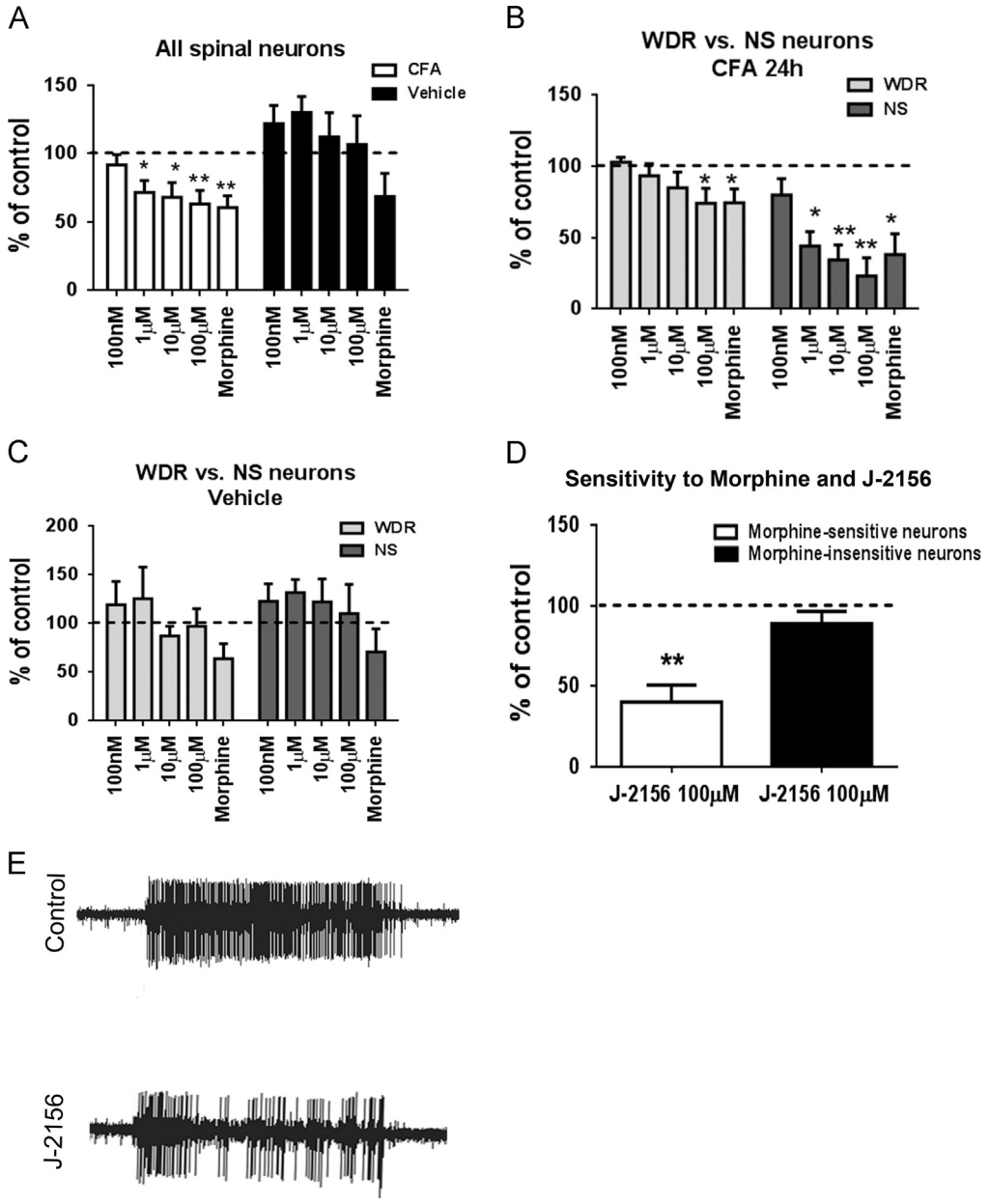

Fig. 2. (A) J-2156 significantly reduced spinal firing rate in CFA-treated animals, but had no effect in sham animals. The effect was dose dependent with the highest dose having a comparable inhibitory effect as morphine. (B) The observed inhibitory effect was mainly driven by inhibition of nociceptive-specific (NS) neurons, whereas wide dynamic range (WDR) neurons were less sensitive to the SSTR4 agonist (n=5–13 neurons). (C) In sham animals, the SSTR4 agonist or morphine had no significant effect in WDR or NS neurons (n=2–6 neurons). (D) Sensitivity of spinal neurons to J-2156 correlates with sensitivity to morphine. (E) An original spike train of a NS neuron from a CFA-treated animal before and after topical administration of 100 μM J-2156.

Table 1
Plasma concentrations of J-2156 after intraperitoneal, intravenous and topical spinal administration. Concentrations of J-2156 in the cerebrospinal fluid were measured after i.p. administration. The plasma concentrations after topical spinal administration remained below the lower quantification limit. Concentrations are means of 6–12 samples per group.

Administration route	**i.p. [mg/kg]**	**i.v. [mg/kg]**		**Topical spinal [μM]**			
	1	1	5	0.1	1	10	100
Plasma conc. (nM)	67	205	1537	LLoQ	LLoQ	LLoQ	LLoQ
CSF[a] conc. (nM)	LLoQ[b]						
Time point of sampling	1.5–2 h	45 min	45 min	15 min			

[a] Cerebrospinal fluid.
[b] Lower quantification limit (2.5 nM).

We showed for the first time that a SSTR4 agonist, like J-2156, can reduce the mechanosensitivity of peripheral nerve afferents as well as spinal neurons in the CFA rat model for inflammatory pain. In addition this effect is pronounced in morphine sensitive neurons compared to other spinal neurons not responsive to morphine. At the spinal level, J-2156 selectively inhibited NS neurons. After systemic administration (1 mg/kg, i.p.), the CSF exposure of J-2156 was below the detection limits suggesting low or no contribution of SSTR4 in the spinal cord to the analgesic responses measured in the behavioral study.

4.1. J-2156 is a potent analgesic in the CFA model

J-2156 has previously been described as an efficacious analgesic in different acute and chronic pain models. Partial nerve ligation was used to assess neuropathic pain, where J-2156 significantly reversed mechanical hyperalgesia. The adjuvants induced chronic inflammatory model was also used, where mechanical allodynia was assessed over a 21 day time course and significant improvements were seen (Sandor et al., 2006). J-2156 also reduces inflammatory reactions in acute inflammatory pain models (Helyes et al., 2006), however direct neuronal inhibition might be implicated. We have shown efficacy of J-2156 in a more acute inflammatory pain model, where hyperalgesia was assessed.

4.2. J-2156 exhibits peripheral antinociceptive effects

The fact that we could not measure a significant increase in the firing rate of afferents after inflammation has been reported before in other studies using in-vitro skin nerve preparations (Brederson et al., 2012; Wenk et al., 2006). It is speculated that mechanically insensitive fibers are recruited and become mechanosensitive under inflammatory conditions. This would result in an overall increased population of responding cells under inflamed conditions (Wenk et al., 2006). This assumption is supported in this study, since more afferents were mechanosensitive in CFA-treated animals. Peripheral antinociceptive mechanisms for the analgesic effects of J-2156 have been previously suggested since SSTR4 is present on sensory nerve terminals (Szolcsanyi et al., 2004; ten Bokum et al., 2000) and inhibition of DRG neuron activity is reported (Gorham et al., 2014a). In this study we were able to show that J-2156 significantly reduced mechanically-evoked firing in single peripheral afferents after i.v. administration in the CFA-treated, but not in the control rats. A higher susceptibility of inflamed afferents to pharmacological intervention has also been described before and allow suggestions that there is a change in the subpopulations of afferents involved in the transmission and/or a change in the functional constitution with receptors involved in nociception (Brederson et al., 2012; Wenk et al., 2006). J-2156 had no effect on spontaneous activity in CFA- and control animals, suggesting that the main peripheral antinociceptive effect was achieved by the reduced mechanosensitivity to evoked stimuli. The effective plasma concentrations under anesthesia are roughly 20 times higher compared to plasma concentrations needed to reach analgesia in the behaving animal. Differences in effective plasma concentrations under anesthesia could be explained by an overall reduced sensitivity of neurons to analgesic compounds due to overlapping mechanisms with the used anesthetic. A recent study describes profound differences of drug effects on electrophysiological endpoints depending on the choice of anesthesia (Hirsch et al., 2014). Even with this limitation, due to the observed analgesic effect with low plasma concentrations in addition to the very low brain penetration of the compound, we can assume that the observed analgesic effect after systemic administration is mediated via peripheral SSTR4 receptors. In conclusion, this study provides in vivo electrophysiological evidence, that J-2156 affects response properties of mechanosensitive peripheral afferents in an inflammatory pain model.

4.3. J-2156 reduces excitability of spinal nociceptive-specific neurons

In this study we recorded spinal neurons that can be grouped due to their response properties. WDR neurons and NS neurons are two known major subgroups of spinal neurons involved in pain transmission (Menetrey et al., 1977; Turnbach et al., 2002; Woolf and King, 1990). Distal inflammation has been shown to sensitize spinal neurons, reflected in an increased firing rate to evoked mechanical stimulation (Martindale et al., 2007; Neugebauer and Schaible, 1990; Schaible et al., 1998). In the present study, topical administration of J-2156 onto the exposed spinal cord significantly reduced mechanosensitivity, specifically in NS neurons at noxious stimulation, but had a smaller effect and only with higher concentrations on WDR neurons at non-noxious or noxious stimulation. Since the strong inhibitory effect of J-2156 on NS neurons in CFA animals was not detectable in vehicle-treated animals we did not expect any effect on WDR neurons in vehicle-treated animals either since we just measured a small effect on WDR neurons in CFA animals. Already a small number of recorded neurons confirmed the assumption of a minor effect on WDR neurons also in control animals. Due to the low number of recorded WDR neurons, we focused our statistical analysis on the comparison of NS neurons in control and CFA animals. Our results are consistent with other studies, reporting an increased mechanical sensitivity of NS neurons (Kitagawa et al., 2005), but not of WDR neurons (McGaraughty et al., 2010) after CFA-induced paw inflammation. We cannot exclude, that some CFA-sensitized NS neurons were characterized as WDR neurons in this study. However, our findings are in line with a previous study showing that 48 h after CFA inflammation NS neurons are sensitized in terms of firing rate to noxious stimuli, but the mechanical threshold remains high enough to clearly identify them as NS neurons (Kitagawa et al., 2005). The spinal CSF concentration of J-2156 after systemic administration of 1 mg/kg (below 2.5 nM) is not sufficient to expect any central effects, considering the spinally applied relative high concentrations of J-2156 (1 μM), needed to induced an inhibition of NS neuronal firing. Therefore, contribution of spinal SST4 receptors to the analgesic effect with the doses used in this study can be excluded. However, these data demonstrated that spinal SSTR4 could contribute to analgesia and therefore higher doses or brain barrier penetrating compounds could also activate spinal SSTR4 which might further contribute the analgesic effect. Since the systemic plasma concentration remained below the detection limit of 2.5 nM after all spinally applied concentrations, a peripheral mediated effect can be excluded in this experiment. A limitation of this study is that with topical spinal application we cannot distinguish between a presynaptic effect on the terminal of the sensory neuron within the spinal cord, which would reduce the synaptic transmission to the spinal neuron, and a postsynaptic effect on the spinal neuron itself. To answer this question slice recordings of the spinal cord would be needed. Since the aim of this study was to assess if a SST4 receptor agonist with a higher penetration of the blood brain barrier could potentially have an effect on spinal neurons this question is out of the scope of this study. Different response properties of WDR and NS neurons to pharmacological interventions have been previously described, suggesting profound differences in their contribution to nociceptive signaling (Sotgiu et al., 2001; Turnbach et al., 2002). Interestingly, in all recorded spinal neurons the inhibitory effect of J-2156 appears to be positively correlated to the inhibitory effect of morphine. Neurons that showed a strong inhibition after J-2156 were also strongly inhibited by morphine. Since J-2156 does not bind per se mu-opiod receptors ($Ki > 10\ \mu M$) this effect can only

be explained by an intracellular signaling pathway. Potential interactions of SST receptors with opioid receptors have been suggested (Betoin et al., 1994; Hatzoglou et al., 2005; Maurer et al., 1982; Pfeiffer et al., 2002; Prinster et al., 2005). A recent study showed, that SSTR4 and delta-opioid receptors exist in a heteromeric complex in the spinal cord and function in synergistic manner (Somvanshi and Kumar, 2014). A potential interaction of spinal SSTR4 and opioid receptors was also supported by the results of this study. This might be a promising property to reduce or replace opioid treatment and avoid undesirable withdrawal symptoms. Since J-2156 targets the SSTR4, it also avoids the most common endocrine side effects of unselective SST agonists as these effects are mainly associated to other subtypes (i.e. SSTR2, 3 and 5) (Weckbecker et al., 2003).

In conclusion, this study shows that the analgesic effect of the selective SST4 receptor agonist J-2156 is mediated most likely via agonism of peripheral receptors. At the spinal level, J-2156 selectively reduces inflammation-induced hyperexcitability of NS neurons, but had a weak effect on WDR neurons. This further consolidates the hypothesis that sensitization of NS neurons seems to be the main driver for inflammatory pain (Kitagawa et al., 2005). However, due to the low CSF concentrations after systemic administration, a spinal contribution to the observed analgesic effect of J-2156 is unlikely. Nevertheless, our observations suggest that this receptor represents a promising target and opens interesting new perspectives for non-opioidergic pain control. The selective anti-nociceptive effect of J-2156 on sensitized spinal NS neurons and its ability to not interfere with physiological nociceptive transmission under control conditions makes this receptor a promising target for further discovery and development work. This would be particularly relevant for chronic pain conditions in which other analgesics are often ineffective. Further research needs to be done to evaluate if centrally acting SSTR4 agonists could actually provide additional analgesic potential under chronic pain conditions.

Acknowledgments

We thank Margot Weiland for her technical assistance in behavioral and pharmacokinetic studies. All authors are employed by Boehringer Ingelheim Pharma GmbH & Co KG.

References

Bar, K.J., Schurigt, U., Scholze, A., Segond Von, B.G., Stopfel, N., Brauer, R., Halbhuber, K.J., Schaible, H.G., 2004. The expression and localization of somatostatin receptors in dorsal root ganglion neurons of normal and monoarthritic rats. Neurosci. 127, 197–206.

Betoin, F., Ardid, D., Herbet, A., Aumaitre, O., Kemeny, J.L., Duchene-Marullaz, P., Lavarenne, J., Eschalier, A., 1994. Evidence for a central long-lasting antinociceptive effect of vapreotide, an analog of somatostatin, involving an opioidergic mechanism. J. Pharmacol. Exp. Ther. 269, 7–14.

Brederson, J.D., Chu, K.L., Reilly, R.M., Brown, B.S., Kym, P.R., Jarvis, M.F., McGaraughty, S., 2012. TRPV1 antagonist, A-889425, inhibits mechanotransmission in a subclass of rat primary afferent neurons following peripheral inflammation. Synapse 66, 187–195.

Carlton, S.M., Zhou, S., Du, J., Hargett, G.L., Ji, G., Coggeshall, R.E., 2004. Somatostatin modulates the transient receptor potential vanilloid 1 (TRPV1) ion channel. Pain 110, 616–627.

Chrubasik, J., Meynadier, J., Blond, S., Scherpereel, P., Ackerman, E., Weinstock, M., Bonath, K., Cramer, H., Wunsch, E., 1984. Somatostatin, a potent analgesic. Lancet 2, 1208–1209.

Clapham, D.E., 2003. TRP channels as cellular sensors. Nature 426, 517–524.

Engstrom, M., Tomperi, J., El-Darwish, K., Ahman, M., Savola, J.M., Wurster, S., 2005. Superagonism at the human somatostatin receptor subtype 4. J. Pharmacol. Exp. Ther. 312, 332–338.

Fioravanti, A., Govoni, M., La, M.G., Perpignano, G., Tirri, G., Trotta, F., Bogliolo, A., Ciocci, A., Mauceri, M.T., Marcolongo, R., 1995. Somatostatin 14 and joint inflammation: evidence for intraarticular efficacy of prolonged administration in rheumatoid arthritis. Drugs Exp. Clin. Res. 21, 97–103.

Gamse, R., Leeman, S.E., Holzer, P., Lembeck, F., 1981. Differential effects of capsaicin on the content of somatostatin, substance P, and neurotensin in the nervous system of the rat. Naunyn Schmiedebergs Arch. Pharmacol. 317, 140–148.

Gorham, L., Just, S., Doods, H., 2014a. Somatostatin 4 receptor activation modulates G-protein coupled inward rectifying potassium channels and voltage stimulated calcium signals in dorsal root ganglion neurons. Eur. J. Pharmacol. 736, 101–106.

Gorham, L., Just, S., Doods, H., 2014b. Somatostatin 4 receptor activation modulates TPRV1 currents in dorsal root ganglion neurons. Neurosci. Lett. 573, 35–39.

Hatzoglou, A., Kampa, M., Castanas, E., 2005. Opioid–somatostatin interactions in regulating cancer cell growth. Front. Biosci. 10, 244–256.

Helyes, Z., Pinter, E., Nemeth, J., Sandor, K., Elekes, K., Szabo, A., Pozsgai, G., Keszthelyi, D., Kereskai, L., Engstrom, M., Wurster, S., Szolcsanyi, J., 2006. Effects of the somatostatin receptor subtype 4 selective agonist J-2156 on sensory neuropeptide release and inflammatory reactions in rodents. Br. J. Pharmacol. 149, 405–415.

Helyes, Z., Pinter, E., Szolcsanyi, J., Horvath, J., 1996. Anti-inflammatory and antinociceptive effect of different somatostatin-analogs. Neurobiology 4, 115–117.

Helyes, Z., Than, M., Oroszi, G., Pinter, E., Nemeth, J., Keri, G., Szolcsanyi, J., 2000. Anti-nociceptive effect induced by somatostatin released from sensory nerve terminals and by synthetic somatostatin analogues in the rat. Neurosci. Lett. 278, 185–188.

Hirsch, S., Dickenson, A., Corradini, L., 2014. Anesthesia influences neuronal activity and drug effectiveness in neuropathic rats. Pain 155, 2583–2590.

Hoyer, D., Perez, J., Schoeffter, P., Langenegger, D., Schupbach, E., Kaupmann, K., Lubbert, H., Bruns, C., Reubi, J.C., 1995. Pharmacological identity between somatostatin SS-2 binding sites and SSTR-1 receptors. Eur. J. Pharmacol. *289*, 151–161.

Iwagaki, N., Garzillo, F., Polgar, E., Riddell, J.S., Todd, A.J., 2013. Neurochemical characterisation of lamina II inhibitory interneurons that express GFP in the PrP-GFP mouse. Mol. Pain 9, 56.

Jiang, N., Furue, H., Katafuchi, T., Yoshimura, M., 2003. Somatostatin directly inhibits substantia gelatinosa neurons in adult rat spinal dorsal horn in vitro. Neurosci. Res. 47, 97–107.

Karalis, K., Mastorakos, G., Chrousos, G.P., Tolis, G., 1994. Somatostatin analogues suppress the inflammatory reaction in vivo. J. Clin. Invest. 93, 2000–2006.

Kardon, A.P., Polgar, E., Hachisuka, J., Snyder, L.M., Cameron, D., Savage, S., Cai, X., Karnup, S., Fan, C.R., Hemenway, G.M., Bernard, C.S., Schwartz, E.S., Nagase, H., Schwarzer, C., Watanabe, M., Furuta, T., Kaneko, T., Koerber, H.R., Todd, A.J., Ross, S.E., 2014. Dynorphin acts as a neuromodulator to inhibit itch in the dorsal horn of the spinal cord. Neuron 82, 573–586.

Kim, S.J., Chung, W.H., Rhim, H., Eun, S.Y., Jung, S.J., Kim, J., 2002. Postsynaptic action mechanism of somatostatin on the membrane excitability in spinal substantia gelatinosa neurons of juvenile rats. Neuroscience 114, 1139–1148.

Kitagawa, J., Kanda, K., Sugiura, M., Tsuboi, Y., Ogawa, A., Shimizu, K., Koyama, N., Kamo, H., Watanabe, T., Ren, K., Iwata, K., 2005. Effect of chronic inflammation on dorsal horn nociceptive neurons in aged rats. J. Neurophysiol. 93, 3594–3604.

Lembeck, F., Donnerer, J., Bartho, L., 1982. Inhibition of neurogenic vasodilation and plasma extravasation by substance P antagonists, somatostatin and [D-Met2, Pro5]enkephalinamide. Eur. J. Pharmacol. 85, 171–176.

Martindale, J.C., Wilson, A.W., Reeve, A.J., Chessell, I.P., Headley, P.M., 2007. Chronic secondary hypersensitivity of dorsal horn neurones following inflammation of the knee joint. Pain 133, 79–86.

Maurer, R., Gaehwiler, B.H., Buescher, H.H., Hill, R.C., Roemer, D., 1982. Opiate antagonistic properties of an octapeptide somatostatin analog. Proc. Natl. Acad. Sci. USA 79, 4815–4817.

McGaraughty, S., Chu, K.L., Perner, R.J., DiDomenico, S., Kort, M.E., Kym, P.R., 2010. TRPA1 modulation of spontaneous and mechanically evoked firing of spinal neurons in uninjured, osteoarthritic, and inflamed rats. Mol. Pain 6, 14.

Menetrey, D., Giesler Jr., G.J., Besson, J.M., 1977. An analysis of response properties of spinal cord dorsal horn neurones to nonnoxious and noxious stimuli in the spinal rat. Exp. Brain Res. 27, 15–33.

Morton, C.R., Hutchison, W.D., Hendry, I.A., Duggan, A.W., 1989. Somatostatin: evidence for a role in thermal nociception. Brain Res. 488, 89–96.

Murase, K., Nedeljkov, V., Randic, M., 1982. The actions of neuropeptides on dorsal horn neurons in the rat spinal cord slice preparation: an intracellular study. Brain Res. 234, 170–176.

Neugebauer, V., Schaible, H.G., 1990. Evidence for a central component in the sensitization of spinal neurons with joint input during development of acute arthritis in cat's knee. J. Neurophysiol. 64, 299–311.

Patel, Y.C., Greenwood, M.T., Warszynska, A., Panetta, R., Srikant, C.B., 1994. All five cloned human somatostatin receptors (hSSTR1-5) are functionally coupled to adenylyl cyclase. Biochem. Biophys. Res. Commun. 198, 605–612.

Pfeiffer, M., Koch, T., Schroder, H., Laugsch, M., Hollt, V., Schulz, S., 2002. Heterodimerization of somatostatin and opioid receptors cross-modulates phosphorylation, internalization, and desensitization. J. Biol. Chem. 277, 19762–19772.

Pinter, E., Helyes, Z., Nemeth, J., Porszasz, R., Petho, G., Than, M., Keri, G., Horvath, A., Jakab, B., Szolcsanyi, J., 2002. Pharmacological characterisation of the somatostatin analogue TT-232: effects on neurogenic and non-neurogenic inflammation and neuropathic hyperalgesia. Naunyn Schmiedebergs Arch. Pharmacol. 366, 142–150.

Prinster, S.C., Hague, C., Hall, R.A., 2005. Heterodimerization of g protein-coupled receptors: specificity and functional significance. Pharmacol. Rev. 57, 289–298.

Reisine, T., Bell, G.I., 1995. Molecular biology of somatostatin receptors. Endocr. Rev. 16, 427–442.
Sandor, K., Elekes, K., Szabo, A., Pinter, E., Engstrom, M., Wurster, S., Szolcsanyi, J., Helyes, Z., 2006. Analgesic effects of the somatostatin sst4 receptor selective agonist J-2156 in acute and chronic pain models. Eur. J. Pharmacol. 539, 71–75.
Schaible, H.G., Neugebauer, V., Geisslinger, G., Beck, U., 1998. The effects of S- and R-flurbiprofen on the inflammation-evoked intraspinal release of immunoreactive substance P—a study with antibody microprobes. Brain Res. 798, 287–293.
Seybold, V.S., Hylden, J.L., Wilcox, G.L., 1982. Intrathecal substance P and somatostatin in rats: behaviors indicative of sensation. Peptides 3, 49–54.
Somvanshi, R.K., Kumar, U., 2014. Delta-opioid receptor and somatostatin receptor-4 heterodimerization: possible implications in modulation of pain associated signaling. PLoS One 9, e85193.
Sotgiu, M.L., Bellomi, P., Biella, G., 2001. Effect of different concentrations of iontophoretic nociceptin on distinct classes of nociceptive neurons in rat spinal cord. Brain Res. 897, 184–187.
Szolcsanyi, J., Bolcskei, K., Szabo, A., Pinter, E., Petho, G., Elekes, K., Borzsei, R., Almasi, R., Szuts, T., Keri, G., Helyes, Z., 2004. Analgesic effect of TT-232, a heptapeptide somatostatin analogue, in acute pain models of the rat and the mouse and in streptozotocin-induced diabetic mechanical allodynia. Eur. J. Pharmacol. 498, 103–109.
Szolcsanyi, J., Helyes, Z., Oroszi, G., Nemeth, J., Pinter, E., 1998a. Release of somatostatin and its role in the mediation of the anti-inflammatory effect induced by antidromic stimulation of sensory fibres of rat sciatic nerve. Br. J. Pharmacol. 123, 936–942.
Szolcsanyi, J., Pinter, E., Helyes, Z., Oroszi, G., Nemeth, J., 1998b. Systemic anti-inflammatory effect induced by counter-irritation through a local release of somatostatin from nociceptors. Br. J. Pharmacol. 125, 916–922.
Szolcsanyi, J., Pinter, E., Helyes, Z., Petho, G., 2011. Inhibition of the function of TRPV1-expressing nociceptive sensory neurons by somatostatin 4 receptor agonism: mechanism and therapeutical implications. Curr. Top. Med. Chem. 11, 2253–2263.
ten Bokum, A.M., Hofland, L.J., van Hagen, P.M., 2000. Somatostatin and somatostatin receptors in the immune system: a review. Eur. Cytokine Netw. 11, 161–176.
Todd, A.J., 2010. Neuronal circuitry for pain processing in the dorsal horn. Nat. Rev. Neurosci. 11, 823–836.
Turnbach, M.E., Spraggins, D.S., Randich, A., 2002. Spinal administration of prostaglandin E(2) or prostaglandin F(2alpha) primarily produces mechanical hyperalgesia that is mediated by nociceptive specific spinal dorsal horn neurons. Pain 97, 33–45.
Weckbecker, G., Lewis, I., Albert, R., Schmid, H.A., Hoyer, D., Bruns, C., 2003. Opportunities in somatostatin research: biological, chemical and therapeutic aspects. Nat. Rev. Drug Discov. 2, 999–1017.
Wenk, H.N., Brederson, J.D., Honda, C.N., 2006. Morphine directly inhibits nociceptors in inflamed skin. J. Neurophysiol. 95, 2083–2097.
Wiesenfeld-Hallin, Z., 1985. Intrathecal somatostatin modulates spinal sensory and reflex mechanisms: behavioral and electrophysiological studies in the rat. Neurosci. Lett. 62, 69–74.
Wiesenfeld-Hallin, Z., 1986. Somatostatin and calcitonin gene-related peptide synergistically modulate spinal sensory and reflex mechanisms in the rat: behavioral and electrophysiological studies. Neurosci. Lett. 67, 319–323.
Woolf, C.J., King, A.E., 1990. Dynamic alterations in the cutaneous mechanoreceptive fields of dorsal horn neurons in the rat spinal cord. J. Neurosci. 10, 2717–2726.
Yasaka, T., Tiong, S.Y., Hughes, D.I., Riddell, J.S., Todd, A.J., 2010. Populations of inhibitory and excitatory interneurons in lamina II of the adult rat spinal dorsal horn revealed by a combined electrophysiological and anatomical approach. Pain 151, 475–488.